

University of Nevada

Reno

✓
Determination of Timing of Recharge for
Geothermal Fluids in The Great Basin Using
Environmental Isotopes and Paleoclimate Indicators

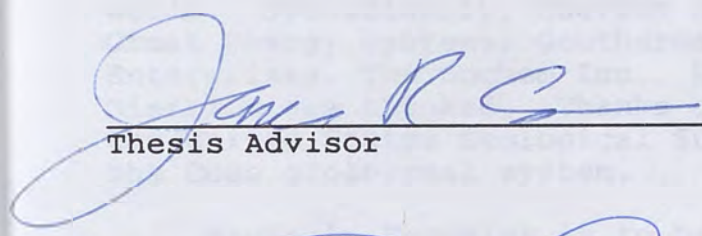
A thesis submitted in partial fulfillment
of the requirements for the degree of
Master of Science, in geology

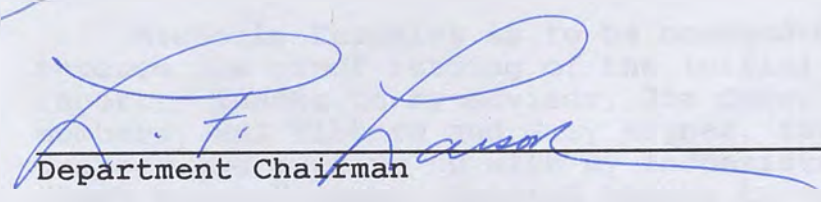
by

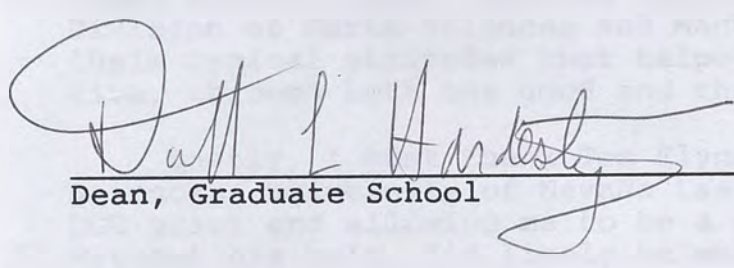
Paul K. Buchanan
111

April, 1990

The thesis of Paul K. Buchanan is approved by


Thesis Advisor


Department Chairman


Dean, Graduate School

University of Nevada
Reno

April, 1990

ACKNOWLEDGEMENTS

This study was made possible by grant DE-FG07-88ID12784 from the United States Department of Energy, Geothermal Technology Division, administered by the Idaho Operations Office, Idaho Falls, Idaho. Additional financial assistance from the Nevada Section of the Geothermal Resources Council aided in the completion of this thesis.

My thanks go to the Nevada geothermal power industry for allowing fluid sampling of deep powerplant production wells. Specifically, Chevron Resources, Oxbow Geothermal, Ormat Energy Systems, Geothermal Food Processors, Tad's Enterprises, Thermochem Inc., Elko Heat Co. and Elko School District are thanked. Thanks also to Dr. Robert Fournier of the United States Geological Survey for providing data on the Coso geothermal system.

Michelle Stickles is to be commended for suffering through the proof reading of the initial drafts of this report. Thanks to my advisor, Jim Carr, and my committee members, Mel Hibbard and Gary Haynes, for taking on this project and putting up with my inconsistent scheduling and "last minute" rush. Special thanks to my cohorts at the Division of Earth Sciences and Mackay School of Mines for their cynical attitudes that helped keep it all in perspective, through both the good and the bad times.

Lastly, I must thank Tom Flynn of the Division of Earth Sciences, University of Nevada Las Vegas, for securing the DOE grant and allowing me to be a part of the project. Without his help, I'd likely be making change at Harrah's right now.

In spite of the numerous citations above, the author accepts full responsibility for the contents that follow.

ABSTRACT

Early theories concerning geothermal system recharge in the Great Basin assumed the fluid source was recent precipitation. Environmental isotopes and paleoclimatic indicators suggest a more plausible paleorecharge scheme.

Polar region isotopic studies demonstrate that a depletion in stable light-isotopes of precipitation existed during the late Pleistocene due to the colder, wetter climate. Isotopic analysis of calcite veins and packrat midden megafossils confirm the depletion event occurred in the Great Basin.

In this study, non-thermal springs represent local, recent precipitation. Thermal waters are generally more isotopically depleted than non-thermal waters, and represent Pleistocene precipitation. Isolated areas where thermal water is more isotopically enriched than non-thermal water correspond to the location of major Pleistocene lakes, suggesting isotopically enriched lake water contributed to recharge. Carbon age dates and isotopic data from Great Basin thermal waters correlate with the polar paleoclimatic studies. Recharge occurred along range-bounding faults.

TABLE OF CONTENTS

ACKNOWLEDGEMENTS.	iii
ABSTRACT.	iv
LIST OF FIGURES	vii
LIST OF TABLES.	ix
CHAPTER 1. INTRODUCTION.	1
CHAPTER 2. PHYSICAL SETTING.	5
2.1 GEOGRAPHY.	5
2.2 GEOLOGY.	7
2.3 THERMAL CHARACTERISTICS AND GEOTHERMAL RESOURCES .	9
2.3.1 Thermal Characteristics	
2.3.2 Geothermal Resources	
CHAPTER 3. THEORY OF ENVIRONMENTAL ISOTOPES.	16
3.1 STABLE LIGHT ISOTOPES.	17
3.1.1 Hydrogen	
3.1.2 Oxygen	
3.1.3 Carbon	
3.2 ISOTOPE FRACTIONATION PROCESSES.	22
3.2.1 Isotope Exchange	
3.2.2 Other Fractionation Processes	
3.3 UNSTABLE LIGHT ISOTOPES AND AGE DATING	31
3.3.1 Tritium	
3.3.2 Carbon	
3.4 CORRECTION OF CARBON-AGE DATES	35
3.4.1 Atmospheric Correction	
3.4.2 Soil and Rock Correction	
CHAPTER 4. DATA SET COMPILATION.	42
4.1 LITERATURE SEARCH	42
4.1.1 Water Samples	
4.1.2 Carbon Age Date Samples	
4.1.3 Paleoclimatic Data	
4.2 FIELD SAMPLING PROGRAM	45
CHAPTER 5. LABORATORY METHODS.	49
5.1 HYDROGEN AND OXYGEN STABLE LIGHT ISOTOPES.	49
5.2 WATER CHEMISTRY	50
5.3 TRITIUM ANALYSIS	50
5.4 CARBON ISOTOPES.	51
5.4.1 Water Samples	
5.4.2 Carbonate Scale	
5.4.3 Analytical Method	
5.5 PACKRAT MIDDENS.	53
5.5.1 Hydrogen and Oxygen Isotopes	
5.5.2 Carbon-Age Determination	

CHAPTER 6.	PLEISTOCENE PALEOCLIMATE DATA	55
6.1	GLOBAL ISOTOPIC DEPLETION EVENTS	55
	6.1.1 Greenland, Arctic Evidence	
	6.1.2 Sub-Polar Indian Ocean, Antartic Evidence	
	6.1.3 Devils Hole, Amargosa Desert, Great Basin	
6.2	PACKRAT MIDDENS.	59
	6.2.1 Initial Midden Studies	
	6.2.2 Isotopic Analysis of Midden Macrofossils	
6.3	PLEISTOCENE LAKES.	67
CHAPTER 7.	WATER ANALYSES.	71
7.1	COMPUTER CONTOURING OF STABLE LIGHT-ISOTOPE DATA .	71
	7.1.1 Undifferentiated Set	
	7.1.2 Non-Thermal Springs and Precipitation	
	7.1.3 Thermal Waters	
	7.1.4 Non-Thermal vs. Thermal Fluids: Isotopic Differences	
7.2	GROUNDWATER AGE DATING USING RADIOACTIVE ISOTOPES.	87
	7.2.1 Tritium	
	7.2.2 Carbon-14	
CHAPTER 8.	DISCUSSION: EFFECT OF PLEISTOCENE LAKES, AND RECHARGE SCHEMES.	92
8.1	EFFECT OF PLEISTOCENE LAKES.	92
8.2	RECHARGE SCHEMES	97
CHAPTER 9.	SUMMARY	104
9.1	CONCLUSIONS.	104
9.2	RECOMMENDATIONS.	105
REFERENCES	CITED	106
APPENDIX A	CURRENT STUDY - STABLE LIGHT ISOTOPE AND GEOCHEMICAL ANALYSES.	116
APPENDIX B	LITERATURE SEARCH - STABLE LIGHT ISOTOPES .	119
APPENDIX C	CARBON AGE ANALYSES	151
APPENDIX D	PALEOCLIMATE DATA	156

LIST OF FIGURES

Figure 2.1	Location map.	6
Figure 2.2	Basin and Range structural models	10
Figure 2.3	Late Cenozoic extensional faults.	11
Figure 3.1	Relative isotopic depletion scale	20
Figure 3.2	Temperature vs. ^{18}O , Fractionation factor	24
Figure 3.3	Temperature dependence of isotopic composition of precipitation	26
Figure 3.4	Rayleigh distillation	27
Figure 3.5	Diagrammatic example of storm rain-out.	29
Figure 3.6	Carbon isotopes in the hydrologic cycle	34
Figure 3.7	The "Suess effect", recent isotopic depletion of atmospheric carbon.	37
Figure 3.8	Carbon isotope content of several types of material	40
Figure 4.1	Fluid sample locations, this study.	48
Figure 4.2	Packrat midden sample locations	48
Figure 6.1	Comparison of ^{18}O vs. stratigraphic age from Greenland and Sub-Polar Indian Ocean	58
Figure 6.2	Comparison of ^{18}O vs. U/TH age from Devils Hole and Sub-Polar Indian Ocean.	58
Figure 6.3	Deuterium vs. radiocarbon age Snake Range packrat middens	62
Figure 6.4	Deuterium vs. radiocarbon age this study, all midden samples.	65
Figure 6.5	Deuterium vs. radiocarbon age this study, Painted Hills midden.	65
Figure 6.6	Deuterium vs. radiocarbon age, Snake Range and Painted Hills middens	66
Figure 6.7	Maximum extent of Pleistocene Lake Lahontan and Lake Bonneville	68
Figure 6.8	Lake level chronology of Pleistocene Lake Lahontan and Lake Bonneville	70
Figure 7.1	Contoured deuterium, all fluid samples.	73
Figure 7.2	Contoured oxygen-18, all fluid samples.	73
Figure 7.3	Deuterium vs. ^{18}O , non-thermal springs.	75
Figure 7.4	Contoured deuterium, non-thermal springs.	77
Figure 7.5	Stormtracks which bring precipitation to the Great Basin.	77
Figure 7.6	Contoured oxygen-18, non-thermal springs.	78

LIST OF FIGURES, Continued

Figure 7.7	Contoured deuterium, thermal springs.	79
Figure 7.8	Contoured deuterium, thermal wells.	79
Figure 7.9	Contoured oxygen-18, thermal springs.	81
Figure 7.10	Contoured oxygen-18, thermal wells.	81
Figure 7.11	Deuterium vs. ^{18}O , Beowawe, Nevada, area.	82
Figure 7.12	Deuterium vs. ^{18}O , Caliente, Nevada, area	82
Figure 7.13	Contoured deuterium, thermal springs minus non-thermal springs	84
Figure 7.14	Contoured deuterium, thermal wells minus non-thermal springs	84
Figure 7.15	Contoured oxygen-18, thermal springs minus non-thermal springs	86
Figure 7.16	Deuterium vs. ^{18}O , demonstrating worldwide occurrence of oxygen shift	86
Figure 7.17	Location of radiocarbon age analyses.	90
Figure 7.18	Deuterium vs. radiocarbon age, northern Nevada thermal waters.	91
Figure 8.1	Location of Painted Hills and Snake Range midden studies in relation to Pleistocene Lake Lahontan and Lake Bonneville	93
Figure 8.2	Deuterium vs. radiocarbon age for Painted Hills middens, compared to Lake Lahontan level chronology.	94
Figure 8.3	Deuterium vs. radiocarbon age for Snake Range middens, compared to Lake Bonneville level chronology.	94
Figure 8.4	Deuterium vs. radiocarbon age for northern Nevada thermal waters, compared to Pleistocene lake level variations.	95
Figure 8.5	Areas where non-thermal waters are more depleted than thermal waters, in relation to location of Pleistocene lakes.	96
Figure 8.6	Historical recharge model	98
Figure 8.7	Ground water flowpath for a lake with inhomogeneous sub-surface	100
Figure 8.8	Pleistocene recharge models involving lake waters	101
Figure 8.9	Conceptual model for recharge of geothermal fluids.	103

LIST OF TABLES

Table 3.1	Isotopes employed in this study.	19
Table 3.2	Possible combinations of hydrogen and oxygen isotopes in water	28
Table 3.3	Effect of hydrogen isotopes on the thermodynamic properties of water.	28
Table 3.4	Correction factors for soil zone carbon. . .	38
Table 4.1	Distribution of fluid sample data set by sample type and temperature. . .	44
Table 4.2	Fluid sampling program analyses.	47
Table 5.1	Water chemistry techniques employed by UURI	51
Table 7.1	Tritium analyses, this study	88
Table 7.2	Radiocarbon-age analyses, this study	89

CHAPTER 1.

INTRODUCTION

The age of geothermal fluids in the Great Basin has long been debated, and is an important factor affecting the future development of the geothermal industry. Reservoir size, longevity, and replenishment all relate to when the thermal fluids entered the cycle. Stable light-isotopes, also known as environmental isotopes, are a natural tracer which can be used to compare the geothermal fluids to other paleoclimatic records from throughout the world.

The development of geothermal resources in the Great Basin has accelerated in the last 10 years, and currently supplies nearly 200 megawatts electricity (MWe) to the western United States. The potential for development of this energy source in the Great Basin was initially long overlooked. White (1965) described production potential at only three sites in Nevada: Steamboat Springs, Beowawe and Brady's Hot Springs. The thermal resources at all three of these locations are today being utilized. Subsequently, Muffler (1979) rated the potential of the Great Basin as 3,000 Megawatts (MWe) of electrical production from 17 hydrothermal systems. In addition to the electric power currently being produced, other applications of geothermal energy currently include vegetable dehydration, district space-heating, and aquaculture.

Although the technology for production and economic utilization is well established, the age, source, and longevity of the resource are as yet unknown, and our lack of knowledge limits further geothermal development. The goal of the research reported here is to establish a model of geothermal fluid genesis throughout the Great Basin, and thus begin to fill the gaps in our understanding.

Thermal waters from across the Great Basin typically have different chemical and stable light-isotope signatures when compared to precipitation and non-thermal waters from the same area. Chemical differences can be attributed to rock-water interaction during deep circulation at elevated temperatures. The geothermal fluids are more isotopically enriched than local non-thermal fluids. This difference has historically been attributed to recharge of geothermal fluids by recent precipitation falling at elevations higher than the discharge zones. Craig (1963) stated that "most geothermal fluids are of meteoric origin", citing their isotopic similarity to meteoric waters throughout the world.

Drawing on classical hydrology and looking for a source that explained the usually strong artesian flow, other workers compared the depleted stable light-isotope signatures of the thermal fluids to those of precipitation falling in nearby high mountain ranges, and found them to

be similar. Nehring (1980) concluded the thermal fluids of Steamboat Springs, Nevada, were quite young and recharged by recent precipitation falling in the nearby Carson Range. Fournier and Thompson (1980) recorded similar observations in a study of the Coso, California, geothermal system, and assigned the recharge zone to the southern Sierra Nevada Mountains, 30 kilometers to the west. The mechanism by which these fluids could be transported this long distance across major fault zones, and the extremely high fluid-flow rates required for modern recharge, were not specified.

Clayton (1966) found that water in oil field brines of the Michigan basin were isotopically depleted relative to modern precipitation. With no high mountain recharge zone nearby to account for these depleted fluids, he concluded the precipitation must have fallen when a colder, wetter climate was prevalent in the region, perhaps during the late Pleistocene. Welch (1981) drew similar conclusions from his study of the Leach Hot Springs system of Grass Valley, north-central Nevada. He pointed out the nearest mountain range high enough to account for the isotopically depleted thermal fluids discharging from the springs is more than 160 kilometers away from Grass Valley. Assuming a high groundwater flow rate of 10 meters per year, the fluid cycle from infiltration to discharge would require 16,000 years. Therefore, modern recharge of the system, in

less than 1,000 years, requires an unrealistic groundwater flow rate of 1,600 meters per year.

This study addresses the question of the age of geothermal fluids in the Great Basin, and investigates the feasibility of paleorecharge. The central question addressed is whether paleorecharge, associated with the wetter climates of the glacial/pluvial climate during the late Pleistocene, accounts for the isotopically depleted nature of geothermal fluids. The study was carried out in northern Nevada, where the majority of high-temperature fluids, deep geothermal production wells, and other components critical to the study are located. I compared stable light isotopic data from thermal fluids to isotopic data from recent precipitation and from paleoclimatic studies. Isotopic data obtained from macrofossil analyses of packrat (genus *Neotoma*) middens were used to determine the magnitude of changes in isotopic composition of paleo-meteoric fluids that resulted from the changing climatic conditions in the Great Basin.

CHAPTER 2.

PHYSICAL SETTING

The Great Basin is a topographically elevated and relatively dry area that is characterized by north and northeast-trending mountains and valleys. It is a region that has undergone extensive geological faulting and has a relatively high heat flow. This combination of factors has produced the present distribution of geothermal systems.

2.1 GEOGRAPHY

The Great Basin of the western United States (Figure 2.1) is a physiographic province covering all or portions of six states. It is defined by regional internal drainage (Fenneman, 1931) and characterized by north to northeast trending mountains and valleys. The major drainage basins in the region are The Great Salt Lake and Sevier (Dry) Lake of Utah, and the Humboldt and Carson Sinks and Pyramid and Walker Lakes of western Nevada. Included within the Great Basin are the east slopes of the northern Sierra Nevada Mountains, California, and the west slopes of the Wasatch Range, Utah. Typical valley elevations range from 1300 to 1600 m and have a semi-arid to desert climate. Many mountain ranges have an alpine climate, with elevations frequently exceeding 3,000 m. The Great Basin is often

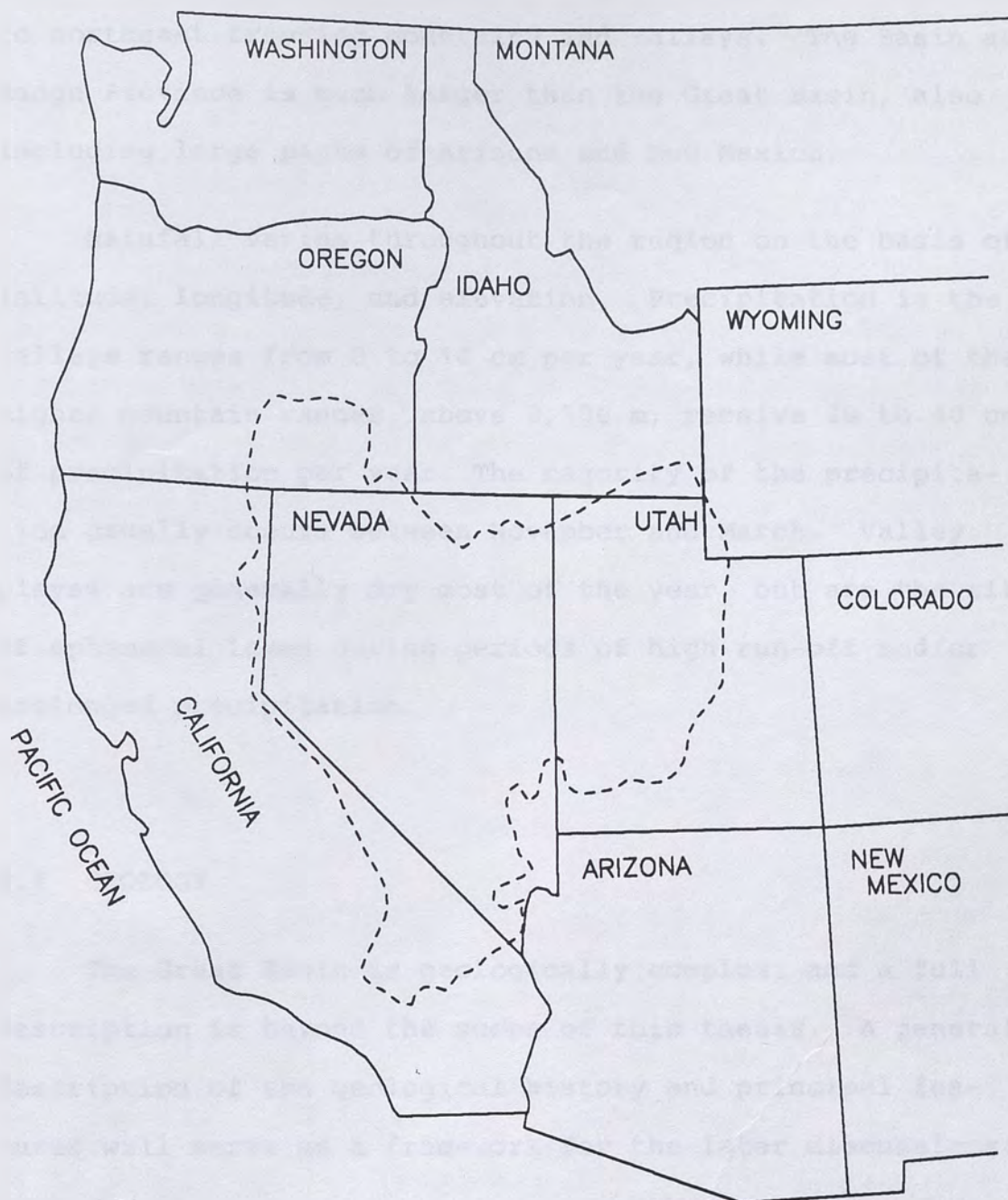


Figure 2.1: Location map for the western United States, and the Great Basin physiographic province as defined by the dashed line.

confused with the Basin and Range, a regionally extensive geologic province of block faulting characterized by north to northeast trending mountains and valleys. The Basin and Range Province is much larger than the Great Basin, also including large parts of Arizona and New Mexico.

Rainfall varies throughout the region on the basis of latitude, longitude, and elevation. Precipitation in the valleys ranges from 0 to 10 cm per year, while most of the higher mountain ranges, above 2,500 m, receive 20 to 40 cm of precipitation per year. The majority of the precipitation usually occurs between November and March. Valley playas are generally dry most of the year, but are the site of ephemeral lakes during periods of high run-off and/or prolonged precipitation.

2.2 GEOLOGY

The Great Basin is geologically complex, and a full description is beyond the scope of this thesis. A general description of the geological history and principal features will serve as a framework for the later discussions.

Rocks units in the Great Basin vary in age from Precambrian to very young. The oldest rocks, ranging in age from Precambrian through middle Paleozoic, occur in the southern and eastern portion of the province. They are the

product of extensive clastic and carbonate deposition in shallow seas, with the estimated thickness of the sediments in eastern Nevada and western Utah exceeding 6,000 m. Paleozoic and Mesozoic rocks in western Nevada are largely deep sea shales and siliceous siltstones that were thrust over the eastern assemblage in a series of orogenies that began in the Devonian Period (270 mya) and lasted through the middle of the Mesozoic Era. Much of western Nevada is underlain by granitic plutons of Mesozoic age, which are best exposed in the Sierra Nevada Mountains of western Nevada and eastern California.

Throughout the Great Basin, valleys contain sediments that are derived locally from the ranges, and vary in size from coarse fan-glomerates near the ranges to fine silts, clays, and evaporites in the playas. Valley sediment accumulations may be up to 3000 m thick.

Widespread volcanism began approximately 43 million years ago and resulted in the formation of siliceous caldera complexes. Volcanic activity was initiated in western Utah and eastern Nevada, spreading west and south across the region. Six mya, the volcanism changed from bi-modal (silicious and basaltic), to principally basaltic. The most recent episode of volcanism produced basalt-basaltic andesite lava flows and cinder cones in west central Nevada, less than 100,000 years ago.

Widespread faulting throughout the region also began approximately 43 million years ago, and is thought to be associated with the volcanic activity. Basin and Range style faulting, which produced the present-day topography of elongated mountains and valleys, is a result of regional extensional tectonics that began approximately 13 million years ago. This style of faulting produces sub-parallel mountains that are, on average, 10 to 20 km wide and 25 to 35 km from crest to crest. Several different models have been developed to explain this structural style (Figure 2.2). A generalized map of the late Cenozoic extensional faults (Figure 2.3) in the Great Basin shows their wide distribution and general north-northeast trend. Range-bounding faults are responsible for the widespread earthquake activity in the Great Basin, and are also believed to be the principal conduits for convecting geothermal fluids.

2.3 THERMAL CHARACTERISTICS AND GEOTHERMAL RESOURCES

In addition to a complex geologic history, the Great Basin is located within an area of elevated heat flow. Heat flow is defined as the product of the thermal conductivity of a rock and the measured thermal gradient. An extended, highly permeable upper crust and the relatively high geothermal gradient of the Great Basin controls the distribution of heat flow and geothermal systems.

2.3.1 Thermal Characteristics

Many authors have documented the physical and chemical characteristics of the high-temperature geothermal systems in the Great Basin (GRC, 1983), and illustrated the close relationships between the anomalous heat flow and the development of energy and mineral resources.

Two dominant regional thermal effects -- those related to tectonic extension and those related to volcanism -- were identified by Blackwell (1983). He argued that the observed heat flow in the Great Basin is a product of the

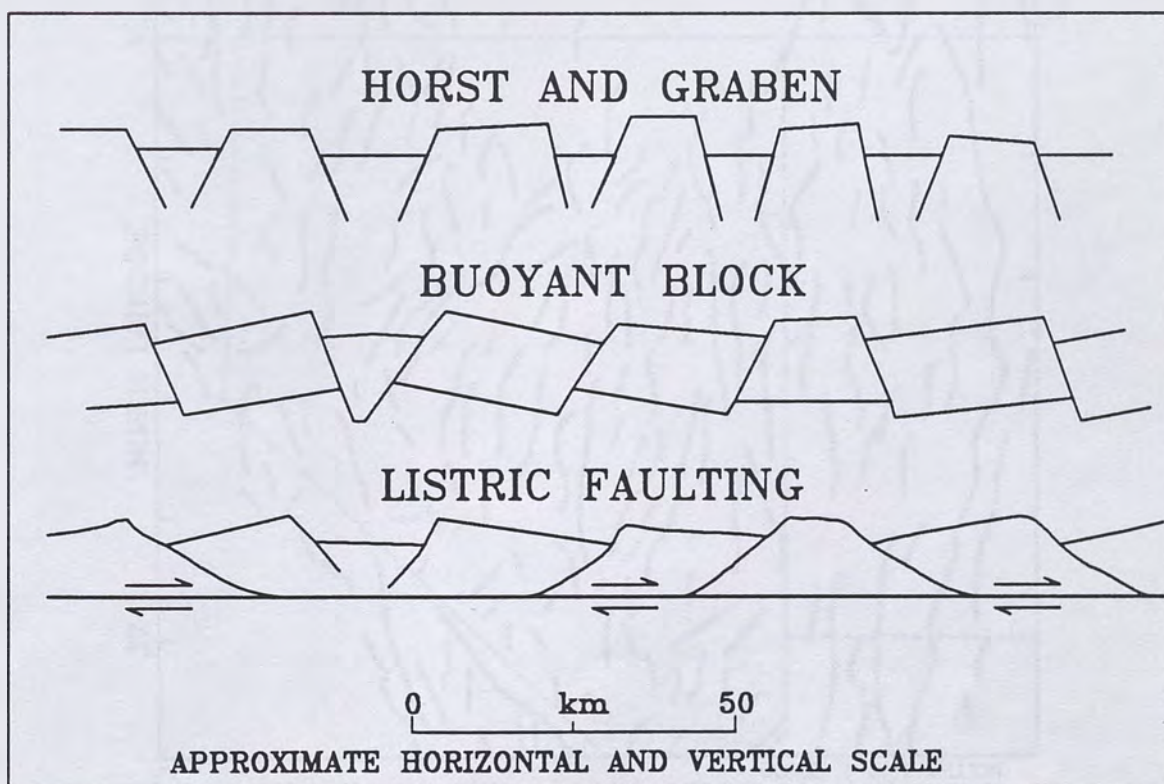


Figure 2.2: Models of Basin and Range structure, after Stewart (1983).

superposition of the effects of regional extension and igneous activity, modified by the local conductive effects of thermal refraction, variations in radiogenic heat production, erosion, and sedimentation. A conceptual heat flow model was proposed that included a heat source, at a depth of 10 to 20 km, with a temperature of 1350°C. Disturbances in observed heat flow at the surface were credited to deeply circulating groundwater.

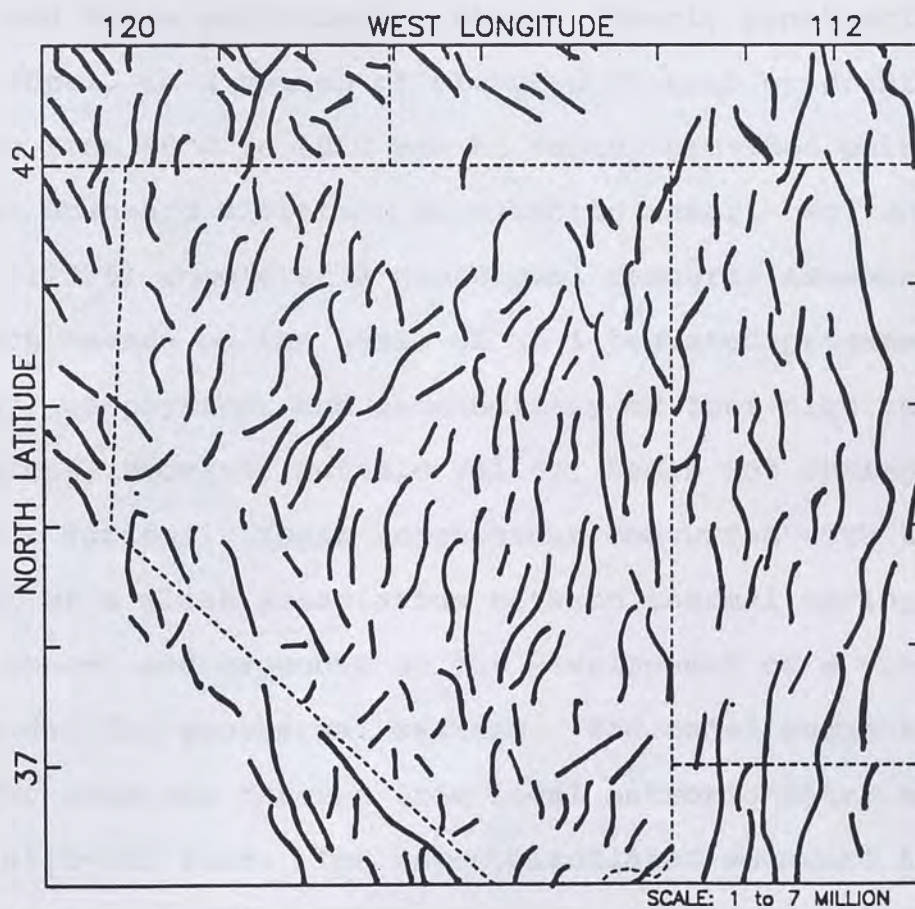


Figure 2.3: Distribution of late Cenozoic extensional faults in the Great Basin, from Stewart (1983).

2.3.2 Geothermal Resources

Serious scientific investigation of the geothermal resources in the western United States were not initiated until the mid 1970s. Garside (1974) documented the initial exploration efforts in Nevada, and identified approximately 300 hot springs and wells throughout the state. Included in the report are the location of thirteen areas that the U.S. Department of the Interior had previously classified as Known Geothermal Resource Areas (KGRA's).

Hose and Taylor (1974) first proposed a model for Basin and Range geothermal systems. Deeply penetrating fault zones, in a region of elevated thermal gradients ranging from 40°C to 60°C per km depth, provided pathways for the downward migration of meteoric water. Wollenberg et al. (1975) completed a geothermal resource assessment of northern Nevada on the basis of an integrated program of geology, geophysics, and geochemistry of four high temperature areas; Beowawe, Buffalo Valley, Leach Hot Springs, and Kyle Hot Springs. Their conclusions concurred with the concept of a close association between thermal springs and fault zones, and expanded on the development of a conceptual model for geothermal systems. The model suggested that recharge was derived from local meteoric water saturating alluvial fans. The water circulated downward to a depth of four to five kilometers, reaching temperatures

ranging from 150°C to 200°C. Fault zones were identified as the permeable passage ways for the upwardly migrating hot water.

As the volume of data for geothermal systems continued to grow, and in the wake of the "energy crisis", efforts were accelerated to develop geothermal energy in the United States. In 1978, Muffler completed an assessment of geothermal resources in the United States. In Nevada, he identified seventeen systems with estimated subsurface temperatures in excess of 150°C, twenty-four with temperatures between 90°C and 150°C, and twenty-eight with temperatures less than 90°C. Virtually all of the systems were believed to involve deep circulation along fault zones.

Garside and Schilling (1979) subsequently completed an inventory of Nevada's geothermal resources that included chemical and isotopic data, in addition to the development history of selected geothermal areas. Following this, a series of assessment programs were completed for various parts of Nevada (Trexler et al., 1980a; Trexler et al., 1980b; Trexler et al., 1981; Trexler et al., 1982). These studies consisted of a series of synoptic surveys, covering geology, geophysics, and geochemistry. Most near-surface geothermal systems were found to be fault-controlled, and

both chemically and isotopically distinct from local non-thermal fluids.

A significant effort was focused on the development of high temperature geothermal resources in Utah and Nevada in the late 1970s to early 1980s. This project was known as the Industry Coupled Drilling Program and was funded by the U.S. Department of Energy and the geothermal industry. In Nevada, large-scale drilling programs were completed at ten sites, including Beowawe, Dixie Valley, Stillwater, Colado, Soda Lake, Humboldt House, Desert Peak, Leach Hot Springs, McCoy, and Tuscarora. In Utah, drilling programs were completed at Cove Fort and Roosevelt Hot Springs. Both of the Utah sites and five of the ten Nevada Sites presently support geothermal power plants.

Edmiston and Benoit (1985) reviewed the chemical characteristics of six geothermal systems in the Great Basin with temperatures between 150° and 200°C. They concluded that most of the systems were associated with hot springs that discharge NaCl type fluids in northwest Nevada or with major centers of Quaternary volcanism along the western border. Two exceptions are the Cove Fort and Roosevelt field in southwestern Utah.

In summary, geothermal systems in the Great Basin have an extensive history of exploration and subsequent development. The data base consists of an integrated package of

geological, geophysical, and geochemical surveys, supplemented by logs of subsurface temperature and lithologies. Most of the geothermal power plants have been developed in the vicinity of known high-temperature geothermal springs.

CHAPTER 3.

THEORY OF ENVIRONMENTAL ISOTOPES

The atomic structure of most matter consists of a nucleus, containing protons and neutrons, surrounded by electrons. The number of protons in an atom dictates the atomic number and the elemental properties of that atom.

Isotopes, the term applied to different forms of an element, possess the same number of protons but a variable number of neutrons. Since isotopes possess the same number of protons, they occupy the same location in the periodic table of the elements and derive their name from the Latin roots iso = same, topos = position (Aswathanarayana, 1985). The combined total of protons and neutrons determines the atomic mass (measured as atomic mass units or AMU) of an element. A convenient way to denote isotopes is to place the atomic mass to the upper left and the atomic number to the lower left of the elemental symbol. For example, the element oxygen contains 8 protons and either 8, 9 or 10 neutrons, hence the notation $^{16}_8\text{O}$, $^{17}_8\text{O}$, and $^{18}_8\text{O}$. In practice, only the atomic mass, not the atomic number, is normally displayed.

Approximately 1700 isotopes have been identified, of which 256 are stable (or non-radioactive). Most elements are a mixture of two or more isotopes; only 21 elements are purely composed of a single isotope. In multiple isotopic

elements, one isotope is usually predominant, while the others are present in only trace amounts (Hoefs, 1987).

Unstable (radioactive) isotopes "decay" to a different isotope or element by emitting atomic particles. They will be discussed later in Section 3.3. Stable isotopes do not undergo decay, but may be exchanged with other materials during chemical equilibrium reactions.

3.1 STABLE LIGHT ISOTOPES

Isotopes of "lighter" elements (with a mass less than 24 AMU) have been shown to be effective natural indicators of environmental conditions (Fritz and Fontes 1980, Faure 1986). The large percent difference between the atomic masses of isotopes of light elements allows the relative abundance of each isotope to be easily quantified through instrumental analysis, such as mass spectrometry. For example, the mass difference of hydrogen (1 AMU) and deuterium (2 AMU) is calculated by:

$$\frac{{}^2\text{H}-{}^1\text{H}}{{}^1\text{H}} = \frac{2 - 1}{1} = 1 = 100\% , \quad (3.1)$$

whereas the difference in oxygen, isotopic mass of 16 AMU and 18 AMU, is calculated by:

$$\frac{{}^{18}\text{O}-{}^{16}\text{O}}{{}^{16}\text{O}} = \frac{18 - 16}{16} = .125 = 12.5\% . \quad (3.2)$$

These percent differences are far more significant than those of the heavier elements. For example, uranium, with isotopic masses of 238 AMU and 235 AMU, has the following percent mass difference between isotopes:

$$\frac{238\text{U}-235\text{U}}{235\text{U}} = \frac{238 - 235}{235} = .0128 = 1.28\% \quad (3.3)$$

The stable light-isotopes of three elements, hydrogen, oxygen, and carbon, were employed in this study, because of their large isotopic mass differences and natural abundances. Isotope ratios are measured as deviation from an internationally accepted standard, usually assigned the value 0, and reported in units of permil (parts per thousand) deviation from that standard. Permil is represented by the symbol ‰. Samples of the accepted standards are distributed to laboratories for instrument calibration to assure reproducibility of results. The standards used vary among elements and will be discussed individually below.

3.1.1 Hydrogen

The element hydrogen contains one proton and has three isotopes, two stable and one unstable. The isotopes are shown in Table 3.1 along with their relative abundance. The internationally accepted standard for measurement of stable hydrogen isotope ratios in water is known as SMOW (Standard Mean Ocean Water) which was initially standardized by Craig (1961). A sample of water with the same

Table 3.1: Isotopes employed in this study and their average worldwide abundances (Aswathanarayana, 1985).

ISOTOPE	COMMON SYMBOL	P	N	AMU	PERCENT ABUNDANCE	COMMENTS
Hydrogen	H, ^1H	1	0	1	99.984	
Deuterium	D, ^2H	1	1	2	0.0154	
Tritium	T, ^3H	1	2	3	$\leq 10^{-15}$	unstable
Oxygen-16	^{16}O	8	8	16	99.763	
Oxygen-17	^{17}O	8	9	17	0.0372	not used
Oxygen-18	^{18}O	8	10	18	0.1995	
Carbon-12	^{12}C	6	6	12	98.90	
Carbon-13	^{13}C	6	7	13	1.10	
Carbon-14	^{14}C	6	8	14	$\approx 10^{-10}$	unstable

P - # of protons in the element
 N - # of neutrons in the isotope
 AMU - Atomic Mass Units

composition as SMOW, referred to as Vienna-SMOW, is maintained by the International Atomic Energy Agency (IAEA) in Vienna, Austria, and distributed to laboratories worldwide for calibration of equipment. The deuterium(D)/hydrogen(^1H) ratio present in this water is assigned a value of 0⁰⁰/₀, and all other values are reported as a deviation (δ) from this standard, using the formula:

$$\delta D^{00}/_0 = 10^3 \times \frac{(D/^1H)_{\text{SAMPLE}} - (D/^1H)_{\text{SMOW}}}{(D/^1H)_{\text{SMOW}}} \quad (3.4)$$

A second standard distributed by the IAEA is based on the D/H content of Standard Light Antarctic Precipitation

(SLAP), and has a value of $-428^{00}/_0$ on the SMOW Scale. All values in this study are reported relative to Vienna SMOW.

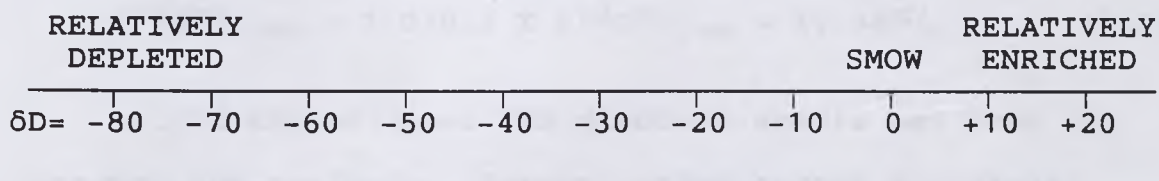
On a relative scale, more positive permil values contain more deuterium and are considered to be enriched, more negative values are considered to be depleted (Figure 3.1). Enriched samples are commonly referred to as "heavy", while depleted samples are considered to be "light".

3.1.2 Oxygen

The element oxygen contains eight protons and has three stable isotopes, as shown in Table 3.1 along with their relative worldwide abundance. The accepted standard for oxygen isotope ratios in water is also Vienna SMOW. The $^{18}\text{O}/^{16}\text{O}$ ratio found in SMOW is zero permil. Oxygen-17 exists in such minute quantities it is not used for isotope studies. The formula for oxygen permil deviation from SMOW is similar to that for hydrogen:

$$\delta^{18}\text{O}^{00}/_0 = 10^3 \times \frac{(^{18}\text{O}/^{16}\text{O})_{\text{SAMPLE}} - (^{18}\text{O}/^{16}\text{O})_{\text{SMOW}}}{(^{18}\text{O}/^{16}\text{O})_{\text{SMOW}}} \quad (3.5)$$

Figure 3.1: Deuterium isotope relative scale.



The IAEA also distributes a SLAP standard for oxygen, corresponding to $-55.5^{00}/_0$ on the SMOW scale. A different standard is used to express the isotope composition of oxygen in carbonates, and is discussed in the carbonate section (3.1.3) that follows.

3.1.3 Carbon

As shown in Table 3.1, the element carbon contains six protons and has two stable isotopes. The internationally accepted standard for carbon is called the Pee Dee Belemnite (PDB). The PDB standard ($0^{00}/_0$ PDB), corresponds to the $^{13}\text{C}/^{12}\text{C}$ ratio of carbon dioxide (CO_2) gas prepared from fossil Belemnites collected from the Cretaceous Pee Dee Formation in South Carolina, USA. Deviation from the PDB standard is calculated in the same manner as deviation from SMOW for hydrogen and oxygen isotopes:

$$\delta^{13}\text{C}^{00}/_0 \text{ PDB} = 10^3 \times \frac{(^{13}\text{C}/^{12}\text{C})_{\text{SAMP}} - (^{13}\text{C}/^{12}\text{C})_{\text{PDB}}}{(^{13}\text{C}/^{12}\text{C})_{\text{PDB}}} . \quad (3.6)$$

A PDB standard also exists for the oxygen isotopes of carbon compounds wherein the $^{18}\text{O}/^{16}\text{O}$ of the CO_2 gas liberated is assigned the value $0^{00}/_0$ PDB. The relationship between the PDB and SMOW oxygen standards is:

$$\delta^{18}\text{O}^{00}/_0 \text{ SMOW} = 1.03037 \times \delta^{18}\text{O}^{00}/_0 \text{ PDB} + 30.86^{00}/_0 . \quad (3.7)$$

All of the original PDB standard sample has been consumed for analysis. Several other carbon standards,

initially calibrated against the PDB standard before it was exhausted, are in use today for reference and calibration. They include the National Bureau of Standards (NBS)-16 and -17 carbon dioxide gas ($-41.48^{00}/_{0}$ PDB and $-4.41^{00}/_{0}$ PDB, respectively), NBS-20 Solenhofen Limestone ($-1.06^{00}/_{0}$ PDB), and the NBS-21 Graphite ($-28.10^{00}/_{0}$ PDB) (Hoefs, 1987).

3.2 ISOTOPE FRACTIONATION PROCESSES

The partitioning of isotopes between two substances or phases is known as isotope fractionation. For environmental isotopes, isotope exchange is the primary process of concern. Variation in temperature (a function of latitude and elevation) and degree of "rain-out" (distance from vapor source) are the primary controlling factors affecting exchange. Other processes include kinetic effects, diffusion, filtration, chemical composition and crystal structure (Hoefs, 1987).

3.2.1 Isotope Exchange

Isotope exchange reactions are similar to general chemical equilibrium and can be represented by the formula:



with the equilibrium constant, K, for the reaction being:

$$K = \frac{(A_2/A_1)^a}{(B_2/B_1)^b} . \quad (3.9)$$

Introducing the concept of the partition function, Q , demonstrates the reliance of fractionation upon temperature (Hoefs, 1987). The calculation to determine Q for any chemical species is:

$$Q = \sum_i (g_i e^{-E_i/kT}) , \quad (3.10)$$

and the equilibrium constant becomes:

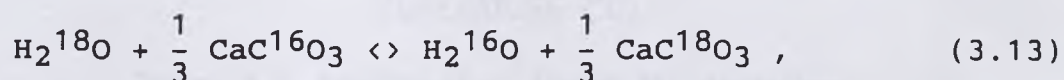
$$K = \frac{(Q_{A2}/Q_{A1})^a}{(Q_{B2}/Q_{B1})^b} . \quad (3.11)$$

Derivation of the Q calculation is beyond the scope and focus of this thesis, but the important factor to note is the strong dependence upon temperature, T , due to its position in the exponential function.

Of more interest than the equilibrium constant is the closely related isotope fractionation factor, α . It is defined as the ratio of the isotopic ratio (R_x) in two compounds or phases (A & B):

$$\alpha_{(A,B)} = \frac{R_A}{R_B} , \quad (3.12)$$

where $\alpha = K^{1/n}$, K is the equilibrium constant and n is equal to the number of atoms exchanged (Hoefs, 1987). For example, the fractionation factor for the exchange of ^{18}O and ^{16}O between water and calcium carbonate (CaCO_3) according to the equilibrium equation:



is given by:

$$\alpha = \frac{(^{18}\text{O}/^{16}\text{O})_{\text{CaCO}_3}}{(^{18}\text{O}/^{16}\text{O})_{\text{H}_2\text{O}}} = 1.031 \text{ at } 25^\circ\text{C} . \quad (3.14)$$

Since temperature is a critical factor in the determination of K , it is equally critical for α as displayed graphically in Figure 3.2.

As just demonstrated, a close relationship exists between temperature and isotopic ratios. With lower average ambient temperatures, which occur with higher latitudes and/or higher elevations, water vapor becomes isotopically lighter (more depleted). The relationship between isotope content of precipitation and temperature

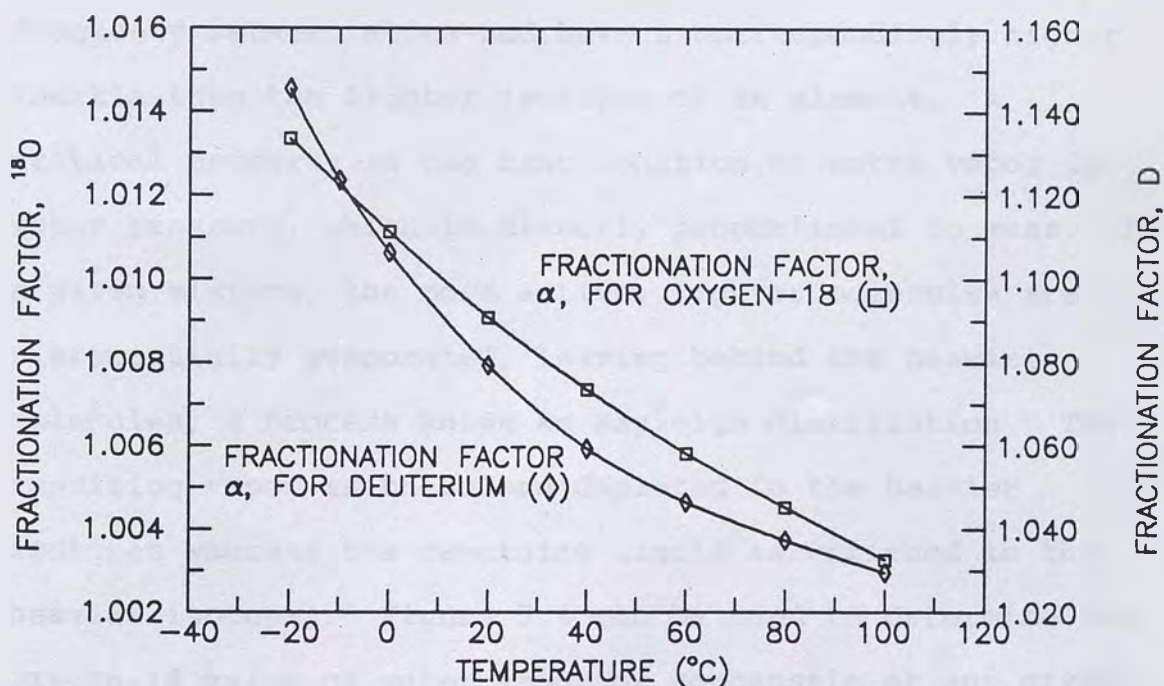


Figure 3.2: Fractionation factor for deuterium and oxygen-18 (Fritz and Fontes, 1980).

was determined by Dansgaard (1964) to be linear and represented by the equation:

$$\delta^{18}\text{O} = 0.695T - 13.6 , \quad (3.15)$$

and subsequently determined by Yurtsever (1975) as:

$$\delta^{18}\text{O} = (0.521 \pm 0.014)T - (14.96 \pm 0.21) . \quad (3.16)$$

However, Gat (1981) demonstrated that, worldwide, the relationship is not linear, but actually is best represented by a series of regional curves converging near $\delta^{18}\text{O} = 0\text{‰}$ and $T = 30^\circ\text{C}$. This temperature relationship is shown graphically in Figure 3.3.

Atomic mass is a crucial factor affecting many of the thermodynamic properties of an element, such as vapor pressure, boiling and freezing point, fractionation, and so forth. Heavier isotopes possess a reduced vibrational frequency between atoms and have a correspondingly higher inertia than the lighter isotopes of an element. A critical property in the fractionation of water vapor is vapor pressure, which is directly proportional to mass. In a given mixture, the more active, lighter molecules are preferentially evaporated, leaving behind the heavier molecules, a process known as Rayleigh distillation. The resulting vapor is therefore depleted in the heavier isotopes whereas the remaining liquid is enriched in the heavier isotopes. Figure 3.4 can be used to determine the Oxygen-18 value of water vapor or condensate at any given temperature.

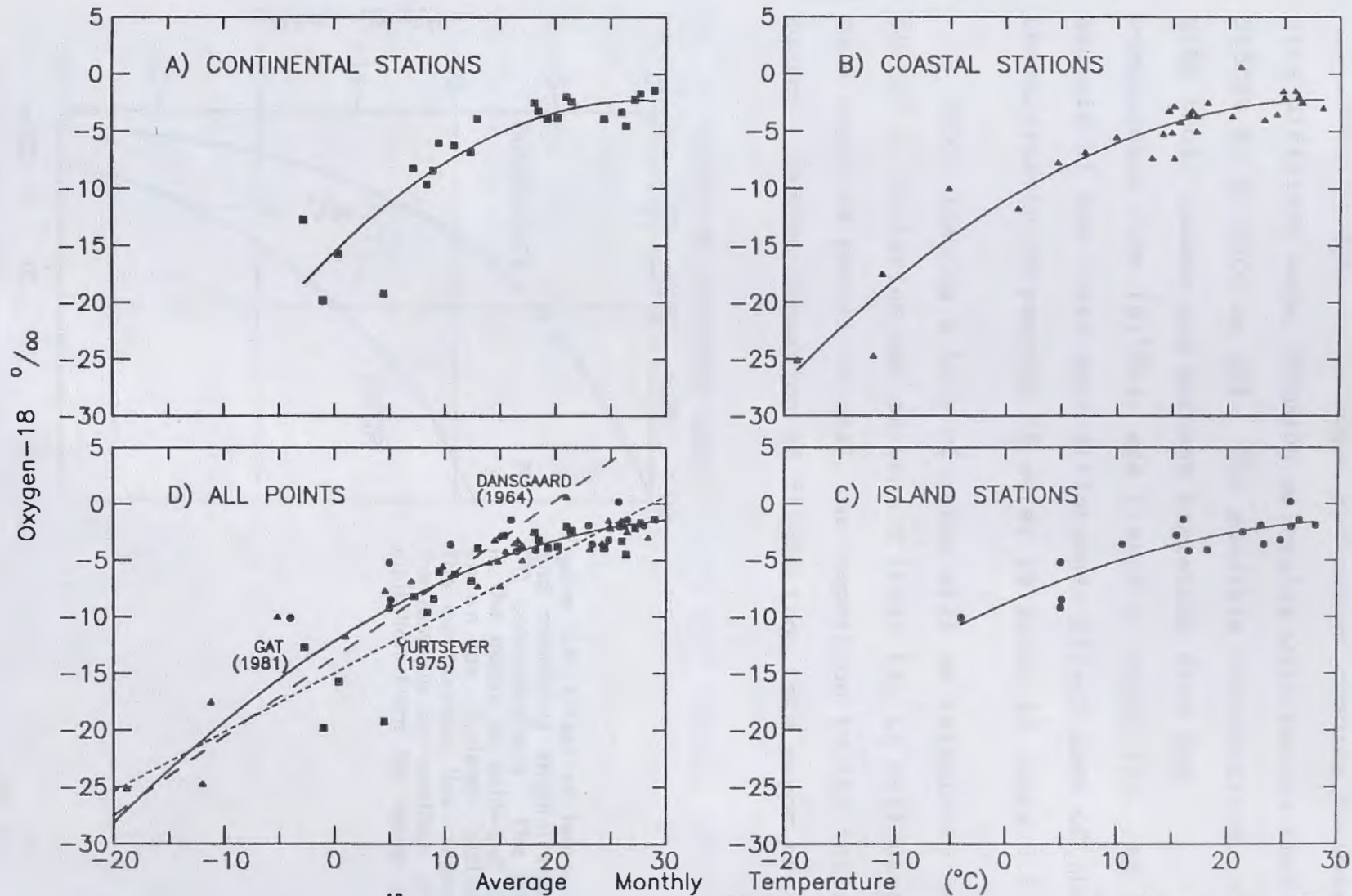


Figure 3.3: Depletion of ^{18}O permil values with decreasing temperature for stations worldwide (Gat, 1981). Dashed lines on D) represent best

fit estimates of Dansgaard and Yurtsever. Solid lines are second degree polynomial best fit lines estimating Gat's converging regional curves.

The isotopes of hydrogen and oxygen combine in water nine different ways, forming molecules with masses that differ by as much as 20%. The possible combinations, along with their masses and percent variation from the predominant form (H_2^{16}O), are listed in Table 3.2. An example of how these mass differences affect some of the thermodynamic properties of water is shown in Table 3.3.

Vapor leaving a body of water will be relatively depleted in deuterium and oxygen-18 (that is, it will display more negative permil values), in comparison to the initial source. During formation of clouds from this vapor the

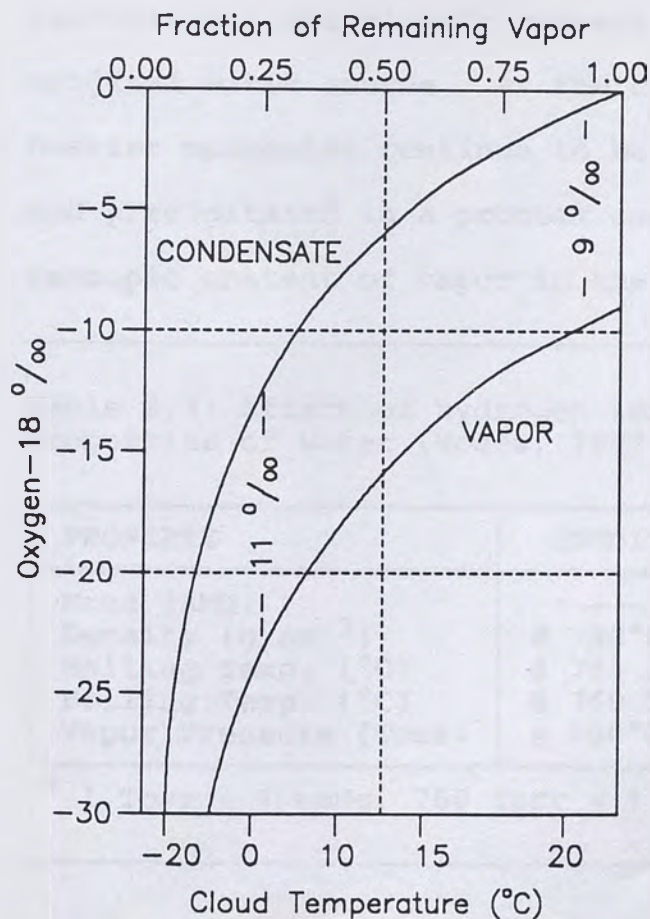


Figure 3.4: Effect of temperature and remaining original vapor on ^{18}O concentrations. The process is the cause of rain-out and is known as Rayleigh distillation. The condensate line represents the isotopic composition of precipitation from the water vapor.

Table 3.2: Combinations of hydrogen and oxygen isotopes in water, the molecular atomic masses, and the percent variation as compared to H_2^{16}O .

FORM	AMU	%	FORM	AMU	%	FORM	AMU	%
H_2^{16}O	18	--	HD^{16}O	19	06	D_2^{16}O	20	11
H_2^{17}O	19	06	HD^{17}O	20	11	D_2^{17}O	21	17
H_2^{18}O	20	11	HD^{18}O	21	17	D_2^{18}O	22	22

heaviest water molecules evaporated will be more likely to condense, and the raindrops formed are relatively enriched isotopically and closely resemble the composition of the original water source. As the cloud moves inland, the heavier molecules continue to be preferentially condensed and precipitated in a process called "rain-out". The isotopic content of vapor in the cloud and subsequent

Table 3.3: Affect of hydrogen isotopes on the thermodynamic properties of water (Hoefs, 1987).

PROPERTY	CONDITION	H_2^{16}O	D_2^{16}O
Mass (AMU)	---	18.0	20.0
Density (g cm^{-3})	@ 20°C	0.9979	1.1051
Melting Temp. ($^\circ\text{C}$)	@ 760 Torr*	0.00	3.81
Boiling Temp. ($^\circ\text{C}$)	@ 760 Torr	100.00	101.42
Vapor Pressure (Torr)	@ 100°C	760.00	721.60

* 1 Torr = 1 mmHg, 760 Torr = 1 Atmosphere

precipitation from the cloud become continually more depleted in the heavy isotopes (Figure 3.5).

Fractionation within each droplet of precipitation continues to take place after each droplet falls from the cloud. Isotopic exchange now occurs between the droplet and water vapor in the surrounding air. As in the initial evaporation process, the lighter molecules are preferentially evaporated, causing the raindrops to become more isotopically enriched in the heavier isotopes. Length of fall is therefore important in determining the final isotopic ratios within the precipitation. Precipitation that reaches lower elevations undergoes a longer fall and

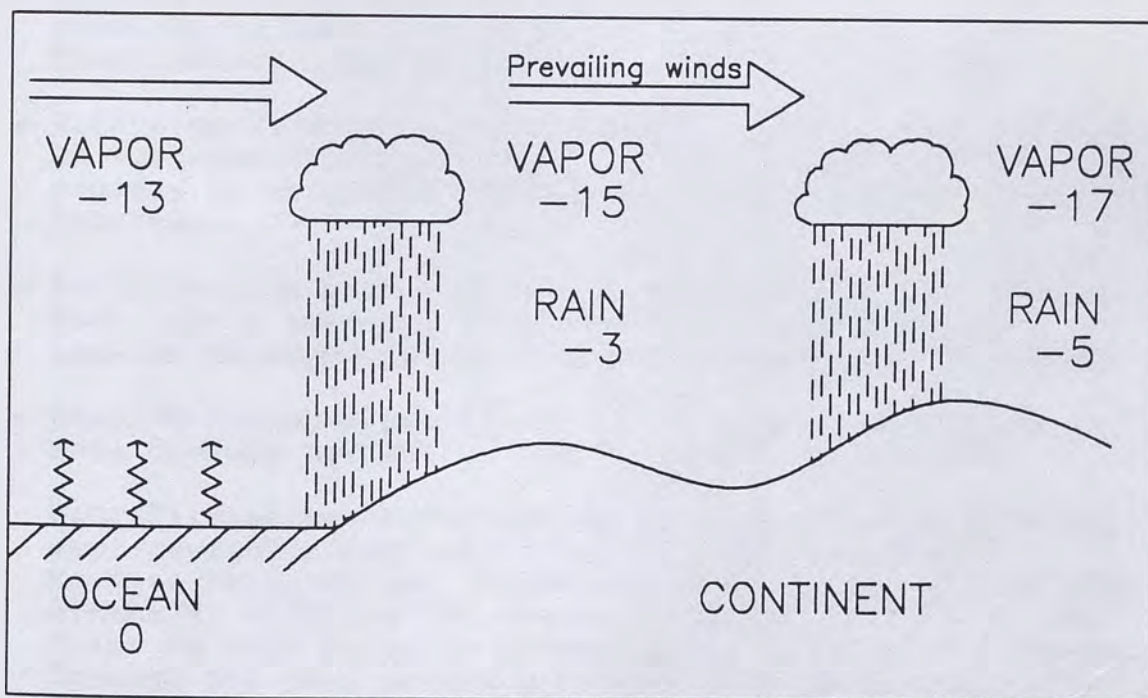


Figure 3.5: Diagrammatic example of storm rain-out. As a cloud moves inland, the vapor becomes progressively more depleted in the heavier isotopes (deuterium and oxygen-18) as they are preferentially condensed and removed.

a longer period of exchange, and becomes more enriched in deuterium and oxygen-18 than precipitation which falls at higher elevations. The duration of each rainfall event is also an important variable affecting depletion. The atmosphere will eventually approach isotopic equilibrium with the precipitation, slowing or halting the fractionation process. Initial precipitation from a storm is therefore more enriched than subsequent rainfall from the same storm.

3.2.2 Other Fractionation Processes

Several other processes can effect isotope fractionation, but none to the extent of exchange. Hoefs (1987) summarized these processes:

- Kinetic isotope effects occur when the rate of chemical reaction is mass sensitive at a particular position. These effects can give clues to reaction pathways.
- Diffusion is primarily of importance for oxygen isotopes in rock-water interaction at elevated temperatures. The process is extremely complex and varies between different minerals.
- Bonds to ions with high ionic potential and low atomic mass have a tendency to preferentially incorporate heavier isotopes making chemical composition important.
- Heavier isotopes are likely to be more concentrated in more closely packed or ordered crystal structures.
- Ultrafiltration occurs during passage of water through semi-permeable membranes such as clays and shales. Heavier isotopes are preferentially adsorbed at the clay minerals, shifting the residual waters retained by the clays to more positive permil values. Water that passes through the clay membrane is then isotopically depleted (Coplen and Hanshaw, 1973). Laboratory experiments showed a deuterium depletion of 2.5⁰⁰/0 and an oxygen-18 depletion of 0.8⁰⁰/0 by this process.

3.3 UNSTABLE LIGHT ISOTOPES AND AGE DATING

Most isotopes are unstable and decay spontaneously in a fission reaction, at a constant rate, to produce energy and a daughter element. The standard exponential decay reaction for this process is:

$$N = N_0 e^{-\epsilon t} \quad \begin{array}{ll} N = \text{current amount} & t = \text{time} \\ N_0 = \text{initial amount} & \\ \epsilon = \text{decay constant} & e = \ln^{-1} \end{array} \quad (3.17)$$

Decay constants are virtually unaffected by temperature and pressure (Aswathanarayana, 1985). A common reference point for a radioactive substance is its "half-life" ($T_{1/2}$), which is the amount of time required for one-half of the mass of the substance to decay. By rearranging reaction 3.17 to:

$$t = - \frac{\ln (N/N_0)}{\epsilon} , \quad (3.18)$$

and setting the ratio N/N_0 equal to one-half, the half-life of an unstable isotope can be calculated from:

$$T_{1/2} = 0.693/\epsilon . \quad (3.19)$$

The two unstable isotopes included in this study, tritium and ^{14}C , both decay by emission of a high-energy, negatively charged beta particle (β^-) from the nucleus of the atom. In this process a neutron disintegrates to a proton and a β^- , raising the atomic number by one which produces a different element. β^- particles are similar to electrons in mass and charge, differing only in the mode of formation.

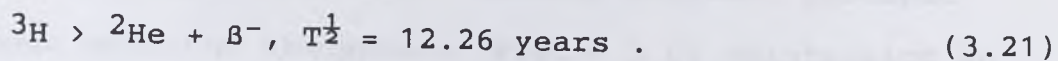
3.3.1 Tritium

Tritium (^3H), the unstable isotope of hydrogen, is naturally produced in the upper atmosphere by cosmic ray neutron (n) bombardment of nitrogen-14 according to the reaction:



The natural production rate for tritium is estimated to be approximately 0.5 ± 0.3 atoms $^3\text{H}/\text{cm}^2/\text{sec}$ (Faure, 1986). Tritium concentrations are measured in tritium units (TU). One TU equals one tritium atom per 10^{18} atoms of hydrogen, and is equivalent to a tritium activity (A) of 7.1 disintegrations of tritium per minute per liter of water (dpm/l) (Faure, 1986). A disintegration is the spontaneous decay of one atom. Natural background concentrations of tritium are normally less than 25 TU (Fritz and Fontes), but may vary greatly locally with latitude, altitude, and season. The advent of above-ground nuclear weapons testing in the mid 1950's flooded the atmosphere with man-made tritium, increasing the background levels by two to three orders of magnitude. With the cessation of above-ground testing in 1963, atmospheric tritium levels have almost returned to pre-testing background levels (Faure, 1986). Minor amounts of man-made tritium continue to enter the atmosphere from the nuclear and defense industries.

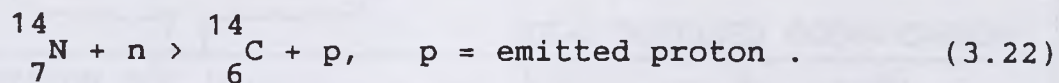
Tritium, with a half life of 12.26 years, decays to helium by emission of a β^- particle by the equation:



After isolation from the atmosphere, the decay of tritium occurs at a constant rate according to the standard exponential decay equation (3.17). The short half-life of tritium limits its usefulness as an indicator of groundwater age to less than 50 years (Campana, 1981). It is nearly impossible to obtain meaningful quantitative dates from tritium samples due to the extreme difficulty of quantifying the initial activity (A_0) of the sample. Most researchers have found it useful to qualitatively associate high tritium activity of groundwater with precipitation that fell in the late 1950's and early 1960's.

3.3.2 Carbon

Carbon has one radioactive isotope, ${}^{14}\text{C}$, which is also produced in the upper atmosphere by cosmic ray neutron (n) bombardment of nitrogen (${}^{14}\text{N}$). The reaction replaces a proton in the nitrogen nucleus with a neutron:



The ${}^{14}\text{C}$ is rapidly oxidized to ${}^{14}\text{CO}_2$ and mixes with the atmospheric CO_2 reservoir, becoming available for incorporation into the hydrosphere and biosphere.

Certain types of material exposed to the atmosphere (living matter, water, etc.) undergo constant isotopic exchange with the atmosphere (Figure 3.6) maintaining an equilibrium ^{14}C activity of $A_0 = 13.56$ disintegrations per minute per gram (dpm/g). This standard activity is 95% of the activity of NBS-4990 oxalic acid in 1950 (Fritz and Fontes, 1980). Activity of ^{14}C is frequently reported as percent modern carbon (PMC), and is calculated by:

$$A_{\text{PMC}} = \frac{(^{14}\text{C}/^{12}\text{C})_{\text{SAMP}}}{(^{14}\text{C}/^{12}\text{C})_{\text{STAND}}} \times 100, \text{ STAND} = 13.56 \text{ dpm/g} \quad (3.23)$$

A sample with a PMC of 100 is equivalent to 13.56 dpm/g.

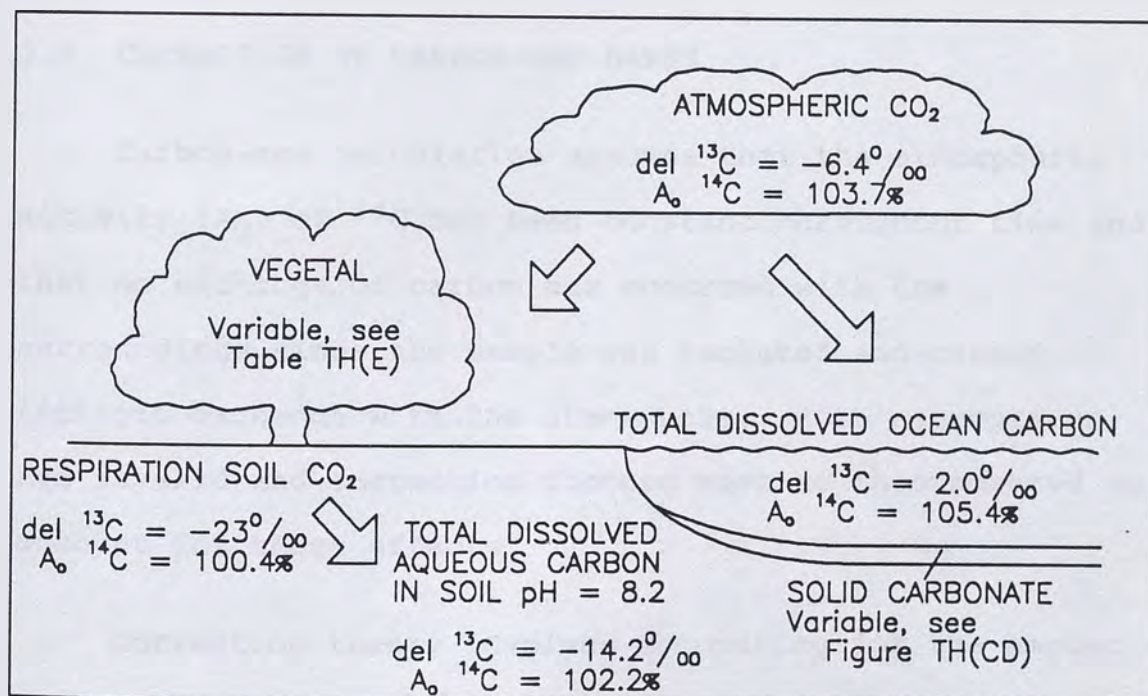
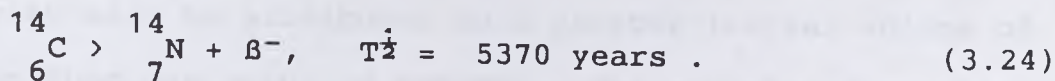


Figure 3.6: The carbon cycle, and the concentration of carbon expected in various materials that may contribute 'dead' carbon to groundwater.

When water is isolated from the atmosphere, or when organisms die, isotopic exchange ceases and the ^{14}C activity (A) decreases as the unstable ^{14}C decays. The decay process is a beta decay and the reaction is:



The "uncorrected" age of the sample is obtained by rearranging the standard exponential decay equation (3.17) to give:

$$t = \frac{-T_{1/2}}{\ln 2} \ln \frac{A}{A_0} \quad \begin{array}{l} A = \text{measured sample activity} \\ t = \text{age} \quad T_{1/2} = 5730\text{y} \\ A_0 \approx 13.56\text{dpm/g} . \end{array} \quad (3.25)$$

All carbon-age dates are calculated as radiocarbon, not calendar, years prior to a reference date of 1950.

3.4 CORRECTION OF CARBON-AGE DATES

Carbon-age calculation assumes that the atmospheric activity (A_0) of ^{14}C has been constant throughout time and that no exchange of carbon has occurred with the surroundings since the sample was isolated and ceased isotopic exchange with the atmosphere. Both assumptions are invalid and correction factors must be incorporated to account for these effects.

Correction theory involves accounting for the amount of "dead" carbon introduced after exchange with the atmosphere has ceased. Activity of ^{14}C is measured as the

number of disintegrations per minute that occur per gram of total carbon present. If additional carbon introduced to the sample after isolation provided no initial ^{14}C activity (in other words, "dead" carbon was added) the measured ^{14}C activity will be attributed to a greater initial volume of carbon than was actually present. The calculated age is then older than the actual age. Referring again to Figure 3.6, the ^{13}C content of several types of material likely to contribute "dead" carbon to groundwater during circulation is demonstrated. During interaction with these materials, the ^{13}C content of the water will be drawn toward the values listed.

3.4.1 Atmospheric Correction

Seuss (1955) showed that A_0 of ^{14}C from twentieth century wood was 2% lower than that of nineteenth century wood (the Suess effect), due to the combustion of fossil fuels and the corresponding introduction of "dead" carbon to the atmosphere (Figure 3.7). Subsequently, DeVries (1958) showed that A_0 of ^{14}C from 1500 to 1700 AD was 2% greater than in the nineteenth century (the DeVries effect). The reason for this change is unclear. More recent studies indicate that A_0 regularly fluctuates through time, within limits of $\pm 5\%$ (Fritz and Fontes, 1980). A comparison of tree ring ^{14}C dates with their dendrochronological age (Michael and Ralph, 1970) has

provided correction tables valid to 8,000 years Before Present (BP). Correction tables for older dates were developed from seasonal glacial lake varves (Stuiver, 1970). Above ground nuclear weapons testing in the late 1950s introduced large quantities of ^{14}C into the atmosphere resulting in a marked increase in the atmospheric A_0 of ^{14}C .

3.4.2 Soil and Rock Correction

The science of correcting carbon-age dates for interaction of the water with soil (organic input), rock (dissolution) and clay (cation exchange) is, unfortunately, not as advanced as the atmospheric corrections. To make an

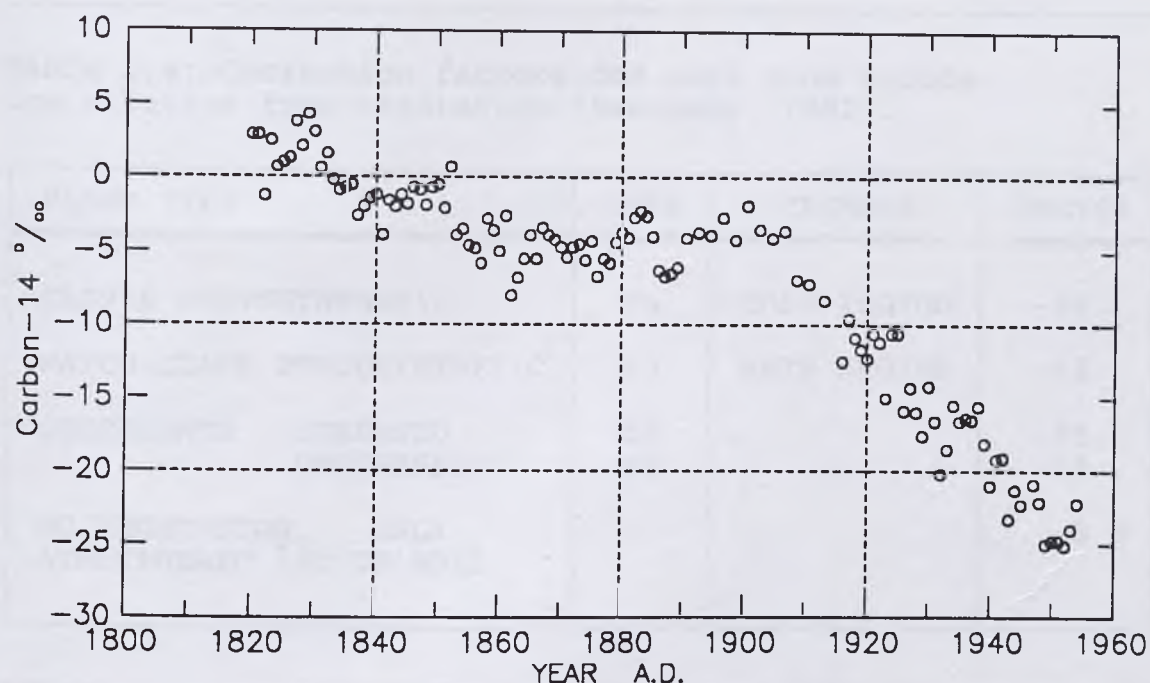


Figure 3.7: The Suess effect. Depletion of atmospheric Carbon-14 values that has occurred over the past 150 years (Stuiver, 1981) due to the combustion of fossil fuels and the resulting introduction of 'dead' carbon into the atmosphere.

accurate correction, the conditions present at the time of recharge and the flow path the water has followed must be determined. This is a worthy but currently unrealistic goal.

Carbon incorporated in the soil zone is derived primarily from root respiration, and the correction factor depends upon the vegetation type (Table 3.4). The factors listed have been determined through field measurement of soil gas carbon content.

The unquantifiable unknown in this correction is the soil condition at the time of fluid recharge, several thousand to tens of thousands of years BP. Many authors have

Table 3.4: Correction factors for soil zone carbon contribution from vegetation (Szecsody, 1982).

PLANT TYPE	TYPE	CLIMATE	FACTOR
CALVIN PHOTOSYNTHETIC	C4	COLD REGION	-25
HATCH-SLACK PHOTOSYNTHETIC	C3	ARID REGION	-12
SUCCULENTS STRESSED	C4		-25
UNSTRESSED	C3		-12
NO VEGETATION, ONLY ATMOSPHERIC ^{13}C IN SOIL			-6.4

used present day soil conditions as a proxy for paleoconditions (Szecsody 1982, Glancy 1986), but this approach is flawed due to the rapid rate of Pleistocene and Holocene climate fluctuations. Use of paleoclimate indicators to suggest conditions at the time of recharge may seem to be more reliable, but is also flawed. The correction factors may result in adjustments of thousands of years, possibly invalidating the paleo condition assumption that was made as a basis for the initial correction. This type of circular reasoning does not provide a reliable correction.

Making a proper correction for rock-water interaction is equally challenging. Precisely determining the flow path of the fluids, the rock types encountered, and the physio-chemical conditions present at the time of encounter is impossible. However, estimates can be made based upon the rock types and temperatures likely to be encountered, and the geochemical ratios present. Isotopic exchange with limestone, for example, is the most likely source of "dead carbon" input. The correction factor depends on whether the limestone is a freshwater ($-4.93 \pm 2.75^{00}/_{0}$ PDB) or salt-water ($+0.56 \pm 1.55^{00}/_{0}$ PDB) carbonate (Faure, 1986). Figure 3.8 shows the range of ^{13}C values for various rock types.

Corrected ^{14}C activity for soil (sl) and rock (rk) can be calculated by:

$$^{14}\text{A}_{\text{corr}} = ^{14}\text{A}_{\text{measured}}/P, \text{ where } P = \text{sl}/(\text{sl}+\text{rk}), \quad (3.26)$$

and:

$$\delta\text{C}_{\text{samp}} = \frac{\text{sl}}{\text{sl}+\text{rk}} \delta\text{C}_{\text{sl}} + \frac{\text{rk}}{\text{sl}+\text{rk}} \delta\text{C}_{\text{rk}}, \quad (3.27)$$

which rearranges to:

$$P = \frac{\delta\text{C}_{\text{samp}} - \delta\text{C}_{\text{rk}}}{\delta\text{C}_{\text{sl}} - \delta\text{C}_{\text{rk}}}. \quad (3.28)$$

$\delta^{13}\text{C}/^{12}\text{C}$ permil values are then inserted to calculate the correction factor, P.

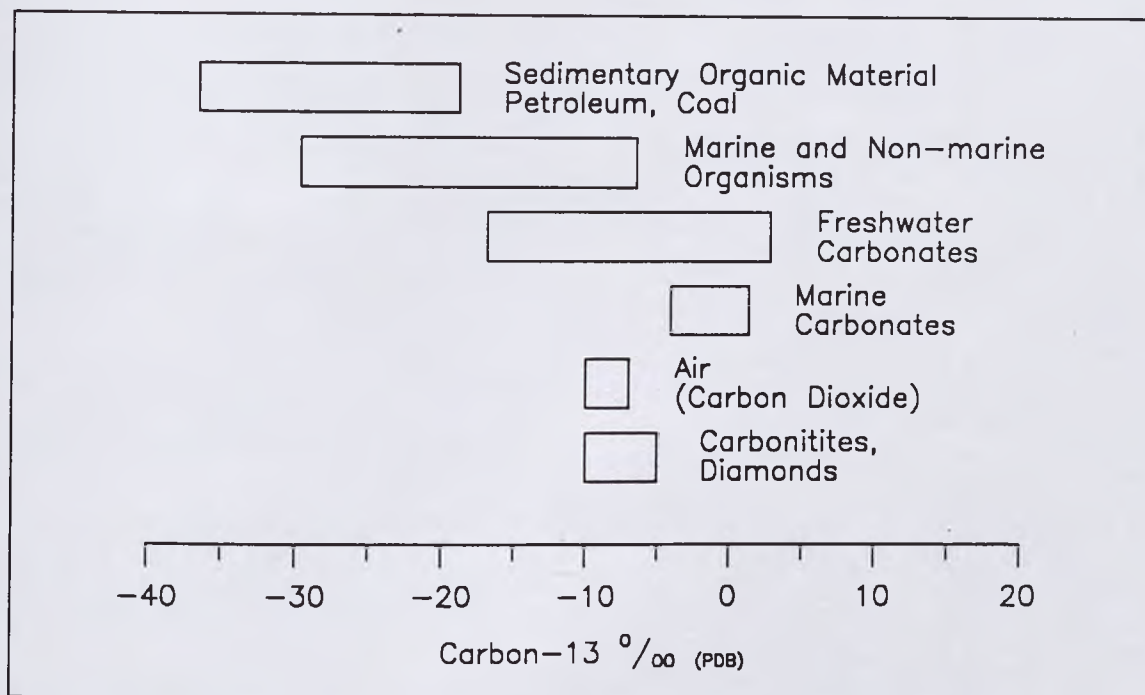


Figure 3.8: Carbon-13 content of various materials that may interact with groundwater and introduce 'dead' carbon during circulation.

Cation exchange with clays relates to the ultrafiltration mentioned in section 3.2.2. The heavier isotopes are preferentially adsorbed by the clay minerals, thereby isotopically depleting the water as it passes through. Any clayey soil, rock, or sediment could serve to slightly isotopically deplete groundwater flowing through it.

LIBRARY

CHAPTER 4.

DATA SET COMPILATION

Data collection consisted of a compilation and assessment of existing isotope and geochemical data, and a fluid sampling program designed to fill data voids and incorporate data from deep geothermal wells.

4.1 LITERATURE SEARCH

An initial base of stable light-isotope data from the Great Basin was assembled through an extensive literature search. A Computer search of GEOREF, CHEM ABSTRACTS and POLLUTION ABSTRACTS was initiated and used the following combination of key words: "Nevada" or "Utah" or "Great Basin"; and "stable light-isotopes" or "deuterium" or "oxygen-18" or "tritium"; and "geothermal" or "water". The results of this search were augmented by searching the following publication lists:

- Utah Geological and Mineralogical Survey,
- Nevada Bureau of Mines and Geology,
- California Division of Oil and Gas,
- University of Nevada Las Vegas,
Division of Earth Sciences,
- University of Nevada Desert Research Institute,
- University of Nevada, thesis and dissertation list.

4.1.1 Water Samples

A 1200+ point data base of stable light-isotope and major geochemical water analyses for thermal and non-thermal springs and wells has been created. Unfortunately, some of the data points are of limited use due to a lack of supporting data, such as sample temperature, collection date or precise location. If sample location was not provided in a longitude-latitude format, such information was determined from the largest scale map available for the area. Table 4.1 shows the distribution of the data set by sample and analysis type. A complete listing of the data set is provided in Appendix B.

4.1.2 Carbon Age Date Samples

Numerous carbon-age dates for moderate temperature (<50°C) water from southern Nevada were discovered during the literature search. The majority of these samples are from the Las Vegas Valley, Nevada Test Site, and Amargosa Desert Areas. These dates were considered to be of limited worth due to their low temperature and distance from northern Nevada, where most of the other data critical to the study is concentrated. Very few dates from high temperature (>90°C) sources in northern Nevada were found. All supporting data for carbon age-dates used in this study are listed in Appendix C.

Table 4.1: Distribution of fluid sample data set by sample and analysis type. Number in parentheses indicates the number of these samples taken during this study.

DEUTERIUM AND OXYGEN-18 ANALYSES

SAMPLE TYPE	TOTAL	TEMP >20°C	TEMP ≤20°C	NO TEMP LISTED
SPRINGS	739(19)	450(19)	259	30
WELLS	399(21)	261(21)	100	30
SURFACE river or stream	77	--	--	--
LAKE	6	--	--	--
UNDETERMINED spring or stream	30	--	--	--
CARBON AGE DATE	154(9)	--	--	--
PACKRAT MIDDENS	44(25)	--	--	--

TRITIUM ANALYSES

SPRINGS	(7)	(7)	--	--
WELLS	(9)	(9)	--	--

GEOCHEMICAL ANALYSES

SPRINGS	703(19)	544(19)	136	23
WELLS	464(18)	364(18)	88	12
UNDETERMINED spring or stream	13	--	--	--

4.1.3 Paleoclimatic Data

Four unique sets of paleoclimate indicators were found in the search. They include:

- Greenland Ice Sheet ice core; oxygen-18 analysis of water,
- Sub-polar Indian Ocean deep-sea core; oxygen-18 analysis of plankton,
- southern Great Basin; oxygen-18 analysis of continuously deposited layered calcite,
- northern Great Basin packrat middens; deuterium analysis of extracted microfossils.

Studies involving isotopic analysis of ice cores from Great Basin sources (Sierra Nevada Mountains, Ruby Mountains, etc.) and Great Basin archaeological artifacts that would benefit this study were not found. A list of the assembled paleoclimatic data is provided in Appendix D.

4.2 FIELD SAMPLING PROGRAM

The goals of the fluid sampling program associated with this study were three-fold:

- 1) Voids identified in the established data set were to be filled. Where a void was present, the highest temperature water source available was sampled,
- 2) Duplicate samples were to be taken for time variant analysis. Hot springs with an extensive history of isotopic analysis were chosen for resampling,
- 3) Geothermal power plant production wells were sampled, through the industry-cooperative program, to directly access deep geothermal reservoirs.

Of the fluid sample analyses, 42 were conducted for deuterium and oxygen-18 isotopes, 38 for bulk chemical analysis, 16 for tritium analysis, and 12 for carbon age dating of high temperature sources. Carbonate scale was obtained from geothermal power plant production wells at Dixie Valley (Oxbow Geothermal), Beowawe and Desert Peak (Chevron Resources) for radiocarbon dating. The details of the collection, preparation and analysis of these samples are given in Section 5.4.2. Table 4.2 lists the fluid samples taken during this study and Figure 4.1 shows their locations. A complete listing of the data can be found in Appendix A.

Analysis of packrat middens from northern Nevada was desired to support the one existing midden study that provided hydrogen isotope analyses. Dr. Peter Wigand of the Desert Research Institute in Reno, Nevada, provided dated midden macrofossils which were submitted for isotope analysis. Figure 4.2 provides the location of the packrat midden sample sites. Packrat midden analytical results are listed in Appendix D.

Table 4.2: Fluid sampling program, this study. DT-deuterium, OX-oxygen 18, TR-tritium, CH-chemistry, CA-carbon age, T-°C.

GF-	SAMPLE NAME	TYPE	LONG	LAT	DT	OX	TR	CH	CA	T	DATE
1	Bradys Hot Sp	WL	119.01	39.79	X	X	X	X		141	1 89
2	Great Boiling Sp	SP	119.37	40.66	X	X	X	X		91	1 89
3	Patua Hot Spring	SP	119.11	39.60	X	X	X	X		60	1 89
4	Steamboat/Ormat	WL	119.72	39.40	X	X	X	X		113	1 89
5	Wabuska Tads #2	WL	119.15	39.16	X	X	X	X		107	1 89
6	Warren Estates	WL	119.83	39.48	X	X	X	X		88	1 89
7	Soda Lake #1	WL	118.86	39.56	X	X	X	X		183	1 89
8	Desert Pk 67-21	WL	118.95	39.75	X	X	X	X		163	1 89
9	Desert Pk 86-21	WL	118.95	39.76	X	X		X		163	1 89
10	Beowawe 1-13	WL	116.62	40.55	X	X	X	X		150	1 89
11	Beowawe 2-13	WL	116.62	40.56	X	X		X		150	1 89
12	Lee Hot Springs	SP	118.72	39.21	X	X		X		93	2 89
13	Alkali Hot Sp	SP	117.34	37.83				X	X	52	2 89
14	Hicks HS	SP	116.72	36.81	X	X	X	X		40	2 89
15	Grapevine Spring	SP	117.38	37.02	X	X	X	X		32	2 89
16	Nevares Spring	SP	116.79	36.51	X	X		X		31	2 89
17	Tecopa Hot Sp	SP	116.23	35.87	X	X		X		42	2 89
18	Rogers Spring	SP	114.44	36.38	X	X	X	X		31	2 89
19	Ash Spring	SP	115.20	37.47	X	X		X		30	2 89
20	Warm Spring	SP	116.38	38.19	X	X	X	X		61	2 89
21	Golconda Hot Sp	SP	117.49	40.96	X	X		X		58	2 89
23	Elko Jr High	WL	115.76	40.84	X	X	X	X		82	2 89
24	Elko Heat Co.	WL	115.78	40.83	X	X	X	X		78	2 89
25	Bruffeys Hot Sp	SP	116.07	40.07	X	X		X		62	2 89
26	Williams Hot Sp	SP	115.23	38.95	X	X		X		53	2 89
27	Morman Spring	SP	115.14	38.76	X	X		X		38	2 89
28	Chimney Hot Sp	SP	115.79	38.47	X	X		X		66	2 89
29	Hot Creek Upper	SP	116.36	38.52	X	X		X		82	2 89
30	Darroughs Hot Sp	WL	117.18	38.82	X	X		X		76	2 89
31	Surprise Val hs	SP	119.98	41.17	X	X		X		47	3 89
32	Soda Lake #1	WL	118.86	39.56	X	X		X	X	183	4 89
33	Desert Pk 67-21	WL	118.95	39.75	X	X		X	X	163	4 89
34	Beowawe 1-13	WL	116.62	40.55	X	X		X		150	4 89
34	Beowawe Inj	WL	116.62	40.55					X	100	4 89
35	Wabuska Tads #2	WL	119.15	39.16		X		X		107	5 89
36	Warm Springs	SP	116.38	38.19	X	X		X	X	61	5 89
37	Elko Jr High	WL	115.76	40.84	X	X		X	X	78	5 89
38	Elko Heat Co.	WL	115.78	40.83	X	X		X		81	5 89
39	Golconda Hot Sp	SP	117.49	40.96	X	X		X		63	5 89
40	Beowawe 1-13 Sc	WL	116.62	40.55					X	150	4 89
41	Oxbow 45-5 Scale	WL	117.89	39.97					X	225	88
42	Oxbow 74-7 Scale	WL	117.91	39.96					X	225	88
43	Oxbow 76-7 Scale	WL	117.90	39.95					X	225	88
44	Soda Lake #1	WL	118.86	39.56	X	X				183	9 89
46	Beowawe 2-13	WL	116.62	40.56	X	X			X	150	9 89
47	Steamboat/Ormat	WL	119.72	39.40	X	X				113	9 89
48	Wabuska Tads #2	WL	119.15	39.16	X	X			X	107	9 89
49	Desert Peak Sc	WL	118.95	39.75					X	163	89

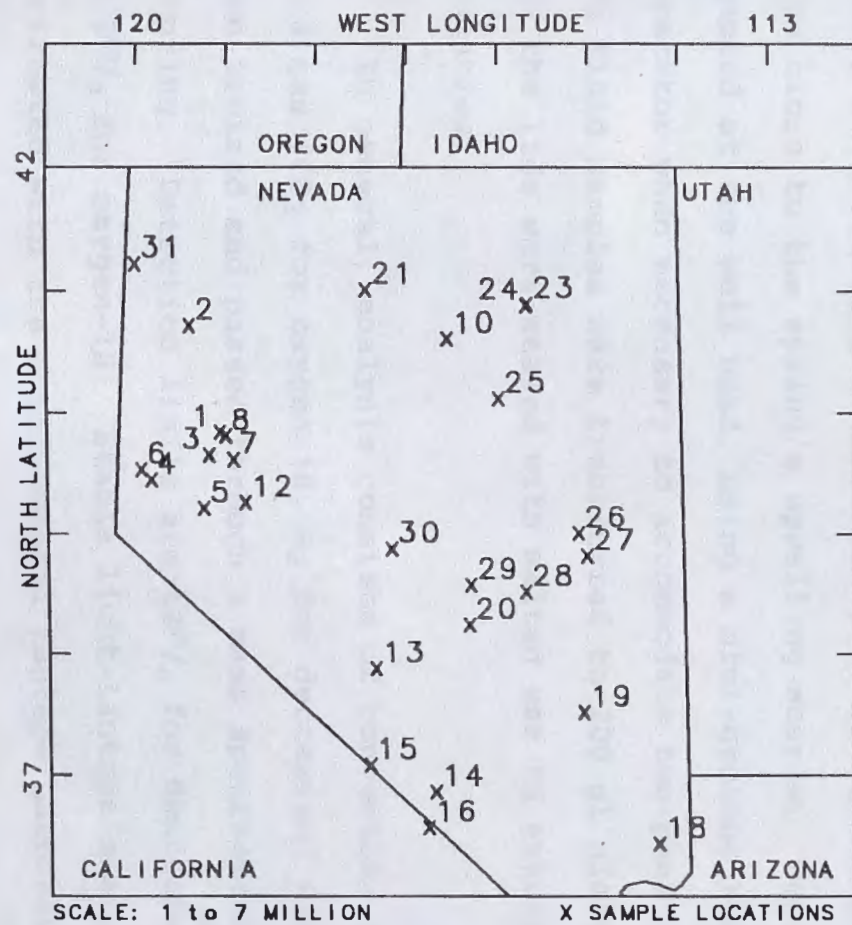


Figure 4.1: Location of fluid samples taken for stable light-isotope analysis during this study. Refer to GF- numbers in Table 4.2 for analyses.

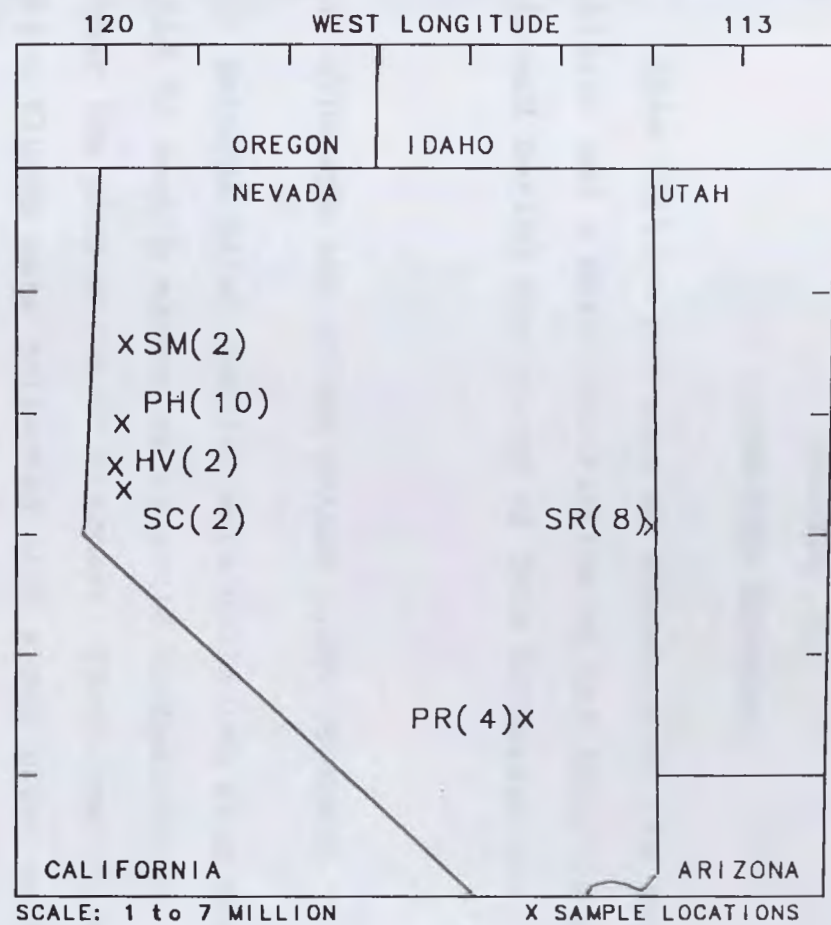


Figure 4.2: Packrat midden sample locations. Number of samples taken at each location shown in parentheses. SR=Snake Range, SC=Silver City, PR=Pahranagat Range, SM=Smoke Creek Desert, HV=Hidden Valley, PH=Painted Hills.

CHAPTER 5.

LABORATORY METHODS

This section provides an inventory of the laboratories utilized and a brief description of the analytic procedures followed during the course of this investigation.

5.1 HYDROGEN AND OXYGEN STABLE LIGHT ISOTOPES

Natural water samples were collected from springs and wells in such a manner as to avoid contamination, from either the atmosphere or stagnant, fractionating water. Spring fluids were collected with a one liter polyethylene bottle attached to a retractable 3 meter sampling device, from close to the spring's upwelling source. Wells were sampled at the well head, using a mini-cyclone steam separator when necessary to accommodate two-phase flow. The fluid samples were transferred to 200 ml glass bottles and the lids were sealed with melted wax to ensure isolation.

In general, analysis consists of converting the sample to a gas (CO_2 for oxygen-18, H_2 for deuterium) which is then ionized and passed through a mass spectrometer for counting. Detection limits are $\pm 2^{00}/_0$ for deuterium and $\pm 0.2^{00}/_0$ for oxygen-18. Stable light-isotope analyses were contracted with the Environmental Isotope Laboratory of the

University of Arizona, Tucson. Oxygen-18 analyses of water samples GF-1 through GF-39 were completed by the University of Arizona, although an equipment calibration problem prevented completion of the contract. Deuterium analysis for samples GF-1 through GF-39 and complete stable light-isotopes analyses for samples GF-40 through GF-48 were performed at the University of Waterloo, Ontario, Canada.

5.2 WATER CHEMISTRY

Water chemistry samples were collected in one liter plastic bottles and submitted to the University of Utah Research Institute (UURI), Salt Lake City, Utah, for analysis. Table 5.1 lists the techniques used for analysis of the elements included in the data set.

5.3 TRITIUM ANALYSIS

Tritium samples were collected from selected springs and deep wells in one liter glass bottles and sealed with Teflon tape. Tritium analysis was performed by the Desert Research Institute Water Resources Center Analytical Laboratory of the University of Nevada System, Reno, Nevada. Samples were distilled by hydrolysis, followed by slow electrolysis at a constant temperature to evaporate

Table 5.1: Water chemistry techniques employed by UURI.

METHOD	ELEMENT(S)
Inductively Coupled Plasma Laboratory Titration Specific Ion Electrode Gravimetric Turbidimetric	Ca, Na, K, SiO ₂ , Mg, Li, B HCO ₃ , Cl F TDS SO ₄

the hydrogen (protium and deuterium) and concentrate the tritium. Counting was then performed with a scintillation counter. The process requires approximately 3 months to complete and has detection limits of 5 TU.

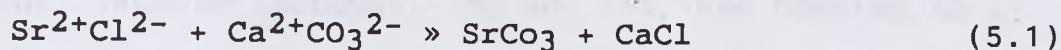
5.4 CARBON ISOTOPES

Carbon isotope analysis was performed by Beta Analytic, Coral Gables, Florida. Approximately 4 grams of carbon are required for each analysis. Two types of material were submitted for carbon isotope analysis: carbonate precipitated from thermal waters, and carbonate scale collected from geothermal production wells. The analysis reported ¹⁴C activity and the ¹³C/¹²C ratio.

5.4.1 Water Samples

Thirty-five gallons of water for each sample were collected from selected hot springs and geothermal power plant production wells deemed to have sufficient carbon for analysis. Wells that use chemicals to inhibit carbonate scale were not sampled.

The water was placed in a stainless steel carbonate precipitator and titrated with 50 to 500 ml sodium hydroxide to raise the pH to approximately 10. One liter of 8 molar strontium chloride solution was then added to produce a strontium carbonate precipitate according to the reaction:



The speed at which the precipitate formed and settled out varied from instantaneous to several days. Some samples produced a gelatinous precipitate which proved, upon analysis, to be devoid of carbon. A more detailed description of the carbonate precipitator and procedure can be found in Szecsody (1982).

5.4.2 Carbonate Scale

Calcium carbonate scale removed from power plant wells was also submitted for analysis. Surface contamination was mechanically removed from the samples prior to submission.

The samples were etched with acid by Beta Analytic in the laboratory to further remove any surface contamination.

5.4.3 Analytical Method

A general description of the analytical method used by Beta Analytic follows. A detailed description of these procedures and equipment can be found in Faure (1986) and Fritz and Fontes (1980).

The water samples are filtered to remove the strontium carbonate, which is allowed to dry. Samples (water and scale) are then acidified to generate CO₂ gas which is purified in a vacuum. The sample is then synthesized to benzene. Stable isotopes, ¹³C and ¹²C, are counted in a mass spectrometer while unstable ¹⁴C is measured by a proportional counter.

5.5 PACKRAT MIDDENS

Packrat middens were collected by Dr. Peter Wigand of the Quaternary Sciences Center, Desert Research Institute, Reno, Nevada. Midden preparation involves several cleaning, soaking and separation processes which isolate the constituent macrofossils (twigs, seeds, dung, etc.).

5.5.1 Hydrogen and Oxygen Isotopes

All of the packrat midden hydrogen and oxygen analyses from this study were completed at the University of Arizona and the University of Miami, Department of Biology. Juniper twigs from 25 middens in western Nevada were obtained from Dr. Wigand and submitted for analysis.

Midden analysis requires liberation of hydrogen and oxygen isotopes from the alpha cellulose structure of plant macrofossils removed from the midden. A more detailed account of the preparation and analysis of cellulose for stable light-isotopes is available in Siegel (1983).

5.5.2 Carbon-Age Determination

The packrat middens had been previously dated by Beta Analytic. Macrofossil fecal pellets (dung) from the same stratigraphic horizon as the twigs provided the carbon for dating. Duplicate dates on pellets have yielded ages agreeing within 2%, well within 1 σ range of each date.

CHAPTER 6.

PLEISTOCENE PALEOCLIMATE DATA

6.1 GLOBAL ISOTOPIC DEPLETION RECORDS

Recharge models that assume geothermal fluid recharge is a recent event requiring meteoric waters from a high elevation fail to consider the significant changes in the isotopic composition of precipitation over the last 40,000 years. It has been known for over twenty years that the isotopic composition of precipitation varies as a function of climate, and that climate varies as a function of time. The magnitude and global extent of those variations are the subject of the following sections.

6.1.1 Greenland, Arctic Evidence

Initial evidence for temporal variations in isotopic composition was presented by Dansgaard et al. (1969). Using ice from a core-hole at Camp Century that penetrated the entire thickness of the Greenland Ice Sheet (1390 m), they were able to reconstruct the isotopic variation in precipitation for the last 15,000 years. Stratigraphic age was determined by counting back through the annual layers in the ice. In addition to the anticipated variations by season, they discovered that modern precipitation is sig-

nificantly enriched in oxygen-18 when compared to ancient precipitation. More specifically, the transition from ancient, isotopically depleted fluids to modern, enriched fluids took place over a 2,000 year period of time between 11,000 and 9,000 years BP. This timing corresponds to the termination of the last major continental glaciation, and is in general agreement with reported climate change timing in other parts of the world. Following the work at Camp Century, additional core holes were completed throughout Greenland. The deepest is Dye 3 in south Greenland, drilled to bedrock at a depth of 2037 m. Oxygen-18 values from Camp Century and Dye 3 (Dansgaard et al, 1985) show a remarkable correlation for the timing of enrichment and depletion events for the last 90,000 years.

6.1.2 Sub-Polar Indian Ocean, Antarctic Evidence

Martinson et al. (1987) developed a "high-resolution" chronostratigraphy based on the oxygen isotope ratio of tests from benthic foraminifera (forams) obtained from drill hole RC11-120, in the southwestern sub-polar Indian Ocean. The procedure utilized the "standard" deep-sea sediment stratigraphy of Pisias et al. (1984), five climatically sensitive data sets, and four separate orbital tuning methods to establish the chronology. According to orbital tuning theory, originally proposed by Milankovitch

(1941), climatic changes, including glaciation, result from solar radiation fluctuations determined by variations of the Earth's orbital elements and axial inclination. Figure 6.1 demonstrates the close correlation in the timing of isotopic variation on opposite ends of the globe, from the Dansgaard and Martinson studies. The curves are presented on a normalized scale to facilitate comparison of the different data types, ice and foraminifera, respectively.

6.1.3 Devils Hole, Amargosa Desert, Great Basin

Devils Hole is a 1 to 5 m wide, open fault zone in the modern spring lineament at Ash Meadows, Amargosa Desert, Nevada. The Hole extends more than 100 m below the water table, which is about 15 m below ground surface. Winograd et al. (1988) analyzed a layered calcite (CaCO_3) vein found approximately 21 m below water table. The absence of dissolved Thorium (<0.01 ppb) in the groundwater allowed dating of the layers in the calcite vein by the $^{230}\text{Th}/^{234}\text{U}$ method. Oxygen isotope analysis of the dated vein layers allowed plotting of a paleoclimate curve similar to that of Martinson et al. (1987). A comparison of these curves is shown in Figure 6.2. The phase difference in the Winograd curve with respect to the Martinson curve ranges from about 17,000 years at point A (fig. 6.2), increasing linearly to 25,000 years at point H. Winograd et al. (1988) attribute

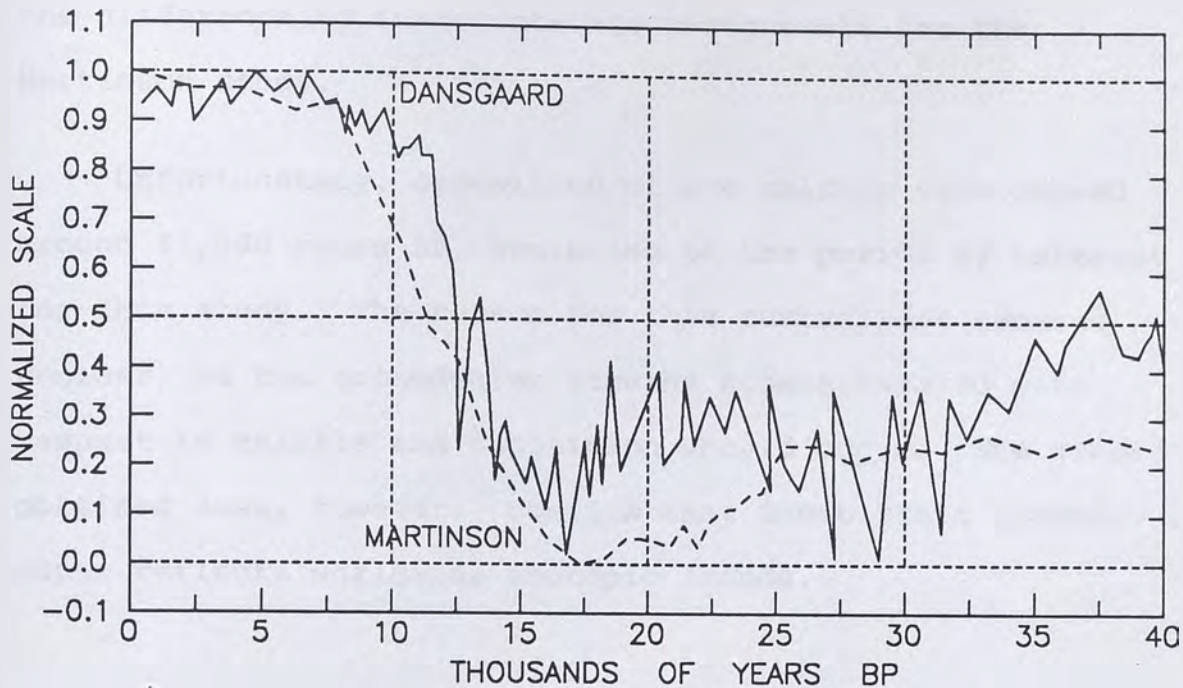


Figure 6.1: Planktonic ^{18}O vs. stratigraphic age from sub-polar Indian Ocean deep sea cores (Martinson et al., 1987), compared to ice ^{18}O vs. ice calculated age from Greenland ice cores (Dansgaard et al. 1969). Timing of changes in isotopic content is in good agreement.

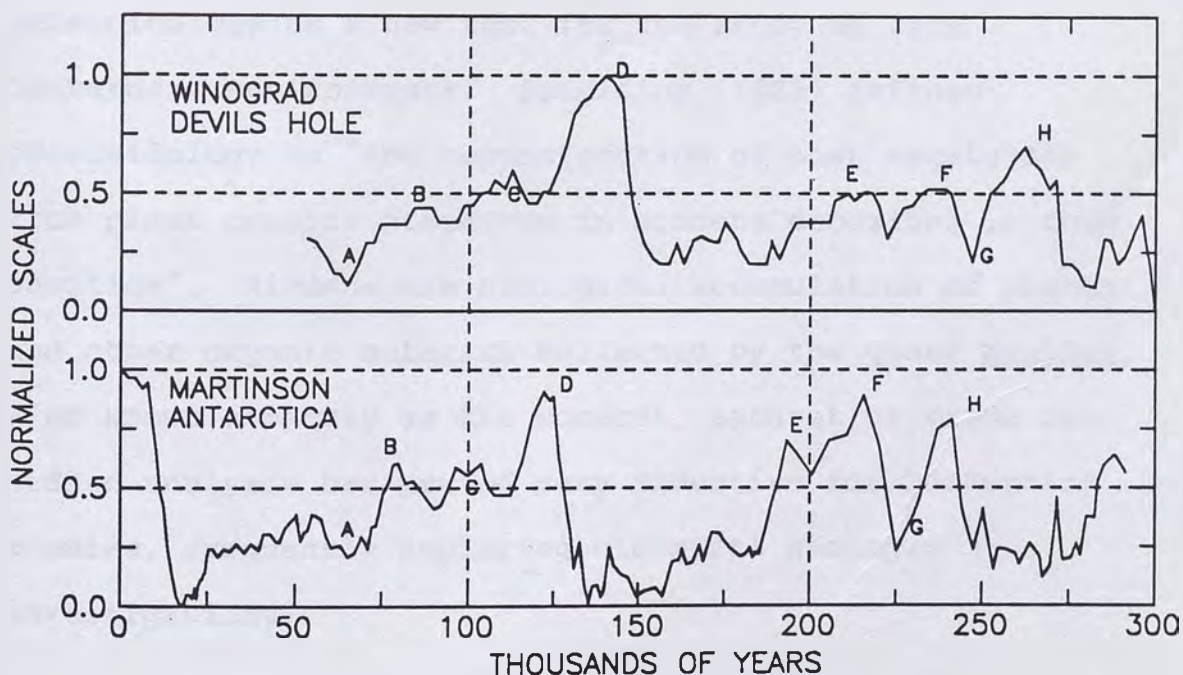


Figure 6.2: Comparison of Martinson et al. (1987) data with ^{18}O of groundwater recorded in calcite at Devils Hole, Amargosa Desert, Great Basin (Winograd et al., 1988). Letters on the curves represent major peaks and troughs thought by Winograd to be correlative.

the difference to inaccurate age assignments for the Martinson study.

Unfortunately, deposition of the calcite vein ceased around 51,000 years BP, beginning of the period of interest for this study. The reason for this curtailment remains unclear, as the groundwater remains supersaturated with respect to calcite and deposition should occur. The record obtained does, however, confirm that Great Basin groundwater reflects worldwide isotopic trends.

6.2 PACKRAT MIDDENS

Wells and Jorgenson (1964) introduced the science of paleonidology as a new tool for the study of late Quaternary environments. Spaulding (1985) defined paleonidology as "the reconstruction of past vegetation from plant remains preserved in middens deposited in rock cavities". Middens are biological accumulation of plants and other organic material collected by the genus Neotoma, also known commonly as the woodrat, packrat or trade-rat. Midden analysis has proved very effective for Quaternary studies, frequently replacing classical geologic investigations.

6.2.1 Initial Midden Studies

Spaulding (1985) also provided a description of midden composition, construction, preservation and morphology. The following is paraphrased from his description.

Currently active middens are loose debris piles, while ancient middens are masses solidified by dehydrated urine. Middens often serve as urination points, and cementation is caused by saturation with urine which, upon drying, encases the refuse in a cohesive, crystalline mass. Indurated packrat middens are self sealing, with typically convoluted rinds that vary in thickness from a few millimeters to several centimeters. Middens must be sheltered from rain in a cave or beneath a rock overhang to be preserved. Some middens are more than 50,000 years old and are among the oldest fossils preserved by mummification.

All Neotoma species share the acquisitive behavior trait and build houses and dens from collected plant debris from within a limited foraging radius, estimated to be approximately 30 m. In addition to plant debris, middens contain fecal pellets, pollen, and skeletal remains. All are tightly cemented by dried and crystallize urine, which is sometimes known colloquially as amberat. The variety of fossil preserved material, the focused location and elevation, and the continuity (some middens provide continuous documentation over a period of 50,000 years), have allowed

workers to reconstruct paleoenvironments and paleoclimates throughout the American west.

Wells and Jorgenson (1964) working at the Nevada Test Site in southern Nevada, identified Utah juniper, pinyon, and curl-leaf mahogany in areas where these high-elevation species no longer flourish. This led them to speculate that, between 40,000 and 7,800 years BP, the climate was colder and perhaps more moist than present conditions. Subsequently, Thompson and Mead (1981) confirmed the existence of a widespread subalpine forest in the southern Great Basin between 25,000 and 11,000 years ago. Midden analysis indicated that the forest habitats were isolated islands subject to cool summer climates. They suggested that the extensive pluvial lakes were the result of a combination of reduced summer temperatures and lower evaporation rates.

More recently, Spaulding (1985) documented major climatic changes in south-central Nevada over the last 45,000 years on the basis of packrat-midden analysis. Again, the macrofossil assemblage indicated a widespread juniper (high-elevation species) flourished throughout the region between 45,000 and 10,000 years ago.

6.2.2 Isotopic Analysis of Midden Macrofossils

Siegel (1983) was one of the first to take the midden technique a step further and extract cellulose from plant debris contained within packrat middens collected in the Snake Range, Nevada-Utah border. The deuterium content of organic matter is known to vary systematically on the basis of origin of the sample (Schiegl and Vogel, 1969). The age of the material collected ranged from 34,000 years BP to present, and he identified a significant deuterium depletion between 34,000 and 13,000 years BP (Figure 6.3). This time frame corresponds to the period that previous authors (Wells and Jorgenson, 1964; Thompson and Mead, 1981; and

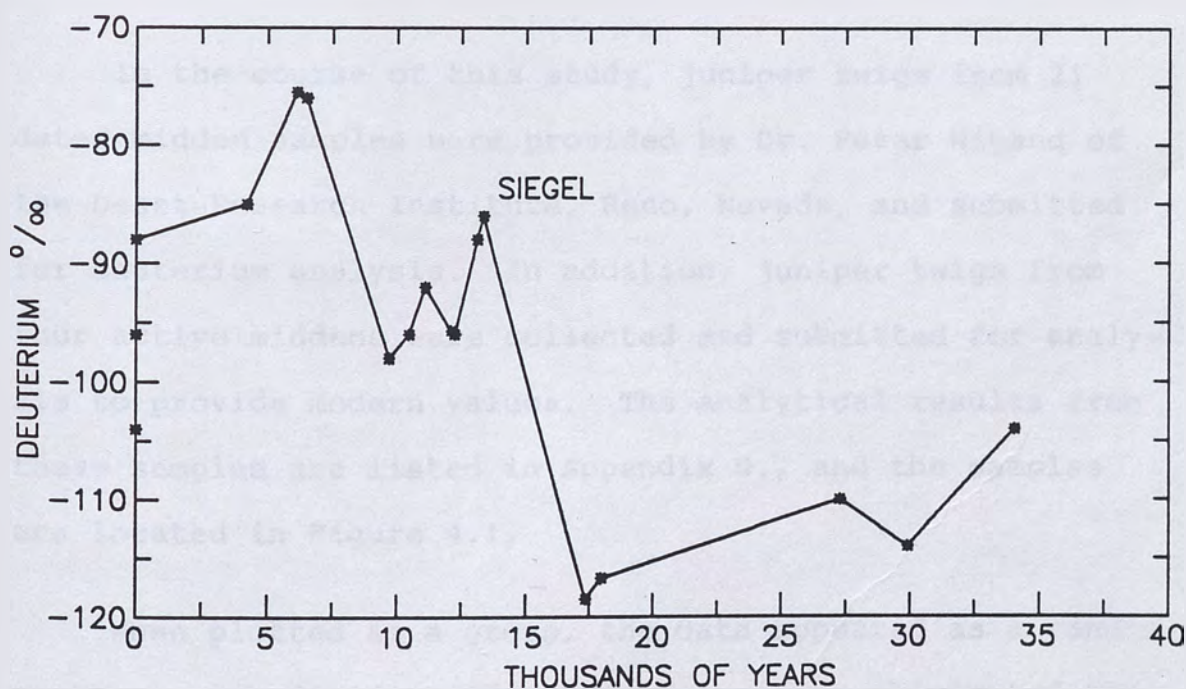


Figure 6.3: Deuterium vs. carbon-14 age of packrat middens from the Snake Range (Siegel, 1983).

Spaulding, 1985) have identified from 40,000 to 10,000 years BP on the basis of plant material alone. Seigel undertook an extensive analysis of the validity of isotopic analyses from twig cellulose. After assessing the possible effects of biosynthesis, photosynthesis, evapotranspiration, and root respiration, he concluded deuterium analyses

... should represent a weighted average for annual precipitation in the area. Thus, it should be possible to infer δD of ancient environmental water and its temperature dependent variation from analysis of cellulose C-H hydrogen in ancient wood (Siegel, 1983, p.75).

He also recommended restricting the sampling and analysis to one type of plant material (ie. twigs of Utah juniper), due to a significant intramidden variation in deuterium content.

In the course of this study, juniper twigs from 21 dated midden samples were provided by Dr. Peter Wigand of the Desert Research Institute, Reno, Nevada, and submitted for deuterium analysis. In addition, juniper twigs from four active middens were collected and submitted for analysis to provide modern values. The analytical results from these samples are listed in Appendix D., and the samples are located in Figure 4.1.

When plotted as a group, the data appeared as a random scatter. Sub-dividing the data by location eliminated the effects of latitude and elevation, and revealed a more

systematic trend. Figure 6.4 shows all the samples on a deuterium vs. radiocarbon age plot, with samples from the same location connected by a line. The two sites with more than two analyses, the Painted Hills and the Pahrnagat Range, both reflect isotopic variations in the anticipated time period.

One concern that arose is the apparent erratic nature of isotopic analyses of modern juniper samples. The modern sample is nearly always more isotopically depleted than anticipated, when compared to the ancient samples. A modern analysis may only reflect the isotopic composition of water in the most recent growing season. Ancient samples are usually an amalgam of twigs covering many years, and single season effects are averaged out. Modern samples were more enriched than expected in the Siegel (1983) study, but this irregularity was not addressed.

Figure 6.5 shows the relationship between radiocarbon age and deuterium content of middens from the Painted Hills, located just north of Reno, Nevada. The Painted Hills site was chosen for detailed study due to its long history of occupation, large number of analyses, and its nearness to Lake Lahontan. As in the Siegel (1983) study, the data reveal a significant deuterium depletion extending from approximately 25,000 to 12,000 years BP. The two data sets are shown together in Figure 6.6. Although both show

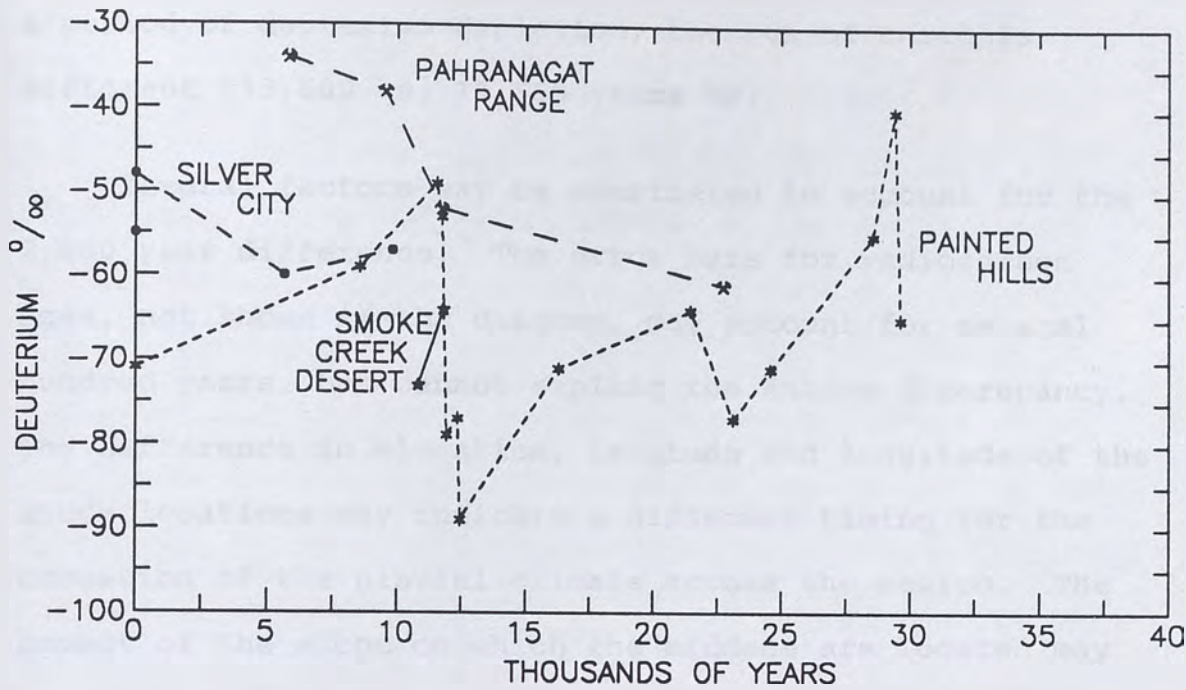


Figure 6.4: Deuterium vs. carbon-14 age of packrat middens from this study, all points. Lines connect samples from the same location.

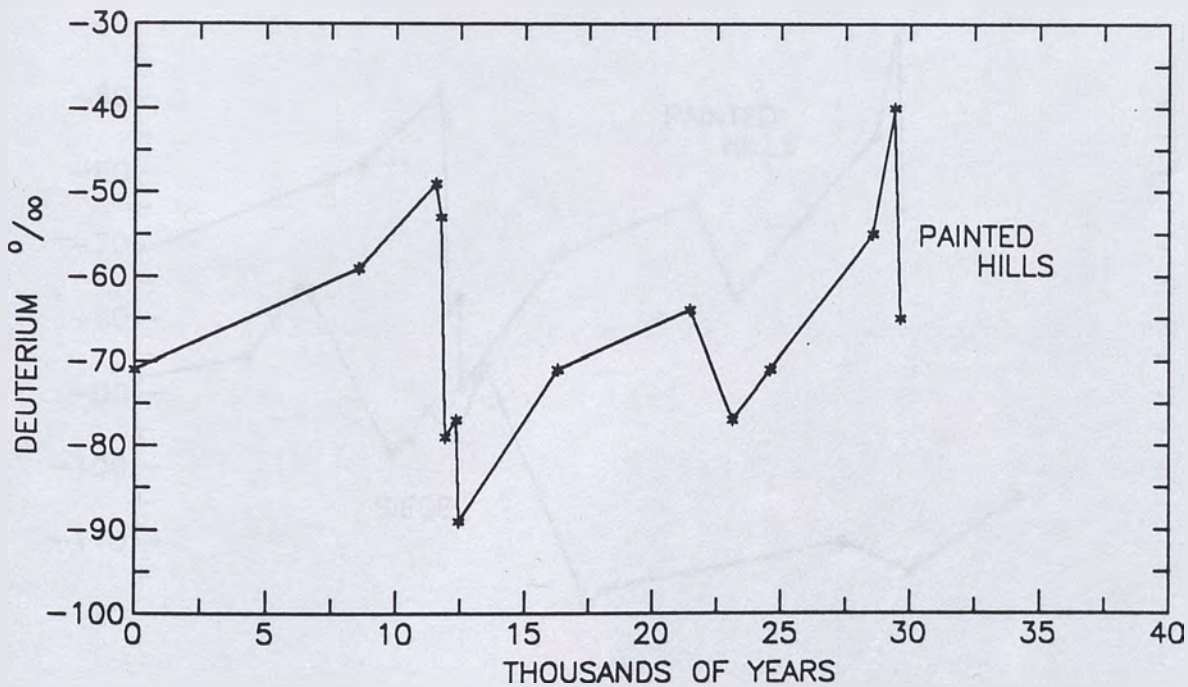


Figure 6.5: Deuterium vs. carbon-14 age of packrat middens from the Painted Hills location only.

a period of deuterium depletion, the age of onset is different (13,500 vs. 11,500 years BP).

Several factors may be considered to account for the 2,000 year difference. The error bars for radiocarbon ages, not shown in the diagram, may account for several hundred years, but cannot explain the entire discrepancy. The difference in elevation, latitude and longitude of the study locations may indicate a different timing for the cessation of the pluvial climate across the region. The aspect of the slope on which the middens are located may also be important. Slopes facing south and west receive greater solar insolation, which may be reflected in the

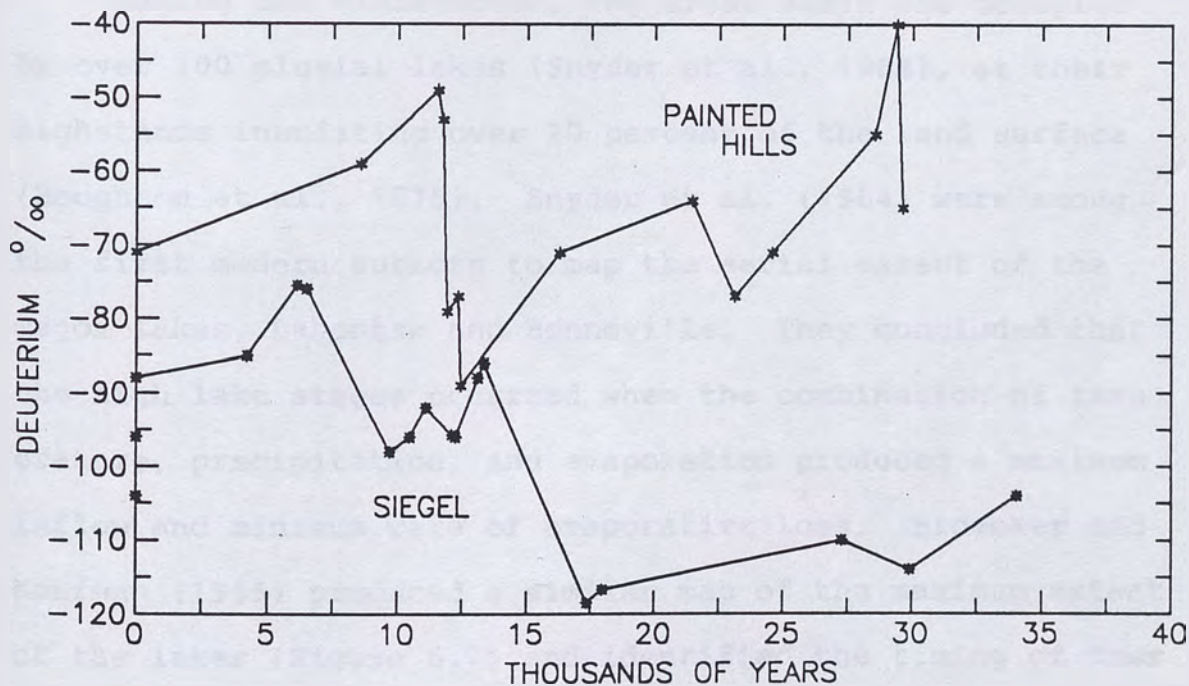


Figure 6.6: Deuterium vs. carbon-14 age of packrat middens from the Snake Range (Siegel, 1983) and the Painted Hills (this study).

isotopes of the collected material. A final factor, to be discussed in detail in a subsequent chapter, is the location of the two sites relative to late Pleistocene lakes. The Snake Range is located on the Nevada-Utah border, adjacent to an arm of pluvial Lake Bonneville (Snyder and others, 1964). Most of the midden material collected during this investigation was derived from the Lake Lahontan Basin, with the Painted hills midden located only a few hundred meters away from the Lahontan highstand shoreline.

6.3 PLEISTOCENE LAKES

During the Pleistocene, the Great Basin was occupied by over 100 pluvial lakes (Snyder et al., 1964), at their highstands inundating over 20 percent of the land surface (Houghton et al., 1975). Snyder et al. (1964) were among the first modern authors to map the aerial extent of the major lakes, Lahontan and Bonneville. They concluded that the high lake stages occurred when the combination of temperature, precipitation, and evaporation produced a maximum inflow and minimum rate of evaporative loss. Broecker and Kaufman (1965) produced a similar map of the maximum extent of the lakes (Figure 6.7) and identified the timing of four highstands in the Late Wisconsin: 17,000, 14,500, 12,000 and 9,500 years BP.

Benson (1978) identified two high stands of 1330 m; the earliest occurred between 25,000 and 22,000 years BP and the most recent extended from 13,500 to 11,000 years BP. Benson (1981) also suggested that percentage of cloud cover was an important factor in the filling and evaporative loss equation for the lakes. In 1987, Benson and Thompson identified the timing of a high stand (1330 meters at 13,500 years BP) and a low stand (1170 meters at 5,000 years BP) for Lake Lahontan.

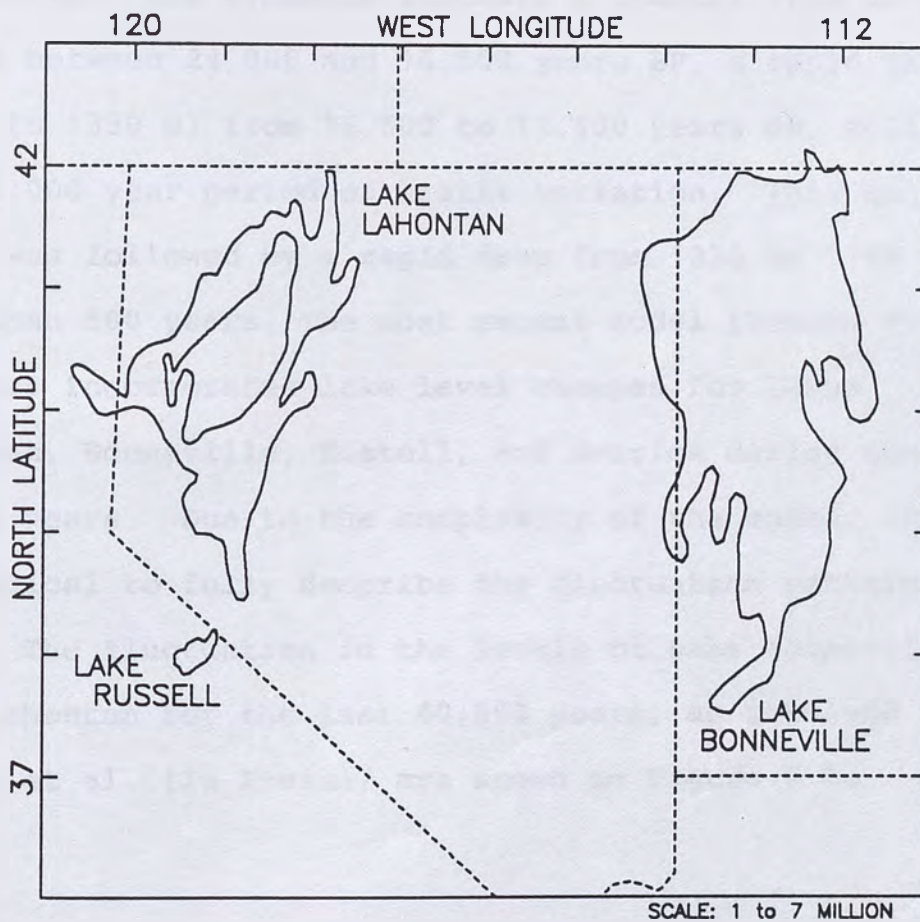


Figure 6.7: Maximum extent of major pluvial lakes in the Great Basin, from Benson et al. (In Press)

In the Walker Lake Basin, Benson (1987) identified the timing of two high stands (14,000 and 12,500 years B.P) and three low stands (21,000 to 15,000, 4,700, and 2,600 years BP), based on interpretation of cored lake sediments. The high stands correlate with most data from the northern portions of Lake Lahontan.

Thompson et al. (1986) show that the last major high stand of Lake Lahontan terminated before 12,070 years BP and that major fluctuations were nearly synchronous with Lake Russell (Mono Lake Basin, California) and Lake Bonneville. The evidence suggests a gradual rise in lake levels between 24,000 and 16,500 years BP, a rapid rise (1270 to 1330 m) from 16,500 to 13,500 years BP, followed by a 1,000 year period of little variation. This quiescent stage was followed by a rapid drop from 1330 to 1170 m in less than 500 years. The most recent model (Benson et al. in press incorporates lake level changes for Lakes Lahontan, Bonneville, Russell, and Searles during the last 35,000 years. Due to the complexity of the model, it is impractical to fully describe the fluctuation patterns here. The fluctuation in the levels of Lake Bonneville and Lake Lahontan for the last 40,000 years, as obtained from Benson et al. (In Press), are shown in Figure 6.8.

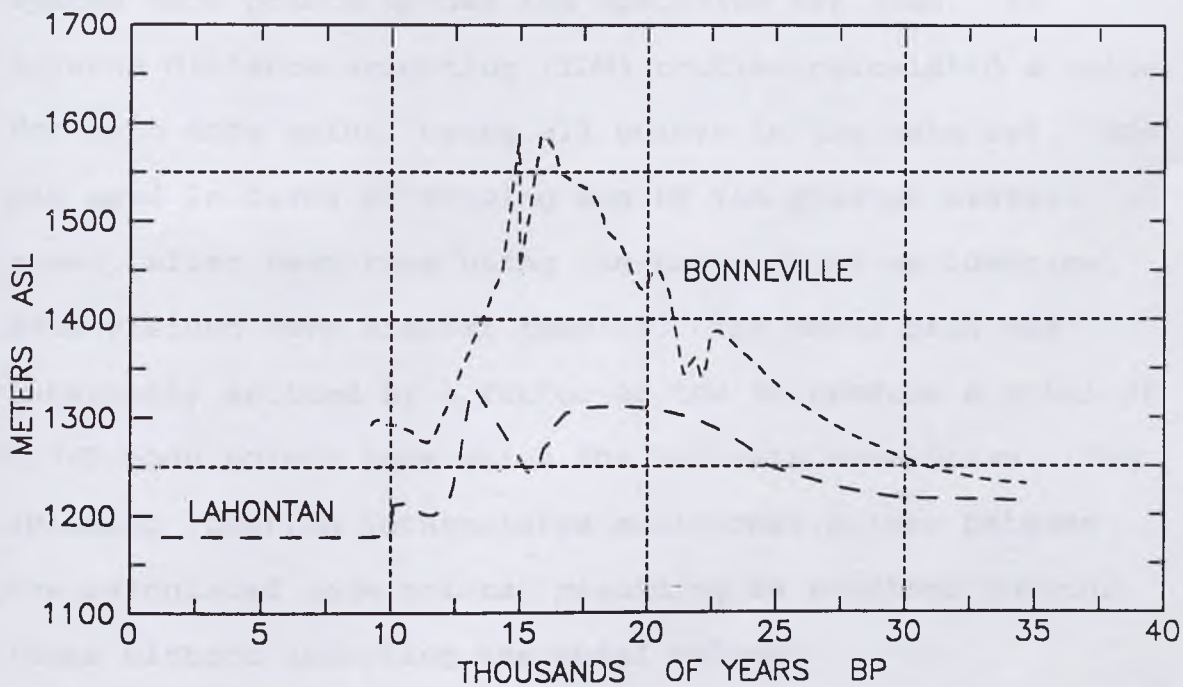


Figure 6.8: Lake level chronology of pluvial Lake Lahontan and Lake Bonneville, from Benson et al. (In Press).

CHAPTER 7.

WATER ANALYSES

7.1 COMPUTER CONTOURING OF STABLE LIGHT-ISOTOPE DATA

The data sets were contoured using the Surfer^R contouring package from Golden Software, Inc. In a study of this type, where data points are at irregular intervals, adjusting the contouring parameters can produce drastically different results from the same data set. All plots presented here were contoured using the same parameters to avoid the introduction of bias, such as manipulating the parameters to produce a desired result.

A grid setting of 15 by 15 established 225 equally spaced node points across the specified map area. An inverse distance weighting (IDW) routine calculated a value for each node point, using all points in the data set. IDW was used in favor of Kriging due to its greater overall speed, after test-runs using the two methods on identical sets yielded very similar results. The nodal grid was internally splined by a factor of two to produce a total of 1,749 node points upon which the contours were drawn. The splining function interpolates additional points between the calculated node points, resulting in smoother contour lines without affecting the nodal values.

All data points from the set being contoured were used for each nodal calculation due to the irregularity of the

data set distribution, and the above mentioned possibility of bias. No single search radius, method, and specified number of nearest points to use adequately served all the data sets. A liability of using the "ALL" points parameter is that contours will be drawn regardless of whether data exists locally. Data points upon which the contours were drawn are provided with each plot to allow the reader to assess the validity of the contouring routine.

7.1.1 Undifferentiated Set

An initial culling of the data set was performed based on the fluid sample source. Data from surface waters such as lakes and streams was excluded from the contouring process. These samples are likely to have undergone exchange with the atmosphere and become isotopically enriched, and would improperly influence the contoured plots.

In order to assess any general trend in the data, contour plots utilizing all remaining points were generated. The plots of deuterium (Figure 7.1) and oxygen-18 (Figure 7.2) show the same pattern, a general depletion from south to north and from west to east. Since the fractionation of isotopes is temperature dependent, meaningful interpretation can come only when the data set is sub-divided by temperature. The set was also divided into two source types; springs and wells.

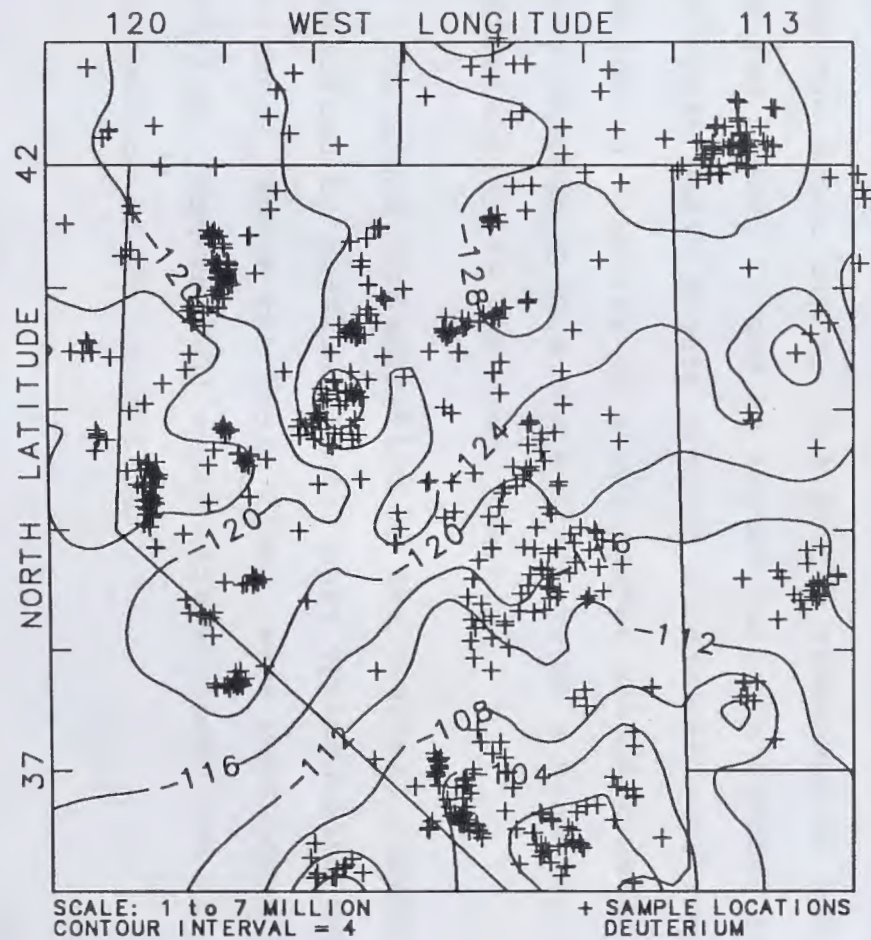


Figure 7.1: Deuterium permil concentration for all points, regardless of sample temperature, from across the Great Basin study area.

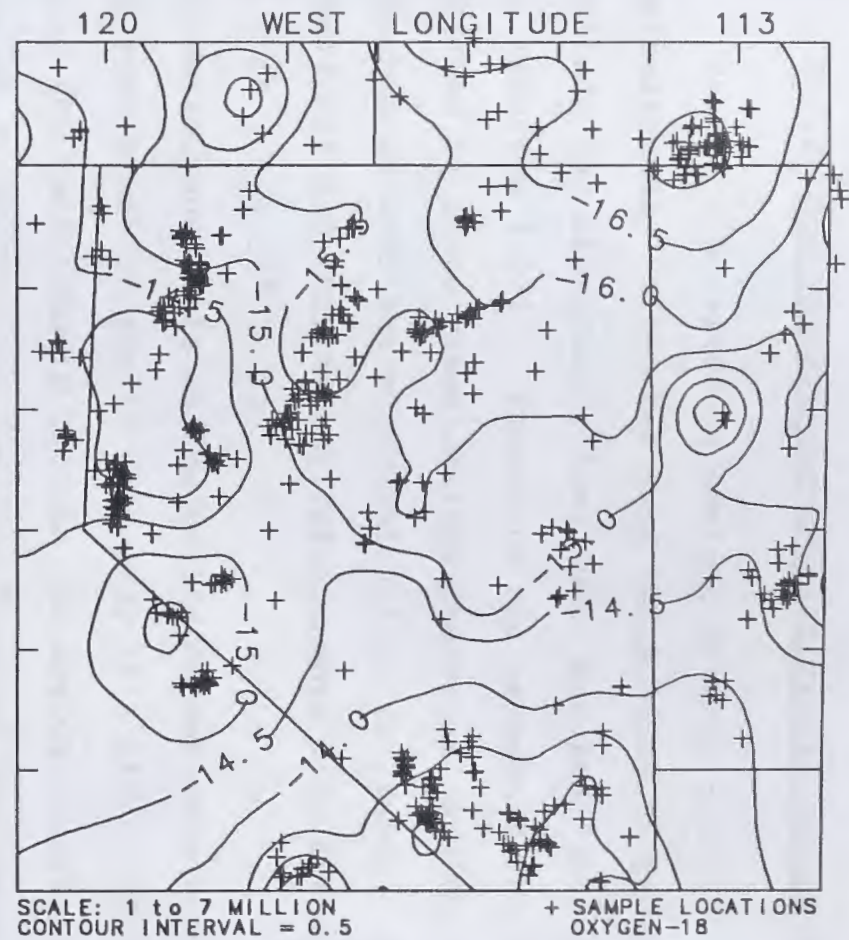


Figure 7.2: Oxygen-18 permil concentration for all points, regardless of sample temperature, from across the Great Basin study area.

7.1.2 Non-Thermal Springs and Precipitation

Stable light-isotope content of precipitation varies systematically on the basis of temperature (a function of latitude and elevation), longitude, and the "rain-out" factor (section 3.2.1). Deuterium and oxygen-18 are equally affected by these fractionation processes, and the relationship between their concentrations is linear. Craig (1961) defined this linear relationship with the equation:

$$\delta D = 8 \times \delta^{18}O + 10 \quad (7.1)$$

and established this as the worldwide meteoric water line. All precipitation should plot near this line. Figure 7.3 shows the relationship between the worldwide meteoric water line of Craig, and the best fit line for non-thermal waters from the Great Basin. Due to the closeness of the slope of the two lines, it can be argued that non-thermal springs in the Great Basin should provide a reasonable estimation of the isotopic ratios in local recent meteoric water. The above described data set will serve as a proxy for modern precipitation in the Great Basin.

To avoid contamination by the regional interbasin flow identified by Mifflin (1968), only springs discharging in the range, above the basin floor, were used for this determination. Non-thermal wells were excluded due to the same possibility of contamination.

The anticipated pattern of isotope concentrations in precipitation includes the effects of oceanic storm tracks and distance from the ocean. The two principal storm tracks that bring precipitation into the Great Basin are northern winter storms that originate in the eastern Pacific Ocean, and southern summer storms that originate in the southern Pacific Ocean and Sea of Cortez.

In order to delineate the distribution of stable isotopes in meteoric waters, deuterium and oxygen-18 data from non-thermal springs (less than 20°C) were contoured on

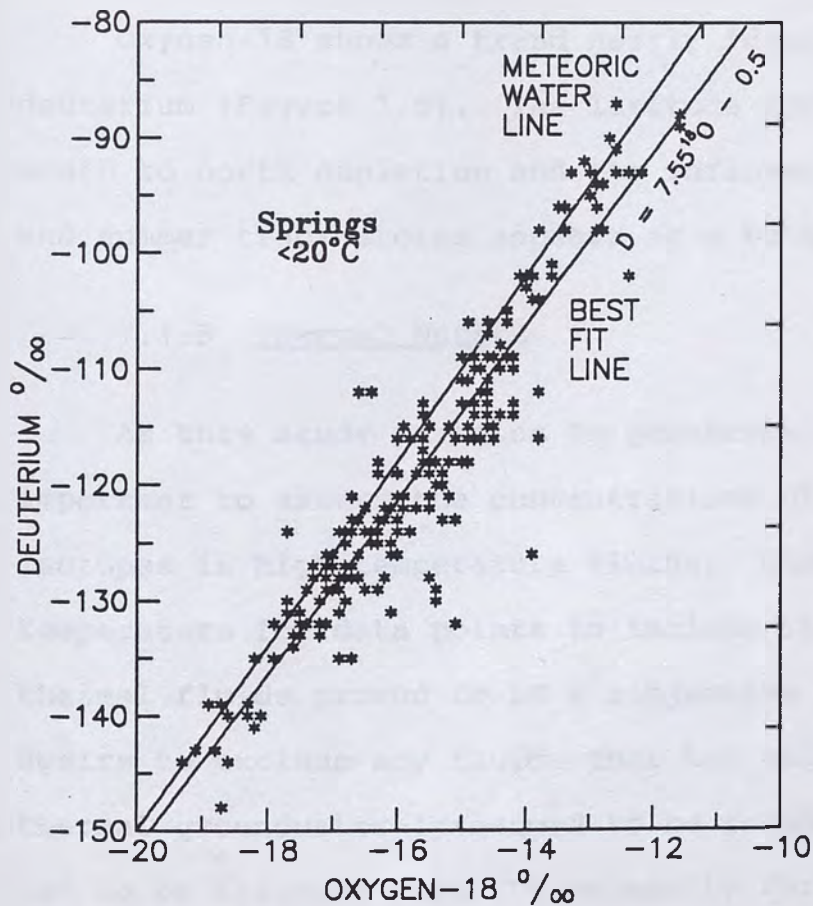


Figure 7.3: Deuterium vs. ^{18}O for cold springs from across the Great Basin. Agreement with the worldwide meteoric water line of Craig is very good. Equation of Craig's line is:

$$D = 8 \times ^{18}\text{O} + 10$$

base maps of the Great Basin. Figure 7.4 shows the variation concentration of deuterium in these springs. The diagram illustrates the effects of latitude and longitude, and the winter and summer storm tracks which are shown in Figure 7.5. The non-thermal fluids generally become more depleted from south to north, reflecting the latitude effect and the summer storm track, and from west to east reflecting the winter storm track. Both trends also show the inland depletion effect of storm rain-out. The most depleted meteoric waters are located in the northeast corner of the study area, while the most enriched fluids are located in southern Nevada.

Oxygen-18 shows a trend nearly identical to that of deuterium (Figure 7.6). The latitude effect produces a south to north depletion and the influence of the winter and summer track storms appears as a bulge in the contours.

7.1.3 Thermal Waters

As this study pertains to geothermal fluids, it is important to assess the concentrations of stable light-isotopes in high temperature fluids. Choosing a cut-off temperature for data points to include in the plots of thermal fluids proved to be a subjective process. The desire to exclude any fluids that had mixed with non-thermal groundwater (presumed to be recent meteoric water) had to be balanced with the necessity for a large enough

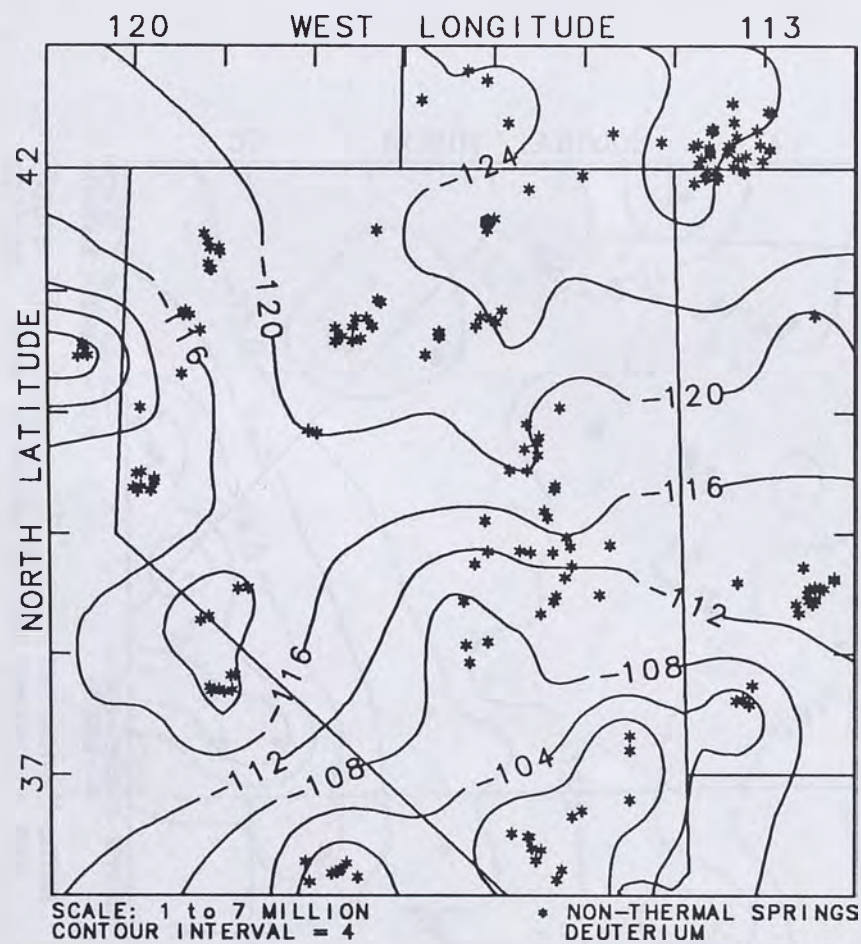


Figure 7.4: Deuterium permil for non-thermal springs. Note trend of isotopic depletion from south to north and from west to east. Lack of data in southeast Oregon deflects contours west.

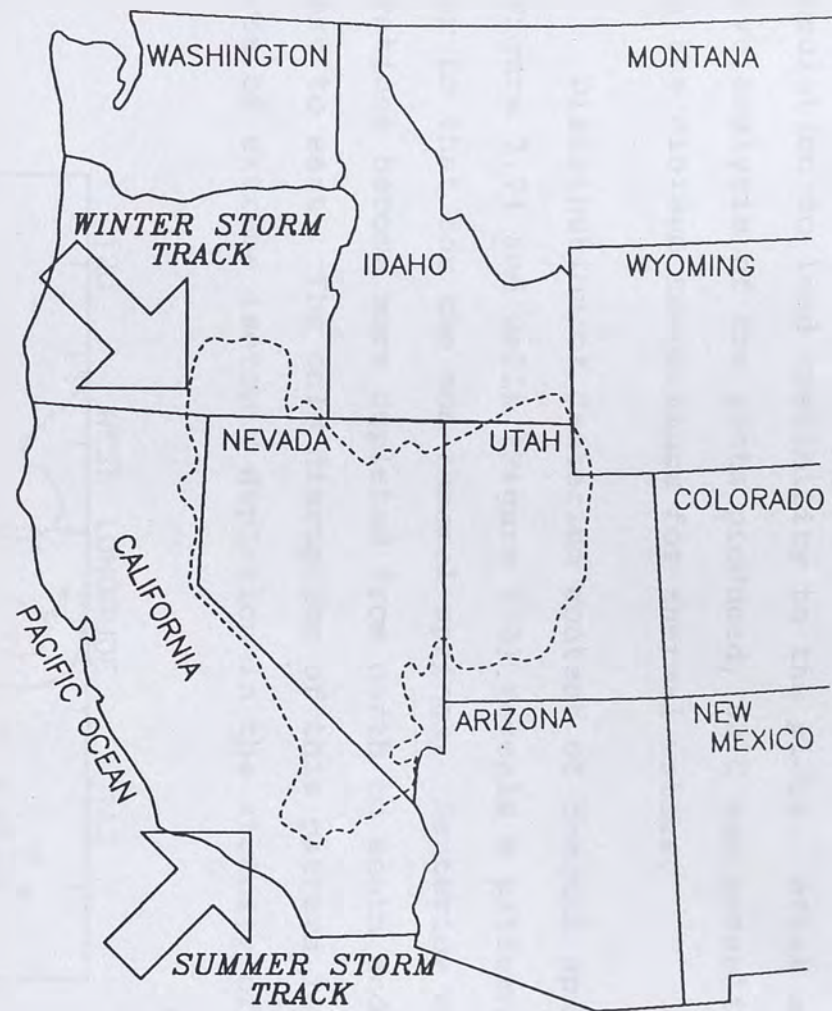


Figure 7.5: Map of the western United States showing the predominant seasonal storm tracks of the Great Basin.

population to lend credibility to the plots. After extensive analysis of the plots produced, 80°C was established as the minimum temperature for thermal waters.

Distribution of deuterium content of thermal springs (Figure 7.7) and wells (Figure 7.8) reveals a pattern similar to that for the non-thermal springs. Deuterium concentrations become more depleted from north to south and from west to east. The only disruption of this pattern is an area of extreme isotopic depletion in the vicinity of Elko,

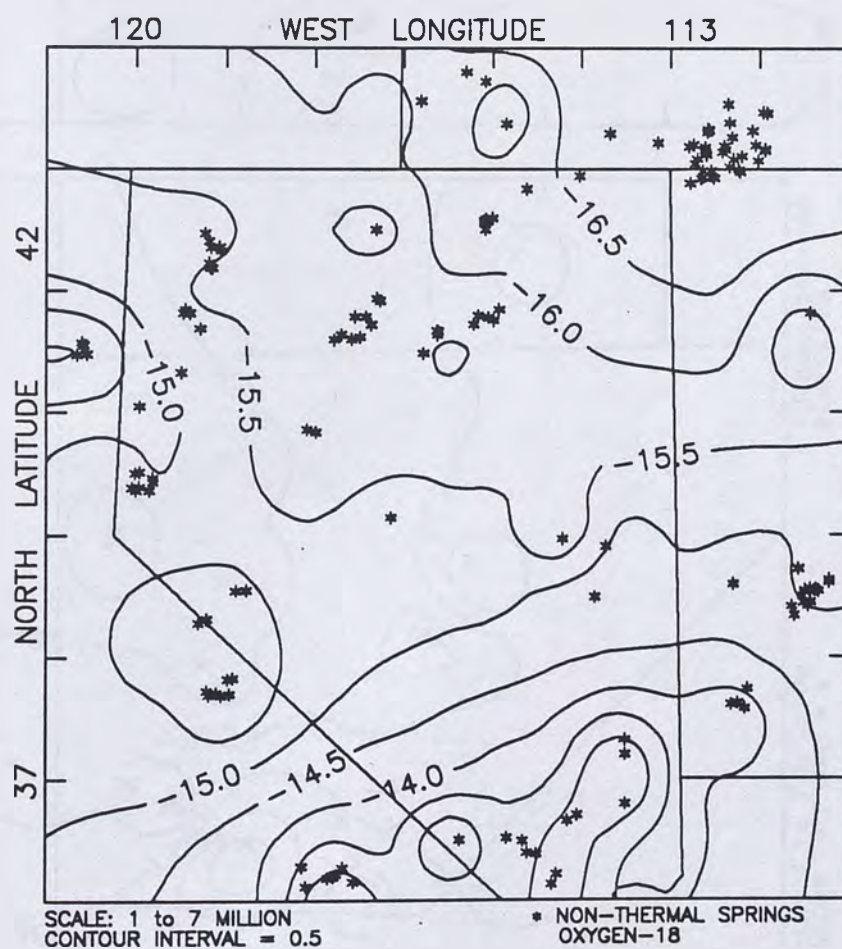


Figure 7.6: Oxygen-18 permil for non-thermal springs. Note similarity to the deuterium plot.

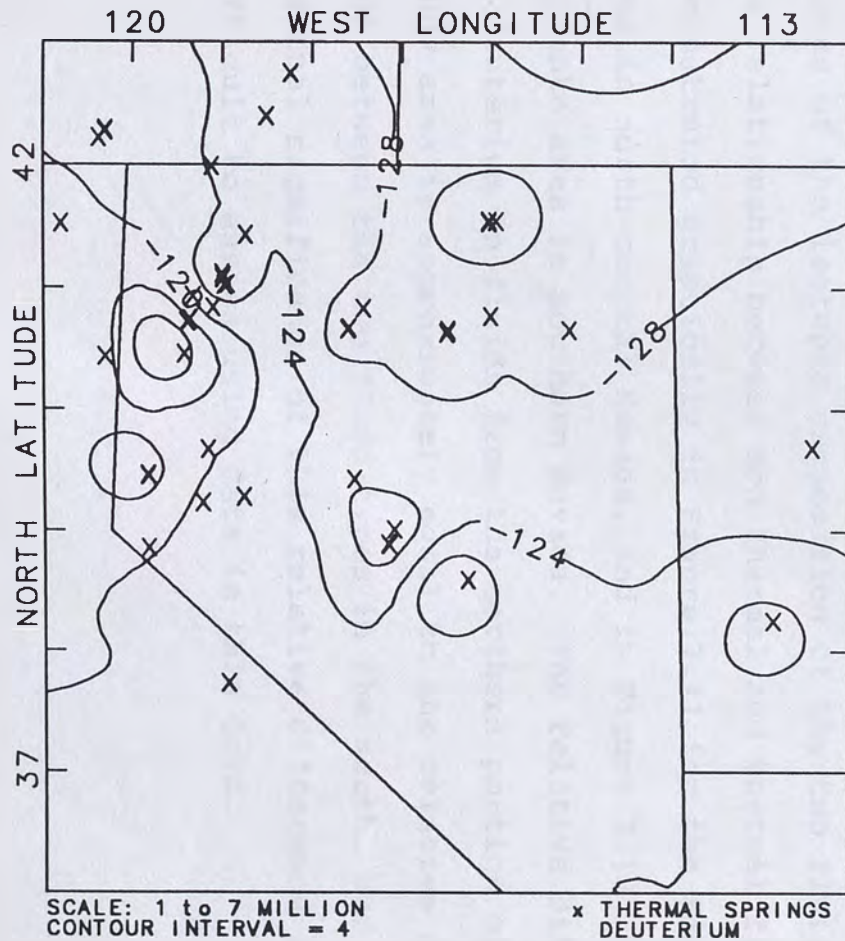


Figure 7.7: Deuterium permil for thermal springs. Note the pattern of isotopic depletion resembles that of the non-thermal springs, becoming more depleted from south to north and west to east.

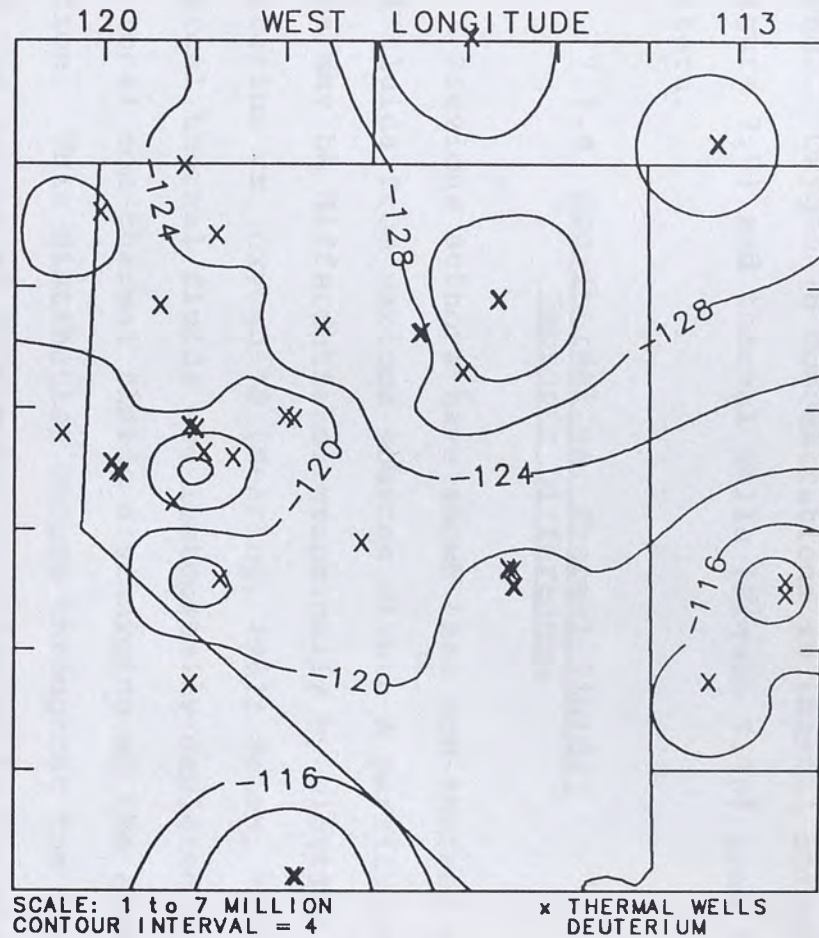
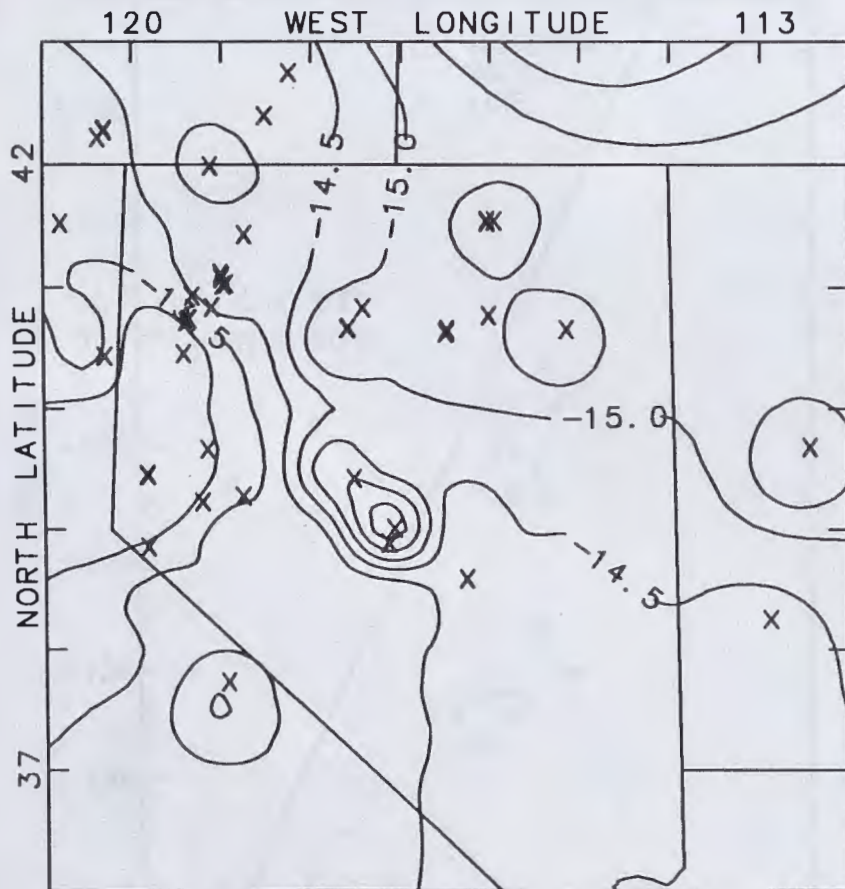


Figure 7.8: Deuterium permil for thermal wells. Note the pattern of isotopic depletion resembles that of the thermal and non-thermal springs.

Nevada. Oxygen-18 concentrations in thermal springs (Figure 7.9) and thermal wells (Figure 7.10) show the same pattern.

7.1.4 Non-Thermal vs. Thermal Fluids: Isotopic Differences

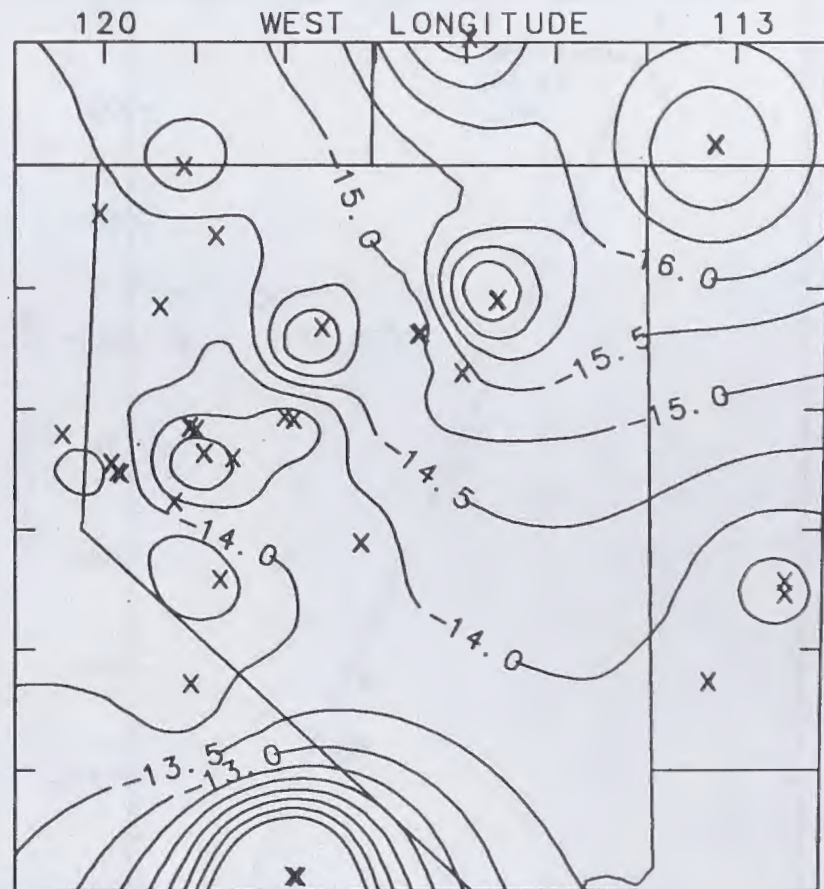
Previous authors have shown that non-thermal and thermal fluids from various sources within a particular study area may be differentiated graphically by plotting deuterium vs. oxygen-18 (Nehring, 1981; Welch, 1983). Typical thermal fluids are isotopically depleted compared to local non-thermal fluids discharging at the same elevation. This distinction occurs throughout the Great Basin and the degree of difference is relative to the absolute values of the isotopic composition of the two fluid types. The relationship between non-thermal and thermal fluids is demonstrated graphically in Figure 7.11 for the Beowawe area in north-central Nevada, and in Figure 7.12 for the Caliente area in southern Nevada. The relative difference of deuterium in fluids from the northern portion of the study area is approximately equal to the relative difference between the two fluid types in the south, but the regional significance of this relative difference is difficult to assess using data in this form.



SCALE: 1 to 7 MILLION
CONTOUR INTERVAL = 0.5

x THERMAL SPRINGS
OXYGEN-18

Figure 7.9: Oxygen-18 permil for thermal springs. Note similarity to the deuterium plot.



SCALE: 1 to 7 MILLION
CONTOUR INTERVAL = 0.5

x THERMAL WELLS
OXYGEN-18

Figure 7.10: Oxygen-18 permil for thermal wells. Note similarity to the previous plots.

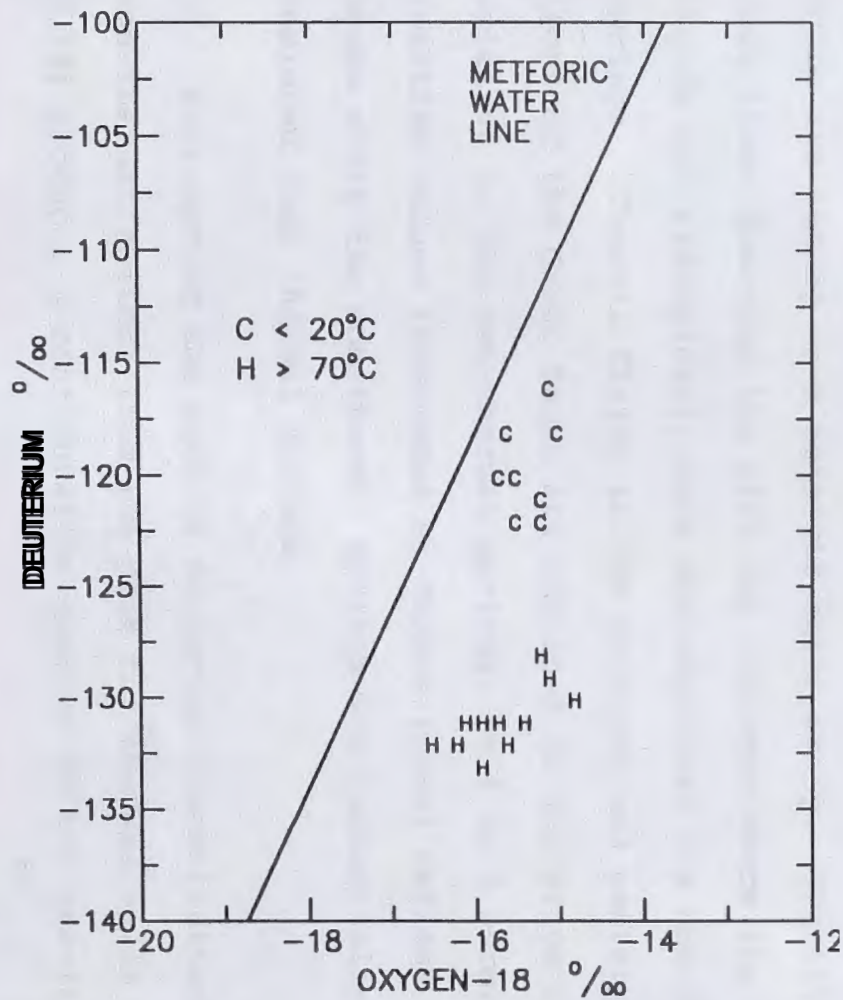


Figure 7.11: Plot of Beowawe, Nevada, area waters showing distinct split between non-thermal springs (C) and thermal springs and geothermal wells (H).

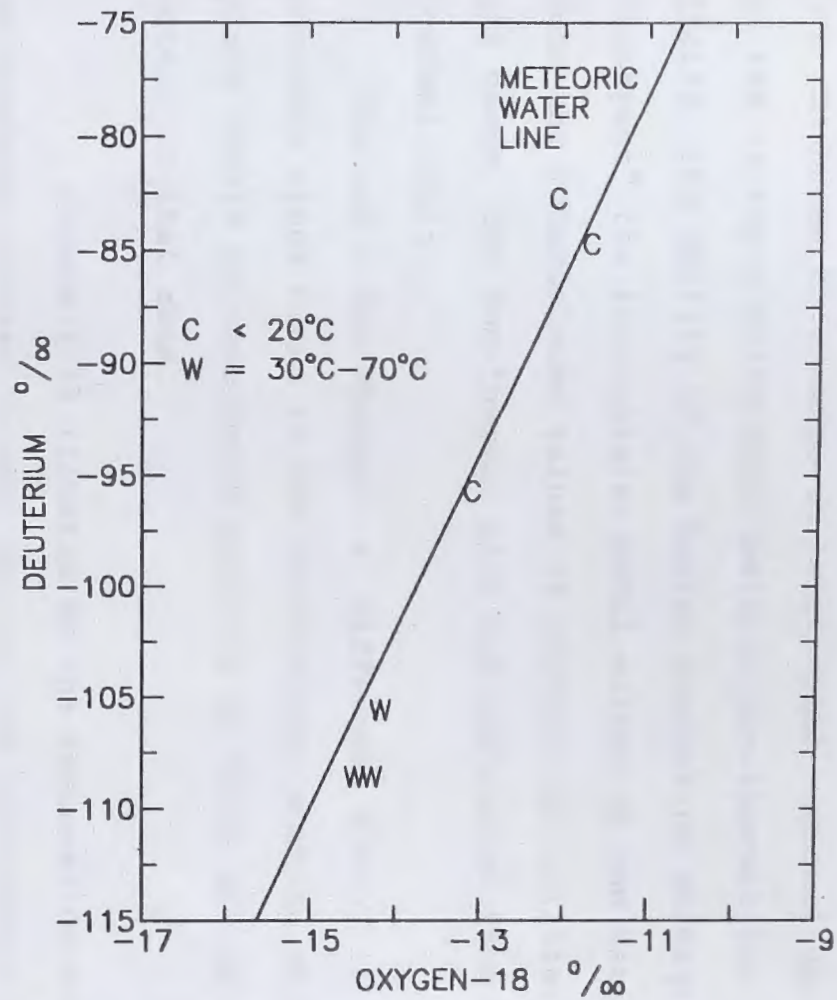


Figure 7.12: Plot of Caliente, Lincoln County, Nevada, area waters showing distinct split between non-thermal springs (C) and warm thermal wells (W).

In order to examine the systematic regional variations in the isotopic differences between non-thermal and thermal fluids, the ability of the Surfer contouring package to "subtract" the interpolated nodal values of one data grid from the interpolated values of another was utilized. In all cases, the non-thermal plot was subtracted from the thermal plot:

$$\text{Thermal} - \text{Non-Thermal} = \text{Difference Plot.} \quad (7.2)$$

Contours lines drawn in the southeastern portion of the plots should be considered spurious as there are no thermal waters in that area.

Figure 7.13 illustrates the regional deuterium differences between thermal springs and non-thermal springs which are acting as a meteoric water proxy. Negative contour lines dominate the plot and indicate where the thermal fluids are isotopically more depleted than the non-thermal springs. Thermal fluids in the northern and western portions of the Great Basin are depleted in deuterium content, relative to the non-thermal springs, by 4 to 8 permil. Positive values (indicated by dashed lines) reflect the few areas where the non-thermal springs are isotopically more depleted than thermal springs.

Subtracting the plot of deuterium concentrations from non-thermal springs from the plot for thermal wells (Figure 7.14) produces a configuration similar to the previous

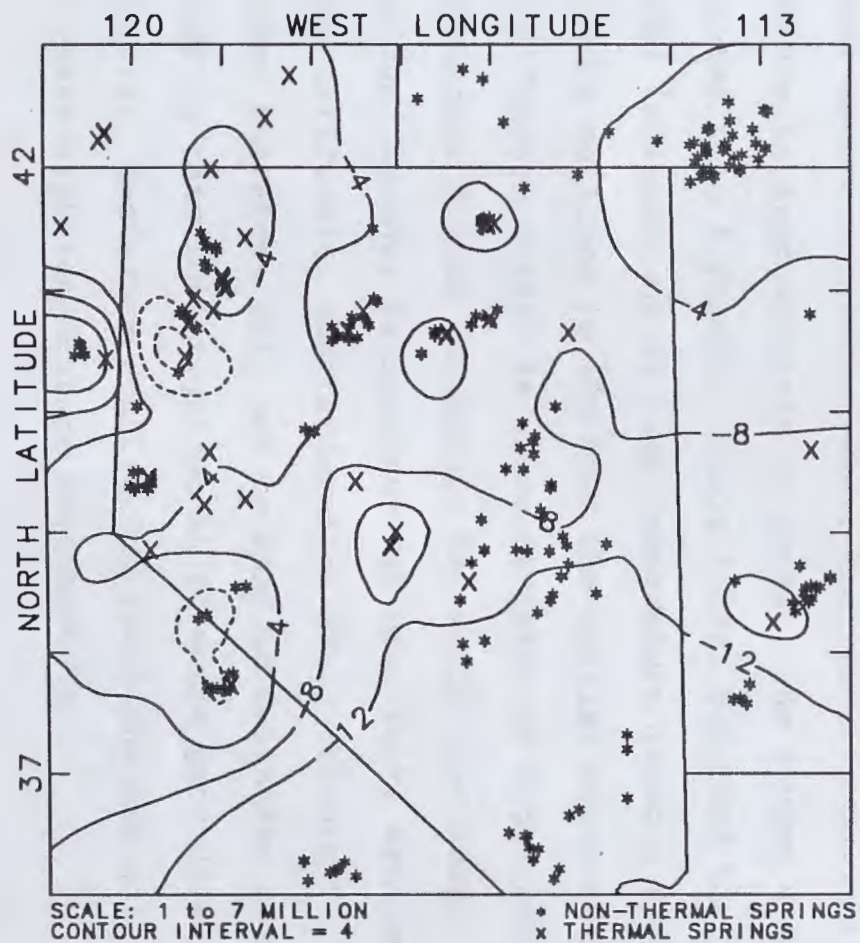


Figure 7.13: Deuterium permil difference for thermal springs minus non-thermal springs. Thermal springs are generally more isotopically depleted than the non-thermal springs, as indicated by the negative (solid) contour lines.



Figure 7.14: Deuterium permil difference for thermal well minus non-thermal springs. The thermal wells are also more isotopically depleted than the non-thermal springs, as indicated by the negative (solid) contour lines.

plot. The thermal fluids are generally more isotopically depleted than the non-thermal fluids, as represented by the solid contour lines. Dashed lines again represent the few areas where non-thermal springs are isotopically more depleted than thermal wells.

If the non-thermal and thermal oxygen-18 plots are compared, a different pattern appears (Figure 7.15). The diagram shows the thermal fluids are generally not more depleted than the non-thermal fluids, as was the case with deuterium. This seeming contradiction may be explained by the behavior of oxygen isotopes at high temperature.

Figure 7.11, which shows $\delta^{18}\text{O}$ vs. δD for the Beowawe area, demonstrates that while the relative deuterium difference is approximately 12 permil, the oxygen difference is less than 1 permil. Craig (1963) reported that rock-water interactions at high temperature yield a fluid that is more enriched in ^{18}O than the initial concentration. This "oxygen shift" is characteristic of high-temperature geothermal fields throughout the world, including Steamboat Springs, Nevada, Yellowstone National Park, Wyoming, Salton Sea, California, and Larderello, Italy (Figure 7.16). Oxygen therefore will not be used to delineate recharge areas in this investigation as it would provide erroneous results. Deuterium equilibrium reactions are not induced by these high temperature environments.

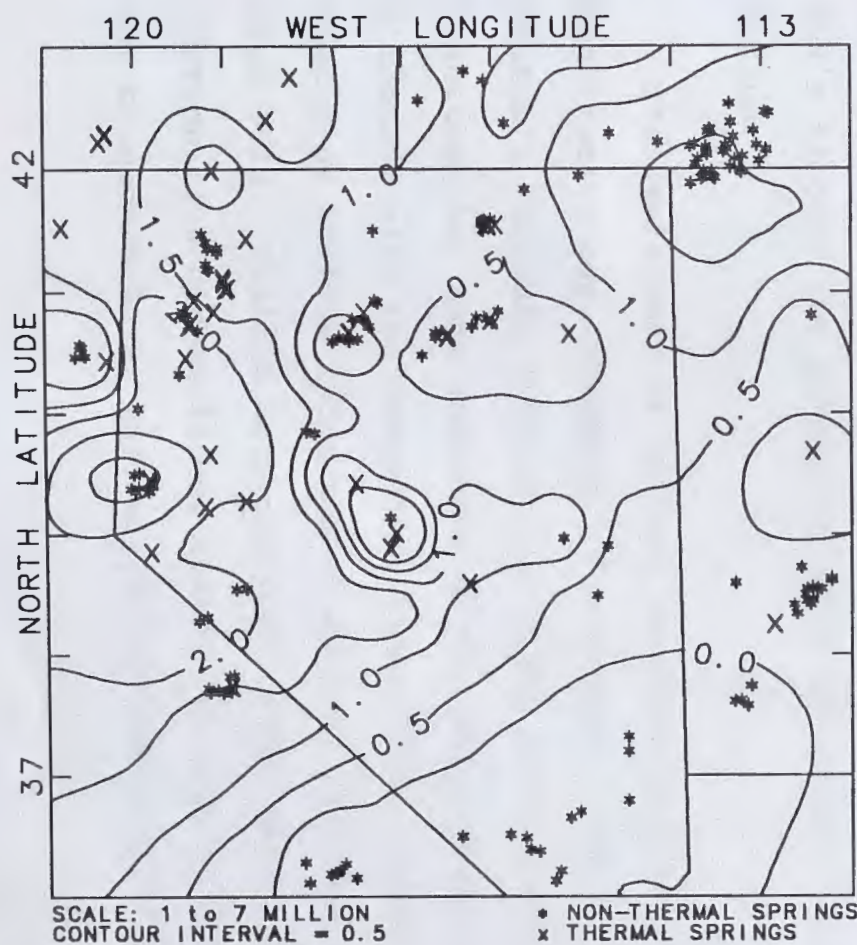


Figure 7.15: Oxygen-18 permil difference for thermal springs minus non-thermal springs. Non-thermal springs are generally more isotopically depleted than the thermal springs, opposite the occurrence with plots of deuterium.

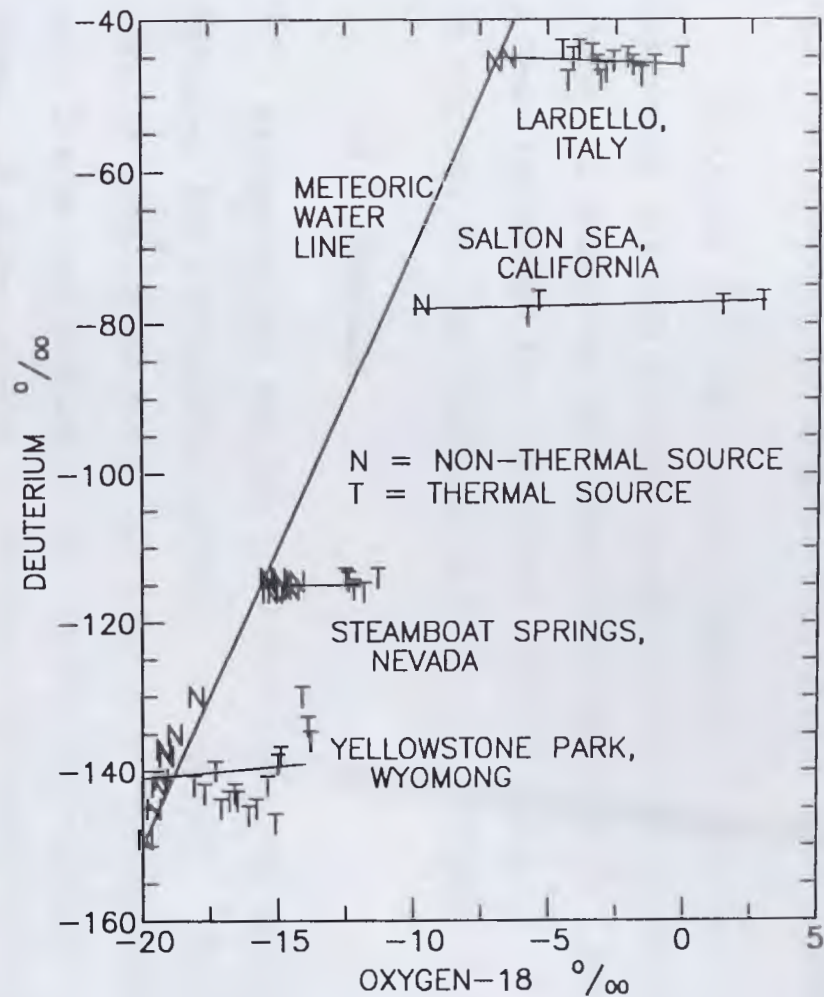


Figure 7.16: Examples of 'oxygen-shift' from famous geothermal fields throughout the world. T represents thermal fluids, while N represents non-thermal waters.

7.2 GROUNDWATER AGE-DATING USING RADIOACTIVE ISOTOPES

Analysis for radioactive isotopes of two elements was performed for the purpose of age-dating fluid samples. The theory of obtaining age dates from radioactive isotopes and a description of the laboratory methods used can be found in Section 3.3 and Sections 5.3 and 5.4, respectively.

7.2.1 Tritium

Sixteen fluid samples were collected for analysis of tritium, the radioactive isotope of hydrogen. With a half-life of only 12.26 years, tritium has been used worldwide as a tracer and indicator of "modern" groundwater. The advent of above ground thermonuclear testing in the early 1950's flooded the atmosphere with artificially produced tritium.

The usefulness of tritium analyses is limited to semi-quantitative age estimates. For example, the presence of tritium in amounts greater than a few tritium units (TU), indicates that some component of the fluid sampled has been in contact with the atmosphere since 1952. Conversely, an absence of tritium indicates no contact with the atmosphere since 1952. Tritium data are most useful when used in conjunction with carbon-14 age dating, to indicate the presence of modern water that would invalidate the ^{14}C date.

Tritium data for all samples analyzed in the course of this study are listed in Table 7.1. All samples contain less than 5 TU tritium, the limit of detection for the procedure used. Typical values for surface water in northern Nevada range from 15 to 21 TU (Szecsody, 1982). The data indicate that no component of the fluid samples have had contact with the atmosphere since 1952.

7.2.2 Carbon-14

Twelve samples were collected for carbon dating during this study, three of which proved to have insufficient carbon for analysis. Additional high-temperature carbon age data were derived from studies in the Steamboat-Moana Area (Flynn et al., 1984; Nehring, 1980). A total of 12 carbon age-dates from fluid samples greater than 90°C, listed in Table 7.2, were utilized during the course of this investigation. Those sites are identified in Figure 7.17.

Table 7.1: Tritium analyses, this study.

GF#	TU	LOCATION	GF#	TU	LOCATION
1	<5	Brady's Hot Sp	10	<5	Beowawe 1-13
2	<5	Gerlach Hot Sp	13	<5	Alakli Hot Sp
3	<5	Patua Hot Sp	14	<5	Bailey Hot Sp
4	<5	Steamboat Hot Sp	15	<5	Grapevine Sp, DV
5	<5	Wabuska Tads #2	18	<5	Rogers Sp, Lk Mead
6	<5	Reno Warren Est	20	<5	Warm Springs
7	<5	Soda Lake 33-14	23	<5	Elko Sch Dist.
8	<5	Des Peak 67-21	24	<5	Elko Heat Co

Table 7.2: Carbon-age date analyses used. GF #'s refer to samples from this study, letter codes refer to data from previous studies. See Appendix C for a complete listing of all carbon-age data.

GF #	SAMPLE NAME	TEMP (°C)	¹⁴ C pmc	¹³ C/ ¹² C ‰	UNCORR AGE
34	Beowawe Batz Inj.	160	6.1	-0.7	23100
36	Warm Spring	65	<0.6	-0.6	>42300
37	Elko School Dist.	90	<1.6	-0.8	>34200
40	Beowawe 1-13 Scale	160	8.3	-4.0	20200
41	Oxbow 45-5 Scale	350	2.1	-5.1	30900
42	Oxbow 74-7 Scale	350	2.4	-5.8	29800
43	Oxbow 76-7 Scale	350	3.7	-6.2	26500
46	Beowawe 2-13	160	8.7	-4.4	20500
49	Desert Peak Scale	160	<0.5	-2.2	>43800
	Steamboat #26 (NEH)	90	0.5	--	44500
	Steamboat #8 (NEH)	90	1.0	--	38300
	Steamboat Sp (FLY)	96	0.2	-6.2	51376
	Warren Est. (FLY)	90	11.5	-10.3	13700

FLY - Flynn et al., 1984

NEH - Nehring, 1980

The complexity and difficulties associated with carbon age-dating have been previously discussed (sections 3.3 and 3.4). However, a deuterium vs. radiocarbon age plot of thermal waters from northern Nevada (Figure 7.18) shows excellent agreement with previous plots. A significant isotopic depletion is recorded from 30,000 to 10,000 years BP. Standing alone, this plot would be unconvincing. In association with the evidence previously presented, it confirms that geothermal fluids have a Pleistocene origin.

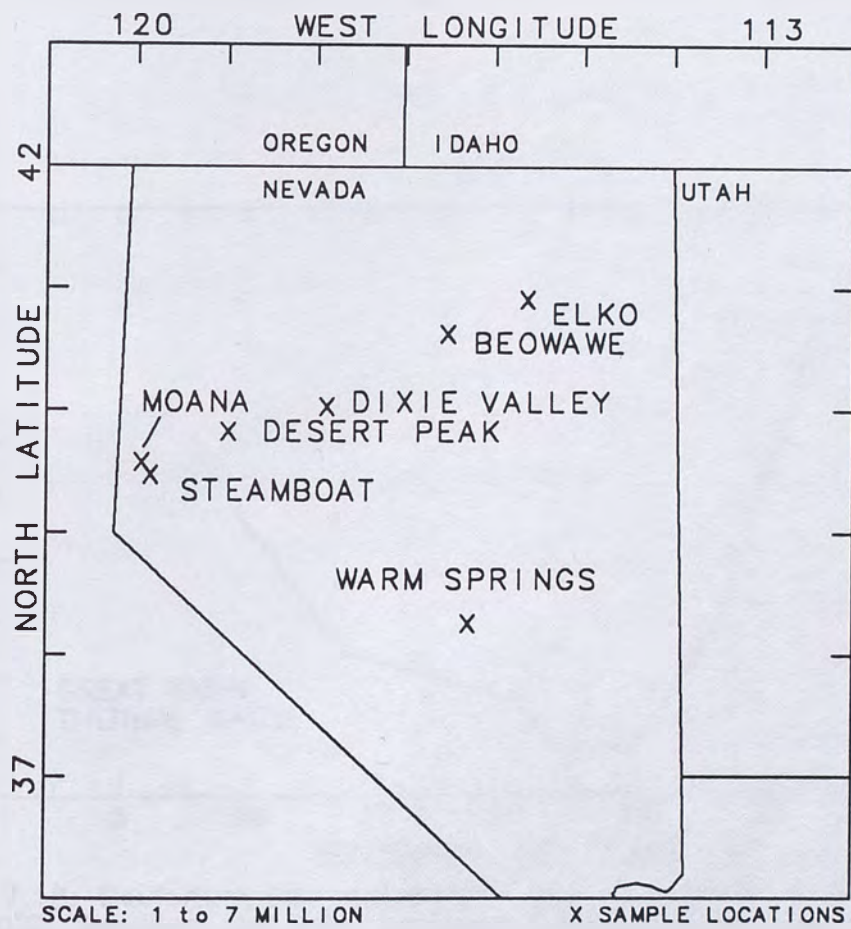


Figure 7.17: Location of high temperature carbon age dates used in this study.

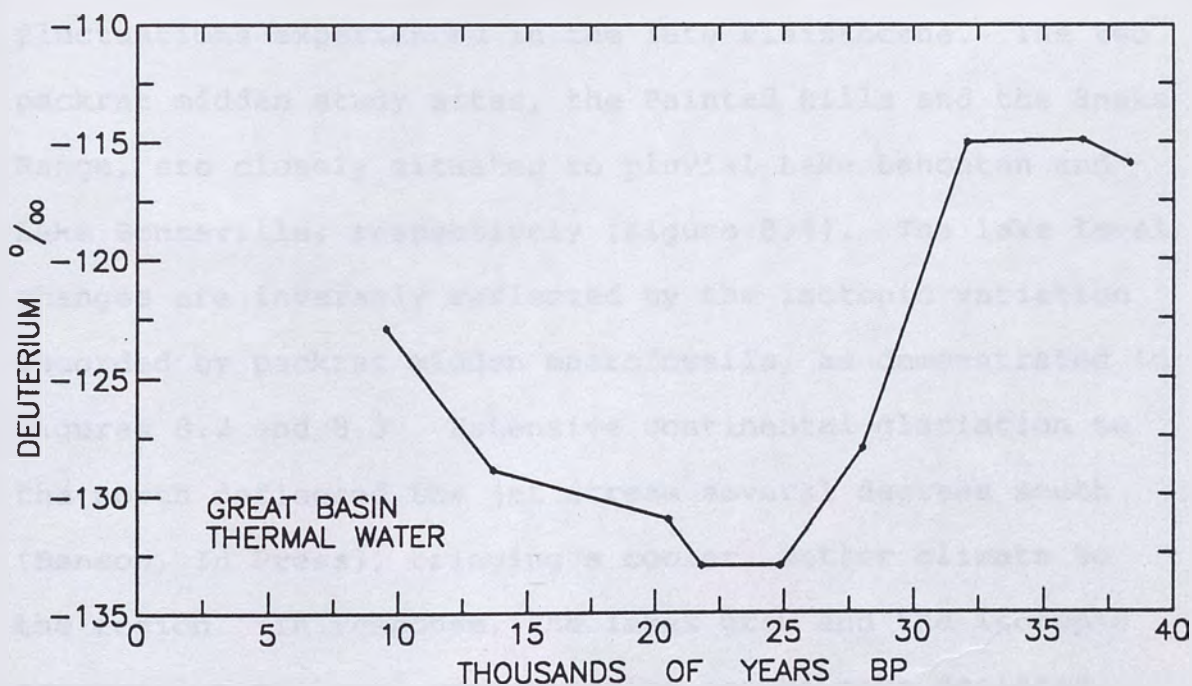


Figure 7.18: Deuterium vs. radiocarbon age of thermal waters greater than 90°C. Samples are from northern Nevada, where the majority of deep geothermal power plant production wells are located.

CHAPTER 8.

DISCUSSION: EFFECT OF PLEISTOCENE LAKES,
AND RECHARGE SCHEMES

Evidence presented to this point is clearly indicates a major worldwide depletion in stable light-isotopes during the late Pleistocene, 30,000 to 10,000 years BP. But how does this data interrelate and apply to the recharge of geothermal fluids in the Great Basin?

8.1 EFFECT OF PLEISTOCENE LAKES

The rise and fall of Pleistocene Lake Lahontan and Lake Bonneville (Figure 6.8) reflected the rapid climatic fluctuations experienced in the late Pleistocene. The two packrat midden study sites, the Painted Hills and the Snake Range, are closely situated to pluvial Lake Lahontan and Lake Bonneville, respectively (Figure 8.1). The lake level changes are inversely reflected by the isotopic variation recorded by packrat midden macrofossils, as demonstrated in Figures 8.2 and 8.3. Extensive continental glaciation to the north deflected the jet stream several degrees south (Benson, In Press), bringing a cooler, wetter climate to the region. In response, the lakes grew and the isotopic composition of local precipitation became more depleted, and this was recorded in the flora of the day. Similarly,

when the glaciers receded and the jet stream returned to the north, the lakes fell and the midden macrofossils recorded a rapid isotopic enrichment.

The same relationship is displayed in comparing the lake level chronologies to the deuterium vs. radiocarbon age of thermal waters from northern Nevada (Figure 8.4). The geothermal fluids are most isotopically depleted at the time the lakes are rising, reflecting the cooler, wetter climate.

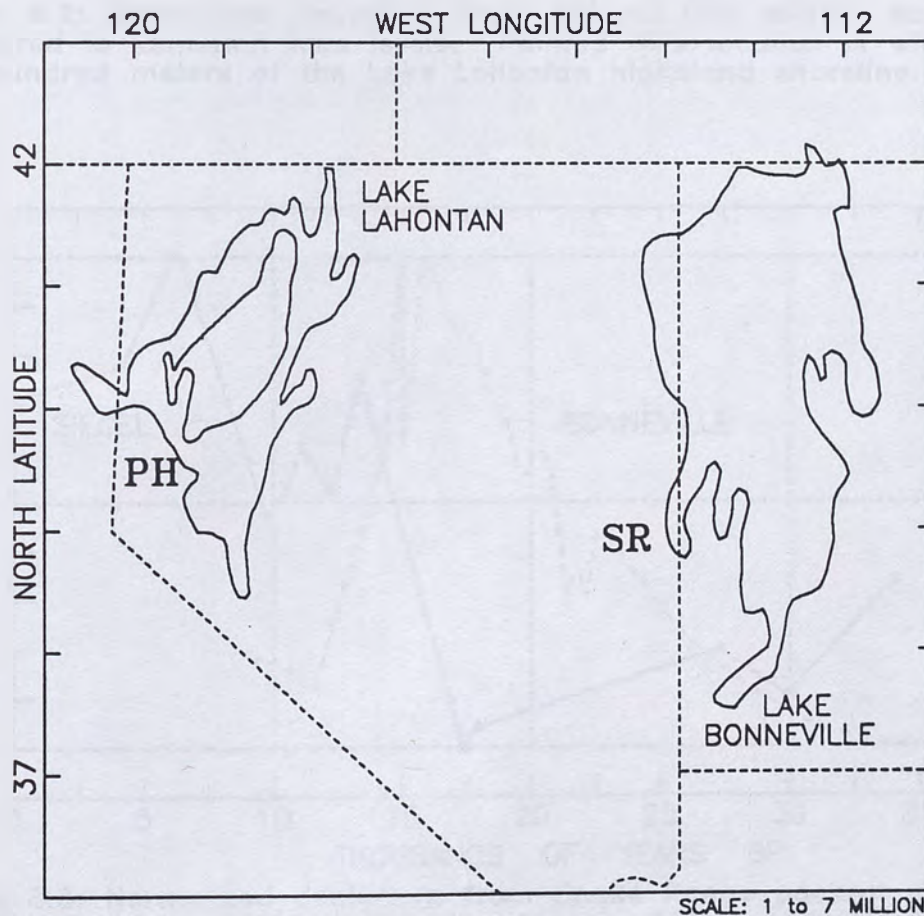


Figure 8.1: Location of the Painted Hills (PH) and Snake Range (SR) midden studies in relation to Lake Lahontan and Lake Bonneville.

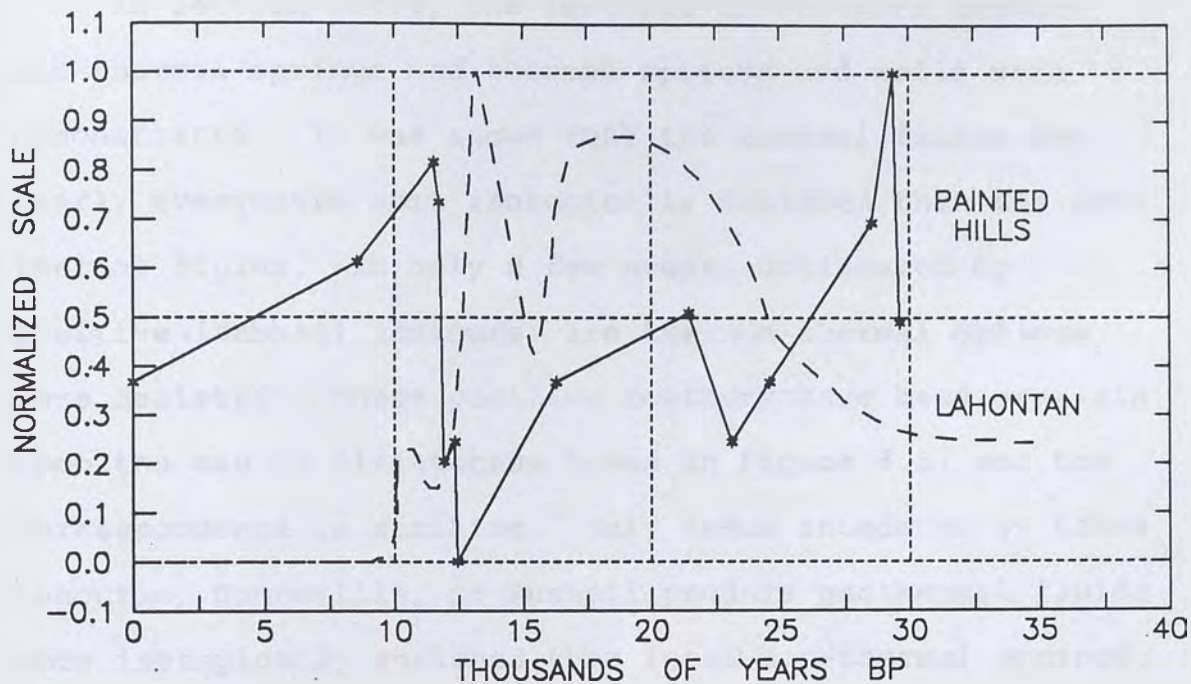


Figure 8.2: Normalized deuterium from Painted Hills midden samples compared to Lahontan lake levels. Painted Hills location is within a few hundred meters of the Lake Lahontan highstand shoreline.

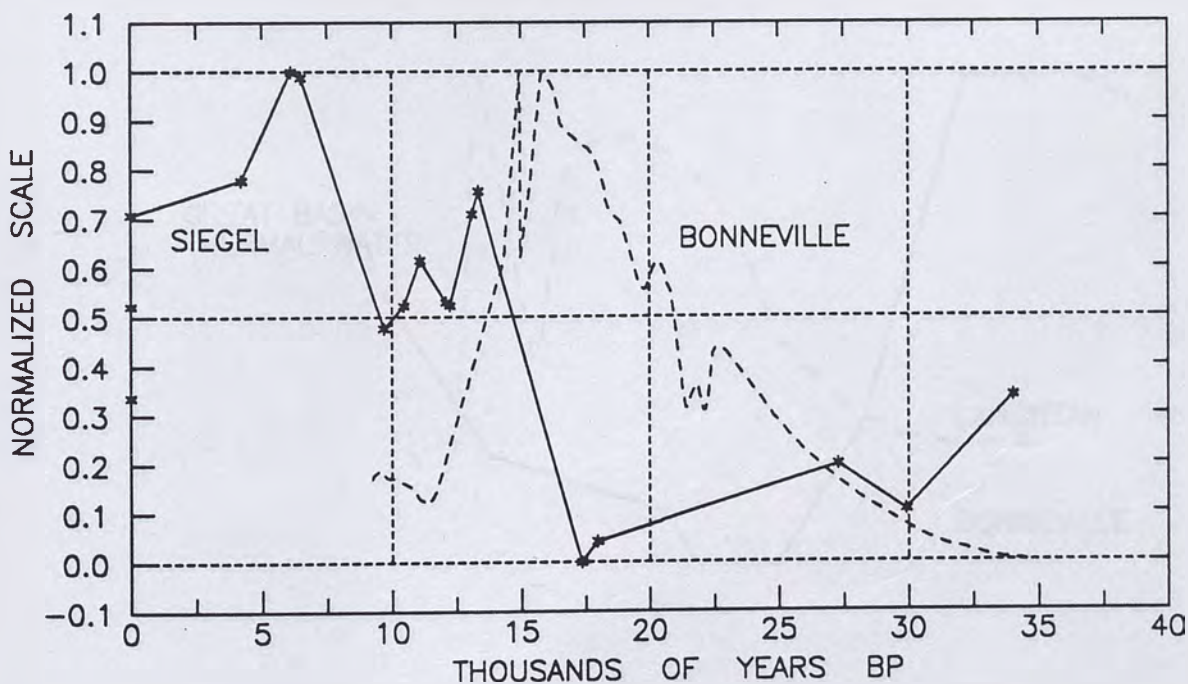


Figure 8.3: Normalized deuterium from Snake Range packrat middens and Bonneville lake level variations. Siegel midden study location is quite near the southwest arm of Lake Bonneville.

In section 7.1.4, the isotopic differences between non-thermal springs and thermal springs and wells were demonstrated. It was shown that the thermal fluids are nearly everywhere more isotopically depleted than the non-thermal fluids. In only a few areas, delineated by positive (dashed) contours, are the non-thermal springs more depleted. These positive contours have been overlain upon the map of Pleistocene lakes in Figure 8.5, and the correspondence is striking. Only areas inundated by Lakes Lahontan, Bonneville, or Russell produce geothermal fluids more isotopically enriched than local non-thermal springs. A lack of thermal water causes the absence of positive contours in the northern Bonneville Basin.

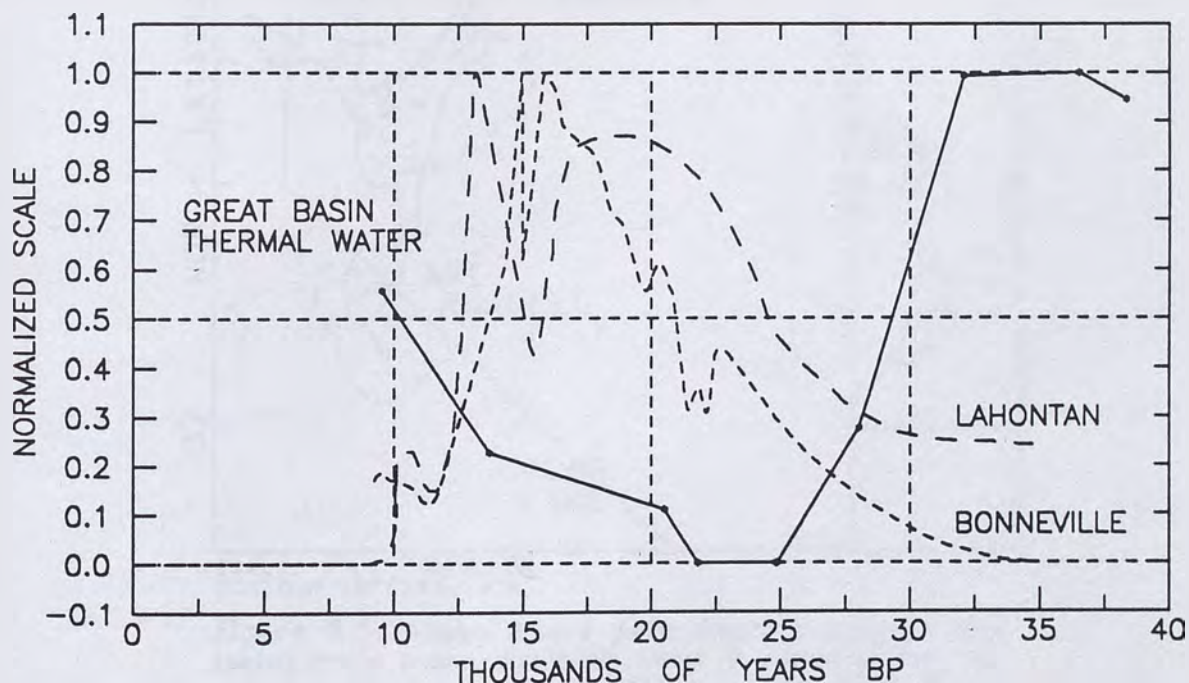
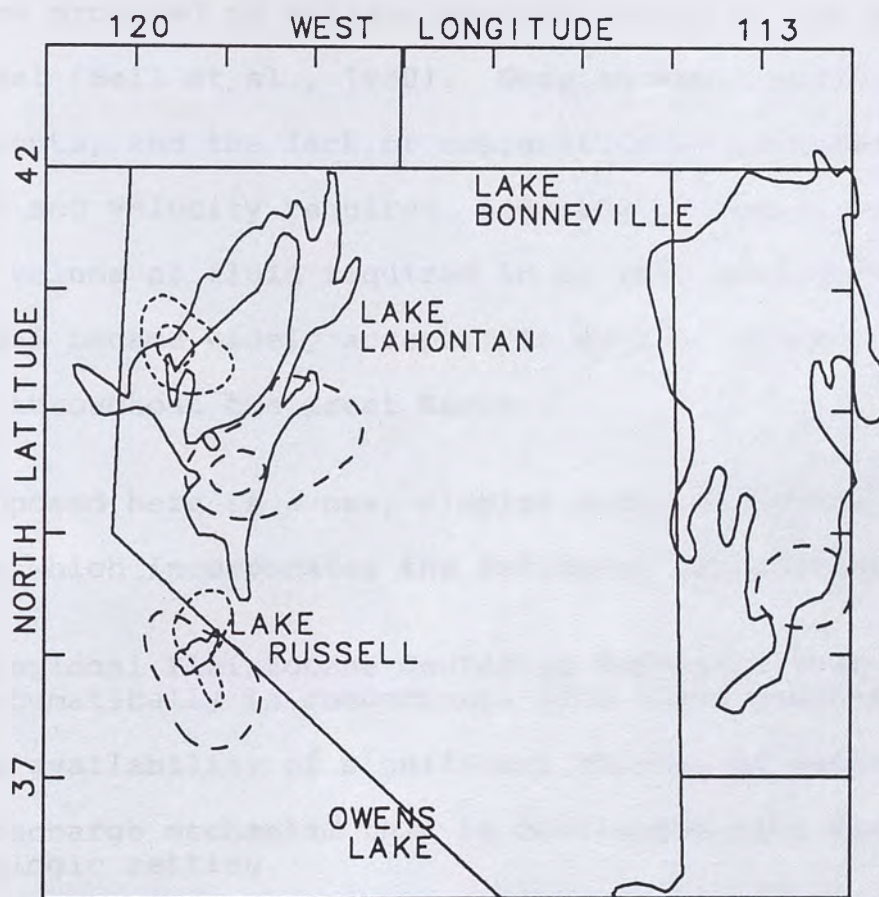


Figure 8.4: Deuterium vs. radiocarbon age of thermal waters greater than 90°C, compared to the level chronology of Lake Lahontan and Lake Bonneville. Note how the trends are inversely related.

A standing body of water will undergo isotopic exchange with the atmosphere, and be moved to more enriched levels (section 3.2). It is apparent that isotopically enriched lake water, leaking from beneath the Pleistocene lakes, contributed to the recharge of geothermal fluids. How this recharge took place is the subject of the following section.



SCALE: 1 to 7 MILLION
CONTOUR INTERVAL = 4

Figure 8.5: Areas where non-thermal springs are isotopically more depleted than thermal water in relation to major pluvial lakes. Long dash lines indicate thermal wells and short dash lines indicate thermal springs. Contours represent permil deuterium difference from Figures 7.13 and 7.14.

8.2 RECHARGE SCHEMES

Geothermal recharge models have previously relied upon local precipitation falling at high elevations to account for isotopic concentrations in geothermal fluids (Nehring, 1980; Fournier et al., 1980). It was proposed that these fluids rapidly circulated downward to a high-temperature zone, and returned along vertical faults (Figure 8.6). Complicated models involving fluid mixing and/or evaporation were produced to explain contradictions to the standard model (Bell et al., 1980). Despite the complicated requirements, and the lack of explanation of groundwater flowpath and velocity required, and lack of source to supply the volume of fluid required in an arid environment, this model became widely accepted to explain geothermal systems throughout the Great Basin.

Proposed here is a new, simpler model of Pleistocene recharge which incorporates the following key elements:

- a regional Pleistocene deuterium depletion that varies systematically in concurrence with fluid geochemistry,
- the availability of significant volumes of water,
- a recharge mechanism that is consistent with the known geologic setting,
- a provides for an extended period of time for fluid recharge to occur.

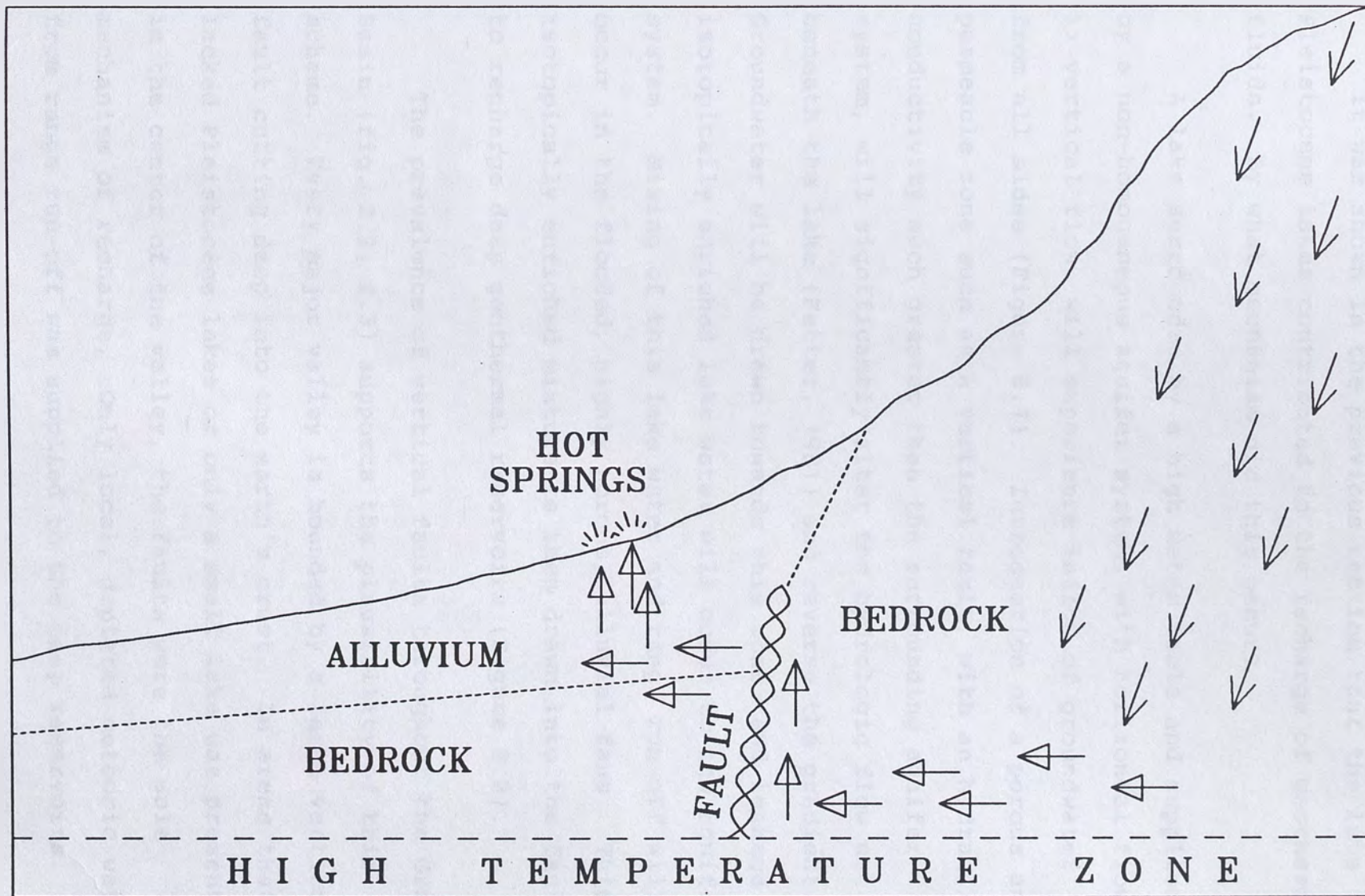


Figure 8.6: Historical recharge model, which relied upon rapid recharge to circulate modern meteoric water great

distances, laterally from the range-top source as well as vertically to and from the heat source or reservoir.

It was shown in the previous section that the late Pleistocene lakes contributed to the recharge of geothermal fluids. By what mechanism did this occur?

A lake surrounded by a high water table and supplied by a non-homogeneous aquifer system, with horizontal flow >> vertical flow, will experience inflow of groundwater from all sides (Figure 8.7). Introduction of a porous and permeable zone such as a vertical fault, with an hydraulic conductivity much greater than the surrounding aquifer system, will significantly alter the hydrologic flow net beneath the lake (Fetter, 1981) and reverse the gradient. Groundwater will be drawn towards this zone, and leakage of isotopically enriched lake water will occur to the aquifer system. Mixing of this lake water and range run-off will occur in the flooded, highly porous, alluvial fans. This isotopically enriched mixture is then drawn into the fault to recharge deep geothermal reservoirs (Figure 8.8).

The prevalence of vertical faults throughout the Great Basin (fig. 2.2, 2.3) supports the plausibility of this scheme. Every major valley is bounded by a large vertical fault cutting deep into the earth's crust. In areas that lacked Pleistocene lakes or only a small lake was present in the center of the valley, the faults were the sole mechanism of recharge. Only local, depleted meteoric water from range run-off was supplied to the deep reservoirs.

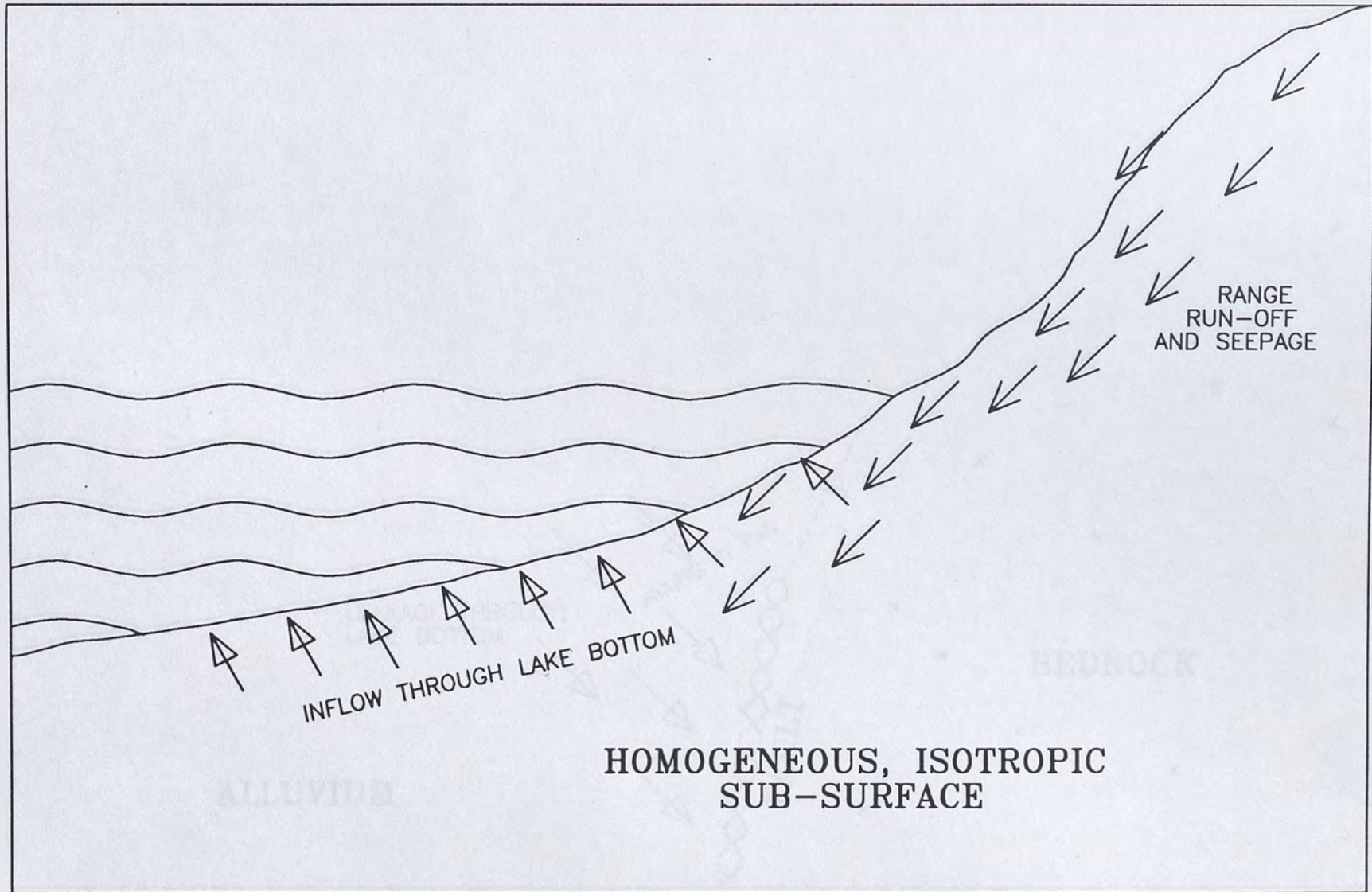


Figure 8.7: Flowpath for lake seepage and range run-off when homogeneous, isotropic sub-surface conditions exist

beneath a lake (Fetter, 1981). The lake will experience seepage through its bottom from all sides.

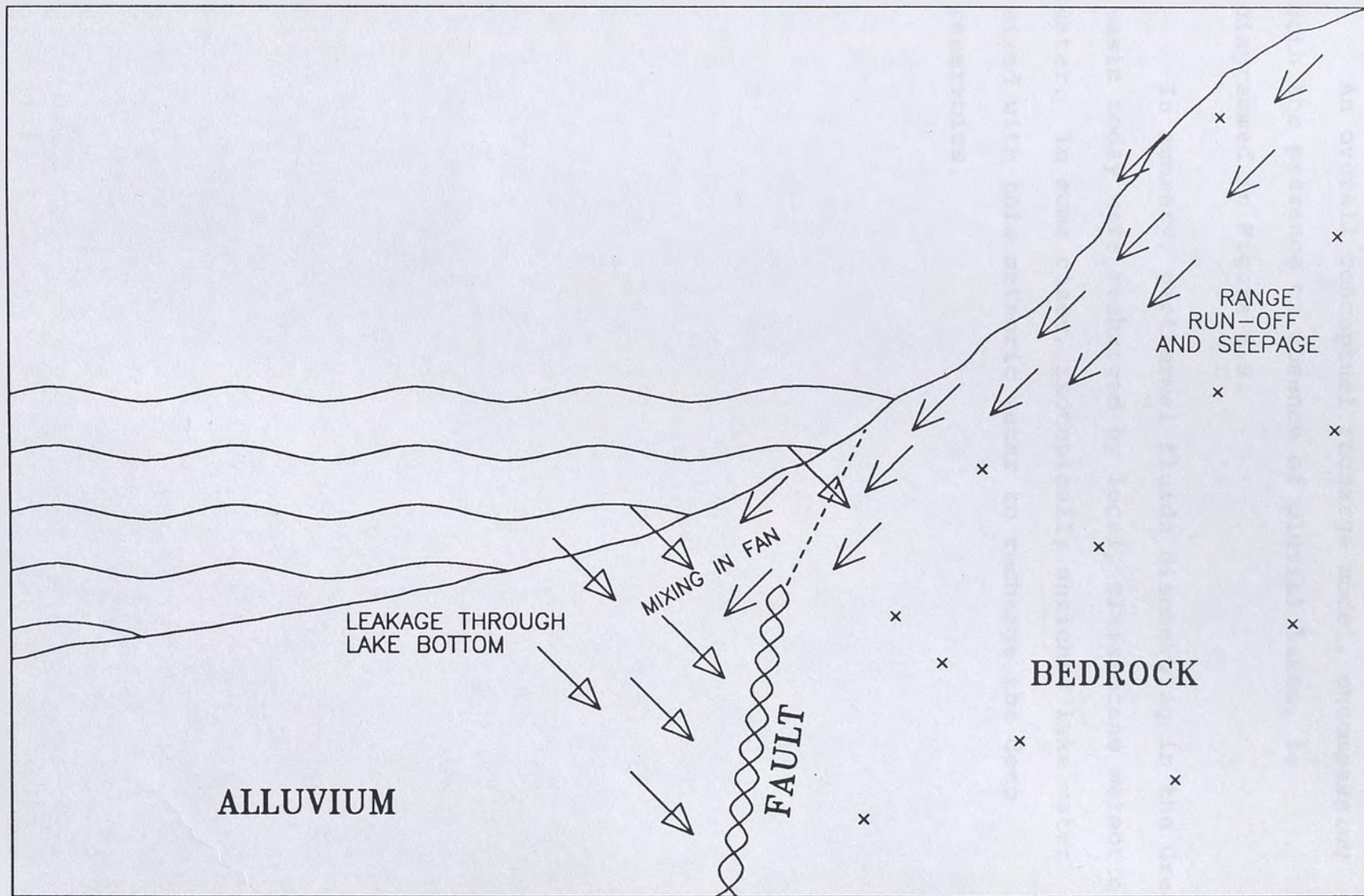


Figure 8.8: Suggested flowpath for lake seepage and range run-off. Mixing occurs in the flooded fan. The fault serves as a conduit to recharge deep, geothermal reservoirs with a slightly isotopically enriched mixture.

An overall conceptual recharge model, encompassing both the presence or absence of pluvial lakes, is diagrammed in Figure 8.9.

In summary, geothermal fluids discharging in the Great Basin today were recharged by local, Pleistocene meteoric water. In some cases, isotopically enriched lake water mixed with this meteoric water to recharge the deep reservoirs.

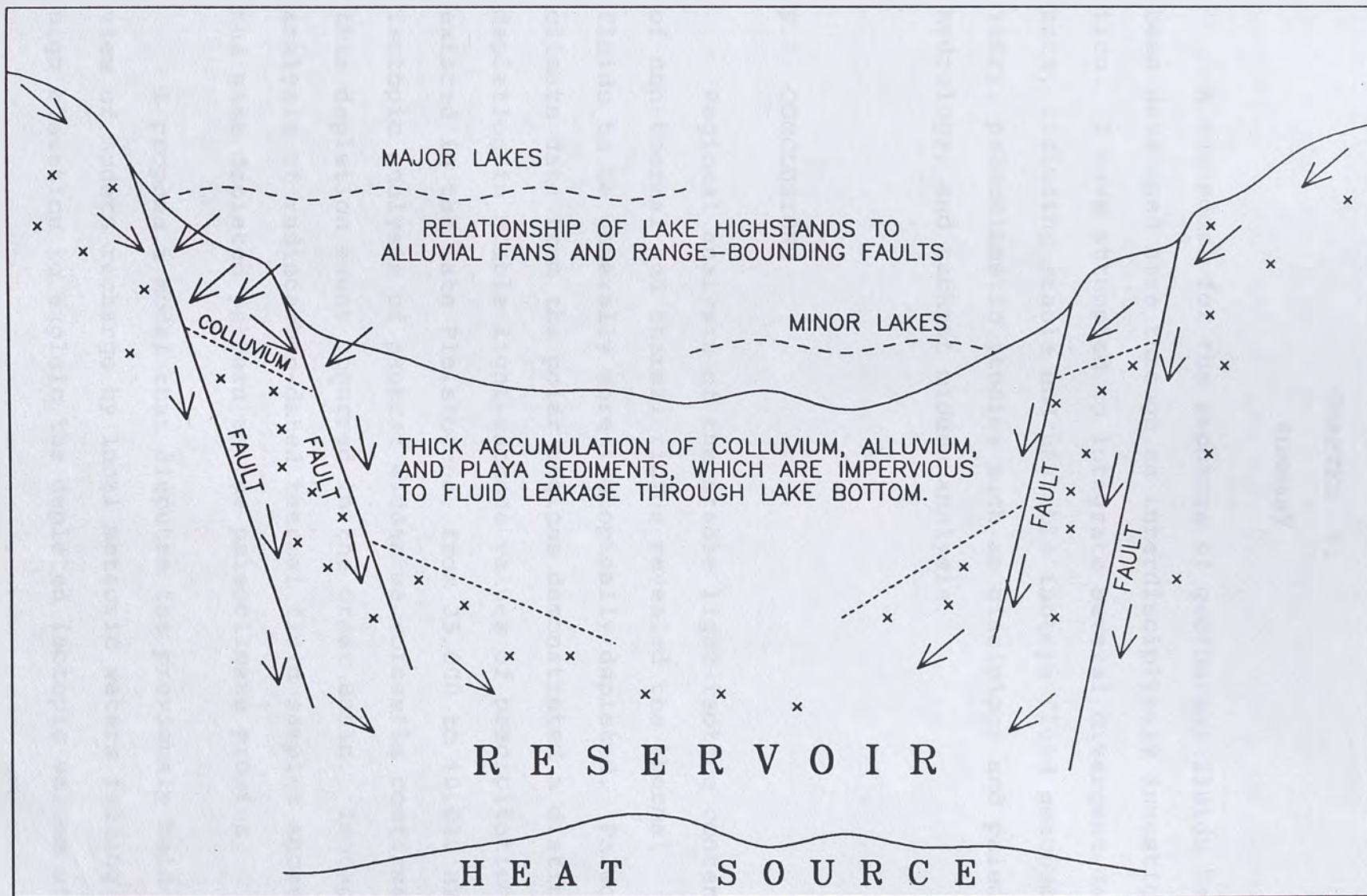


Figure 8.9: New conceptual model of geothermal recharge involving high-angle Basin and Range style faulting, range

run-off, and fluid contribution from pluvial lakes where large enough to saturate the alluvial fans above faults.

CHAPTER 9.

SUMMARY

A new model for the recharge of geothermal fluids has been developed here through an interdisciplinary investigation. I have attempted to integrate several divergent data sets, including stable and unstable isotope fluid geochemistry, paleoclimatic studies such as glaciology and paleohydrology, and packrat midden analysis.

9.1 CONCLUSIONS

Regional analysis of the stable light-isotope content of non-thermal and thermal fluids revealed the thermal fluids to be generally more isotopically depleted. Paleoclimate data from the polar regions demonstrated a distinct depletion in stable light-isotope values of precipitation existed in the late Pleistocene, from 35,000 to 10,000 BP. Isotopic analysis of packrat midden macrofossils confirmed this depletion event occurred in the Great Basin. Isotopic analysis of radiocarbon-dated thermal fluid samples showed the same depleted pattern as the paleoclimate proxies.

I propose a model that disputes the previously held view of modern recharge by local meteoric waters falling at high elevation to explain the depleted isotopic values of

geothermal fluids. Instead, I propose that recharge of the geothermal reservoirs occurred in the late Pleistocene, during a colder, wetter phase of climate. In a few areas, major Pleistocene lakes contributed some component of the fluid recharge.

9.2 RECOMMENDATIONS

Isotopic analysis of packrat midden macrofossils would appear to provide an excellent record of local climatic change. Extensive sampling and analysis of middens could provide accurate information on the timing of climate change across the Great Basin.

Time-variant isotopic analysis of geothermal fluids from power plant production wells spanning a full decade, could potentially give clues to reservoir life. A gradual enrichment in the isotopic value of the fluids would suggest younger fluids are being tapped. Where possible (Beowawe, Steamboat Springs, Dixie Valley), local hot springs should be studied in conjunction with the geothermal fluids. Geothermal wells by-pass the upward migration phase of the circulatory system, and may produce an isotopically different water than the hot springs.

REFERENCES CITED

- Aswathanarayana, 1985, Principles of Nuclear Geology, A.A. Balkema, Rotterdam, 397p.
- Bell, E.J. and L.T. Larson, eds., 1980, Geothermal reservoir assessment case study, northern Basin and Range Province, northern Dixie Valley, Nevada; Volume III: Mackay Minerals Research Institute, University of Nevada Reno, 117p.
- Benoit, W.R., J.E. Hiner, and R.T. Forest, 1982, Discovery and geology of the Desert Peak geothermal field; A case history: Nevada Bureau of Mines and Geology Bulletin 97, 82p.
- Benson, L.V., D.R. Curry, R.I. Dorn, K.R. Lajoie, C.G. Oviatt, S.W. Robinson, G.I. Smith, S. Stine, and R.S. Thompson, In Press, Variation in sizes of four Great Basin lake systems during the past 35,000 years: Unpublished Manuscript, to be published in a special issue of Paleo-3, "Paleolakes and Oceans".
- Benson, L.V., 1988, Preliminary paleolimnologic data for the Walker Lake subbasin, California and Nevada: U.S. Geological Survey Water Resources Investigations Report 87-4258, 50p.
- Benson, L.V. and R.S. Thompson, 1987, Lake level variation in the Lahontan Basin for the past 50,000 years: Quaternary Research, v.28, p.69-85.
- Benson, L.V., J.H. Robinson, R.K. Blankennagel, and A.E. Ogard, 1983, Chemical composition of groundwater and the locations of permeable zones in the Yucca Mountain area, Nevada: U.S. Geological Survey Open-File Report 83-854, 19p.
- Benson, L.V., 1981, Paleoclimatic significance of lake level fluctuations in the Lahontan Basin: Quaternary Research, v.16, p.390-403.
- Benson, L.V., 1978, Fluctuation in the level of Pluvial Lake Lahontan during the last 40,000 years: Quaternary Research, v.9, p.300-318.

- Berger, D.L., K.C. Kilroy, and D.H. Schaefer, 1987, Geophysical logs and hydrologic data for eight wells in the Coyote Spring Valley area, Clark and Lincoln Counties, Nevada: U.S. Geological Survey Open-File Report 87-679, 58p.
- Blackett, R.E., M.A. Shubat, D.S. Chapman, C.B. Forster, and C.B. Schlinger, 1989, An assessment of geothermal resources at Newcastle, Utah: Geothermal Resources Council Transactions, v.13, p.109-116.
- Blackwell, D.D., 1983, Heat Flow in the northern Basin and Range Province: Geothermal Resources Council Special Report 13, p.81-91.
- Boughton, C.J., 1986, Integrated geochemical and hydraulic analyses of Nevada Test Site groundwater systems: University of Nevada Reno, Masters Thesis #2090, 135p.
- Bowman, J.R. and D. Cole, 1982, Hydrogen and oxygen isotope geochemistry of cold and warm springs from the Tuscarora, Nevada, thermal area: Geothermal Resources Council Transactions, v.6, p.77-80.
- Broecker, W.S. and A. Kaufman, 1965, Radiocarbon chronology of lake Lahontan and Lake Bonneville II, Great Basin: Geological Society of America Bulletin, v.76, p.537-566.
- Campana, M.E., 1981, Environmental isotopes in natural recharge investigations: Water Resources Research Conference.
- Claassen, H.C., 1985, Sources and mechanisms of recharge for groundwater in the west-central Amargosa Desert, Nevada - A geochemical interpretation: U.S. Geological Survey Professional Paper 712-F, 31p.
- Clayton, R.N., I. Freidman, D.L. Graff, T.K. Mayeda, W.F. Meets, and N.F. Shimp, 1966, Origin of saline formation waters. I. - Isotopic Composition: Journal of Geophysical Research, v.71, p.3869-3882.
- Cole, D.R., 1983, Chemical and isotopic investigation of warm springs associated with normal faults in Utah: Journal of Volcanology and Geothermal Research, v.16, p.65-98.
- Coplen, T.B. and B.B. Hanshaw, 1973, Ultrafiltration by a compacted clay membrane - I. Oxygen and hydrogen isotopic fractionation: Geochimica et Cosmochimica Acta, v.37, p.2295-2310.

- Coplen, T.B., 1988, Normalization of oxygen and hydrogen isotope data: Chemical Geology - Isotope Geoscience Section, v.72, p.293-297.
- Craig, H., 1961, Standard for reporting concentrations of deuterium and oxygen-18 in natural waters: Science, v.133, p.1833-1934.
- Craig, H., 1963, The isotope geochemistry of water and carbon in geothermal areas: Consiglio Nazionale delle Ricerche, Laboratorio di Geologia Nucleare, Pisa, 53p.
- Dansgaard, W., H.B. Clausen, N. Gundestrup, S.J. Johnsen, and C. Rygner, 1985, Dating and climatic interpretation of two Greenland ice cores: in, Langway, C.C., H. Oerscher, and W. Dansgaard, eds., Greenland Ice Core: Geophysics, Geochemistry, and the Environment, p.71-76.
- Dansgaard, W., S.J. Johnsen, J. Moller, and C.C. Langway, Jr., 1969, One thousand centuries of climatic record from Camp Century on the Greenland Ice Sheet: Science, v.166, p.377-381.
- Dansgaard, W., 1964, Stable isotopes in precipitation: Tellus, v.16, n.4, p.436-468.
- Day, G.A., 1987, Source of recharge to the Beowawe geothermal system, north-central Nevada: University of Nevada Reno, Masters Thesis #2170, 82p.
- de Vries, H., 1958, Variation in concentration of radiocarbon with time and location on earth: Proceeding Koninkl. Ned. Akad. Wetenschap, B61, p.94-102.
- Edmiston, R.C. and W.R. Benoit, 1985, Basin and Range geothermal systems with fluid temperatures of 150° to 200°C: Geothermal Resources Council Bulletin, v.14, n.4, p.3-10.
- Faure G., 1986, Principles of Isotope Geology, 2nd ed., John Wiley, New York, 589p.
- Fenneman, N.M., 1931, Physiography of Western United States, McGraw Hill, New York.
- Fetter, C.W. Jr., Applied Hydrology, Charles Merrill, Columbus, Ohio, 488p.

- Flynn, T. and G. Ghush, Jr., 1984, Geologic and hydrologic research on the Moana geothermal system, Washoe County, Nevada, final report: Division of Earth Sciences, Environmental Research Center, University of Nevada Las Vegas, 148p.
- Fournier, R.O., 1981, Application of water geochemistry to geothermal systems: in Ryback, L. and L.J.P. Muffler, eds., Geothermal Systems: Principles and Case Histories, John Wiley and Sons, New York, p.109-143.
- Fournier, R.O. and J.M. Thompson, 1980, The recharge area for the Coso, California, geothermal system deduced from δD and $\delta^{18}O$ in thermal and non-thermal waters in the region: U.S. Geological Survey Open-File Report 80-454, 25p.
- Fournier, R.O., M.L. Sorey, R.H. Mariner, and A.H. Truesdell, 1979, Chemical and isotopic prediction of aquifer temperatures in the geothermal system at Long Valley, California: Journal of Volcanology and Geothermal Research, v.5, p.17-34.
- Fournier, R.O., 1977, Chemical geothermometers and mixing models for geothermal systems: Geothermics, v.5, p.41-50.
- Fournier, R.O. and J.J. Rowe, 1966, Estimation of underground temperatures from the silica content of water from hot springs and wet-steam wells: American Journal of Science, v.64, p.685-697.
- Fritz, P. and J.Ch. Fontes, eds., 1980, Handbook of Environmental Isotope Geochemistry, Volume 1: The Terrestrial Environment, A: Elsevier Scientific Publishing Company, Amsterdam, 545p.
- Garside, L.J. and J.H. Schilling, 1979, Thermal waters of Nevada: Nevada Bureau of Mines and Geology Bulletin 91, 163p.
- Garside, L.J., 1974, Geothermal exploration and development in Nevada through 1973: Nevada Bureau of Mines and Geology Report 21, 12p.
- Gat, J.R., 1981, The isotopes of hydrogen and oxygen in precipitation: In P. Fritz and J.Ch. Fontes, eds., Handbook of Environmental Isotope Geochemistry, Volume 1: The Terrestrial Environment, A, p.21-47.

- Glancy, P.A., 1986, Geohydrology of the basalt and unconsolidated sedimentary aquifers in the Fallon area, Churchill County, Nevada: U.S. Geological Survey Water Supply Paper 2263, 62p.
- Higgins, C.T., T. Flynn, R.H. Chapman, D.T. Trexler, G.W. Chase, C.F. Bacon, and G. Ghosn, Jr., 1985, Geothermal systems of the Mono Basin - Long Valley region, eastern California and western Nevada: California Division of Mines and Geology, Open-File Report 85-19, 159p.
- Higgins, C.T., R.H. Chapman, and G.W. Chase, 1983, Geothermal resources of the Bridgeport-Bodie Hills region, California: California Division of Mines and Geology, Open-File Report 83-14, 105p.
- Hoefs, J., 1987, Stable Isotope Geochemistry, 3rd ed., Springer-Verlag, Heidelberg, 208p.
- Hose, R.K. and B.E. Taylor, 1974, Geothermal systems of northern Nevada: U.S. Geological Survey Open-File Report 74-271, 27p.
- Houghton, J.G., C.M. Sakamoto and R.O. Gifford, 1975, Nevada's Weather and Climate: Nevada Bureau of Mines and Geology Special Publication 2, 78p.
- Ingraham, N.L., 1986, Environmental isotope hydrology of the Dixie Valley geothermal system, Dixie Valley, Nevada: University of Nevada Reno, Masters Thesis #1620, 96p.
- Ingraham, N.L. and B.E. Taylor, 1982, Hydrogen isotope study of large scale meteoric water transport in northern California and Nevada: Journal of Hydrology, v.85, p.183-197.
- Jacobson, R.L., N.L. Ingraham, and M.E. Campana, 1983, Isotope hydrology of a Basin and Range geothermal system: University of Nevada System - Desert Research Institute, Water Resources Center Publication #41087, 18p.
- Janik, C.J., N.L. Nehring, and A.H. Truesdell, 1983, Stable isotope geochemistry of thermal fluids from Lassen Volcanic National Park, California: Geothermal Resources Council Transactions, v.7, p.295-300.
- Kirk, S.T., 1987, Analysis of the White river groundwater flow system using a deuterium calibrated discrete state compartment model: University of Nevada Reno, Masters Thesis #2248, 81p.

- Lyles, B.F., 1985, Time-variant hydrogeologic and geochemical study of selected thermal springs in western Nevada: University of Nevada Reno, Masters Thesis #2008, 202p.
- Lyles, B.F. and J.W. Hess, 1988, Isotope and ion geochemistry in the vicinity of the Las Vegas Valley Shear Zone: University of Nevada System - Desert Research Institute, Water Resources Center Publication #41111, 78p.
- McKay, A.W. and D.E. Zimmerman, 1983, Hydrogeochemical investigation of thermal springs in the Black Canyon - Hoover Dam area, Nevada and Arizona: University of Nevada System - Desert Research Institute, Water Resources Center Publication #41092, 40p.
- Mariner, R.H., H.W. Young, and T.S. Presser, 1989, Geochemistry of thermal water from selected wells, Boise, Idaho: Geothermal Resources Council Transactions, v.13, p.173-178.
- Mariner, R.H., T.S. Presser, and W.C. Evans, 1983, Geochemistry of active geothermal systems in the northern Basin and Range Province: Geothermal Resources Council, Special Report 13, p.95-119.
- Mariner, R.H., T.S. Presser, and W.C. Evans, 1976, Chemical data of eight springs in northwestern Nevada: U.S. Geological Survey Open-File Report, 13p.
- Mariner, R.H., T.S. Presser, J.B. Rapp, and L.M. Willey, 1975, The minor and trace elements, gas, and isotope compositions of the principal hot springs of Nevada and Oregon: U.S. Geological Survey Open-File Report, 27p.
- Mariner, R.H., J.B. Rapp, L.M. Willey, and T.S. Presser, 1974, The chemical composition and estimated minimum thermal reservoir temperatures of the principal hot springs of northern and central Nevada: U.S. Geological Survey Open-File Report, 32p.
- Martinson, D.G., N.G. Pisias, J.D. Hayes, J. Imbrie, T.C. Moore, Jr., and N.J. Shackleton, 1987, Age dating and the orbital theory of the Ice Ages; Development of a high resolution 0 to 300,000 year chronostratigraphy: Quaternary Research, v.27, p.1-27.
- Michael, H.N. and E.K. Ralph, 1970, Correction factors applied to Egyptian radiocarbon dates from the era before Christ: In I.U. Olsson, ed., Radiocarbon Variations and Absolute Chronology, p.109-119.

- Mifflin, M.D., 1968, Delineation of groundwater flow systems in Nevada: University of Nevada System - Desert Research Institute, Water Resources Center Publication #42004, 103p.
- Milankovitch, M., 1941, Kanon der Erdbestrahlung und sei Eiszeitenproblem. Acad. R. Serbe (Belgrade), ed. Spec. 133 Sect. Sci. Math. Naturales, 633p.
- Muffler, L.J.P., ed., 1978, Assessment of geothermal resources of the United States - 1978: U.S. Geological Survey Circular 790, 163p.
- Nathenson, M., N.L. Nehring, E.G. Croswaithe, R.S. Harmon, C. Janik, and J. Borthwick, 1982, Chemical and light-stable isotope characteristics of waters from the Raft River geothermal area and environs, Cassia County, Idaho, Box Elder County, Utah: Geothermics, v.11, n.4, p.215-237.
- Nehring, 1980, Geochemistry of Steamboat Springs, Nevada: U.S. Geological Survey Open-File Report 80-887, 61p.
- Reed, M.J., 1975, Chemistry of thermal waters in selected geothermal area of California: California Division of Oil and Gas Publication TR-15, 31p.
- Rohrs, D.T. and J.R. Bowman, 1980, A light stable isotope study of the Roosevelt Hot Springs area, southwestern Utah: Department of Geology and Geophysics, University of Utah, Topical Report, 89p.
- Roth, J.G., 1988, Delineation of the Railroad Valley flow system using a deuterium calibrated groundwater model: University of Nevada Reno, Masters Thesis #2439, 156p.
- Schiegl, W.E. and J.C. Vogel, 1969, Deuterium content of organic matter: Earth and Planetary Science Letters, v.7, p.307-313.
- Seuss, H.E., 1955, Radiocarbon concentration in modern wood: Science, v.122, p.415-417.
- Siegel, R.D., 1983, Paleoclimatic significance of D/H and $^{13}\text{C}/^{12}\text{C}$ ratios in Pleistocene and Holocene wood: University of Arizona, Masters Thesis, 105p.
- Snyder, C.T., G. Hardman, and F.F. Zdenk, 1964, Pleistocene lakes in the Great Basin: U.S. Geological Survey Miscellaneous Geologic Investigations Map I-416, Scale 1:1,000,000.

- Spaulding, W.G., 1985, Vegetation and climates of the past 45,000 years in the vicinity of the Nevada Test Site, south-central Nevada: U.S. Geological Survey Professional Paper 1329, 83p.
- Spaulding, W.G., 1981, The late Quaternary vegetation of a southern Nevada mountain range: University of Arizona, Ph.D. Dissertation, Tucson, Arizona, 271p.
- Stewart, J.H., 1983, Cenozoic structure and tectonics of the northern Basin and Range Province, California, Nevada, and Utah: Geothermal Resources Council Special Report 13, p.25-40.
- Stuiver, M., 1981, Atmospheric ^{14}C changes resulting from fossil fuel CO_2 release and cosmic ray flux variability: Earth and Planetary Science Letters, v.53, p.349-362.
- Stuiver, M., 1970, Long term ^{14}C variations: In I.U. Olsson, ed., Radiocarbon Variations and Absolute Chronology, p.197-213.
- Szecsody, J.E., 1982, Use of major ion chemistry and environmental isotopes to delineate subsurface flow in Eagle Valley, Nevada: University of Nevada Reno, Masters Thesis #1715, 195p.
- Thompson, R.S., L.V. Benson, and E.M. Hattori, 1986, A revised chronology of the last Pleistocene lake cycle in the central Lahontan Basin: Quaternary Research, v.25, p.1-9.
- Thompson, R.S. and J.I. Mead, 1981, Late Quaternary environments and biogeography in the Great Basin: Quaternary Research, v.17, p.39-55.
- Trexler, D.T., T. Flynn, B.A. Koenig, E.J. Bell, and G. Ghusn, Jr., 1982, Low to moderate temperature geothermal resource assessment for Nevada; area specific studies; Pumpernickel Valley, Carlin and Moana: Division of Earth Sciences, Environmental Research Center, University of Nevada Las Vegas, 178p.
- Trexler, D.T., B.A. Koenig, T. Flynn, J.L. Bruce, and G. Ghusn, Jr., 1981, Area specific geothermal assessment, Nevada; Hawthorne, Paradise Valley, Carson Sink, and state wide assessment: Nevada Bureau of Mines and Geology, 203p.

- Trexler, D.T., B.A. Koenig, T. Flynn, and J.L. Bruce, 1980b, Assessment of the geothermal resources of Carson-Eagle Valleys and Big Smoky Valley, Nevada, Final Report: Nevada Bureau of Mines and Geology, 162p.
- Trexler, D.T., T. Flynn, B.A. Koenig, and J.L. Bruce, 1980a, Assessment of the geothermal resources of Caliente, Nevada, Final Report: Nevada Bureau of Mines and Geology, 23p.
- U.S. Geological Survey, GEOTHERM; Geothermal data base for California.
- Vuatz, F.D. and F. Goff, 1987, Water geochemistry and hydrogeology of the shallow aquifer at Roosevelt Hot Springs, southern Utah: Los Alamos National Laboratories Report LA-11160-HDR, 63p.
- Welch, A.H. and A.M. Preissler, 1986, Aqueous geochemistry of the Brady's Hot Springs Geothermal Area, Churchill County, Nevada: U.S. Geological Survey Water Supply Paper 2290, p.17-36.
- Welch, A.H., 1985, Geothermal Resources of the western Black Rock Desert, northwestern Nevada; hydrology and aqueous geochemistry: University of Nevada Reno, Doctoral Dissertation #2040, 139p.
- Welch, A.H., M.L. Sorey, and F.H. Olmstead, 1981, The hydrothermal system in southern Grass Valley, Pershing County, Nevada: U.S. Geological Survey Open-File Report 81-915, 193p.
- Wells, P.V. and C.D. Jorgenson, 1964, Pleistocene woodrat middens and climatic change in Mohave Desert; A record of Juniper woodlands: Science, v.143, p.1171-1174.
- White, A.F. and N.J. Chuma, 1987, Carbon and isotopic mass balance models of the Oasis Valley - Fortymile Canyon groundwater basin, southern Nevada: Water Resources Research v.23, n.4, p.571-582.
- White, D.E. and D.L. Williams, 1975, Assessment of geothermal resources of the United States - 1975: U. S. Geological Survey Circular 726, 155p.
- White, D., 1965, Geothermal energy: U.S. Geological Survey Circular 519, 17p.

- Winograd, I.J., B.J. Sabo, T.B. Coplen, and A.C. Riggs, 1988, A 250,000 year climatic record from vein calcite; implications for the Milankovitch Theory: *Science*, v.242, p.1275-1280.
- Winograd, I.J. B.J. Sabo, A.C. Riggs, and P.T. Kolesar, 1985, Two million year record of deuterium depletion in Great Basin groundwaters: *Science*, v.227, p.39-55.
- Winograd, I.J. and F.J. Pearson, Jr., 1976, Major Carbon-14 anomaly in a regional carbonate aquifer; possible evidence for megascale channelling, south-central Great Basin: *Water Resources Research* v.12, n.6, p.1125-1143.
- Winograd, I.J. and I. Friedman, 1972, Deuterium as a tracer of regional groundwater flow, southern Great Basin, Nevada and California: *Geological Society of America Bulletin*, v.83, p.3691-3708.
- Wollenberg, H.A., 1975, Radioactivity of geothermal systems: *Proceedings, Second United Nations Symposium on the Development and use of Geothermal Systems, San Francisco, California*, p.1283-1292.
- Young, H.W., 1985, Geochemistry and hydrology of thermal springs in the Idaho Batholith and adjacent areas, central Idaho: *U.S. Geological Survey Water Resource Investigations Report 85-4172*, 44p.
- Young, H.W. and R.E. Lewis, 1982, Geohydrology of geothermal systems: *U.S. Geological Survey Professional Paper 1044-J*, p.J1-J20.
- Yurtsever, Y., 1975, Worldwide survey of stable isotopes in precipitation: *Report Section Isotope Hydrology, International Atomic Energy Agency, Vienna*, 40p.

APPENDIX A

CURRENT STUDY - STABLE LIGHT-ISOTOPES AND GEOCHEMISTRY

GF #	SAMPLE NAME	REF	LOC	TYPE	LONG	LAT	ELEV meters	DEUT ‰	OX18 ‰	TEMP °C	DATE MO YR
1	Bradys Hot Springs	GFG	BDY	WELL	119.012	39.787	1253	-127	-14.2	141	1 89
2	Great Boiling Spring	GFG	BRD	SPRG	119.365	40.661	1207	-103	-10.9	91	1 89
3	Patua Hot Spring	GFG	CSK	SPRG	119.113	39.597	1237	-121	-12.4	86	1 89
4	Steamboat/Ormat	GFG	SMA	WELL	119.715	39.395	1433	-121	-12.4	113	1 89
5	Wabuska Tads #2	GFG	MSV	WELL	119.152	39.161	1311	-115	-15.8	107	1 89
6	Warren Estates #1	GFG	SMA	WELL	119.825	39.481	1402	-126	-15.9	88	1 89
7	Soda Lake 33-14	GFG	CSK	WELL	118.859	39.564	1213	-105	-10.8	183	2 89
8	Desert Peak 67-21	GFG	DPK	WELL	118.951	39.754	1340	-115	-12.3	158	2 89
9	Desert Peak 86-21	GFG	DPK	WELL	118.946	39.758	1366	-114	-12.1	159	2 89
10	Beowawe Ginn 1-13	GFG	BEO	WELL	116.616	40.554	1506	-132	-16.2	151	2 89
11	Beowawe Ginn 2-13	GFG	BEO	WELL	116.617	40.555	1506	-133	-15.9	153	2 89
12	Lee Hot Springs	GFG	FAL	SPRG	118.722	39.209	1222	-126	-13.4	93	2 89
13	Alkali Hot Spring	GFG	CLV	SPRG	117.335	37.825	1529	B	B	52	2 89
14	Hicks (Bailey) HS	GFG	AMG	SPRG	116.721	36.805	1097	-116	-14.5	40	2 89
15	Grapevine Spring	GFG	DVY	SPRG	117.384	37.024	756	-112	-13.9	32	2 89
16	Nevares Spring	GFG	DVY	SPRG	116.791	36.512	293	-105	-13.4	31	2 89
17	Tecopa Hot Spring	GFG	DVY	SPRG	116.231	35.872	427	-99	-12.6	42	2 89
18	Rogers Spring	GFG	MRV	SPRG	114.443	36.377	485	-95	-13.7	31	2 89
19	Ash Spring	GFG	WRV	SPRG	115.195	37.465	1100	-111	-14.2	30	2 89
20	Warm Spring	GFG	HCV	SPRG	116.377	38.187	1682	-118	-14.2	61	2 89
21	Golconda Hot Sp	GFG	PDV	SPRG	117.491	40.955	1341	-132	-15.8	58	2 89
23	Elko Jr Hi	GFG	ELK	WELL	115.761	40.839	1554	-151	-17.9	82	2 89
24	Elko Heat Company	GFG	ELK	WELL	115.775	40.825	1541	-149	-18.1	80	2 89
25	Bruffeys Hot Sp	GFG	PNE	SPRG	116.067	40.067	1783	-133	-16.3	62	2 89
26	Williams Hot Sp	GFG	WRV	SPRG	115.231	38.953	1931	-121	-15.6	53	2 89
27	Morman Spring	GFG	WRV	SPRG	115.142	38.763	1609	-125	-16.1	38	2 89
28	Chimney Hot Sp	GFG	RRV	SPRG	115.788	38.467	1465	-124	-15.9	66	2 89
33	Desert Peak 67-21	GFG	DPK	WELL	118.951	39.754	1340	-118	-12.1	163	5 89
34	Beowawe 1-13	GFG	BEO	WELL	116.616	40.554	1506	-131	-15.9	150	5 89
35	Wabuska Tads #2	GFG	MSV	WELL	119.152	39.161	1311	B	-16.2	107	5 89
36	Warm Spring	GFG	HCV	SPRG	116.377	38.187	1682	-119	-14.8	61	5 89
37	Elko Jr Hi	GFG	ELK	WELL	115.761	40.839	1554	-150	-18.6	80	5 89
38	Elko Heat Company	GFG	ELK	WELL	115.775	40.825	1541	-147	-18.4	81	5 89
39	Golconda Hot Spring	GFG	PDV	SPRG	117.491	40.955	1341	-132	-16.3	63	5 89
44	Soda Lake 33-14	GFG	CSK	WELL	118.859	39.564	1213	-106	-11.2	185	9 89
46	Beowawe Ginn 2-13	GFG	BEO	WELL	116.617	40.555	1506	-131	-16.1	154	9 89
47	Steamboat/Ormat	GFG	SMA	WELL	119.715	39.395	1433	-119	-13.0	113	9 89
48	Wabuska Tads #2	GFG	MSV	WELL	119.152	39.161	1311	-133	-16.4	107	9 89

APPENDIX A, continued

Current Study Data Set

GF #	pH	Ca	SO ₄	Na (All	K Analyses	SiO ₂	CO ₃ ⁺		Mg PPM)	Li	F	B	SPEC	SUM	MEAS
							HCO ₃	Cl In					COND mmhos	TDS	TDS
1	7.2	35	323	694	53	210	112	872	0.2	1.5	5.5	4.4		2311	2120
2	7.3	73	416	1488	113	169	97	2180	1.4	1.7	4.4	8.2		4552	4152
3	7.6	52	405	656	52	198	93	829	0.6	1.7	4.7	6.1		2298	2100
4	6.3	15	120	611	58	278	369	790	0.3	6.9	2.0	41.8		2292	2056
5	7.5	35	549	292	14	111	73	47	0.0	0.3	6.8	1.0		1129	1038
6	8.1	27	528	277	8	126	93	55	0.0	0.2	4.1	2.0		1120	950
7	5.7	109	48	2000	232	284	108	3400	0.4	3.8	1.0	13.4	10000	6200	6140
8	8.1	96	77	2190	235	303	38	3550	0.2	3.0	4.6	15.1	12000	6512	7320
9	8.0	87	70	2230	249	319	36	3740	0.2	3.0	4.3	15.6	12000	6754	7570
10	9.7	0	74	169	21	335	213	41	0.2	1.0	9.6	0.9	850	865	887
11	9.8	0	75	171	21	308	163	42	0.2	1.0	8.8	0.9	850	791	824
12	7.3	40	465	458	26	164	114	381	0.6	0.7	7.0	2.2		1659	1601
13	7.0	45	504	320	22	55	326	62	3.1	1.7	6.7	1.1		1347	1116
14	7.7	17	139	168	7	65	228	54	0.5	0.3	5.2	0.3		684	542
15	7.8	41	138	183	15	44	453	80	19.1	0.2	2.7	1.1		977	680
16	7.6	44	179	148	11	26	360	44	21.2	1.2	2.6	0.9		838	600
17	8.4	4	569	798	16	89	713	439	1.7	0.2	2.5	8.8		2641	2148
18	7.2	443	1740	323	21	20	163	338	140.4	0.6	1.4	0.9		3191	3064
19	7.6	47	37	28	6	29	257	14	19.0	0.0	0.5	0.1		438	272
20	6.8	70	98	193	23	48	704	36	22.0	0.6	3.0	0.4		1198	798
21	7.3	33	59	147	22	60	449	22	7.4	0.5	1.6	1.4		803	580
23	7.0	61	77	114	37	73	496	15	11.0	0.3	1.5	1.0		887	600
24	6.6	63	70	110	35	65	493	15	12.3	0.3	2.0	0.9		867	582
25	7.0	47	37	39	8	55	279	13	17.1	0.1	0.7	0.3		496	326
26	9.6	2	15	63	0	59	60	11	0.2	0.0	13.8	0.2		224	180
27	7.5	62	46	27	5	27	296	11	19.8	0.1	1.3	0.1		495	328
28	6.8	68	48	67	15	43	412	11	14.0	0.2	1.8	0.3		680	448
29	7.0	24	58	208	13	162	524	43	4.0	1.0	8.8	0.6		1046	745
30	9.2	1	47	104	2	104	126	13	0.0	0.3	14.5	0.3		412	348
31	9.1	4	119	110	1	51	63	39	0.0	0.0	4.6	1.0	505	393	362
32	5.9	100	59	1830	212	273	105	3220	0.7	3.4	1.1	12.6	10000	5817	6110
33	8.0	103	87	2220	238	302	42	3610	0.2	3.0	4.5	15.2	13000	6625	7300
34	9.8	0	66	168	20	330	224	40	0.2	0.9	9.9	0.9	1000	860	748
35	7.8	36	638	309	14	109	68	48	0.0	0.3	7.6	1.0	1250	1231	1198
36	6.6	72	101	211	24	52	686	36	23.7	0.7	3.8	0.4	1210	1211	864
37	6.8	61	74	120	36	76	471	21	11.7	0.3	2.1	0.9	850	874	637
38	6.7	63	73	109	35	67	477	20	12.3	0.3	1.8	26.3	850	885	624
39	7.2	32	58	148	22	60	419	28	7.5	0.5	2.6	10.3	815	788	576
44	5.5	105	62	1940	230	284	109	3310	0.7	3.6	0.7	12.8	9900		6040
46	9.8	1	77	184	22	331	269	48	0.2	1.1	11.1	1.0	845		831
47															
48															

B - Broken in shipment

GF-22 was not submitted for analysis

APPENDIX A, continued

LOC Symbol Key

LOC	BASIN NAME	LOC	BASIN NAME	LOC	BASIN NAME
AMG	AMARGOSA DESERT	HVU	HAMLIN VALLEY	SCY	SILVER CITY
AVY	ANTELOPE VALLEY	IDA	IDAHO	SFB	SARCOBATUS FLAT
BDY	BRADY'S HOT SPRINGS	IMP	IMPERIAL VALLEY	SHM	SHEEP MOUNTAINS
BEO	BEOWAWE	JVY	JAKES VALLEY	SHR	SHEEP RANGE
BOI	BOISE, IDAHO	KBV	KOBEH VALLEY	SMA	STEAMBOAT-MOANA
BRD	BLACK ROCK DESERT	LKT	LAKE TAHOE	SMD	SMOKE DESERT
BSV	BIG SMOKY VALLEY	LSV	LITTLE SMOKY VALLEY	SMV	SMITH CREEK VALLEY
BTV	BUTTE VALLEY	LVC	LONG VALLEY CALDERA	SNR	SNAKE RANGE
BUF	BUFFALO VALLEY	LVS	LAS VEGAS SHEAR ZONE	SPM	SPRING MOUNTAINS
BVY	BUENA VISTA VALLEY	MDC	MODOC PLATEAU	SPR	SPRING VALLEY
CAL	CALIENTE	MIN	MINERAL COUNTY	SPV	SURPRISE VALLEY
CAR	CARLIN	MIS	MISCELLANEOUS	SSN	SOUTHERN SIERRA
CEV	CARSON-EAGLE VALLEY	MON	MONITOR VALLEY	STV	STEPTOE VALLEY
CLV	CLAYTON VALLEY	MRV	MUDDY RIVER VALLEY	SVY	SIERRA VALLEY
COL	COLADO	MSV	MASON VALLEY	SWI	SOUTHWEST IDAHO
COS	COSO	NEN	NORTHEAST NEVADA	TMD	TAHOE MEADOWS
CRF	CRATER FLAT	NTS	NEVADA TEST SITE	TSC	TUSCARORA
CSK	CARSON SINK	NWK	NEWARK VALLEY	UDV	UTAH DUGWAY VALLEY
CSR	COSO RANGE	OAV	OASIS VALLEY	UFS	UTAH FISH SPRING FLAT
CSV	COYOTE SPRING VALLEY	ORE	OREGON	UNC	UTAH NEWCASTLE
CVY	COAL VALLEY	PAH	PAHRANAGAT VALLEY	UPV	UTAH PINE VALLEY
DLV	DELAMAR VALLEY	PDV	PARADISE VALLEY	USC	UTAH SOUTH-CENTRAL
DPK	DESERT PEAK	PHM	PAHUTE MESA	USD	UTAH SEVIER DESERT
DXV	DIXIE VALLEY	PHS	PAINTED HILLS	USL	UTAH GREAT SALT LAKE
ECV	EDWARDS CREEK VALLEY	PHV	PAHRUMP VALLEY	USV	UTAH SNAKE VALLEY
ELK	ELKO AREA	PLK	PYRAMID LAKE	USW	UTAH SOUTH-WESTERN
FAL	FALLON AREA	PLV	PLEASANT VALLEY	UTL	UTAH LAKE
FLV	FISH LAKE VALLEY	PNE	PINE VALLEY	UTV	UTAH TOOLE VALLEY
FMC	FORTYMILE CANYON	PNV	PENOYER VALLEY	UWC	UTAH WEST-CENTRAL
FVY	FAIRVIEW VALLEY	PPV	PUMPERNICKEL VALLEY	UWV	UTAH WAH WAH VALLEY
GDV	GARDEN VALLEY	PRG	PAHRANAGAT RANGE	UWW	UTAH WHIRLWIND VALLEY
GSV	GRASS VALLEY	RBV	RUBY VALLEY	WKL	WALKER LAKE
GVY	GABBS VALLEY	RFT	RAFT RIVER IDAHO/UTAH	WKR	WALKER RIVER
HAW	HAWTHORNE	RNV	RALSTON VALLEY	WLS	WELLS
HCV	HOT CREEK VALLEY	RRV	RAILROAD VALLEY	WPR	WHITE PINE RANGE
HLV	HONEY LAKE VALLEY	RSE	REESE RIVER VALLEY	WRV	WHITE RIVER VALLEY
HUM	HUMBOLDT RIVER	RSV	ROSE VALLEY	WSV	WASHOE VALLEY
HVA	HIDDEN VALLEY	SCD	SMOKE CREEK DESERT	YCF	YUCCA FLAT
HVD	HOOVER DAM	SCV	STONE CABIN VALLEY	YCM	YUCCA MOUNTAIN

APPENDIX B

LITERATURE SEARCH - STABLE LIGHT-ISOTOPE DATA

Isotopic data acquired from literature search. When no name was given, sample name taken from the Township and Range designation. LOC is general sample location, see Appendix A for key to letter symbols. REF is source of data, key follows this appendix.

SAMP #	SAMPLE NAME	REF	LOC	TYPE	LONG	LAT	ELEV meters	DEUT ‰	OX18 ‰	TEMP °C	DATE MO YR
1	Shoshone Range W1	DAY	BEO	SPRG	116.682	40.563	1707	-118	-15.0	12	5 85
2	Mule Creek Seep W2	DAY	BEO	SPRG	116.676	40.594	1932	-116	-15.1	-1	5 85
3	Mule Creek Spring W3	DAY	BEO	SPRG	116.687	40.599	1996	-118	-15.6	-1	5 85
4	North Windmill W4	DAY	BEO	WELL	116.589	40.591	1477	-120	-15.5	16	5 85
5	Southwest Windmill W5	DAY	BEO	WELL	116.643	40.535	1563	-122	-15.2	18	5 85
6	Artesian Well W6	DAY	BEO	WELL	116.605	40.574	1463	-126	-15.3	35	5 85
7	Horshoe Ranch Well G1	DAY	BEO	WELL	116.462	40.606	1428	-121	-15.2		5 85
8	Long Draw Spring G2	DAY	BEO	SPRG	116.435	40.617	1457	-121	-15.2		5 85
9	I-80 Rest Stop Well G3	DAY	BEO	WELL	116.475	40.681	1454	-130	-16.5		5 85
10	I-80 Rest Stop Well G4	DAY	BEO	WELL	116.475	40.681	1454	-131	-16.5		9 85
11	Bob's Flat Windmill G5	DAY	BEO	WELL	116.406	40.662	1546	-124	-15.7		5 85
12	Emigrant Pass Sp G6	DAY	BEO	SPRG	116.289	40.651	1792	-122	-15.5	-1	3 85
13	T-S Ranch Well G7	DAY	BEO	WELL	116.651	40.694	1396	-121	-16.0		5 85
14	Maysville Sum Sp G9	DAY	BEO	SPRG	116.831	40.413	2048	-121	-15.2	-1	5 85
15	Beowawe Mid Geyser B1	DAY	BEO	SPRG	116.585	40.562	1554	-128	-15.2	999	3 85
16	Beowawe Lower Hot Sp B2	DAY	BEO	SPRG	116.583	40.586	1451	-131	-15.4	999	5 85
17	Beowawe West Geyser B3	DAY	BEO	SPRG	116.595	40.559	1496	-132	-15.6	999	5 85
18	Beowawe Mid Geyser B4	DAY	BEO	SPRG	116.585	40.562	1554	-131	-15.7	999	9 85
19	Beowawe Blowing Well B5	DAY	BEO	WELL	116.584	40.562	1479	-129	-15.1	999	9 85
20	Hot Springs Point T1	DAY	BEO	SPRG	116.517	40.404	1448	-132	-16.5	75	3 85
21	Carlin Warm Spring T2	DAY	CAR	SPRG	116.153	40.685	1484	-126	-16.2		3 85
22	Carlin Hot Spring T3	DAY	CAR	SPRG	116.127	40.697	1484	-126	-17.1	80	5 85
23	Horseshoe Rch HS T4	DAY	BEO	SPRG	116.462	40.606	1428	-133	-16.9	58	7 85
24	Carlin Hot Springs T5	DAY	CAR	SPRG	116.127	40.697	1484	-122	-15.0	80	9 85
25	Humboldt R, Beowawe H1	DAY	BEO	SURF	116.473	40.593	1430	-120	-15.7	19	3 85
26	Humboldt R, Beowawe H2	DAY	BEO	SURF	116.473	40.593	1430	-121	-15.5		6 85
27	Humboldt R, Beowawe H3	DAY	BEO	SURF	116.473	40.593	1430	-114	-14.2		9 85
28	Humboldt R, Carlin H4	DAY	HUM	SURF	116.129	40.699	1487	-116	-15.5		5 85
29	Humboldt R, Carlin H5	DAY	HUM	SURF	116.129	40.699	1487	-117	-14.5		9 85
30	Stillwater Range DV-21	ING	DXV	STSP	117.991	39.908	1036	-117	-14.0	13	3 79
31	Stillwater Range DV-22	ING	DXV	STSP	118.017	39.896	1170	-113	-15.0	11	3 79
32	Stillwater Range DV-45	ING	DXV	STSP	118.053	39.903	1463	-116	-14.7	14	5 79
33	Stillwater Range DV-46	ING	DXV	STSP	118.053	39.903	1463	-114	-14.2	16	5 79
34	Stillwater Range DV-47	ING	DXV	STSP	118.053	39.903	1463	-108	-14.0	18	5 79
35	Stillwater Range DV-48	ING	DXV	STSP	118.053	39.903	1463	-107	-14.3	14	5 79
36	Stillwater Range DV-49	ING	DXV	STSP	118.028	39.907	1268	-107	-14.1	16	5 79
37	Stillwater Range DV-53	ING	DXV	STSP	118.079	39.819	1292	-124	-14.1	18	6 79
38	Stillwater Range DV-61	ING	DXV	STSP	118.204	39.716	1399	-114	-14.3	16	6 79
39	Stillwater Range DV-78	ING	DXV	STSP	118.148	39.799	1298	-124	-14.0	22	7 79

APPENDIX B, continued

Literature Search - Isotope Data

SAMP #	SAMPLE NAME	REF	LOC	TYPE	LONG	LAT	ELEV meters	DEUT ‰	OX18 ‰	TEMP °C	DATE MO YR
40	Stillwater Range DV-102	ING	DXV	STSP	117.914	40.016	1646	-115	-13.5	14	6 79
41	Stillwater Range DV-103	ING	DXV	STSP	117.958	40.001	1743	-121	-14.5	14	6 79
42	Stillwater Range DV-110	ING	DXV	STSP	117.809	40.087	1472	-129	-14.9	16	6 79
43	Dixie Valley DV-13	ING	DXV	WELL	118.042	39.684	1044	-134	-16.0	19	3 79
44	Dixie Valley DV-14	ING	DXV	WELL	118.042	39.684	1044	-133	-16.5	19	3 79
45	Dixie Valley DV-43	ING	DXV	WELL	118.042	39.684	1044	-127	-16.3	18	5 79
46	Dixie Valley DV-44	ING	DXV	WELL	118.042	39.684	1044	-126	-16.4	18	5 79
47	Dixie Valley DV-65	ING	DXV	WELL	118.042	39.684	1044	-130	-16.7	20	6 79
48	Dixie Valley DV-34	ING	DXV	WELL	117.707	40.066	1091	-122	-15.3	20	5 79
49	Dixie Valley DV-37	ING	DXV	WELL	117.673	40.079	1111	-115	-15.4	16	5 79
50	Dixie Valley DV-38	ING	DXV	WELL	117.652	40.078	1113	-127	-16.0	19	5 79
51	Dixie Valley DV-39	ING	DXV	WELL	117.617	40.064	1123	-125	-16.4	23	5 79
52	Dixie Valley DV-40	ING	DXV	WELL	117.652	40.078	1113	-115	-15.7	16	5 79
53	Dixie Valley DV-100	ING	DXV	WELL	117.784	39.964	1067	-126	-15.4	19	6 79
54	Pleasant Valley DV-20	ING	PLV	STSP	117.671	40.241	1280	-126	-15.3	21	3 79
55	Dixie Hot Spring DV-23	ING	DXV	SPRG	118.071	39.788	1042	-120	-15.3	73	3 79
56	Dixie Hot Spring DV-24	ING	DXV	SPRG	118.071	39.788	1042	-126	-15.3	55	3 79
57	Dixie Hot Spring DV-6	ING	DXV	SPRG	118.071	39.788	1042	-125	-15.4	73	7 79
58	Dixie Hot Spring DV-9	ING	DXV	SPRG	118.071	39.788	1042	-134	-15.8	73	7 79
59	Dixie Hot Spring DV-15	ING	DXV	SPRG	118.071	39.788	1042	-133	-15.7	52	7 79
60	Dixie Hot Spring DV-16	ING	DXV	SPRG	118.071	39.788	1042	-129	-15.4	26	7 79
61	Dixie Hot Spring DV-17	ING	DXV	SPRG	118.071	39.788	1042	-121	-15.8	20	7 79
62	Hyder Hot Spring DV-4	ING	DXV	SPRG	117.719	40.003	1093	-132	-15.0	63	3 79
63	Hyder Hot Spring DV-33	ING	DXV	SPRG	117.719	40.003	1093	-135	-15.0	66	5 79
64	Hyder Hot Spring HHS-1	ING	DXV	SPRG	117.719	40.003	1093	-130	-15.8	75	7 79
65	Sou Hot Spring DV-1	ING	DXV	SPRG	117.725	40.087	1125	-131	-15.0	55	3 79
66	Sou Hot Spring DV-2	ING	DXV	SPRG	117.725	40.087	1125	-137	-14.7	51	3 79
67	Sou Hot Spring DV-35	ING	DXV	SPRG	117.725	40.087	1125	-127	-15.3	53	5 79
68	Sou Hot Spring DV-36	ING	DXV	SPRG	117.725	40.087	1125	-123	-15.3	73	5 79
69	Carson Sink CS-1	ING	CSK	STSP	117.851	40.177	1463	-124	-15.2	15	7 79
70	Carson Sink CS-4	ING	CSK	STSP	117.846	40.158	1545	-123	-15.9	16	7 79
71	Carson Sink CS-3	ING	CSK	STSP	117.983	40.102	1251	-122	-14.7	21	7 79
72	Carson Sink CS-4	ING	CSK	STSP	117.922	40.055	1753	-122	-15.2	16	7 79
73	Carson Sink CS-6	ING	CSK	STSP	118.193	39.848	1500	-122	-15.7	21	7 79
74	Carson Sink CS-8	ING	CSK	STSP	118.231	39.791	1353	-121	-14.2	24	7 79
75	Clan Alpine Mts DV-3	ING	DXV	STSP	117.622	39.847	1554	-121	-15.1	11	3 79
76	Clan Alpine Mts DV-10	ING	DXV	STSP	117.571	40.033	1509	-122	-15.2	15	3 79
77	Clan Alpine Mts DV-12	ING	DXV	STSP	117.832	39.734	1475	-117	-14.3	11	3 79
78	Clan Alpine Mts DV-60	ING	DXV	STSP	117.856	39.633	1853	-113	-14.7	9	6 79
79	Clan Alpine Mts DV-63	ING	DXV	STSP	117.896	39.643	1560	-117	-15.2	18	6 79

APPENDIX B, continued

Literature Search - Isotope Data

SAMP #	SAMPLE NAME	REF	LOC	TYPE	LONG	LAT	ELEV meters	DEUT ‰	OX18 ‰	TEMP °C	DATE MO YR
80	Clan Alpine Mts DV-64	ING	DXV	STSP	117.765	39.731	1634	-120	-13.4	-1	6 79
81	Clan Alpine Mts DV-83	ING	DXV	STSP	117.667	39.801	1463	-128	-16.1	28	8 79
82	Buckbrush Spring DV-42	ING	DXV	SPRG	117.977	39.768	1033	-124	-16.3	15	5 79
83	Thermal Test Well DV-30	ING	DXV	WELL	118.011	39.866	1045	-123	-14.5	65	5 79
84	McCoy Hot Spring DV-5	ING	DXV	SPRG	117.604	40.081	1210	-131	-15.8	39	3 79
85	McCoy Hot Spring DV-6	ING	DXV	SPRG	117.636	40.036	1122	-135	-14.6	29	3 79
86	McCoy Hot Spring DV-7	ING	DXV	SPRG	117.636	40.036	1122	-130	-15.8	30	3 79
87	McCoy Hot Spring DV-8	ING	DXV	SPRG	117.636	40.036	1122	-134	-15.6	30	3 79
88	McCoy Hot Spring DV-9	ING	DXV	SPRG	117.636	40.036	1122	-131	-15.2	30	3 79
89	McCoy Hot Spring DV-11	ING	DXV	SPRG	117.604	40.081	1134	-124	-15.4	43	3 79
90	McCoy Hot Spring DV-116	ING	DXV	SPRG	117.604	40.081	1134	-134	-15.7	40	3 79
91	Deep Well DV-69	ING	DXV	WELL	118.011	39.866	1045	-109	-10.5	69	7 79
92	Deep Well DV-70	ING	DXV	WELL	118.011	39.866	1045	-117	-12.6	76	7 79
93	Deep Well DV-71	ING	DXV	WELL	118.011	39.866	1045	-113	-12.8	82	7 79
94	Deep Well DV-72A	ING	DXV	WELL	118.011	39.866	1045	-109	-12.6	77	7 79
95	Deep Well DV-72B	ING	DXV	WELL	118.011	39.866	1045	-119	-12.6	77	7 79
96	Deep Well DV-90	ING	DXV	WELL	118.011	39.866	1045	-115	-14.4	94	9 79
97	Deep Well DV-126	ING	DXV	WELL	118.011	39.866	1045	-119	-14.6	87	12 79
98	Deep Well DV-128	ING	DXV	WELL	118.011	39.866	1045	-119	-14.8	49	3 79
99	Deep Well DV-81	ING	DXV	WELL	117.917	39.846	1031	-124	-12.6	51	8 79
100	Deep Well DV-82	ING	DXV	WELL	117.917	39.846	1031	-126	-12.7	86	8 79
101	Deep Well DV-93	ING	DXV	WELL	117.917	39.846	1031	-101	-11.7	83	9 79
102	Deep Well DV-125	ING	DXV	WELL	117.917	39.846	1031	-120	-13.9	33	12 79
103	Edwards Ck Valley ECV-1	ING	ECV	STSP	117.586	39.722	1576	-117	-17.2	14	10 79
104	Edwards Ck Valley ECV-2	ING	ECV	STSP	117.644	39.682	1559	-112	-15.5	13	10 79
105	Edwards Ck Valley ECV-3	ING	ECV	SURF	119.785	39.521	1591	-114	-16.6	13	10 79
106	Fairview Valley DV-120	ING	FVY	STSP	117.992	39.312	1439	-111	-15.6	12	10 79
107	Pupfish Spring, NV - 1	MCK	HVD	SPRG	114.742	36.013	220	-98	-12.6	32	
108	Arizona Hot Spot - 2	MCK	HVD	SPRG	114.742	36.006	220	-106	-12.9	58	
109	Nevada Hot Spot, NV - 3	MCK	HVD	SPRG	114.734	36.001	400	-98	-12.9	62	
110	Sauna Cave, NV - 4	MCK	HVD	SPRG	114.743	36.003	220	-105	-13.7	50	
111	Palm Tree Hot, AZ - 6	MCK	HVD	SPRG	114.739	35.995	220	-98	-14.0	57	
112	Palm Tree Cold, AZ - 7	MCK	HVD	SPRG	114.738	35.995	220	-82	-10.5	24	
113	Ringbolt Rapids, AZ - 10	MCK	HVD	SPRG	114.724	35.961	232	-84	-10.9	50	
114	Bighorn Sheep, NV - 12	MCK	HVD	SPRG	114.735	35.939	320	-81	-10.1	36	
115	Arizona Seep, AZ - 13	MCK	HVD	SPRG	114.708	35.928	232	-82	-10.0	32	
116	Lake Mead - LM	MCK	HVD	LAKE	114.751	36.033	372	-114	-14.6	10	
117	Soldier Meadow Sp #2	WCH	BRD	SPRG	119.218	41.358	1390	-130	-16.6	54	1 74
118	Well near Gerlach	WCH	BRD	WELL	119.378	40.781	1463	-121	-14.7	80	1 74
119	Sulphur TH SP#1	WCH	BRD	SPRG	118.999	40.953	1180	-121	-12.9	89	7 80

APPENDIX B, continued

Literature Search - Isotope Data

SAMP #	SAMPLE NAME	REF	LOC	TYPE	LONG	LAT	ELEV meters	DEUT ‰	OX18 ‰	TEMP °C	DATE MO YR
120	Soldier Cr TH SP#1	WCH	BRD	SPRG	118.999	40.953	1180	-124	-15.7	46	6 80
121	Black Rock Spring	WCH	BRD	SPRG	119.007	40.974	1205	-127	-15.4	77	6 80
122	Well BRD51A	WCH	BRD	WELL	119.009	40.995	1204	-124	-14.4	28	6 81
123	Well BRD51B	WCH	BRD	WELL	119.009	40.985	1200	-124	-14.8	24	6 81
124	Soldier Cr TH SP#4	WCH	BRD	SPRG	119.016	41.003	1205	-128	-15.0	87	6 80
125	Soldier Cr TH SP#3	WCH	BRD	SPRG	119.015	41.013	1205	-128	-15.6	78	6 80
126	Soldier Cr TH SP#3	WCH	BRD	SPRG	119.015	41.013	1205	-131	-15.8	47	6 80
127	Soldier Cr TH SP#2	WCH	BRD	SPRG	119.014	41.024	1210	-128	-15.1	91	6 80
128	Well BRD57A	WCH	BRD	WELL	119.019	41.037	1210	-128	-15.8	41	12 80
129	Double Hot Springs #1	WCH	BRD	SPRG	119.028	41.049	1212	-121	-15.6	82	12 79
130	Double Hot Springs #2	WCH	BRD	SPRG	119.028	41.049	1212	-121	-17.1	78	12 79
131	Double Hot Springs #4	WCH	BRD	SPRG	119.028	41.049	1212	-120	-15.1	60	12 79
132	Double Hot Springs #5	WCH	BRD	SPRG	119.028	41.049	1212	-120	-15.7	78	12 79
133	Double Hot Springs #6	WCH	BRD	SPRG	119.028	41.049	1212	-119	-15.6	79	12 79
134	Well DHS4	WCH	BRD	WELL	119.027	41.054	1207	-130	-16.0	35	8 80
135	Well DHS4	WCH	BRD	WELL	119.027	41.054	1207	-129	-16.0	37	11 80
136	Well DHS5	WCH	BRD	WELL	119.027	41.054	1207	-130	-16.4	36	8 80
137	Well DHS6	WCH	BRD	WELL	119.027	41.054	1207	-127	-14.6	26	11 80
138	Great Boiling Sp #23	WCH	BRD	SPRG	119.365	40.661	1207	-98	-11.3	100	1 80
139	Great Boiling Sp #46	WCH	BRD	SPRG	119.365	40.661	1207	-105	-10.4	89	1 80
140	Great Boiling Sp #48	WCH	BRD	SPRG	119.365	40.661	1207	-99	-10.6	94	1 80
141	Ditch	WCH	BRD	SPRG	119.355	40.673	1202	-95	-11.5	97	11 79
142	Mud Springs #1	WCH	BRD	SPRG	119.384	40.651	1200	-95	-11.3	79	2 80
143	Mud Springs #2	WCH	BRD	SPRG	119.384	40.651	1200	-98	-11.0	91	1 80
144	Well BRO4	WCH	BRD	WELL	119.018	41.075	1227	-127	-15.4	24	4 81
145	Hardin City TH SP	WCH	BRD	SPRG	119.001	41.116	1213	-131	-16.1	51	7 80
146	Well BR12	WCH	BRD	WELL	119.001	41.132	1221	-130	-16.0	25	5 81
147	Soldier B or TH SP#1	WCH	BRD	SPRG	119.021	41.148	1221	-130	-15.9	70	7 80
148	Well BRD53B	WCH	BRD	WELL	119.006	41.083	1233	-129	-15.4	21	7 81
149	Trego Hot Springs #A	WCH	BRD	SPRG	119.111	40.767	1199	-125	-15.1	86	4 80
150	Well GRB'	WCH	BRD	WELL	119.265	40.727	1195	-77	-5.6	12	11 80
151	Well GRD	WCH	BRD	WELL	119.217	40.772	1190	-98	-9.2	12	12 80
152	Well GRL	WCH	BRD	WELL	119.051	40.845	1191	-90	-7.8	13	11 80
153	Well GRL'	WCH	BRD	WELL	119.051	40.845	1191	-82	-6.2	14	11 80
154	Well BRO6	WCH	BRD	WELL	119.099	40.999	1190	-89	-8.4	17	8 80
155	Well BRO7	WCH	BRD	WELL	119.063	41.022	1191	-108	-12.0	16	7 80
156	Well BRO8	WCH	BRD	WELL	119.098	40.936	1190	-69	-7.6	14	7 80
157	Well BRO9	WCH	BRD	WELL	119.138	40.906	1190	-79	-6.8	15	7 80
158	Well BRO10	WCH	BRD	WELL	119.103	40.878	1190	-86	-8.4	13	10 80
159	Well BRO11	WCH	BRD	WELL	119.169	40.873	1190	-99	-10.8	15	7 80

APPENDIX B, continued

Literature Search - Isotope Data

SAMP #	SAMPLE NAME	REF	LOC	TYPE	LONG	LAT	ELEV meters	DEUT ‰	OX18 ‰	TEMP °C	DATE MO YR
160	Granite Basin Spring	WCH	BRD	SPRG	119.367	40.743	1570	-114	-14.8	15	8 79
161	Summit Spring	WCH	BRD	SPRG	119.415	40.774	2548	-109	-14.8	11	8 79
162	Railroad Springs	WCH	BRD	SPRG	119.436	40.743	1493	-112	-16.4	12	1 80
163	Middle Mustang Spring	WCH	BRD	SPRG	119.116	41.356	1803	-124	-16.1	23	8 79
164	Mud Meadow SP#1	WCH	BRD	SPRG	119.194	41.339	1335	-129	-16.3	10	4 80
165	Mud Meadow SP#2	WCH	BRD	SPRG	119.194	41.339	1335	-125	-16.4	11	5 80
166	Soldier Meadow SP#1	WCH	BRD	SPRG	119.238	41.403	1571	-115	-14.5	12	5 80
167	Donnelly Creek SP#1	WCH	BRD	SPRG	119.147	41.116	1509	-122	-15.5	14	4 80
168	Donnelly Creek SP#2	WCH	BRD	SPRG	119.167	41.118	1816	-120	-15.4	17	5 80
169	Donnelly Creek	WCH	BRD	SURF	119.133	41.114	1280	-110	-15.0	6	2 80
170	SP below Little Big Mtn	WCH	BRD	SPRG	119.062	41.257	1951	-127	-16.7	15	8 79
171	Wheeler Spring	WCH	BRD	SPRG	119.169	41.287	1274	-115	-14.9	18	3 80
172	Running Water Spring	WCH	BRD	SPRG	119.073	41.291	2140	-114	-14.6	10	3 80
173	Mud Meadow SP#3	WCH	BRD	SPRG	119.206	41.339	1323	-118	-15.1	25	8 79
174	Mud Meadow TH SP#5	WCH	BRD	SPRG	119.168	41.339	1320	-128	-16.0	27	5 80
175	Mud Meadow TH SP#10	WCH	BRD	SPRG	119.192	41.339	1321	-116	-15.3	53	3 80
176	Mud Meadow TH SP#2	WCH	BRD	SPRG	119.217	41.339	1366	-131	-16.6	53	5 80
177	Mud Meadow TH SP#3	WCH	BRD	SPRG	119.224	41.339	1372	-125	-16.6	44	1 80
178	Mud Meadow TH SP#1	WCH	BRD	SPRG	119.188	41.339	1365	-127	-16.4	57	1 80
179	Mud Meadow TH SP#6	WCH	BRD	SPRG	119.223	41.361	1386	-124	-16.5	51	1 80
180	Mud Meadow TH SP#9	WCH	BRD	SPRG	119.216	41.339	1377	-131	-16.7	35	4 80
181	Soldier Meadow TH SP#4	WCH	BRD	SPRG	119.187	41.380	1359	-131	-16.4	55	4 80
182	Soldier Meadow TH SP#1	WCH	BRD	SPRG	119.181	41.381	1353	-131	-16.6	38	5 80
183	Soldier Meadow TH SP#3	WCH	BRD	SPRG	119.166	41.398	1396	-119	-16.0	30	3 80
184	A. Jackson Ranch Well	WCH	BRD	WELL	119.130	41.018	1195	-114	-15.5	17	3 80
185	A. Jackson Ranch Well	WCH	BRD	WELL	119.130	41.018	1195	-121	-15.6	17	2 80
186	WW3921	WCH	BRD	WELL	119.114	41.055	1195	-118	-15.0	20	2 80
187	WW3922T1	WCH	BRD	WELL	119.110	41.073	1195	-118	-15.8	24	12 79
188	WW3922T1	WCH	BRD	WELL	119.110	41.073	1195	-123	-15.8	24	12 79
189	WW3922T2	WCH	BRD	WELL	119.110	41.074	1195	-123	-15.8	26	12 80
190	WW3922T3	WCH	BRD	WELL	119.105	41.083	1195	-123	-16.0	24	12 80
191	WW3922T4	WCH	BRD	WELL	119.104	41.083	1195	-115	-15.7	23	12 80
192	PW290	WCH	BRD	WELL	119.102	41.128	1215	-121	-15.9	34	1 80
193	PW1636	WCH	BRD	WELL	119.101	41.121	1210	-122	-16.0	34	1 80
194	FL WL WW3985T1 SO CR	WCH	BRD	WELL	119.125	41.127	1215	-115	-15.7	15	1 80
195	Well at Wagner Springs	WCH	BRD	WELL	119.138	41.136	1219	-124	-15.6	32	4 80
196	Flother Well No2 3989T	WCH	BRD	WELL	119.127	41.144	1216	-126	-16.6	14	1 80
197	Calico Mountains Spring	WCH	BRD	SPRG	119.184	41.160	1609	-124	-16.0	-1	1 80
198	Calico Mountains Spring	WCH	BRD	SPRG	119.184	41.160	1609	-112	-16.6	-1	8 79
199	Hobo Hot Spring	TRX	CEV	SPRG	119.811	39.058	1451	-115	-13.7	46	

APPENDIX B, continued

Literature Search - Isotope Data

SAMP #	SAMPLE NAME	REF	LOC	TYPE	LONG	LAT	ELEV meters	DEUT ‰	OX18 ‰	TEMP °C	DATE MO YR
200	Walley's Hot Spring	TRX	CEV	SPRG	119.833	38.981	1426	-132	-16.3	58	
201	Job's Canyon Stream	TRX	CEV	SURF	119.824	38.901	1463	-117	-15.4	3	
202	Carson River	TRX	CEV	SURF	119.780	38.944	1437	-116	-14.6	4	
203	City of Minden Well	TRX	CEV	WELL	119.769	38.955	1434	-120	-14.8	12	
204	Unruh's Well	TRX	CEV	WELL	119.744	39.036	1433	-118	-15.2	12	
205	Saratoga Well	TRX	CEV	WELL	119.746	39.054	1426	-133	-16.0	26	
206	Saratoga Hot Spring	TRX	CEV	SPRG	119.742	39.057	1432	-130	-16.2	50	
207	Carson Sewage Plant	TRX	CEV	SURF	119.731	39.163	1410	-123	-15.4	32	
208	Noble Murray Well	TRX	CEV	WELL	119.706	39.148	1402	-130	-16.2	41	
209	Carson Hot Springs	TRX	CEV	SPRG	119.752	39.194	1439	-128	-14.9	50	
210	Carson River	TRX	CEV	SURF	119.765	39.147	1403	-121	-14.0	5	
211	Dodd Well	TRX	CEV	WELL	119.782	39.293	1542	-120	-14.2	16	
212	Saratoga Well	TRX	CEV	WELL	119.746	39.054	1426	-133	-16.1	26	
213	Darrough's Well	TRX	BSV	WELL	117.186	38.822	1719	-131	-8.4	91	
214	Darrough's North Spring	TRX	BSV	SPRG	117.183	38.821	1695	-130	-6.7	71	
215	Darrough's South Spring	TRX	BSV	SPRG	117.185	38.811	1707	-128	-15.1	68	
216	Darrough's Pool	TRX	BSV	SPRG	117.195	38.821	1708	-129	-8.1	96	
217	Aqueduct Stream	TRX	BSV	SURF	117.208	38.813	1975	-123	-10.8	2	
218	Barker Creek	TRX	BSV	SURF	117.029	38.086	2042	-125	-15.6	4	
219	Spencer 73	TRX	BSV	WELL	116.858	39.327	1725	-141	-15.4	73	
220	Spencer 39 (Dead Burrow)	TRX	BSV	WELL	116.858	39.327	1725	-143	-15.9	39	
221	Well N of Linka Mine	TRX	BSV	WELL	116.829	39.341	1752	-141	-17.8		
222	Upper Ophir Creek	TRX	BSV	SURF	117.267	38.945	2243	-132	-16.0	6	
223	Lower Ophir Creek	TRX	BSV	SURF	117.244	38.941	1935	-126	-11.2	4	
224	McLeod 88 Spring	TRX	BSV	SPRG	117.131	38.941	1669	-132	-17.7	88	
225	McLeod 66 spring	TRX	BSV	SPRG	117.131	38.941	1951	-125	-16.3	63	
226	Fault Spring	TRX	BSV	SPRG	117.161	39.073	1707	-132	-15.1	14	
227	Wallis Well	TXL	CAL	WELL	114.513	37.625	1350	-109	-14.6	67	11 79
228	Hospital Injection Well	TXL	CAL	WELL	114.514	37.623	1344	-109	-14.4	29	11 79
229	Hot Springs Motel Well	TXL	CAL	WELL	114.511	37.621	1343	-106	-14.3	45	11 79
230	Clover Valley Wash	TXL	CAL	SURF	114.502	37.618	1341	-86	-11.7	12	11 79
231	Meadow Valley Wash	TXL	CAL	SURF	114.501	37.624	1343	-97	-13.1	5	11 79
232	Van Kirk Well	TXL	CAL	WELL	114.512	37.621	1342	-109	-14.4	43	11 79
233	Caliente City Well	TXL	CAL	WELL	114.514	37.616	1340	-84	-12.1	15	11 79
234	HAAP Well #1 HAW-1	DTT	HAW	WELL	118.676	38.558	1265	-126	-15.2	52	
235	HAAP Well #5 HAW-2	DTT	HAW	WELL	118.673	38.551	1292	-127	-15.3	41	
236	HAAP Well #6 HAW-3	DTT	HAW	WELL	118.639	38.538	1283	-124	-13.6	24	
237	HAAP Well #3 HAW-4	DTT	HAW	WELL	118.559	38.521	1338	-123	-15.6	40	
238	HAAP Well #4 HAW-5	DTT	HAW	WELL	118.622	38.494	1402	-132	-15.3	23	
239	El Capitan Well HAW-6	DTT	HAW	WELL	118.642	38.514	1341	-130	-15.4	99	

APPENDIX B, continued

Literature Search - Isotope Data

SAMP #	SAMPLE NAME	REF	LOC	TYPE	LONG	LAT	ELEV meters	DEUT ‰	OX18 ‰	TEMP °C	DATE MO YR
240	Alum Creek HAW-7	DTT	HAW	SURF	118.644	38.441	1707	-117	-14.8	7	
241	Cottonwood Ck HAW-8	DTT	HAW	SURF	118.778	38.645	1463	-119	-15.2	10	
242	Cottonwood Ck HAW-9	DTT	HAW	SURF	118.828	38.591	2286	-115	-15.4	7	
243	Cottonwood Ck HAW-10	DTT	HAW	SURF	118.803	38.555	2743	-124	-16.1	3	
244	Walker Warm (1) HAW-11	DTT	MSV	SPRG	118.971	38.494	1631	-127	-16.2	34	
245	Correyville (1) HAW-12	DTT	HAW	SPRG	118.778	38.476	2341	-119	-15.7	6	
246	Corey Canyon HAW-13	DTT	HAW	SPRG	118.667	38.481	1554	-123	-15.1	15	
247	HUD Well #5 HAW-14	DTT	HAW	WELL	118.628	38.513	1347	-122	-15.2	35	
248	Corey Canyon Well HAW-15	DTT	HAW	WELL	118.739	38.489	1920	-124	-15.2	11	
249	Walker Warm (2) HAW-16	DTT	MSV	SPRG	118.971	38.494	1631	-132	-16.2	34	
250	Correyville (2) HAW-17	DTT	HAW	SPRG	118.778	38.476	2341	-124	-15.8	6	
251	Artesian Well (1)	DTT	PDV	WELL	117.571	41.106	1317	-132	-17.1	68	
252	Artesian Well (2)	DTT	PDV	WELL	117.571	41.106	1317	-136	-17.0	68	
253	Dutch Flat Well	DTT	PDV	WELL	117.564	41.153	1316	-130	-16.5	13	
254	Golconda Hot Spring	DTT	PDV	SPRG	117.491	40.955	1341	-119	-15.8	42	
255	Segerstrom (5) Sp.	DTT	PDV	SPRG	117.493	40.961	1335	-120	-15.3	61	
256	Segerstrom (1) Sp.	DTT	PDV	SPRG	117.493	40.961	1335	-120	-15.8	71	
257	Paradise Well	DTT	PDV	WELL	117.691	41.308	1366	-119	-15.2	18	
258	L Humboldt R @ Bullhead	DTT	HUM	SURF	117.319	41.399	1376	-122	-15.4	18	
259	The Hot Springs	DTT	PDV	SPRG	117.388	41.421	1366	-134	-15.8	56	
260	Klauman Well	DTT	PDV	WELL	117.429	41.421	1356	-123	-15.4	18	
261	Home Ranch Well	DTT	PDV	WELL	117.517	41.338	1333	-116	-14.9	18	
262	Humboldt R @ Preble	DTT	HUM	SURF	117.397	40.972	1326	-107	-12.5	18	
263	Segerstrom Well (1)	DTT	PDV	WELL	117.488	40.957	1333	-126	-15.7	67	
264	Day Warm Springs	DTT	PDV	SPRG	117.373	41.417	1368	-131	-16.4	36	
265	Big Cottonwood Creek	DTT	PDV	SURF	117.532	41.491	1378	-110	-13.7	15	
266	Segerstrom Well (2)	DTT	PDV	WELL	117.491	40.953	1341	-128	-15.7	42	
267	Buckbrush Spring	DTT	PDV	SPRG	117.368	41.436	1433	-126	-13.9	9	
268	Wash O'Neal Creek	DTT	PDV	SURF	117.628	41.402	1594	-112	-14.7	5	
269	Humboldt R @ Golconda	DTT	HUM	SURF	117.482	40.897	1322	-114	-14.2	5	
270	Blossom Hot Pot	DEN	PPV	SPRG	117.111	40.922	1349	-128	-16.3	58	10 81
271	Humboldt R @ Ellison	DEN	HUM	SURF	117.185	40.891	1343	-128	-14.5	13	10 81
272	Stonehouse Spring	DEN	PPV	SPRG	117.311	40.846	1349	-129	-16.5	17	10 81
273	Brooks Hot Spring	DEN	PPV	SPRG	117.304	40.829	1358	-127	-16.5	35	10 81
274	Sulfur Spring	DEN	PPV	SPRG	117.348	40.865	1365	-124	-16.0	18	10 81
275	Tipton 2 Cold Spring	DEN	PPV	SPRG	117.464	40.712	1506	-125	-16.1	15	10 81
276	Tipton 2 Warm Spring	DEN	PPV	SPRG	117.462	40.713	1515	-120	-16.0	27	10 81
277	Hot Sp W of Tipton 1	DEN	PPV	SPRG	117.492	40.761	1475	-131	-14.8	80	10 81
278	Hot Sp SW of Tipton 1	DEN	PPV	SPRG	117.494	40.758	1444	-128	-16.3	49	10 81
279	Spanish Basin Cold Sp	DEN	PPV	SPRG	117.582	40.714	1949	-114	-15.6	2	10 81

APPENDIX B, continued

Literature Search - Isotope Data

SAMP #	SAMPLE NAME	REF	LOC	TYPE	LONG	LAT	ELEV meters	DEUT ‰	OX18 ‰	TEMP °C	DATE MO YR
280	Strm N End of Tobin Rg	DEN	PPV	SURF	117.501	40.611	1649	-114	-15.3	10	10 81
281	Summit Spring	DEN	PPV	SPRG	117.403	40.651	1664	-121	-16.0	14	10 81
282	Kent Spring	DEN	PPV	SPRG	117.402	40.648	1667	-121	-15.5	10	10 81
283	Tipton Warm Well	DEN	PPV	WELL	117.508	40.717	1451	-134	-15.5	23	10 81
284	Long John Warm Spring	DEN	CAR	SPRG	116.154	40.685	1524	-135	-15.9	23	11 81
285	S.P. Spring	DEN	CAR	SPRG	116.129	40.706	1500	-130	-15.4	10	11 81
286	Rye Patch Spring	DEN	CAR	SPRG	116.075	40.681	1658	-129	-15.4	13	11 81
287	Barrows Well	DEN	CAR	WELL	116.136	40.698	1493	-131	-15.9	79	11 81
288	Dry Susie Hot Spring	DEN	CAR	SPRG	116.042	40.765	1548	-137	-17.2	65	11 81
289	Dry Susie Lower Spring	DEN	CAR	SPRG	116.013	40.774	1559	-128	-15.5	15	11 81
290	Humboldt R Downstream	DEN	HUM	SURF	116.133	40.699	1484	-120	-14.7	19	11 81
291	Carlin Hot Springs (1)	DEN	CAR	SPRG	116.127	40.697	1484	-132	-15.9	82	11 81
292	Carlin Hot Springs (2)	DEN	CAR	SPRG	116.127	40.697	1484	-125	-15.6	49	11 81
293	Humboldt R Upstream	DEN	HUM	SURF	116.125	40.701	1484	-117	-14.3	12	11 81
294	Cherry Spring	DEN	CAR	SPRG	116.243	40.723	1833	-126	-16.0	-1	11 81
295	Maggie Ck Ranch Well	DEN	CAR	WELL	116.107	40.741	1509	-129	-15.6		11 81
296	Ash Canyon Creek - 77	SZE	CEV	SURF	119.851	39.168	2134	-111	-14.6		5 81
297	Ash Canyon Creek - 85	SZE	CEV	SURF	119.842	39.173	1890	-108	-15.3		5 81
298	Ash Canyon Creek - 156	SZE	CEV	SURF	119.871	39.165	2484	-103	-14.0		8 81
299	Ash Canyon Creek - 158	SZE	CEV	SURF	119.856	39.169	2271	-103	-14.6		8 81
300	Ash Canyon Creek - 159	SZE	CEV	SURF	119.851	39.168	2134	-103	-14.2		8 81
301	Ash Ck, Blw Confl - 162	SZE	CEV	SURF	119.846	39.168	2018	-101	-14.5		8 81
302	N Ash Ck, Ab Confl - 163	SZE	CEV	SURF	119.842	39.176	1887	-107	-14.8		8 81
303	Ash Ck, Ab Confl - 164	SZE	CEV	SURF	119.842	39.172	1887	-109	-14.4		8 81
304	Ash Canyon Creek - 166	SZE	CEV	SURF	119.815	39.177	1612	-102	-14.9		8 81
305	Well - 3	SZE	CEV	WELL	119.765	39.221	1463	-109	-15.2	10	1 81
306	Well - 4	SZE	CEV	WELL	119.843	39.175	1829	-101	-15.7	13	1 81
307	Well - 5	SZE	CEV	WELL	119.798	39.185	1536	-108	-15.8		1 81
308	Well - 9	SZE	CEV	WELL	119.801	39.101	1500	-119	-17.7		1 81
309	Well - 10	SZE	CEV	WELL	119.761	39.136	1433	-126	-17.9	12	1 81
310	Well - 12	SZE	CEV	WELL	119.791	39.106	1748	-96	-15.1	2	3 81
311	Well - 13	SZE	CEV	WELL	119.834	39.121	1731	-113	-13.5	7	1 81
312	Well - 48	SZE	CEV	WELL	119.801	39.101	1450	-111	-15.1	15	4 81
313	Well - 52	SZE	CEV	WELL	119.791	39.179	1438	-110	-14.9	15	4 81
314	Well - 172	SZE	CEV	WELL	119.792	39.185	1524	-113	-14.4	16	9 81
315	Well - 173	SZE	CEV	WELL	119.767	39.181	1437	-111	-13.2	22	9 81
316	Well - 174	SZE	CEV	WELL	119.724	39.196	1411	-102	-13.3	14	9 81
317	Well - 175	SZE	CEV	WELL	119.744	39.161	1420	-104	-14.4	9	9 81
318	Well - 176	SZE	CEV	WELL	119.724	39.163	1425	-111	-13.4	10	10 81
319	Well - 177	SZE	CEV	WELL	119.724	39.163	1425	-108	-12.9	14	10 81

APPENDIX B, continued

Literature Search - Isotope Data

SAMP #	SAMPLE NAME	REF	LOC	TYPE	LONG	LAT	ELEV meters	DEUT ‰	OX18 ‰	TEMP °C	DATE MO YR
320	Well - 178	SZE	CEV	WELL	119.735	39.159	1430	-111	-15.0	35	10 81
321	Well - 179	SZE	CEV	WELL	119.744	39.161	1423	-114	-14.4	10	10 81
322	Well - 180	SZE	CEV	WELL	119.778	39.165	1448	-105	-13.8	13	10 81
323	Cold Spring - 1A	BOW	TSC	SPRG	116.165	41.502	1878	-119	-16.3	11	
324	Cold Spring - 2A	BOW	TSC	SPRG	116.157	41.521	1951	-122	-16.2	12	
325	Cold Spring - 3A	BOW	TSC	SPRG	116.181	41.511	1890	-125	-16.8	15	
326	Cold Spring - 3B	BOW	TSC	SPRG	116.181	41.507	1888	-124	-16.7	17	
327	Cold Spring - 3C	BOW	TSC	SPRG	116.175	41.508	1888	-116	-16.0	10	
328	Cold Spring - 3D	BOW	TSC	SPRG	116.163	41.483	1579	-118	-15.5	10	
329	Cold Spring - 4A	BOW	TSC	SPRG	116.087	41.529	2042	-123	-15.3	8	
330	Cold Spring - 5A	BOW	TSC	SPRG	116.169	41.486	1859	-135	-16.9	15	
331	Cold Spring - 5B	BOW	TSC	SPRG	116.182	41.487	1981	-131	-16.1	19	
332	Cold Spring - 5C	BOW	TSC	SPRG	116.171	41.491	1878	-135	-16.7	19	
333	Cold Spring - 6A	BOW	TSC	SPRG	116.166	41.436	1719	-134	-16.6	20	
334	Hot Spring - 7A	BOW	TSC	SPRG	116.066	41.474	1766	-137	-16.1	89	
335	Hot Spring - 7B	BOW	TSC	SPRG	116.067	41.474	1766	-129	-15.6	82	
336	Hot Spring - 7C	BOW	TSC	SPRG	116.161	41.471	1762	-133	-16.6	56	
337	Hot Spring - 8A	BOW	TSC	SPRG	116.146	41.477	1766	-128	-16.1	73	
338	Hot Spring - 8B	BOW	TSC	SPRG	116.147	41.476	1766	-137	-14.0	95	
339	Hot Spring - 8C	BOW	TSC	SPRG	116.147	41.481	1766	-136	-15.7	59	
340	Hot Spring - 8D	BOW	TSC	SPRG	116.146	41.479	1766	-135	-15.8	85	
341	Steamboat M1	FLN	SMA	WELL	119.753	39.409	1460	-115	-12.0	96	
342	Zolezzi M2	FLN	SMA	SPRG	119.766	39.431	1369	-94	-10.5	27	
343	Miles M3	FLN	SMA	WELL	119.818	39.477	1400	-131	-15.9	89	
344	Moana Lane M4	FLN	SMA	WELL	119.813	39.483	1378	-113	-14.4	40	
345	McKay M5	FLN	SMA	WELL	119.811	39.481	1378	-109	-14.2	54	
346	Desjardin M6	FLN	SMA	WELL	119.822	39.477	1399	-122	-15.9	77	
347	Warren Estates M7	FLN	SMA	WELL	119.825	39.481	1402	-129	-16.1	87	
348	Newburg M8	FLN	SMA	WELL	119.828	39.483	1414	-128	-15.8	95	
349	Gadda M9	FLN	SMA	WELL	119.816	39.479	1392	-123	-15.9	90	
350	Thomas Creek M10	FLN	SMA	SURF	119.796	39.438	1414	-114	-15.1	6	
351	Farad Spring M11	FLN	SMA	SPRG	120.031	39.421	1646	-115	-13.5	35	
352	Quillicy Well M12	FLN	SMA	WELL	119.803	39.478	1376	-111	-13.8	34	
353	River Inn M13	FLN	SMA	WELL	119.912	39.513	1415	-115	-14.9	58	
354	Steamboat Springs M14	FLN	SMA	WELL	119.753	39.409	1460	-116	-11.6	98	
355	Thomas Creek M15	FLN	SMA	SURF	119.796	39.438	1414	-114	-14.8	7	
356	Miles M16	FLN	SMA	WELL	119.818	39.477	1400	-125	-16.6	90	
357	Edmiston M17	FLN	SMA	WELL	119.815	39.481	1396	-110	-15.5	46	
358	Decapprio M18	FLN	SMA	WELL	119.821	39.479	1378	-97	-12.4	80	
359	S. Bermuda M19	FLN	SMA	WELL	119.821	39.476	1402	-116	-15.8	81	

APPENDIX B, continued

Literature Search - Isotope Data

SAMP #	SAMPLE NAME	REF	LOC	TYPE	LONG	LAT	ELEV meters	DEUT ‰	OX18 ‰	TEMP °C	DATE MO YR
360	Barnett B1	FLN	SMA	WELL	119.821	39.491	1390	-111	-13.1	30	
361	Barnett B2	FLN	SMA	WELL	119.821	39.491	1390	-107	-13.2	30	
362	Gadda G1	FLN	SMA	WELL	119.816	39.479	1392	-122	-15.0	90	
363	Gadda G2	FLN	SMA	WELL	119.816	39.479	1392	-114	-15.1	90	
364	Miles M1	FLN	SMA	WELL	119.818	39.477	1400	-114	-15.6	90	
365	Peppermill - P2	FLN	SMA	WELL	119.801	39.498	1358	-111	-14.8	53	
366	Walker Lake Surface	BEN	WKL	LAKE	118.701	38.701	1210	-42	-1.6		
367	East Walker, Bridgeport	BEN	WKR	SURF	119.221	38.258	1973	-105	-13.6		11 84
368	East Walker, Bridgeport	BEN	WKR	SURF	119.221	38.258	1973	-100	-13.8		6 85
369	East Walker, Bridgeport	BEN	WKR	SURF	119.221	38.258	1973	-101	-12.8		7 85
370	East Walker, Bridgeport	BEN	WKR	SURF	119.221	38.258	1973	-99	-12.2		8 85
371	East Walker, Bridgeport	BEN	WKR	SURF	119.221	38.258	1973	-104	-13.0		10 85
372	East Walker, Bridgeport	BEN	WKR	SURF	119.221	38.258	1973	-107	-13.7		11 85
373	East Walker, Bridgeport	BEN	WKR	SURF	119.221	38.258	1973	-108	-14.0		11 85
374	East Walker, Bridgeport	BEN	WKR	SURF	119.221	38.258	1973	-113	-12.8		1 86
375	East Walker, Bridgeport	BEN	WKR	SURF	119.221	38.258	1973	-112	-14.6		2 86
376	West Walker, Coleville	BEN	WKR	SURF	119.503	38.566	1536	-110	-15.5		6 85
377	West Walker, Coleville	BEN	WKR	SURF	119.503	38.566	1536	-111	-14.9		7 85
378	West Walker, Coleville	BEN	WKR	SURF	119.503	38.566	1536	-105	-14.3		8 85
379	West Walker, Coleville	BEN	WKR	SURF	119.503	38.566	1536	-118	-15.2		10 85
380	West Walker, Coleville	BEN	WKR	SURF	119.503	38.566	1536	-115	-15.3		11 85
381	West Walker, Coleville	BEN	WKR	SURF	119.503	38.566	1536	-119	-15.6		11 85
382	West Walker, Coleville	BEN	WKR	SURF	119.503	38.566	1536	-117	-13.8		1 86
383	West Walker, Coleville	BEN	WKR	SURF	119.503	38.566	1536	-112	-15.2		2 86
384	Walker River, Wabuska	BEN	WKR	SURF	119.108	39.131	1310	-109	-14.2		11 84
385	Walker River, Wabuska	BEN	WKR	SURF	119.108	39.131	1310	-101	-13.7		6 85
386	Walker River, Wabuska	BEN	WKR	SURF	119.108	39.131	1310	-101	-13.5		7 85
387	Walker River, Wabuska	BEN	WKR	SURF	119.108	39.131	1310	-107	-13.3		8 85
388	Walker River, Wabuska	BEN	WKR	SURF	119.108	39.131	1310	-102	-10.8		9 85
389	Walker River, Wabuska	BEN	WKR	SURF	119.108	39.131	1310	-103	-13.2		10 85
390	Walker River, Wabuska	BEN	WKR	SURF	119.108	39.131	1310	-107	-13.5		11 85
391	Walker River, Wabuska	BEN	WKR	SURF	119.108	39.131	1310	-109	-13.8		12 85
392	Walker River, Wabuska	BEN	WKR	SURF	119.108	39.131	1310	-112	-13.6		1 86
393	Walker River, Wabuska	BEN	WKR	SURF	119.108	39.131	1310	-111	-13.7		2 86
394	Walker River, Wabuska	BEN	WKR	SURF	119.108	39.131	1310	-113	-14.2		3 86
395	Trego Spring (near)	MAR	BRD	SPRG	119.112	40.766	1213	-128	-14.9	85	8 75
396	Selenite Range	MAR	BRD	SPRG	119.251	40.617	1676	-119	-15.3	14	8 75
397	San Emidio Desert - 1	MAR	BRD	SPRG	119.403	40.389	1244	-105	-11.5	79	8 75
398	San Emidio Desert - 2	MAR	BRD	SPRG	119.403	40.389	1244	-108	-12.1	89	8 75
399	San Emidio Desert - 3	MAR	BRD	SPRG	119.403	40.389	1244	-106	-11.6	95	8 75

APPENDIX B, continued

Literature Search - Isotope Data

SAMP #	SAMPLE NAME	REF	LOC	TYPE	LONG	LAT	ELEV meters	DEUT ‰	OX18 ‰	TEMP °C	DATE MO YR
400	Gt Boiling (near)	MAR	BRD	SPRG	119.362	40.672	1202	-107	-11.7	90	8 75
401	San Emidio Spring	MAR	BRD	SPRG	119.436	40.257	1532	-110	-14.2	15	8 75
402	Lee Hot Springs CH1	MNR	FAL	SPRG	118.722	39.209	1222	-126	-13.2	88	7
403	Dixie Hot Spring CH2	MNR	DXV	SPRG	118.071	39.788	1042	-126	-15.9	72	7
404	Stillwater Flow Well CH3	MNR	CSK	WELL	118.549	39.522	1189	-110	-12.4	96	7
405	Soda Lakes Res Well CH4	MNR	CSK	WELL	118.853	39.566	1215	-109	-13.5	100	7
406	Soda Lakes Res Well CH5	MNR	CSK	WELL	118.843	39.574	1210	-111	-14.6	22	7
407	Walley's Hot Spring DG1	MNR	CEV	SPRG	119.833	38.981	1426	-120	-15.6	61	7
408	Hot Hole EK1	MNR	ELK	SPRG	115.776	40.811	1542	-145	-15.3	56	7
409	Sulphur Hot Spring EK2A	MNR	RBV	SPRG	115.286	40.586	1841	-130	-16.1	93	7
410	Sulphur Hot Spring EK2B	MNR	RBV	SPRG	115.286	40.586	1841	-126	-14.5	45	7
411	Hot Ck hot spring EK3	MNR	PNE	SPRG	116.059	40.325	1737	-127	-16.3	26	7
412	Nile Spring EK4	MNR	NEN	SPRG	114.069	41.929	1559	-139	-18.2	43	7
413	Mineral Hot Spring EK5	MNR	NEN	SPRG	114.733	41.788	1616	-139	-17.6	60	7
414	Wells hot spring EK6A	MNR	WLS	SPRG	114.985	41.161	1745	-135	-16.9	50	7
415	Wells hot spring EK6B	MNR	WLS	SPRG	114.985	41.161	1745	-138	-17.0	36	7
416	Wells hot spring EK7A	MNR	WLS	SPRG	114.985	41.161	1745	-134	-16.5	61	7
417	Wells hot spring EK7B	MNR	WLS	SPRG	114.985	41.161	1745	-137	-17.0	55	7
418	Wildhorse hot sp EK8	MNR	NEN	SPRG	115.775	41.562	1896	-140	-17.9	54	7
419	Patsville hot sp EK9	MNR	NEN	SPRG	115.921	41.763	1775	-141	-18.2	41	7
420	Hot Sulfur Springs EK10	MNR	TSC	SPRG	116.147	41.468	1768	-135	-16.8	90	7
421	Carlin hot spring EK11	MNR	CAR	SPRG	116.127	40.697	1484	-133	-16.6	79	7
422	Ruby Marsh hot sp EK12	MNR	RBV	SPRG	115.409	40.251	1829	-130	-16.2	65	7
423	Walti Hot Spring EU1	MNR	GSV	SPRG	116.589	39.901	1731	-130	-16.9	72	7
424	Hot Springs Point EU2	MNR	BEO	SPRG	116.671	39.951	1448	-136	-16.0	54	7
425	Beowawe Steam Well EU3	MNR	BEO	WELL	116.591	40.564	1494	-114	-11.1	999	7
426	Beowawe Hot Spring EU4	MNR	BEO	SPRG	116.583	40.586	1451	-130	-14.8	98	7
427	Bartholomae Hot Sp EU5	MNR	AVY	SPRG	116.348	39.404	1933	-128	-16.3	54	7
428	Hot Spring Ranch HU1	MNR	PPV	SPRG	117.493	40.761	1463	-131	-15.7	85	7
429	Golconda hot spring HU2	MNR	PDV	SPRG	117.491	40.955	1341	-126	-15.7	74	7
430	Double Hot Springs HU3	MNR	BRD	SPRG	119.028	41.049	1212	-129	-15.9	80	7
431	Soldier Meadow hs HU4	MNR	BRD	SPRG	119.181	41.381	1353	-130	-16.6	54	7
432	Pinto HS West Well HU5	MNR	BRD	WELL	118.807	41.357	1244	-128	-14.1	92	7
433	Pinto Hot Sp East HU6	MNR	BRD	SPRG	118.785	41.362	1244	-129	-14.5	93	7
434	Dyke Hot Spring HU7	MNR	BRD	SPRG	118.566	41.567	1262	-128	-16.3	66	7
435	Baltazor Flow Well HU8	MNR	BRD	WELL	119.183	41.921	1284	-126	-15.6	90	7
436	Baltazor Hot Sp HU9	MNR	BRD	SPRG	119.183	41.921	1284	-125	-15.3	80	7
437	Bog Hot Springs HU10	MNR	BRD	SPRG	119.781	41.923	1309	-124	-15.3	54	7
438	Howard Hot Springs HU12	MNR	BRD	SPRG	118.505	41.722	1317	-127	-16.2	56	7
439	The Hot Springs HU13	MNR	PDV	SPRG	117.388	41.421	1366	-135	-16.4	58	7

APPENDIX B, continued

Literature Search - Isotope Data

SAMP #	SAMPLE NAME	REF	LOC	TYPE	LONG	LAT	ELEV meters	DEUT ‰	OX18 ‰	TEMP °C	DATE MO YR
440	Spencer Hot Spring LA1	MNR	MON	SPRG	116.589	39.327	1725	-136	-16.0	72	7
441	Valley Moon hot sp LA2	MNR	RSE	SPRG	117.102	40.199	1463	-128	-16.3	53	7
442	Smith Ck hot spring LA3	MNR	RSE	SPRG	117.561	39.354	1884	-130	-16.7	86	7
443	Buff Vly Hot Spring LA4	MNR	BUF	SPRG	117.327	40.368	1425	-132	-15.9	49	7
444	Wabuska Hot Sp LY1A	MNR	MSV	SPRG	119.152	39.161	1311	-132	-16.0	97	7
445	Wabuska Hot Sp LY1B	MNR	MSV	SPRG	119.152	39.161	1311	-130	-15.4	94	7
446	Nevada Hot Springs LY2	MNR	MSV	SPRG	119.411	38.899	1420	-123	-16.0	61	7
447	Patua (Fernley) hs LY3	MNR	CSK	SPRG	119.113	39.597	1237	-122	-13.3	86	7
448	Soda Springs MI1	MNR	MIN	SPRG	118.103	38.342	1425	-130	-16.1	35	7
449	Darrough Steam Well NY1	MNR	BSV	WELL	117.186	38.822	1719	-119	-15.3	94	7
450	Darrough Hot Sp NY2	MNR	BSV	SPRG	117.185	38.811	1707	-123	-15.5	95	7
451	Dianas Punch Bowl NY3	MNR	MON	SPRG	116.665	39.031	2063	-125	-16.2	59	7
452	Dianas Punch Bowl HS NY4	MNR	MON	SPRG	116.665	39.031	2048	-125	-14.8	51	7
453	Pott's Ranch Hot Sp NY5	MNR	BSV	SPRG	116.558	39.081	2027	-128	-16.3	45	7
454	Warm Springs wm sp NY6	MNR	HCV	SPRG	116.377	38.187	1682	-114	-14.3	61	7
455	Jersey Valley hs PE1	MNR	DXV	SPRG	117.491	40.178	1378	-130	-15.6	29	7
456	Kyle Hot Springs PE2	MNR	BVY	SPRG	117.884	40.406	1391	-130	-15.5	77	7
457	Sou Hot Springs PE3	MNR	DXV	SPRG	117.725	40.087	1125	-130	-16.2	73	7
458	Trego hot spring PE5	MNR	BRD	SPRG	119.111	40.767	1199	-125	-14.4	86	7
459	Black Rock hot sp PE6	MNR	BRD	SPRG	118.967	40.961	1205	-122	-13.0	90	7
460	Leach Hot Spring PE7	MNR	PLV	SPRG	117.648	40.603	1421	-129	-15.7	92	7
461	Needle Rocks WA1	MNR	PLK	SPRG	119.676	40.146	1164	-107	-6.3	56	7
462	Great Boiling Sp WA2	MNR	BRD	SPRG	119.365	40.661	1207	-101	-10.8	86	7
463	Gerlach flow well WA3	MNR	BRD	WELL	119.381	40.781	1463	-121	-14.7	80	7
464	Steamboat Springs WA4	MNR	SMA	SPRG	119.741	39.381	1402	-117	-12.2	94	7
465	Bower's Hot Spring WA5	MNR	WSV	SPRG	119.842	39.328	1561	-102	-14.8	46	7
466	Cherry Ck hot sp WP1	MNR	STV	SPRG	114.898	39.887	1900	-128	-16.2	61	7
467	Monte Neva WP2	MNR	STV	SPRG	114.807	39.668	1830	-128	-16.7	79	7
468	Radium HS Well BA1	MNR	ORE	WELL	117.935	44.931	1009	-138	-17.9	57	7
469	East Lake Hot Spring DE1	MNR	ORE	SPRG	121.197	43.723	1944	-76	-9.4	62	7
470	Weberg Hot Spring GR1	MNR	ORE	SPRG	119.648	44.003	1482	-122	-15.1	46	
471	Blue Mountain Hot Sp GR2	MNR	ORE	SPRG	118.576	44.355	1301	-127	-16.1	58	
472	Ritter Hot Springs GR3	MNR	ORE	SPRG	119.137	44.835	884	-119	-14.8	43	
473	Trout Creek hot sp HA1	MNR	ORE	SPRG	118.377	42.188	1414	-127	-16.2	52	
474	Hot Lake HA2	MNR	ORE	SURF	118.603	42.327	1244	-116	-11.6		
475	Hot Lake hot spring HA3	MNR	ORE	SPRG	118.603	42.327	1244	-126	-14.4	96	
476	Alvord/Indian Spring HA4	MNR	ORE	SPRG	118.532	42.544	1241	-124	-13.2	79	
477	Mickey Springs HA5	MNR	ORE	SPRG	118.347	42.678	1228	-124	-13.4	86	
478	Crane Hot Springs HA7	MNR	ORE	SPRG	118.633	43.441	1262	-134	-16.2	78	
479	Olene Gap Hot Spring KL1	MNR	ORE	SPRG	121.618	42.173	1250	-113	-13.0	87	

APPENDIX B, continued

Literature Search - Isotope Data

SAMP #	SAMPLE NAME	REF	LOC	TYPE	LONG	LAT	ELEV meters	DEUT ‰	OX18 ‰	TEMP °C	DATE MO YR
480	Crump's Spring LK2	MNR	ORE	SPRG	119.875	42.251	1370	-116	-13.3	78	
481	Barry Ranch Hot Sp LK3	MNR	ORE	SPRG	120.435	42.153	1442	-119	-13.7	88	
482	Hunters Hot Springs LK4	MNR	ORE	SPRG	120.368	42.221	1454	-119	-14.3	96	
483	Summer Lake Hot Sp LK5	MNR	ORE	SPRG	120.647	42.724	1298	-115	-13.3	43	
484	McDermitt hot sp MA1	MNR	ORE	SPRG	117.831	42.096	1417	-135	-17.0	52	
485	Three Forks hot sp MA2	MNR	ORE	SPRG	117.172	42.626	1219	-127	-16.1	35	
486	Riverside hot spring MA3	MNR	ORE	SPRG	118.199	43.467	1030	-134	-15.2	63	
487	Beulah Hot Springs MA4	MNR	ORE	SPRG	118.127	43.944	1018	-132	-13.2	60	
488	Neal Hot Spring MA5	MNR	ORE	SPRG	117.462	44.024	792	-139	-16.5	88	
489	Little Valley hot sp MA6	MNR	ORE	SPRG	117.503	43.893	756	-140	-16.5	76	
490	Mitchell Butte HS MA7	MNR	ORE	SPRG	117.151	43.763	692	-137	-16.7	62	
491	Vale Hot Spring MA8	MNR	ORE	SPRG	117.232	43.986	680	-135	-15.2	97	
492	Dry Creek	NEH	SMA	SURF	119.821	39.471	1575	-115	-15.1	15	6 77
493	Stock Spring	NEH	SMA	SPRG	119.831	39.441	1783	-118	-15.6	15	6 77
494	Stock Spring	NEH	SMA	SPRG	119.831	39.441	1783	-119	-15.5	13	11 77
495	Thomas Creek Spring	NEH	SMA	SPRG	119.881	39.431	2316	-122	-15.9	13	6 77
496	Thomas Creek Spring	NEH	SMA	SPRG	119.881	39.431	2316	-123	-16.3	13	11 77
497	Slide Mountain Spring	NEH	SMA	SPRG	119.911	39.311	2774	-106	-14.9	6	6 77
498	Slide Mountain Spring	NEH	SMA	SPRG	119.911	39.311	2774	-106	-14.9	9	7 77
499	Slide Mountain Spring	NEH	SMA	SPRG	119.911	39.311	2774	-110	-14.8	-1	8 77
500	Slide Mountain Spring	NEH	SMA	SPRG	119.911	39.311	2774	-109	-15.0	1	11 77
501	Davis Creek Spring	NEH	SMA	SPRG	119.831	39.321	1768	-109	-14.5	13	6 77
502	Davis Creek Spring	NEH	SMA	SPRG	119.831	39.321	1768	-110	-14.7	17	7 77
503	Davis Creek Spring	NEH	SMA	SPRG	119.831	39.321	1768	-109	-14.6	7	11 77
504	Pleasant Valley School	NEH	SMA	WELL	119.781	39.371	1463	-109	-14.9	22	6 77
505	Pleasant Valley School	NEH	SMA	WELL	119.781	39.371	1463	-110	-14.9	25	7 77
506	Pleasant Valley School	NEH	SMA	WELL	119.781	39.371	1463	-112	-14.8	12	11 77
507	Jumbo Grade Spring	NEH	SMA	SPRG	119.721	39.291	1813	-114	-14.4	11	6 77
508	Jumbo Grade Spring	NEH	SMA	SPRG	119.721	39.291	1813	-116	-14.7	9	11 77
509	Scorpion Springs	NEH	SMA	SPRG	119.691	39.361	1980	-116	-14.9	13	6 77
510	Alum Spring	NEH	SMA	SPRG	119.691	39.391	1980	-116	-14.8	12	6 77
511	Alum Spring	NEH	SMA	SPRG	119.691	39.391	1980	-113	-14.2	16	7 77
512	Alum Spring	NEH	SMA	SPRG	119.691	39.391	1980	-115	-14.6	14	8 77
513	Alum Spring	NEH	SMA	SPRG	119.691	39.391	1980	-116	-14.5	12	11 77
514	Guyton Ranch Well	NEH	SMA	WELL	119.171	39.471	1478	-113	-13.6	19	6 77
515	Hidden Valley Well	NEH	SMA	WELL	119.721	39.500	1493	-116	-15.2	17	6 77
516	Washoe Lake	NEH	SMA	LAKE	119.171	39.251	1530	-58	-5.0		3 76
517	Washoe Lake	NEH	SMA	LAKE	119.171	39.251	1530	-17	2.6		11 76
518	Washoe Lake	NEH	SMA	LAKE	119.171	39.251	1530	-64	-6.4		4 78
519	Lake Tahoe	NEH	LKT	LAKE	120.001	39.001	1898	-57	-5.3		7 76

APPENDIX B, continued

Literature Search - Isotope Data

SAMP #	SAMPLE NAME	REF	LOC	TYPE	LONG	LAT	ELEV meters	DEUT ‰	OX18 ‰	TEMP °C	DATE MO YR
520	50	NEH	SMA	SPRG	119.738	39.381	1402	-116	-12.2	53	6 77
521	50	NEH	SMA	SPRG	119.738	39.381	1402	-115	-12.4	50	7 77
522	50	NEH	SMA	SPRG	119.738	39.381	1402	-116	-12.6	52	11 77
523	25SS	NEH	SMA	SPRG	119.739	39.383	1404	-116	-12.5	88	7 75
524	26NW	NEH	SMA	SPRG	119.741	39.383	1413	-114	-10.4	95	7 75
525	26	NEH	SMA	SPRG	119.739	39.381	1410	-116	-12.4	96	6 77
526	26	NEH	SMA	SPRG	119.739	39.381	1410	-116	-12.1	89	7 77
527	26	NEH	SMA	SPRG	119.739	39.381	1410	-116	-12.1	90	11 77
528	Near 1	NEH	SMA	SPRG	119.742	39.386	1417	-118	-12.4	72	11 77
529	3	NEH	SMA	SPRG	119.742	39.386	1417	-117	-12.2	72	11 77
530	4	NEH	SMA	SPRG	119.741	39.387	1410	-110	-10.5	58	5 74
531	4	NEH	SMA	SPRG	119.741	39.387	1410	-107	-10.7	53	3 76
532	4	NEH	SMA	SPRG	119.741	39.387	1410	-110	-11.0	70	7 76
533	4	NEH	SMA	SPRG	119.741	39.387	1410	-111	-11.3	77	6 77
534	4	NEH	SMA	SPRG	119.741	39.387	1410	-113	-11.2	76	7 77
535	4	NEH	SMA	SPRG	119.741	39.387	1410	-114	-11.3	79	8 77
536	4	NEH	SMA	SPRG	119.741	39.387	1410	-114	-11.0	83	11 77
537	4	NEH	SMA	SPRG	119.741	39.387	1410	-114	-11.5	79	12 77
538	5	NEH	SMA	SPRG	119.742	39.387	1410	-115	-12.1	81	7 75
539	5	NEH	SMA	SPRG	119.742	39.387	1410	-115	-12.0	95	6 77
540	Mine Tunnel Near 5	NEH	SMA	SPRG	119.741	39.391	1410	-114	-12.1	70	7 77
541	6	NEH	SMA	SPRG	119.741	39.388	1410	-116	-12.1	97	6 77
542	6	NEH	SMA	SPRG	119.741	39.388	1410	-115	-11.9	97	7 77
543	6	NEH	SMA	SPRG	119.741	39.388	1410	-116	-12.3	98	11 77
544	6	NEH	SMA	SPRG	119.741	39.388	1410	-116	-12.6	97	12 77
545	8	NEH	SMA	SPRG	119.741	39.389	1410	-116	-11.8	93	5 74
546	8	NEH	SMA	SPRG	119.741	39.389	1410	-116	-12.2	90	7 75
547	8	NEH	SMA	SPRG	119.741	39.389	1410	-117	-12.2	96	7 76
548	8	NEH	SMA	SPRG	119.741	39.389	1410	-116	-12.8	91	6 77
549	8	NEH	SMA	SPRG	119.741	39.389	1410	-116	-12.2	93	7 77
550	8	NEH	SMA	SPRG	119.741	39.389	1410	-116	-12.1	87	11 77
551	8	NEH	SMA	SPRG	119.741	39.389	1410	-117	-12.4	90	12 77
552	10	NEH	SMA	SPRG	119.742	39.391	1410	-116	-10.8	85	5 74
553	13	NEH	SMA	SPRG	119.742	39.391	1410	-113	-11.7	90	7 75
554	13	NEH	SMA	SPRG	119.742	39.391	1410	-114	-11.3	91	7 76
555	23	NEH	SMA	SPRG	119.744	39.391	1410	-115	-12.1	95	6 77
556	23	NEH	SMA	SPRG	119.744	39.391	1410	-115	-12.0	95	7 77
557	23	NEH	SMA	SPRG	119.744	39.391	1410	-114	-12.0	95	11 77
558	24	NEH	SMA	SPRG	119.744	39.391	1410	-115	-11.9	97	12 77
559	17S	NEH	SMA	SPRG	119.744	39.391	1410	-112	-10.8	84	7 75

APPENDIX B, continued

Literature Search - Isotope Data

SAMP #	SAMPLE NAME	REF	LOC	TYPE	LONG	LAT	ELEV meters	DEUT ‰	OX18 ‰	TEMP °C	DATE MO YR
560	Near 27	NEH	SMA	SPRG	119.744	39.392	1410	-116	-12.1	78	6 77
561	Near 27	NEH	SMA	SPRG	119.744	39.392	1410	-115	-12.2	90	7 77
562	Near 27	NEH	SMA	SPRG	119.744	39.392	1410	-117	-12.4	85	11 77
563	Near 27	NEH	SMA	SPRG	119.744	39.392	1410	-115	-12.1	79	12 77
564	27	NEH	SMA	SPRG	119.744	39.392	1410	-115	-12.1	87	6 77
565	21N	NEH	SMA	SPRG	119.743	39.393	1410	-113	-11.7	70	6 77
566	21N	NEH	SMA	SPRG	119.743	39.393	1410	-113	-11.5	66	7 77
567	Mormon Well	LYL	LVS	WELL	115.095	36.644	1963	-91	-12.5	10	9 83
568	Wiregrass Spring	LYL	LVS	SPRG	115.208	36.633	2438	-94	-12.9	10	10 86
569	Cow Camp Spring	LYL	LVS	SPRG	115.307	36.584	1756	-93	-12.6	10	10 83
570	Indian Spring AFB	LYL	LVS	WELL	115.681	36.581	954	-96	-13.0	24	6 85
571	Indian Spring	LYL	LVS	SPRG	115.668	36.565	969	-93	-11.9	25	6 86
572	Point B Well	LYL	LVS	WELL	115.565	36.535	975	-98	-13.2	25	6 86
573	Indian Spring Prison	LYL	LVS	WELL	115.554	36.514	1024	-102	-13.7	23	6 85
574	Big Timber Spring	LYL	LVS	SPRG	115.927	36.445	2048	-93	-13.3	11	6 85
575	Corn Creek Spring	LYL	SHR	SPRG	115.357	36.439	895	-96	-13.0	21	6 85
576	Corn Creek Well	LYL	SHR	WELL	115.398	36.465	899	-95	-13.5	19	12 86
577	Willow Spring	LYL	LVS	SPRG	115.763	36.417	1829	-98	-13.4	11	6 85
578	LV Pahute Indian Res	LYL	LVS	WELL	115.357	36.357	927	-98	-14.0	19	7 85
579	Adams Well	LYL	LVS	WELL	115.281	36.331	893	-98	-12.7	23	8 82
580	Courtney Well	LYL	LVS	WELL	115.348	36.328	960	-96	-12.1	21	8 82
581	Holland Well	LYL	LVS	WELL	115.283	36.333	783	-98	-12.6	26	8 82
582	Mifflin Well	LYL	LVS	WELL	115.423	36.326	1183	-100	-12.6	18	8 82
583	Clark Spring	LYL	LVS	SPRG	115.721	36.321	2648	-94	-12.9	10	6 85
584	Tule Spring State Park	LYL	LVS	WELL	115.267	36.321	750	-99	-13.4	21	6 85
585	Stewart Well	LYL	LVS	WELL	115.672	36.319	2530	-100	-13.4	10	6 86
586	Gilbert Well	LYL	LVS	WELL	115.423	36.308	1225	-98	-12.7	16	8 82
587	Deer Creek Spring #2	LYL	LVS	SPRG	115.627	36.308	2652	-98	-13.4	8	6 85
588	Grapevine Spring	LYL	LVS	SPRG	115.491	36.301	1490	-91	-11.6	27	6 85
589	Martin Well	LYL	LVS	WELL	115.243	36.291	715	-100	-13.4	22	6 85
590	Highway Maint. Well	LYL	LVS	WELL	115.594	36.269	1960	-96	-12.2	11	9 82
591	Mt Charleston Lodge	LYL	LVS	WELL	115.647	36.258	2320	-96	-12.4	10	8 82
592	Sky Mtn. Resort	LYL	LVS	WELL	115.579	36.171	1817	-97	-13.3	14	6 85
593	Red Rock Canyon Red Sp	LYL	LVS	SPRG	115.419	36.144	1122	-93	-12.2	19	6 85
594	BLM Visitors Center	LYL	LVS	WELL	115.434	36.129	1125	-89	-12.3		6 85
595	Sandstone Spring	LYL	LVS	SPRG	115.469	36.063	1207	-90	-12.7	17	6 85
596	Travertine Hot Springs	HIG	LVC	SPRG	119.205	38.246	2048	-137	-16.3	69	
597	The Hot Springs	HIG	LVC	SPRG	119.214	38.223	2024	-136	-16.0	38	
598	Big Alkali Spring	HIG	LVC	SPRG	119.159	38.212	2280	-132	-17.2	17	
599	Warm Spring	HIG	LVC	SPRG	119.112	38.203	2347	-130	-17.2	24	

APPENDIX B, continued

Literature Search - Isotope Data

SAMP #	SAMPLE NAME	REF	LOC	TYPE	LONG	LAT	ELEV meters	DEUT OO/O	OX18 OO/O	TEMP °C	DATE MO YR
600	Bodie Water Supply	HIG	LVC	SPRG	119.073	38.245	2804	-124	-16.8	5	
601	8S 1E 20CCA1S	YNG	SWI	SPRG	116.383	42.731	1829	-128	-17.1	10	7 73
602	9S 2E 13CBC1S	YNG	SWI	SPRG	116.167	42.651	1341	-122	-16.5	11	7 73
603	11S 5W 2DAB1S	YNG	SWI	SPRG	116.887	42.493	1704	-118	-15.4	8	6 78
604	13S 4E 12CDD1	YNG	SWI	SPRG	115.934	42.304	1669	-116	-13.8	8	6 78
605	14S 14E 11CAB1S	YNG	SWI	SPRG	114.784	42.222	1558	-126	-17.1	12	6 78
606	46N 60E 13ACC1S	YNG	NEN	SPRG	115.125	41.875	2250	-127	-16.7	4	6 78
607	45N 55E 25DAA1S	YNG	NEN	SPRG	115.711	41.768	2030	-128	-16.6	7	6 78
608	1N 3W 21ACD1S	YNG	SWI	SPRG	116.737	43.411	680	-139	-16.8	56	6 78
609	2S 2W 35ACB1	YNG	SWI	WELL	116.543	43.207	900	-145	-17.8	40	6 78
610	4S 1E 34BAD1	YNG	SWI	WELL	116.324	43.036	783	-145	-17.5	77	6 78
611	5S 3E 26BCB1	YNG	SWI	WELL	116.077	42.963	762	-146	-17.5	81	6 78
612	7S 5E 7ABB1	YNG	SWI	WELL	115.901	42.751	908	-135	-17.6	40	6 78
613	7S 6E 9BAD1	YNG	SWI	WELL	115.767	42.751	878	-142	-18.2	51	6 78
614	8S 14E 30ACD1S	YNG	SWI	SPRG	114.857	42.704	882	-137	-17.2	71	2 78
615	9S 13E 33CBD1	YNG	SWI	WELL	114.946	42.531	1148	-131	-16.2	30	6 78
616	12S 7E 33CBC1S	YNG	SWI	SPRG	115.811	42.366	1133	-130	-16.6	72	6 78
617	14S 9E 2BAA1	YNG	SWI	WELL	115.375	42.244	1603	-124	-16.4	27	6 78
618	16S 9E 24BB1S	YNG	SWI	SPRG	115.362	42.026	1585	-131	-17.3	55	6 78
619	Basset Hot Spring	IGR	MDC	SPRG	121.111	41.644	1265	-119	-14.5	79	7 83
620	Kelly Hot Springs	IGR	MDC	SPRG	120.801	41.454	1340	-117	-13.6	92	7 83
621	Menlo Hot Spring, CA	IGR	SPV	SPRG	120.074	41.241	1375	-117	-14.8	56	7 83
622	Hunters Hot Spring, OR	IGR	ORE	SPRG	120.371	42.204	1333	-125	-13.6	96	7 83
623	Leonards Hot Spring	IGR	SPV	SPRG	120.092	41.598	1375	-117	-13.8	62	7 73
624	Bradys AH-1	WLC	BDY	WELL	119.016	39.788	1242	-125	-14.7	95	3 81
625	Bradys AH-2	WLC	BDY	WELL	119.019	39.783	1242	-126	-14.0	80	3 81
626	Bradys AH-4	WLC	BDY	WELL	119.032	39.779	1240	-127	-14.4	20	3 81
627	Bradys AH-5	WLC	BDY	WELL	119.016	39.812	1251	-123	-14.2	27	3 81
628	Bradys AH-8	WLC	BDY	WELL	119.004	39.776	1244	-123	-14.3	36	3 81
629	Bradys AH-9	WLC	BDY	WELL	119.041	39.766	1240	-123	-14.0	15	3 81
630	Bradys DH-15	WLC	BDY	WELL	119.009	39.789	1257	-124	-14.2	117	4 81
631	Bradys DH-17	WLC	BDY	WELL	119.021	39.787	1240	-126	-14.3	58	2 81
632	Bradys AH-20	WLC	BDY	WELL	119.018	39.774	1250	-126	-14.4	111	3 81
633	Bradys M-8	WLC	BDY	WELL	119.012	39.787	1253	-121	-14.2	100	7 79
634	Desert Peak DH-31	WLC	DPK	WELL	118.995	39.739	1216	-114	-12.2	20	2 81
635	Desert Peak B21-2	BNT	DPK	WELL	118.946	39.764	1414	-116	-12.6	320	3 77
636	Desert Peak B21-2	BNT	DPK	WELL	118.946	39.764	1414	-116	-12.9	320	11 77
637	Spring - 1	NAT	RFT	SPRG	113.462	42.464	1613	-135	-17.9	12	7 75
638	Well - 2	NAT	RFT	WELL	113.441	42.446	1387	-124	-16.8	32	8 75
639	Well - 3	NAT	RFT	WELL	113.432	42.441	1361	-125	-16.8	35	7 75

APPENDIX B, continued

Literature Search - Isotope Data

SAMP #	SAMPLE NAME	REF	LOC	TYPE	LONG	LAT	ELEV meters	DEUT ‰	OX18 ‰	TEMP °C	DATE MO YR
640	Mud Spring - 4	NAT	RFT	SPRG	113.073	42.398	1768	-128	-16.7	3	11 76
641	Spring - 5	NAT	RFT	SPRG	113.036	42.393	1839	-126	-16.6	2	11 76
642	Lake Fork Spring - 6	NAT	RFT	SPRG	113.033	42.388	1804	-126	-16.6	3	11 76
643	Spring - 7	NAT	RFT	SPRG	113.691	42.259	1884	-125	-16.3	10	8 75
644	Spring - 8	NAT	RFT	SPRG	113.678	42.251	1902	-127	-16.8	8	8 75
645	Upper Nibbs Spring - 9	NAT	RFT	SPRG	113.452	42.311	1725	-129	-17.1	9	8 75
646	Rice Spring - 10	NAT	RFT	SPRG	113.444	42.287	1513	-133	-17.0	21	8 75
647	Point Spring - 11	NAT	RFT	SPRG	113.203	42.244	1536	-127	-16.7	19	8 75
648	Spring - 12	NAT	RFT	SPRG	113.701	42.234	2143	-134	-17.6	6	8 75
649	Sears Spring - 13	NAT	RFT	SPRG	113.588	42.241	1597	-132	-16.9	28	8 75
650	Spring - 14	NAT	RFT	SPRG	113.429	42.193	1634	-128	-16.2	11	7 75
651	DH06 - 15	NAT	RFT	WELL	113.425	42.181	1657	-144	-18.3	15	9 79
652	DH06 - 15	NAT	RFT	WELL	113.425	42.181	1657	-145	-18.5	13	11 78
653	I.D.-5 - 16	NAT	RFT	WELL	113.431	42.168	1668	-135	-17.2	12	3 75
654	Well - 17	NAT	RFT	WELL	113.353	42.199	1429	-131	-17.0	24	7 75
655	Spring - 18	NAT	RFT	SPRG	113.855	42.133	2158	-129	-17.4	-1	11 76
656	Wilson Spring - 19	NAT	RFT	SPRG	113.904	42.116	1620	-132	-17.1	16	11 76
657	Indian Grove Sp - 20	NAT	RFT	SPRG	113.729	42.113	2303	-135	-18.2	5	7 75
658	Emery Canyon Sp - 21	NAT	RFT	SPRG	113.734	42.088	2062	-132	-17.4	9	7 75
659	Flowing Well - 22	NAT	RFT	WELL	113.132	42.101	1643	-133	-17.4	37	8 76
660	Almo 2 - 23	NAT	RFT	WELL	113.613	42.075	1603	-132	-17.3	17	2 76
661	Jim Sage Spring - 24	NAT	RFT	SPRG	113.517	42.122	1920	-133	-17.2	18	8 75
662	Spring - 25	NAT	RFT	SPRG	113.506	42.093	1783	-132	-17.0	20	8 75
663	Almo 1 - 26	NAT	RFT	WELL	113.561	42.085	1567	-132	-17.4	59	11 75
664	Spring - 28	NAT	RFT	SPRG	113.541	42.074	1582	-128	-16.8	12	
665	I.D.-1 - 30D	NAT	RFT	WELL	113.354	42.134	1463	-135	-17.5	28	9 74
666	Spring - 31	NAT	RFT	SPRG	113.405	42.122	1554	-128	-16.9		7 74
667	Well - 32	NAT	RFT	WELL	113.414	42.118	1570	-133	-17.2	18	74
668	RRGE-2 - 33	NAT	RFT	WELL	113.378	42.108	1476	-135	-17.5	50	7 75
669	RRGE-2 - 33	NAT	RFT	WELL	113.378	42.108	1476	-136	-17.5	62	10 76
670	Schmidt Well - 35	NAT	RFT	WELL	113.391	42.107	1501	-136	-17.6	95	7 74
671	Schmidt Well - 35	NAT	RFT	WELL	113.391	42.107	1501	-133	-17.6	90	10 76
672	Well - 36	NAT	RFT	WELL	113.374	42.107	1471	-130	-16.9	29	7 75
673	RRGE-1 - 37	NAT	RFT	WELL	113.391	42.101	1495	-132	-17.6	95	10 76
674	RRGE-1 - 37	NAT	RFT	WELL	113.391	42.101	1495	-133	-17.6	95	10 77
675	I.D.-3 - 38	NAT	RFT	WELL	113.394	42.098	1494	-134	-17.4	79	1 75
676	I.D.-3 - 38	NAT	RFT	WELL	113.394	42.098	1494	-133	-17.7	56	4 75
677	Crank Well - 39	NAT	RFT	WELL	113.376	42.098	1473	-135	-17.3	93	7 74
678	Well - 40	NAT	RFT	WELL	113.374	41.097	1471	-130	-16.7	33	7 75
679	Well - 41	NAT	RFT	WELL	113.364	42.101	1465	-131	-17.2	31	7 75

APPENDIX B, continued

Literature Search - Isotope Data

SAMP #	SAMPLE NAME	REF	LOC	TYPE	LONG	LAT	ELEV meters	DEUT ‰	OX18 ‰	TEMP °C	DATE MO YR
680	RRGE-3 - 43	NAT	RFT	WELL	113.362	42.093	1478	-136	-17.6		2 77
681	RRGE-3 - 43	NAT	RFT	WELL	113.362	42.093	1478	-135	-17.7		10 77
682	I.D.-2 - 44	NAT	RFT	WELL	113.361	42.092	1481	-132	-17.0	30	1 75
683	Well - 47	NAT	RFT	WELL	113.323	42.134	1442	-127	-16.9	10	7 75
684	Well - 48	NAT	RFT	WELL	113.335	42.075	1472	-130	-17.2	15	8 75
685	Six Mile Spring - 49	NAT	RFT	SPRG	113.173	42.126	1902	-129	-17.0	8	8 75
686	Mine Tunnel Sp - 50	NAT	RFT	SPRG	113.072	42.094	2158	-123	-16.6	8	8 75
687	Spring - 51	NAT	RFT	SPRG	113.067	42.083	2012	-129	-16.9	8	8 75
688	Spring - 52	NAT	RFT	SPRG	113.821	42.017	1966	-128	-16.9	12	5 76
689	Spring - 53	NAT	RFT	SPRG	113.841	41.994	2012	-128	-16.8		
690	Spring - 54	NAT	RFT	SPRG	113.724	42.067	1975	-134	-17.6	9	12 75
691	Spring - 55	NAT	RFT	SPRG	113.719	42.049	1896	-126	-16.1	5	12 75
692	Well - 56	NAT	RFT	WELL	113.733	42.025	1859	-127	-16.3	10	3 76
693	I.D.-4 - 58	NAT	RFT	WELL	113.447	42.067	1512	-129	-17.4	40	3 75
694	The Narrow Hot Sp - 59	NAT	RFT	SPRG	113.447	42.067	1512	-131	-17.4	38	7 74
695	Spring - 60	NAT	RFT	SPRG	113.423	42.012	1681	-126	-16.6	16	7 75
696	Spring - 61	NAT	RFT	SPRG	113.329	42.038	1537	-126	-17.0	12	7 75
697	Spring - 63	NAT	RFT	SPRG	113.151	42.001	1707	-125	-16.4	14	7 74
698	Gambles Hole Well - 65	NAT	RFT	WELL	114.116	41.889	1580	-134	-17.4	34	11 76
699	Mine Tunnel - 67	NAT	RFT	SPRG	113.849	41.976	2290	-130	-16.8	8	9 75
700	Spring - 68	NAT	RFT	SPRG	113.762	41.919	1900	-134	-17.6	10	9 75
701	Spring - 69	NAT	RFT	SPRG	113.671	41.918	1980	-121	-16.7	7	9 75
702	Dipping Vat Spring - 70	NAT	RFT	SPRG	113.471	41.949	2130	-122	-15.7	8	10 75
703	Spring - 71	NAT	RFT	SPRG	113.367	41.925	2820	-127	-17.0	6	9 75
704	Spring - 72	NAT	RFT	SPRG	113.353	41.907	2895	-130	-17.7	7	9 75
705	Spring - 73	NAT	RFT	SPRG	113.906	41.817	1780	-131	-16.9	9	11 76
706	Spring - 74	NAT	RFT	SPRG	113.787	41.854	2085	-130	-17.2	10	11 76
707	Spring - 75	NAT	RFT	SPRG	113.768	41.864	2145	-133	-17.6	8	11 76
708	Clarkes Basin Sp - 76	NAT	RFT	SPRG	113.659	41.868	2180	-124	-16.4	8	10 75
709	Pine Spring - 77	NAT	RFT	SPRG	113.641	41.857	2310	-133	-17.6	8	10 75
710	Antelope - 1	COL	USC	SPRG	112.865	38.653	1480	-113	-14.6	16	6 75
711	Fish Spring - 2	COL	UWC	SPRG	113.391	39.844	1315	-129	-13.8	21	6 75
712	Fish Spring - 3	COL	UWC	SPRG	113.423	39.908	1305	-127	-12.3	59	6 75
713	Twin Peaks - 4	COL	USC	SPRG	112.716	38.795	1610	-112	-14.6	28	6 75
714	Cudahy - 5	COL	USC	SPRG	112.864	38.762	1520	-114	-14.6	32	6 75
715	Laverkin - 6	COL	USW	SPRG	113.268	37.187	995	-111	-13.1	42	6 75
716	Grantsville - 7	COL	USL	SPRG	112.531	40.646	1295	-107	-13.8	30	6 75
717	Crystal Prison - 8	COL	UTL	SPRG	111.911	40.501	1320	-141	-15.9	62	6 78
718	Red Hill - 10	COL	USC	SPRG	112.103	38.636	1720	-127	-17.0	77	77
719	Monroe - 11	COL	USC	SPRG	112.111	38.634	1645	-128	-17.0	70	77

APPENDIX B, continued

Literature Search - Isotope Data

SAMP #	SAMPLE NAME	REF	LOC	TYPE	LONG	LAT	ELEV meters	DEUT ‰	OX18 ‰	TEMP °C	DATE MO YR
720	Joeseeph - 12	COL	USC	SPRG	112.211	38.613	1680	-133	-17.3	63	77
721	Castilla - 13	COL	UTL	SPRG	111.595	40.011	1875	-123	-16.7	42	6 75
722	Saratoga -14	COL	UTL	SPRG	112.904	40.399	1375	-137	-16.0	44	6 75
723	Thermo - 15	COL	USC	SPRG	113.195	38.184	1535	-118	-14.3	90	77
724	Crater - 16	COL	UWC	SPRG	112.726	39.613	1420	-126	-16.1	84	77
725	Wasatch - 17	COL	USL	SPRG	111.896	40.789	1300	-128	-16.0	42	1 81
726	Beck - 18	COL	USL	SPRG	111.917	40.818	1300	-129	-16.8	56	1 81
727	Deseret - 19	COL	USL	SPRG	112.738	40.557	1320	-114	-15.5	21	6 75
728	Big Spring - 20	COL	USL	SPRG	112.646	40.741	1295	-112	-13.8	19	6 75
729	Blue Warm - 21	COL	USL	SPRG	112.454	41.832	1408	-134	-16.1	27	6 75
730	Crystal Madsen - 22	COL	USL	SPRG	112.088	41.661	1305	-110	-13.1	54	6 75
731	Uddy - 23	COL	USL	SPRG	112.157	41.856	1317	-113	-15.3	53	6 75
732	Cutler - 24	COL	USL	SPRG	112.054	41.834	1305	-131	-15.5	25	6 75
733	Garland - 25	COL	USL	SPRG	112.106	41.731	1292	-143	-16.0	27	6 75
734	Utah - 26	COL	USL	SPRG	112.031	41.303	1300	-136	-15.1	58	6 80
735	Ogden - 27	COL	USL	SPRG	111.922	41.234	1400	-136	-16.0	56	6 80
736	Hooper - 28	COL	USL	SPRG	112.176	41.136	1285	-140	-15.8	57	6 80
737	Hot Well 1 - 29	COL	USW	WELL	113.569	37.668	1595	-121	-13.8	97	6 75
738	D. Tullis 1 - 30	COL	USW	WELL	113.561	37.666	1600	-114	-13.4	27	6 75
739	16S 49E 22DC - 3	CLA	AMG	WELL	116.441	36.627	740	-102	-12.8		11 72
740	16S 49E 5ACC - 4	CLA	AMG	WELL	116.476	36.586	740	-103	-13.2		3 74
741	16S 49E 8ABB - 5	CLA	AMG	WELL	116.475	36.699	735	-100	-13.2	23	11 72
742	16S 49E 9DCC - 8	CLA	AMG	WELL	116.446	36.574	735	-103	-13.4	23	3 74
743	16S 49E 18DC - 9	CLA	AMG	WELL	116.494	36.555	730	-102	-12.6		3 74
744	16S 49E 16CCC - 10	CLA	AMG	WELL	116.465	36.553	727	-98	-13.2		6 79
745	16S 49E 19DAA - 11	CLA	AMG	WELL	116.488	36.546	720	-101	-13.1	26	3 74
746	16S 48E 25AA - 13	CLA	AMG	WELL	116.509	36.538	710	-102	-13.0	27	3 74
747	16S 48E 36AAA - 14	CLA	AMG	WELL	116.509	36.523	705	-99	-12.6		3 74
748	17S 48E 1AB - 15	CLA	AMG	WELL	116.509	36.506	695	-104	-13.0		3 74
749	17S 49E 7BB - 16	CLA	AMG	WELL	116.501	36.491	697	-104	-12.7		3 74
750	17S 49E 9AA - 17	CLA	AMG	WELL	116.444	36.496	696	-105	-12.8		3 74
751	17S 49E 8DDB - 18	CLA	AMG	WELL	116.467	36.482	695	-102	-13.0	24	3 74
752	Ash Tree Spring - 20	CLA	AMG	SPRG	116.411	36.429	690	-102	-12.4	18	3 74
753	16S 49E 23ADD - 21	CLA	AMG	WELL	116.514	36.551	730	-99	-13.2		6 79
754	16S 48E 15AAA - 23	CLA	AMG	WELL	116.546	36.566	720	-103	-13.4	26	3 71
755	16S 48E 10CBA - 25	CLA	AMG	WELL	116.561	36.577	725	-102	-13.4	25	3 71
756	16S 50E 7BCD - 27	CLA	AMG	WELL	116.438	36.631		-105	-13.8	31	4 71
757	16S 49E 15AAA - 29	CLA	AMG	WELL	116.442	36.574		-105	-13.8	24	3 71
758	16S 49E 36AAA - 30	CLA	AMG	WELL	116.442	36.523		-104	-13.7		6 79
759	16S 48E 7CBC - 47	CLA	AMG	WELL	116.611	36.631		-102	-13.1	24	3 71

APPENDIX B, continued

Literature Search - Isotope Data

SAMP #	SAMPLE NAME	REF	LOC	TYPE	LONG	LAT	ELEV meters	DEUT ‰	OX18 ‰	TEMP °C	DATE MO YR
760	16S 48E 18DAD - 50	CLA	AMG	WELL	116.593	36.553		-104	-13.6		6 79
761	Well 8, NTS - 64	CLA	PHM	WELL	116.289	37.167	1750	-104	-13.0	27	3 71
762	Ranch Canyon (Kirk)	ROH	USC	SPRG	112.834	38.428	1960	-113	-15.0	11	2 76
763	Ranch Canyon (Kirk)	ROH	USC	SPRG	112.834	38.428	1960	-110	-14.2	11	8 76
764	Bailey Springs	ROH	USC	SPRG	112.808	38.479	2080	-112	-14.6	7	10 77
765	Bailey Springs	ROH	USC	SPRG	112.808	38.479	2080	-116	-15.6	7	8 76
766	Bailey Springs	ROH	USC	SPRG	112.808	38.479	2080	-111	-14.6	7	8 76
767	Willow	ROH	USC	SPRG	112.753	38.491	2080	-111	-15.0	7	10 77
768	Willow	ROH	USC	SPRG	112.753	38.491	2080	-114	-14.8	7	8 76
769	Willow	ROH	USC	SPRG	112.753	38.491	2080	-112	-14.6	7	10 77
770	Cherry Creek	ROH	USC	SURF	112.816	38.303	2001	-113	-14.7	-1	8 76
771	Griffith	ROH	USC	SPRG	112.951	38.345	1960	-110	-14.4	-1	8 76
772	Antelope	ROH	USC	SPRG	112.865	38.653	1480	-116	-15.1	-1	8 76
773	North	ROH	USC	SPRG	112.925	38.271	1740	-112	-14.7	-1	8 76
774	Rock Corral	ROH	USC	SPRG	112.822	38.374	2160	-109	-14.2	6	8 76
775	Mud Spring	ROH	USC	SPRG	112.781	38.346	2020	-113	-14.8	-1	8 76
776	Mathew	ROH	USC	SPRG	112.751	38.469	2180	-117	-15.6	-1	10 77
777	Jack Rabbit	ROH	USC	SPRG	112.805	38.461	2280	-116	-15.8	-1	10 77
778	Sulferdale North	ROH	USC	SPRG	112.551	38.565	2201	-118	-15.6	-1	8 76
779	Sulferdale South	ROH	USC	SPRG	112.551	38.546	2320	-116	-15.6	-1	8 76
780	Dead Cow	ROH	USC	SPRG	113.554	38.528	2170	-114	-14.6	-1	8 76
781	Four Mile	ROH	USC	SPRG	112.663	38.473	2180	-114	-14.2	-1	8 76
782	Wire Gass	ROH	USC	SPRG	112.709	38.474	2205	-115	-15.2	-1	8 76
783	Cowboy	ROH	USC	SPRG	112.692	38.484	2150	-118	-15.2	-1	8 76
784	Magpie	ROH	USC	SURF	112.451	38.636	2160	-120	-15.6		8 76
785	Milford City	ROH	USC	WELL	113.015	38.396	1520	-117	-15.5	23	2 76
786	Beaver Lake Mine	ROH	USC	SPRG	113.138	38.533	1860	-104	-12.5		8 76
787	Armstrong	ROH	USC	SPRG	113.178	38.592	1720	-107	-13.7		8 76
788	Little Hot Creek Spring	CGT	LVC	SPRG	118.844	37.699	2130	-122	-15.3	79	5 72
789	Casa Diablo Well	FOU	LVC	WELL	118.912	37.647	2222	-116	-14.2	94	
790	Hot Bubbling Pool	FOU	LVC	SPRG	118.854	37.648	2156	-111	-12.4	60	
791	Big Alkali Lake (near)	FOU	LVC	SPRG	118.795	37.674	2096	-124	-16.2	56	
792	Big Alkali Lake SE of	FOU	LVC	SPRG	118.786	37.663	2097	-123	-15.9	49	
793	Whitmore HS North of	FOU	LVC	SPRG	118.809	37.649	2134	-121	-15.2	58	
794	Lake Crowley West of	FOU	LVC	SPRG	118.758	37.639	2082	-125	-16.1	41	
795	Big Springs	FOU	LVC	SPRG	118.833	37.752	2118	-115	-15.9	11	
796	Wilfred Canyon Well	FOU	LVC	WELL	118.728	37.694	2128	-130	-17.1	10	
797	LV 4 (near)	FOU	LVC	SPRG	118.813	37.632	2128	-120	-15.3	16	
798	Laurel Canyon East of	FOU	LVC	SPRG	118.896	37.617	2195	-128	-16.7	12	
799	State Fish Hatchery	FOU	LVC	SPRG	118.947	37.641	2179	-121	-15.9	13	

APPENDIX B, continued

Literature Search - Isotope Data

SAMP #	SAMPLE NAME	REF	LOC	TYPE	LONG	LAT	ELEV meters	DEUT ‰	OX18 ‰	TEMP °C	DATE MO YR
800	McLaughlin Creek	FOU	LVC	SURF	118.863	37.773	2231	-130	-16.9	8	
801	Deadman Creek at US395	FOU	LVC	SURF	118.981	37.747	2280	-124	-16.0	13	
802	Deadman Creek S Trib	FOU	LVC	SURF	119.041	37.703	2489	-112	-14.7	7	
803	NW of O'Harrel Canyon	FOU	LVC	SPRG	118.784	37.761	2249	-131	-16.9	7	
804	Mammoth Mountain	FOU	LVC	SPRG	119.026	37.623	9999	-109	-14.5	2	
805	Minaret Summit (near)	FOU	LVC	SPRG	119.046	37.655	9000	-111	-14.9	5	
806	Endogenous #5 Magma PC	CGT	LVC	WELL	118.914	37.647		-116	-14.2	94	5 72
807	1	WHT	AMG	SPRG	116.769	37.073	1220	-113	-14.5		
808	2	WHT	AMG	SPRG	116.702	37.039	1160	-111	-14.3		
809	3	WHT	AMG	SPRG	116.756	37.031	1170	-102	-13.4		
810	4	WHT	AMG	SPRG	116.729	37.019	1105	-102	-13.4		
811	5	WHT	AMG	SPRG	116.713	37.026	1155	-108	-14.0		
812	6	WHT	AMG	SPRG	116.758	37.025	1180	-102	-13.4		
813	7	WHT	AMG	SPRG	116.716	36.974	1101	-108	-14.0		
814	Hicks (Bailey) HS 8	WHT	AMG	SPRG	116.721	36.805	1097	-110		40	
815	9	WHT	AMG	SPRG	116.718	36.968	1085	-109	-14.0		
816	11	WHT	AMG	SPRG	116.717	36.959	1070	-108	-14.1		
817	12	WHT	AMG	SPRG	116.716	36.948	1055	-109	-14.1		
818	13	WHT	AMG	SPRG	116.738	37.006	1170	-108	-14.1		
819	14	WHT	AMG	SPRG	116.764	36.917	1035	-102	-13.3		
820	15	WHT	AMG	SPRG	116.752	36.907	1001	-108	-13.9		
821	16	WHT	AMG	SPRG	116.749	36.886	990	-106	-13.6		
822	17	WHT	AMG	SPRG	116.761	36.884	1001	-104	-13.3		
823	Spring 1 Carson River	MPE	CEV	SPRG	119.705	38.784	1608	-127	-15.6	84	9 81
824	Spring 2 Carson River	MPE	CEV	SPRG	119.692	38.781	1622	-125	-15.5	65	9 81
825	Basset Hot Spring	MPE	MDC	SPRG	121.111	41.644	1265	-115	-13.5	79	
826	Wendell Hot Springs	MPE	HLV	SPRG	120.249	40.364	1240	-121	-14.0	96	
827	Zamboni Hot Springs	MPE	MDC	SPRG	120.024	39.921	1350	-118	-15.3	41	9 81
828	Benton Hot Springs	MPE	LVC	SPRG	118.531	37.801	1715	-136	-17.5	57	74
829	Fales Hot Springs	MPE	LVC	SPRG	119.366	38.352	2235	-133	-17.5	61	74
830	Hot Creek Gorge	CGT	LVC	SPRG	118.829	37.664	2121	-120	-14.8	90	8 83
831	The Hot Springs	MPE	LVC	SPRG	119.214	38.223	2024	-137	-16.3	38	11 77
832	Travertine Hot Springs	MPE	LVC	SPRG	119.205	38.246	2048	-139	-16.6	69	74
833	Fish Spring	LEA	NEN	SPRG	114.253	42.149	2088	-124	-16.8	5	
834	Buckeye Hot Springs	HIG	LVC	SPRG	119.327	38.239	2109	-138	-17.7	60	74
835	Dechambeau Well	HIG	LVC	WELL	119.082	38.051	1987	-127	-15.7	66	74
836	Little Alkali Lake NE	CGT	LVC	SPRG	118.788	37.668	2103	-124	-16.2	56	5 72
837	Little Alkali Lake SE	HIG	LVC	SPRG	118.773	37.658	2091	-123	-15.9	49	
838	Little Alkali Lake SSW	CGT	LVC	SPRG	118.809	37.649	2134	-121	-15.2	58	5 72
839	Little Alkali Lake SSE	CGT	LVC	SPRG	118.761	37.644	2085	-125	-16.1	41	5 72

APPENDIX B, continued

Literature Search - Isotope Data

SAMP #	SAMPLE NAME	REF	LOC	TYPE	LONG	LAT	ELEV meters	DEUT ‰	OX18 ‰	TEMP °C	DATE MO YR
840	Silver Peak Spring	MPE	CLV	SPRG	117.373	37.759	1280	-118	-13.5	40	
841	Macfarlanes Hot Springs	MPE	BRD	SPRG	118.718	41.051	1247	-127	-12.5	75	
842	Wedell Hot Spring	MPE	GVY	SPRG	118.195	38.923	1260	-132	-15.9	60	
843	Colado	MPE	COL	WELL	118.385	40.244	1240	-126	-14.0	60	
844	Hyder Hot Springs	MPE	DXV	SPRG	117.719	40.003	1093	-133	-15.7	78	
845	Fly Ranch (wards)	MPE	BRD	SPRG	119.332	40.859	1250	-121	-14.7	80	
846	Marble Hot Springs	MJR	SVY	WELL	120.376	39.763	1509	-118	-14.4	73	6 73
847	Marble Hot Springs	MJR	SVY	WELL	120.376	39.763	1509	-118	-14.3	70	6 73
848	W. Hagge	MJR	SVY	WELL	120.348	39.731	1509	-119	-14.9	40	6 73
849	W. Hagge	MJR	SVY	WELL	120.348	39.728	1509	-122	-15.7	39	6 73
850	G. Fillipini	MJR	SVY	WELL	120.351	39.721	1509	-118	-13.9	94	6 73
851	W. Hagge	MJR	SVY	WELL	120.343	39.713	1509	-119	-14.6	44	6 73
852	G. Fillipini	MJR	SVY	WELL	120.357	39.697	1509	-119	-14.9	51	6 73
853	A. Genasci	MJR	SVY	WELL	120.258	39.681	1509	-111	-14.8	18	6 73
854	Campbell Hot Springs	MJR	SVY	SPRG	120.378	39.589	1509	-111	-14.8	37	6 73
855	Church of the LDS	MJR	HLV	WELL	120.679	40.411	1341	-113	-14.5	49	7 73
856	Wendell Hot Springs	MJR	HLV	SPRG	120.249	40.364	1240	-119	-14.1	96	7 73
857	Seyferth Hot Springs	MJR	SPV	SPRG	121.349	41.251	1550	-121	-14.1	85	7 73
858	Hot Springs Motel	MJR	SPV	WELL	120.068	41.539	1374	-117	-13.8	98	7 73
859	Menlo Hot Springs	MJR	SPV	SPRG	120.074	41.241	1375	-112	-15.3	57	8 73
860	Kelly Hot Spring	MJR	MDC	SPRG	120.801	41.454	1340	-115	-13.5	92	7 73
861	Little Hot Springs	MJR	MDC	SPRG	121.399	41.241	1090	-117	-14.2	76	8 73
862	W. Valley Res Hot Sp	MJR	MDC	SPRG	120.168	41.191	1524	-119	-14.1	77	7 73
863	Basset Hot Spring	MJR	MDC	SPRG	121.111	41.644	1265	-116	-14.7	79	8 73
864	Kellog Hot Spring	MJR	MDC	SPRG	121.028	41.125	4229	-116	-14.1	78	8 73
865	Hunt Hot Springs	MJR	MDC	SPRG	121.926	41.034	500	-94	-13.3	58	8 73
866	Holtville Ice Co	MJR	IMP	WELL	115.379	32.809	-7	-94	-10.5	45	11 70
867	Haiwee Spring CT-74-2	FRN	COS	SPRG	117.756	36.117		-98	-13.2	20	74
868	CGEH#1 CF-78-1	FRN	COS	WELL	117.804	36.054		-107	-7.8	195	7 78
869	Coso #1 CF79-2	FRN	COS	WELL	117.766	36.049	1098	-99	-5.8	140	4 79
870	Haiwee Spring CT-79-3	FRN	CSR	SPRG	117.756	36.117		-96	-13.5	17	4 79
871	Wild Rose Ranch CF-79-5	FRN	SSN	SPRG	117.976	36.046		-102	-13.9	-1	4 79
872	Hennis Ranch CF-79-6	FRN	RSV	WELL	117.951	36.084		-112	-14.5	23	4 79
873	Earl Price Rch CF-79-11	FRN	SSN	SPRG	118.023	36.213		-106	-14.3	18	4 79
874	Earl Price Rch CF-79-12	FRN	SSN	SPRG	118.023	36.211		-108	-14.4	18	4 79
875	Dirty Socks HS CF-79-13	FRN	COS	SPRG	117.981	36.329	1093	-121	-15.1	29	4 79
876	China Garden CF-79-14	FRN	CSR	SPRG	117.607	36.201		-92	-13.1	15	4 79
877	Cole Springs CF-79-16	FRN	CSR	SPRG	117.669	36.150		-98	-12.8	13	4 79
878	Dead End Spr CF-79-17	FRN	CSR	SPRG	117.694	36.128		-96	-12.9	12	4 79
879	Junct Ranch Sp Cf-79-18	FRN	CSR	SPRG	117.493	36.086		-94	-12.8	14	4 79

APPENDIX B, continued

Literature Search - Isotope Data

SAMP #	SAMPLE NAME	REF	LOC	TYPE	LONG	LAT	ELEV meters	DEUT ‰	OX18 ‰	TEMP °C	DATE MO YR
880	Mountain Sp CF-79-20	FRN	CSR	SPRG	117.526	35.944		-93	-12.4	13	4 79
881	Mountain Can CF-79-21	FRN	CSR	SPRG	117.565	35.948		-89	-11.6	14	4 79
882	Chimney Pk Sp CF-79-23	FRN	SSN	SPRG	118.058	35.884		-102	-13.6	9	4 79
883	Big Pine Md Sp CF-79-24	FRN	SSN	SPRG	118.081	35.947		-104	-13.8	7	4 79
884	Grumpy Bear CF-79-25	FRN	SSN	WELL	118.099	35.989		-106	-13.5	-1	4 79
885	Naval Base SW CF-79-27	FRN	COS	WELL	117.747	35.684		-95	-12.2	-1	4 79
886	Rose Valley R CF-79-29	FRN	RSV	WELL	117.951	36.076		-109	-13.8	-1	4 79
887	Rose Valley R CF-79-30	FRN	RSV	WELL	117.951	36.076		-111	-13.9	-1	4 79
888	Fallon-Mori	GLA	FAL	WELL				-113	-14.8		
889	Kennametal Inc	GLA	FAL	WELL	118.771	39.508	1206	-114	-14.5		
890	Fallon #3	GLA	FAL	WELL				-108	-14.3		
891	Fallon #1	GLA	FAL	WELL				-108	-14.1		
892	Navy #3	GLA	FAL	WELL	118.743	39.468	1204	-111	-14.1		
893	Howard Wolf	GLA	FAL	WELL	118.721	39.561	1196	-113	-14.4		
894	Ronald Albaugh #1	GLA	FAL	WELL	118.721	39.548	1196	-111	-14.3		
895	Ponte Subdivision	GLA	FAL	WELL	118.781	39.501	1207	-114	-14.8		
896	Ben Peck	GLA	FAL	WELL	118.786	39.494	1207	-110	-13.8		
897	Country Club Estates	GLA	FAL	WELL	118.809	39.489	1210	-111	-14.4		
898	Farad	LLS	TRV	SPRG	120.031	39.421	1646	-108		36	9 83
899	Farad	LLS	TRV	SPRG	120.031	39.421	1646	-115		36	11 83
900	Farad	LLS	TRV	SPRG	120.031	39.421	1646	-106	-13.8	35	1 84
901	Farad	LLS	TRV	SPRG	120.031	39.421	1646	-107		35	3 84
902	Farad	LLS	TRV	SPRG	120.031	39.421	1646	-102		36	5 84
903	Farad	LLS	TRV	SPRG	120.031	39.421	1646	-106	-13.7	36	7 84
904	Steamboat	LLS	SMA	SPRG	119.743	39.389	1421	-112	-11.8	85	10 83
905	Steamboat	LLS	SMA	SPRG	119.743	39.389	1421	-109		93	12 83
906	Steamboat	LLS	SMA	SPRG	119.743	39.389	1421	-106		89	2 84
907	Steamboat	LLS	SMA	SPRG	119.743	39.389	1421	-105	-10.8	88	4 84
908	Steamboat	LLS	SMA	SPRG	119.743	39.389	1421	-109		92	6 84
909	Steamboat	LLS	SMA	SPRG	119.743	39.389	1421	-120		93	8 84
910	Bowers	LLS	WSV	SPRG	119.842	39.328	1561	-109		46	9 83
911	Bowers	LLS	WSV	SPRG	119.842	39.328	1561	-105		45	10 83
912	Bowers	LLS	WSV	SPRG	119.842	39.328	1561	-104	-14.8	46	11 83
913	Bowers	LLS	WSV	SPRG	119.842	39.328	1561	-105		45	12 83
914	Bowers	LLS	WSV	SPRG	119.842	39.328	1561	-108		45	1 84
915	Bowers	LLS	WSV	SPRG	119.842	39.328	1561	-106	-14.9	46	2 84
916	Bowers	LLS	WSV	SPRG	119.842	39.328	1561	-103		45	3 84
917	Bowers	LLS	WSV	SPRG	119.842	39.328	1561	-102		46	4 84
918	Bowers	LLS	WSV	SPRG	119.842	39.328	1561	-105	-14.5	46	5 84
919	Bowers	LLS	WSV	SPRG	119.842	39.328	1561	-101		45	6 84

APPENDIX B, continued

Literature Search - Isotope Data

SAMP #	SAMPLE NAME	REF	LOC	TYPE	LONG	LAT	ELEV meters	DEUT ‰	OX18 ‰	TEMP °C	DATE MO YR
920	Bowers	LLS	WSV	SPRG	119.842	39.328	1561	-104		46	7 84
921	Bowers	LLS	WSV	SPRG	119.842	39.328	1561	-105	-14.7	45	8 84
922	Saratoga	LLS	CEV	SPRG	119.742	39.057	1432	-126		51	9 83
923	Saratoga	LLS	CEV	SPRG	119.742	39.057	1432	-124	-16.3	51	11 83
924	Saratoga	LLS	CEV	SPRG	119.742	39.057	1432	-128		51	1 84
925	Saratoga	LLS	CEV	SPRG	119.742	39.057	1432	-123		51	3 84
926	Saratoga	LLS	CEV	SPRG	119.742	39.057	1432	-119	-15.6	51	5 84
927	Saratoga	LLS	CEV	SPRG	119.742	39.057	1432	-109		51	7 84
928	Walleys	LLS	CEV	SPRG	119.833	38.981	1426	-122		51	9 83
929	Walleys	LLS	CEV	SPRG	119.833	38.981	1426	-115	-15.1	52	11 83
930	Walleys	LLS	CEV	SPRG	119.833	38.981	1426	-113		46	1 84
931	Walleys	LLS	CEV	SPRG	119.833	38.981	1426	-109		45	3 84
932	Walleys	LLS	CEV	SPRG	119.833	38.981	1426	-111	-14.1	46	5 84
933	Walleys	LLS	CEV	SPRG	119.833	38.981	1426	-109		50	7 84
934	Kingsbury Grade Spring	LLS	CEV	SPRG	119.866	39.979	2057	-106	-14.6	-1	6 84
935	Ritter Spring	LLS	SMA	SPRG	119.863	39.289	1975	-106	-14.9	-1	6 84
936	Thomas Creek Spring	LLS	SMA	SPRG	119.881	39.431	2316	-118	-16.3	-1	12 84
937	Stock Spring	LLS	SMA	SPRG	119.831	39.441	1783	-113	-15.6	-1	12 84
938	CSV-2	BER	CSV	WELL	114.722	36.781	666	-98	-12.9	27	1 86
939	CE-DT-4	BER	CSV	WELL	114.892	36.795	662	-102	-13.0	34	12 80
940	CE-DT-5	BER	CSV	WELL	114.891	36.795	661	-100	-12.9	36	7 81
941	CE-DT-6	BER	CSV	WELL	114.787	36.768	693	-97	-13.0	34	9 86
942	CE-VF-2	BER	CSV	WELL	114.929	36.874	752	-101	-13.0	34	2 86
943	SHV-1	BER	CSV	WELL	114.925	36.522	807	-91	-11.2	25	3 86
944	Leach Hot Spring #1	WEL	GSV	SPRG	117.658	40.593	1421	-129	-15.7	85	6 77
945	Leach Hot Spring #1	WEL	GSV	SPRG	117.658	40.593	1421	-129	-16.0	86	9 78
946	Leach Hot Spring #12	WEL	GSV	SPRG	117.658	40.593	1424	-127	-15.4	92	3 79
947	Leach Hot Spring #15	WEL	GSV	SPRG	117.658	40.593	1424	-124	-14.0	92	12 78
948	Leach Hot Spring #22	WEL	GSV	SPRG	117.658	40.593	1421	-131	-16.5	81	6 77
949	Leach Hot Spring #22	WEL	GSV	SPRG	117.658	40.593	1421	-131	-16.9	81	9 78
950	Well DH 13A	WEL	GSV	WELL	117.646	40.609	1440	-134	-16.4	53	8 78
951	Well DH 10A	WEL	GSV	WELL	117.646	40.607	1430	-131	-16.6	86	9 78
952	Well DH 3D	WEL	GSV	WELL	117.668	40.556	1435	-133	-16.8	58	8 78
953	Well DH 3B	WEL	GSV	WELL	117.668	40.562	1435	-129	-16.1	25	8 78
954	Sheep Ranch Spring	WEL	GSV	SPRG	117.613	40.641	1535	-125		13	6 77
955	DH 7B	WEL	GSV	WELL	117.685	40.594	1397	-125	-16.2	16	8 78
956	Point Spring	WEL	GSV	SPRG	117.799	40.631		-124		10	6 77
957	Pertain Spring	WEL	GSV	SPRG	117.523	40.547	1780	-124	-16.5	12	6 77
958	Pertain Spring	WEL	GSV	SPRG	117.523	40.547	1780	-124	-15.8	16	8 78
959	Mud Spring	WEL	GSV	SPRG	117.614	40.529	1474	-123	-16.0	14	6 77

APPENDIX B, continued

Literature Search - Isotope Data

SAMP #	SAMPLE NAME	REF	LOC	TYPE	LONG	LAT	ELEV meters	DEUT ‰	OX18 ‰	TEMP °C	DATE MO YR
960	Well near Mud Spring	WEL	GSV	WELL	117.612	40.531	1481	-122	-15.9	15	6 77
961	DH 8	WEL	GSV	WELL	117.668	40.603	1417	-123	-16.5	15	8 78
962	DH 13A	WEL	GSV	WELL	117.574	40.551	1548	-124	-16.4	18	8 78
963	Spring in SW Grass Vly	WEL	GSV	SPRG	117.726	40.566	1535	-124	-15.2	20	6 77
964	DH1	WEL	GSV	WELL	117.653	40.588	1407	-125	-16.9	16	8 78
965	Spring in Spulding Can	WEL	GSV	SPRG	117.798	40.526	1512	-124	-15.8	13	6 77
966	Clear Creek	WEL	GSV	SURF	117.656	40.731	1463	-122	-15.8	5	3 79
967	Well J12	BNS	YCM	WELL	116.393	36.744	953	-98	-12.8	27	3 71
968	Well J13	BNS	YCM	WELL	116.422	36.804	1011	-98	-13.0	31	3 71
969	Well UE25b#1	BSN	YCM	WELL	116.442	36.804	1200	-100	-13.4	36	8 81
970	Well UE25b#1	BSN	YCM	WELL	116.442	36.804	1200	-101	-13.4	36	9 81
971	Well UE25b#1	BSN	YCM	WELL	116.442	36.804	1200	-100	-13.5	37	7 82
972	Well UE-29a#2	BSN	YCM	WELL	116.363	36.938	1215	-94	-12.8	25	1 82
973	Well UE-29a#2	BSN	YCM	WELL	116.363	36.938	1215	-93	-12.8	23	1 82
974	Well USW G-4	BSN	YCM	WELL	116.442	36.862	1270	-103	-13.8	36	12 82
975	Well USW H-1	BSN	YCM	WELL	116.446	36.873	1302	-103	-13.4	33	10 80
976	Well USW H-1	BSN	YCM	WELL	116.446	36.873	1302	-101	-13.5	35	12 80
977	Well USW H-4	BSN	YCM	WELL	116.441	36.849	1249	-104	-14.0	35	5 82
978	Well USW H-5	BSN	YCM	WELL	116.439	36.861	1478	-102	-13.6	37	7 82
979	Well USW H-5	BSN	YCM	WELL	116.439	36.861	1478	-102	-13.6	35	7 82
980	Well USW H-6	BSN	YCM	WELL	116.472	36.853	1306	-106	-13.8	38	10 82
981	Well USW VH-1	BSN	YCM	WELL	116.541	36.793	955	-108	-14.2	36	2 81
982	Preston Big Spring	KRK	WRV	SPRG	115.081	38.934	1746	-126	-15.6	21	
983	Nicholas Spring	KRK	WRV	SPRG	115.059	38.911	1713	-124	-16.1	21	
984	Cold Spring	KRK	WRV	SPRG	115.066	38.917	1722	-121	-15.8	22	
985	Lund Spring	KRK	WRV	SPRG	115.003	38.851	1707	-121	-15.4		
986	Emigrant Spring	KRK	WRV	SPRG	115.046	38.622	1673	-112	-14.5	21	
987	Morman Spring	KRK	WRV	SPRG	115.142	38.763	1609	-108	-15.7	38	
988	Flag Spring	KRK	WRV	SPRG	115.002	38.423	1612	-105	-14.3	16	
989	Hot Creek Spring	KRK	WRV	SPRG	115.153	38.383	1594	-104	-15.5	32	
990	Moon River Spring	KRK	WRV	SPRG	115.183	38.356	1585	-118	-14.1		
991	Cave Spring	KRK	WRV	SPRG	114.799	38.644	1960	-100	-13.9		
992	Hiko Spring	KRK	WRV	SPRG	115.214	37.598	1181	-107		27	
993	Crystal Spring	KRK	WRV	SPRG	115.323	37.531	1169	-109		28	
994	Ash Spring	KRK	WRV	SPRG	115.195	37.465	1100	-108	-14.1	37	
995	Muddy River Spring	KRK	WRV	SPRG	114.715	36.722	538	-98	-12.9	3	
996	Sand Spring	KRK	WRV	SPRG	115.341	38.897	2558	-123	-16.2	-1	
997	Chimney Rock Spring	KRK	STV	SPRG	114.884	38.835	2306	-109	-14.3	-1	
998	Kane Spring	KRK	WRV	SPRG	114.708	37.251	1305	-87	-12.6	-1	
999	Grapevine Spring	KRK	WRV	SPRG	114.708	37.131	1097	-88	-11.6	-1	

APPENDIX B, continued

Literature Search - Isotope Data

SAMP #	SAMPLE NAME	REF	LOC	TYPE	LONG	LAT	ELEV meters	DEUT ‰	OX18 ‰	TEMP °C	DATE MO YR
1000	JR-7	RTH	NWK	WELL	115.743	39.818	1788	-129		16	7 87
1001	Simonson Warm spring	RTH	NWK	SPRG	115.775	39.811	1890	-128		23	7 87
1002	Barrel Spring	RTH	NWK	SPRG	115.641	39.582	1807	-124		20	7 87
1003	Goicoechea Well	RTH	NWK	WELL	115.606	39.502	1827	-122			7 87
1004	JR-1	RTH	NWK	WELL	115.828	39.386	1810	-122		16	7 87
1005	JR-2	RTH	NWK	WELL	115.801	39.439	1817	-123		15	7 87
1006	Lagori Well	RTH	NWK	WELL	115.755	39.422	1805	-117			7 87
1007	JR-14	RTH	NWK	WELL	115.902	39.297	1833	-118		17	7 87
1008	Fish Creek Spring	RTH	NWK	SPRG	116.035	39.279	1841	-121		21	7 87
1009	JR-16	RTH	NWK	WELL	116.051	39.233	1865	-123		18	7 87
1010	JR-17	RTH	NWK	WELL	116.085	39.123	1963	-119		14	7 87
1011	Green Spring	RTH	WPR	SPRG	115.572	39.118	1850	-118		18	7 87
1012	Big Warm Spring	RTH	RRV	SPRG	115.699	38.951	1707	-120		34	7 87
1013	Pritchard Spring	RTH	HCV	SPRG	116.169	38.781	2018	-102		-1	7 87
1014	JR-38	RTH	RRV	SPRG	115.492	38.784	1634	-119		23	7 87
1015	JR-37	RTH	RRV	SPRG	115.484	38.774	1634	-113		16	7 87
1016	JR-44	RTH	RRV	WELL	115.568	38.736	1489	-110			7 87
1017	Trap #3	RTH	RRV	WELL	115.582	38.602	1445	-122		999	7 87
1018	Trap #9	RTH	RRV	WELL	115.651	38.618	1449	-121		999	7 87
1019	Trap #16	RTH	RRV	WELL	115.641	38.598	1451	-123		999	7 87
1020	Butterfield Spring	RTH	RRV	SPRG	115.547	38.521	1448	-116			7 87
1021	Kate Spring	RTH	RRV	SPRG	115.532	38.554	1448	-114		25	7 87
1022	North Spring	RTH	RRV	SPRG	115.764	38.561	1466	-121		34	7 87
1023	Chimney Hat Spring	RTH	RRV	SPRG	115.788	38.467	1465	-120		66	7 87
1024	Bullwhacker Spring	RTH	RRV	SPRG	115.567	38.439	1451	-113		22	7 87
1025	Grant Canyon #1	RTH	RRV	WELL	115.571	38.457	1445	-114		999	7 87
1026	Bacon Flat #1	RTH	RRV	WELL	115.593	38.463	1439	-114		999	7 87
1027	Storm Spring	RTH	RRV	SPRG	115.862	38.398	1451	-121		32	7 87
1028	JR-51	RTH	RRV	WELL	115.561	38.361	1451	-108		23	7 87
1029	JR-27	RTH	HCV	WELL	116.278	38.312	1591	-106			7 87
1030	Stone Corral Well	RTH	RRV	WELL	115.884	38.256	1478	-114		21	7 87
1031	JR-50	RTH	BSS	WELL	115.728	38.248	1469	-103		21	7 87
1032	Warm Spring	RTH	HCV	SPRG	116.377	38.187	1682	-114		54	7 87
1033	Joe's Well	RTH	HCV	WELL	116.259	38.173	1604	-109		19	7 87
1034	JR-26	RTH	HCV	WELL	116.173	38.209	1564	-112			7 87
1035	JR-55	RTH	RRV	WELL	116.031	38.171	1513	-106		22	7 87
1036	JR-57	RTH	RRV	WELL	116.031	38.135	1513	-115		22	7 87
1037	JR-23	RTH	HCV	WELL	116.345	38.113	1673	-107		19	7 87
1038	JR-58	RTH	RRV	WELL	115.993	37.952	1494	-114		23	7 87
1039	Freds Well JR-59	RTH	RRV	WELL	116.051	38.964	1487	-118		19	7 87

APPENDIX B, continued

Literature Search - Isotope Data

SAMP #	SAMPLE NAME	REF	LOC	TYPE	LONG	LAT	ELEV meters	DEUT ‰	OX18 ‰	TEMP °C	DATE MO YR
1040	Cedar Spring	RTH	HCV	SPRG	116.178	37.762	1771	-101			7 87
1041	Cold Spring	RTH	NWK	SPRG	115.753	39.841	1884	-124		16	7 87
1042	Alligator Ridge Well	RTH	NWK	WELL	115.491	39.743	2073	-127		1	7 87
1043	Moore Spring	RTH	NWK	SPRG	115.625	39.735	2170	-120		1	7 87
1044	JR-9	RTH	NWK	SPRG	115.648	39.681	2128	-124		17	7 87
1045	JR-4	RTH	NWK	SPRG	115.778	39.636	1789	-120		16	7 87
1046	JR-3	RTH	NWK	SPRG	115.748	39.456	1899	-125		13	7 87
1047	JR-13	RTH	NWK	SPRG	115.938	39.457	2225	-117		16	7 87
1048	Sand Spring	RTH	NWK	SPRG	115.454	39.331	2208	-123		1	7 87
1049	JR-62	RTH	NWK	SPRG	115.465	39.301	2365	-121		12	7 87
1050	Snowball spring	RTH	NWK	SPRG	116.194	39.041	2243	-118		18	7 87
1051	Birch Spring	RTH	RRV	SPRG	115.538	39.066	1909	-115		1	7 87
1052	Saddle Spring	RTH	RRV	SPRG	115.398	39.977	2621	-116		1	7 87
1053	Martilleti Spring	RTH	BSS	SPRG	115.831	38.787	2066	-105		15	7 87
1054	Secret Spring	RTH	WRV	SPRG	115.291	38.662	2121	-109		15	7 87
1055	Summit Spring	RTH	WRV	SPRG	115.301	38.823	2082	-109		18	7 87
1056	Indian Spring	RTH	RRV	SPRG	115.721	38.775	1887	-110		1	7 87
1057	N. 6 Mile Can Spring	RTH	HCV	SPRG	116.304	38.679	2536	-108		15	7 87
1058	Hot Spring	RTH	HCV	SPRG	116.366	38.521	1722	-111		34	7 87
1059	Albert Spring	RTH	WRV	SPRG	115.362	38.568	2079	-107		1	7 87
1060	Tybo Spring	RTH	HCV	SPRG	116.417	38.371	2073	-104		1	7 87
1061	Mud Spring	RTH	RRV	SPRG	115.454	38.414	1672	-109		18	7 87
1062	Big Spring	RTH	RRV	SPRG	115.481	38.371	2463	-112		1	7 87
1063	Ox Spring	RTH	RRV	SPRG	115.617	38.266	1737	-105		17	7 87
1064	JR-24	RTH	HCV	SPRG	116.393	38.006	1969	-107		1	7 87
1065	Reveille Spring	RTH	RRV	SPRG	116.167	38.031	1951	-97		16	7 87
1066	Georges Water Spring	RTH	HCV	SPRG	116.353	37.861	2106	-98		1	7 87
1067	Blackburn #3	RTH	RRV	WELL	116.137	40.231	1615	-132	-15.3	200	3 87
1068	Blackburn #16	RTH	RRV	WELL	116.144	40.238	1612	-134	-15.5	150	3 87
1069	Well J13	BOU	YCM	WELL	116.422	36.804	1011	-96	-12.7	31	6 82
1070	Well A, Test	BOU	PHM	WELL	116.041	37.038	1221	-107	-13.0	27	6 82
1071	Well 2, Test	BOU	PHM	WELL	116.084	37.166	1362	-102	-13.2	35	6 82
1072	Well U19c	BOU	PHM	WELL	116.317	37.268	2143	-109	-14.1	39	6 82
1073	Well 8, NTS	BOU	PHM	WELL	116.289	37.167	1750	-101	-12.9	27	6 82
1074	Well Ue16d	BOU	PHM	WELL	116.164	37.071	1428	-96	-12.4	25	6 82
1075	Well Ue16d	BOU	PHM	WELL	116.164	37.071	1428	-106	-13.5	25	6 82
1076	Well 1, Army	BOU	LVS	WELL	116.036	36.595	961	-99	-13.1	32	6 82
1077	Well 5c	BOU	LVS	WELL	115.959	36.785	939	-108	-13.4	26	6 82
1078	Well C	BOU	PHM	WELL	116.014	36.918	1104	-106	-13.3	37	6 82
1079	Well 4	BOU	LVS	WELL	116.031	36.911	1097	-94	-12.6	28	6 82

APPENDIX B, continued

Literature Search - Isotope Data

SAMP #	SAMPLE NAME	REF	LOC	TYPE	LONG	LAT	ELEV meters	DEUT ‰	OX18 ‰	TEMP °C	DATE MO YR
1080	Well C-1	BOU	PHM	WELL	116.013	36.919	1104	-102	-12.8	36	6 82
1081	Well Ue15d	BOU	PHM	WELL	116.041	37.208	1398	0	-14.1	30	6 82
1082	Fairbanks Spring, SW	WNP	AMG	SPRG	116.339	36.491	695	-103	-13.6	27	5 73
1083	Rogers Spring	WNP	AMG	SPRG	116.326	36.481	695	-102			3 75
1084	Longstreet Spring	WNP	AMG	SPRG	116.326	36.467	702	-103			3 75
1085	Scruggs Spring	WNP	AMG	SPRG	116.309	36.434	709	-103			3 75
1086	Crystal Pool	WNP	AMG	SPRG	116.323	36.421	694	-102	-13.7	31	5 73
1087	Crystal Pool	WNP	AMG	SPRG	116.323	36.421	694	-104		31	3 75
1088	King Spring	WNP	AMG	SPRG	116.274	36.408	705	-104			3 75
1089	Big Spring	WNP	AMG	SPRG	116.273	36.374	683	-102	-13.4	27	5 73
1090	Big Spring	WNP	AMG	SPRG	116.273	36.374	683	-102		27	11 73
1091	Hiko Spring	WNF	WRV	SPRG	115.214	37.598	1181	-114		27	8 68
1092	Hiko Spring	WNF	WRV	SPRG	115.214	37.598	1181	-113		27	1 69
1093	Hiko Spring	WNF	WRV	SPRG	115.214	37.598	1181	-113		27	3 70
1094	Crystal Spring	WNF	WRV	SPRG	115.323	37.531	1169	-112		28	8 68
1095	Crystal Spring	WNF	WRV	SPRG	115.323	37.531	1169	-113		28	1 69
1096	Crystal Spring	WNF	WRV	SPRG	115.323	37.531	1169	-112		28	3 70
1097	Ash Spring	WNF	WRV	SPRG	115.195	37.465	1100	-110		37	8 68
1098	Ash Spring	WNF	WRV	SPRG	115.195	37.465	1100	-112		37	1 69
1099	Ash Spring	WNF	WRV	SPRG	115.195	37.465	1100	-115		37	3 70
1100	Trout Spring	WNF	SPM	SPRG	115.682	36.222	2286	-102		8	3 70
1101	Cold Creek Spring	WNF	SPM	SPRG	115.744	36.414	1890	-100		11	8 68
1102	Cold Creek Spring	WNF	SPM	SPRG	115.744	36.414	1890	-105		11	1 69
1103	Cold Creek Spring	WNF	SPM	SPRG	115.744	36.414	1890	-106		11	3 70
1104	Indian Springs	WNF	LVS	SPRG	115.668	36.565	969	-101		25	8 68
1105	Indian Springs	WNF	LVS	SPRG	115.668	36.565	969	-103		25	1 69
1106	Indian Springs	WNF	LVS	SPRG	115.668	36.565	969	-104		25	3 70
1107	Corn Creek Ranch Well	WNF	SHR	WELL	115.398	36.465	899	-98		20	1 69
1108	Corn Creek Ranch Well	WNF	SHR	WELL	115.398	36.465	899	-97		20	3 70
1109	Manse Spring	WNF	PHV	SPRG	115.896	36.157	866	-100		24	8 68
1110	Manse Spring	WNF	PHV	SPRG	115.896	36.157	866	-104		24	3 70
1111	Tule Springs Well	WNF	LVS	WELL	115.267	36.321	750	-103		21	1 69
1112	Fairbanks Spring	WNF	AMG	SPRG	116.339	36.491	695	-106		28	8 68
1113	Fairbanks Spring	WNF	AMG	SPRG	116.339	36.491	695	-106		28	1 69
1114	Fairbanks Spring	WNF	AMG	SPRG	116.339	36.491	695	-107		28	3 70
1115	Crystal Pool	WNF	AMG	SPRG	116.323	36.421	694	-110		32	8 68
1116	Crystal Pool	WNF	AMG	SPRG	116.323	36.421	694	-106		32	1 69
1117	Crystal Pool	WNF	AMG	SPRG	116.323	36.421	694	-107		32	3 70
1118	Point of Rocks Spring	WNF	AMG	SPRG	116.273	36.408	705	-110		32	8 68
1119	Point of Rocks Spring	WNF	AMG	SPRG	116.273	36.408	705	-104		32	1 69

APPENDIX B, continued

Literature Search - Isotope Data

SAMP #	SAMPLE NAME	REF	LOC	TYPE	LONG	LAT	ELEV meters	DEUT ‰	OX18 ‰	TEMP °C	DATE MO YR
1120	Point of Rocks Spring	WNF	AMG	SPRG	116.273	36.408	705	-107		32	3 70
1121	Big Spring	WNF	AMG	SPRG	116.273	36.374	683	-107		28	1 69
1122	Big Spring	WNF	AMG	SPRG	116.273	36.374	683	-107		28	3 70
1123	Nevares Spring	WNF	DVY	SPRG	116.791	36.512	293	-111		39	8 68
1124	Nevares Spring	WNF	DVY	SPRG	116.791	36.512	293	-109		39	3 70
1125	Texas Spring	WNF	DVY	SPRG	116.836	36.458	122	-108		33	3 70
1126	Travertine Spring	WNF	DVY	SPRG	116.824	36.443	122	-109		34	3 70
1127	Muddy Spring	WNF	MRV	SPRG	114.715	36.722	538	-101		32	3 70
1128	Moapa Spring	WNF	MRV	SPRG	114.718	36.714	543	-100		32	3 70
1129	Pedersons Warm Spring	WNF	MRV	SPRG	114.712	36.711	543	-101		33	1 69
1130	Pedersons Warm Spring	WNF	MRV	SPRG	114.712	36.711	543	-100		33	3 70
1131	Iversons Spring	WNF	MRV	SPRG	114.714	36.709	545	-100		32	3 70
1132	Flag Spring	WNF	WRV	SPRG	115.002	38.423	1612	-111		16	3 70
1133	Hot Creek Spring	WNF	WRV	SPRG	115.153	38.383	1594	-124		32	3 70
1134	Well C-1	WNF	PHM	WELL	116.013	36.919	1104	-114		35	1 69
1135	Well 1, Army	WNF	LVS	WELL	116.036	36.595	961	-107		33	1 69
1136	Well 1, Army	WNF	LVS	WELL	116.036	36.595	961	-106		33	3 70
1137	Well 5B	WNF	LVS	WELL	116.969	36.801	942	-110		24	1 69
1138	Well J12	WNF	YCM	WELL	116.393	36.744	953	-102		26	1 69
1139	Nuclear Eng Co Well	WNF	AMG	WELL	116.633	36.689	786	-112		29	8 68
1140	Shannon Spring	VTZ	USC	SPRG	112.754	38.378	2240	-102	-14.1	7	5 82
1141	Old Indian Spring	VTZ	USC	SPRG	112.752	38.388	2414	-105	-14.3	14	5 82
1142	Well OH-5	VTZ	USC	WELL	112.757	38.503	1700	-107	-13.2	83	5 82
1143	Bailey Spring	VTZ	USC	SPRG	112.808	38.479	2080	-107	-14.6	6	4 83
1144	Well OH-1	VTZ	USC	WELL	112.759	38.397	1719	-109	-12.8	54	5 82
1145	Roosevelt Seep	VTZ	USC	SPRG	112.757	38.501	1807	-110	-12.2	26	5 82
1146	WOW Well-3	VTZ	USC	WELL	112.762	38.503	1558	-113	-13.3	24	5 82
1147	Jefferson Well	VTZ	USC	WELL	112.751	38.386	1521	-113	-14.5	18	4 83
1148	Milford Well	VTZ	USC	WELL	113.015	38.396	1520	-114	-15.3	23	5 82
1149	Well 26-9-18	VTZ	USC	WELL	112.761	38.508	1527	-114	-14.4	19	5 82
1150	Utah State Well 14-2	VTZ	USC	WELL	112.756	38.391	1908	-116	-13.6	268	78
1151	Anderson Well	VTZ	USC	WELL	112.759	38.514	1527	-117	-15.6	16	5 82
1152	Hamblin Spring	BLK	UNW	SPRG	113.604	37.543	1783	-91	-12.6	-1	
1153	Escalante Mine	BLK	UNW	WELL				-94	-13.0	-1	
1154	Cove Spring	BLK	UNW	SPRG	113.536	37.554	1853	-95	-13.0	-1	
1155	Joel Spring	BLK	UNW	SPRG	113.433	37.670	1858	-103	-14.0	-1	
1156	Pinto Spring	BLK	UNW	SPRG	113.467	37.509	1990	-104	-13.9	-1	
1157	Hildebrand Well	BLK	UNW	WELL	113.566	37.661	1599	-107	-14.2	999	
1158	NC-10 Well	BLK	UNW	WELL	113.566	37.661	1599	-108	-14.0	102	
1159	3N 2E 2CDCD - #5	MYP	BOI	WELL	116.185	43.621	853	-133	-17.0	72	1 88

APPENDIX B, continued

Literature Search - Isotope Data

SAMP #	SAMPLE NAME	REF	LOC	TYPE	LONG	LAT	ELEV meters	DEUT ‰	OX18 ‰	TEMP °C	DATE MO YR
1160	3N 2E 11ABBC - #7	MYP	BOI	WELL	116.180	43.617	853	-134	-17.2	76	1 88
1161	3N 2E 11ABCB - #8	MYP	BOI	WELL	116.179	43.616	853	-133	-17.2	80	1 88
1162	3N 2E 11BAAA - #9	MYP	BOI	WELL	116.182	43.618	853	-132	-17.1	72	1 88
1163	3N 2E 12CDDD - #10	MYP	BOI	WELL	116.163	43.605	853	-133	-17.0	78	1 88
1164	4N 3E 10BDCB - #11	MYP	BOI	SPRG	116.503	43.634	1920	-123	-16.7	4	5 88
1165	4N 3E 11DDAA - #12	MYP	BOI	SPRG	116.470	43.695	1554	-119	-16.0	8	4 88
1166	4N 3E 35CCDD - #13	MYP	BOI	SPRG	116.487	43.703	1371	-122	-16.1	10	3 88
1167	Lochsa Springs	YOU	IBL	SPRG	115.170	46.411	800	-115	-15.5	11	7 82
1168	Granite Springs	YOU	IBL	SPRG	115.272	46.025	2024	-131	-17.7	3	7 82
1169	Horse Creek Campground	YOU	IBL	SPRG	114.442	45.508	1900	-139	-18.9	12	8 80
1170	24N 4E 19BCA	YOU	IBL	SPRG	116.010	45.422	1050	-125	-16.1	11	6 80
1171	24N 21E 22CDD1s	YOU	IBL	SPRG	113.964	45.382	1150	-140	-18.1	8	6 80
1172	22N 2E 31BBC1s	YOU	IBL	SPRG	116.268	45.205	1500	-124	-16.7	6	6 80
1173	Hazard Lake Campground	YOU	IBL	SPRG	116.140	45.210	2147	-127	-17.3	2	7 82
1174	Jureano Spring	YOU	IBL	SPRG	114.299	45.194	2499	-139	-18.7	3	8 82
1175	20N 22E 17AAC1s	YOU	IBL	SPRG	113.874	45.063	1650	-139	-18.3	14	8 80
1176	20N 25E 16ACC1s	YOU	IBL	SPRG	113.484	45.070	2450	-143	-19.1	5	8 82
1177	19N 6E 38BD1s	YOU	IBL	SPRG	115.710	45.014	1180	-132	-17.5	10	6 80
1178	17N 2E 15BAB1s	YOU	IBL	SPRG	116.209	44.833	1759	-127	-17.1	7	6 79
1179	17N 11E 33DDC1s	YOU	IBL	SPRG	115.104	44.767	1500	-140	-18.6	10	6 80
1180	N15 5E 23DAC1s	YOU	IBL	SPRG	115.816	44.619	1900	-124	-17.7	4	6 79
1181	N15 10E 13CAB1s	YOU	IBL	SPRG	115.187	44.634	1550	-132	-17.9	9	6 80
1182	N14 2E6 10CBC1s	YOU	IBL	SPRG	113.344	44.558	1980	-143	-18.8	10	8 80
1183	N13 5E 21CAA1s	YOU	IBL	SPRG	115.880	44.454	2280	-128	-17.3	7	6 79
1184	11N 16E 30DAA1s	YOU	IBL	SPRG	114.583	44.251	1768	-144	-18.6	9	8 80
1185	11N 20E 17AAB1s	YOU	IBL	SPRG	114.153	44.281	2103	-148	-18.7	14	8 82
1186	10N 6E 19DCD1s	YOU	IBL	SPRG	115.779	44.192	2365	-124	-16.9	5	7 82
1187	9N 9E 32BAD1s	YOU	IBL	SPRG	115.423	44.074	2255	-131	-17.7	5	8 79
1188	9N 17E 22BCA1s	YOU	IBL	SPRG	114.459	44.086	1951	-141	-18.2	9	8 80
1189	7N 1W 10ABD1s	YOU	IBL	SPRG	116.434	43.966	1079	-118	-14.9	10	4 82
1190	7N 7E 32DAC1s	YOU	IBL	SPRG	115.690	43.903	2012	-123	-16.7	6	9 81
1191	Pole Creek Spring	YOU	IBL	SPRG	114.730	43.914	2286	-144	-19.3	5	8 82
1192	5N 6E 28ACB1s	YOU	IBL	SPRG	115.781	43.756	2182	-127	-17.1	6	7 82
1193	5N 11E 2DCC1s	YOU	IBL	SPRG	115.094	43.806	2560	-133	-17.5	8	9 81
1194	3N 11E 5ADA1s	YOU	IBL	SPRG	115.181	43.630	1676	-140	-18.3	10	7 81
1195	3N 13E 2DBA1s	YOU	IBL	SPRG	114.863	43.632	1707	-131	-17.5	6	7 81
1196	2N 10E 5ADB1s	YOU	IBL	SPRG	115.303	43.562	1341	-128	-16.8	10	8 81
1197	Big Creek Hot Springs	YOU	IBL	SPRG	114.341	45.352	1524	-154	-19.4	94	8 80
1198	17N 11E 16ACB1s	YOU	IBL	SPRG	115.136	44.810	1700	-152	-19.4	87	7 79
1199	14N 6E 11BDA1s	YOU	IBL	SPRG	115.709	44.567	1200	-140	-18.6	89	6 80

APPENDIX B, continued

Literature Search - Isotope Data

SAMP #	SAMPLE NAME	REF	LOC	TYPE	LONG	LAT	ELEV meters	DEUT ‰	OX18 ‰	TEMP °C	DATE MO YR
1200	12N 5E 22BBC1s	YOU	IBL	SPRG	115.859	44.363	1228	-134	-17.7	86	6 79
1201	Sunbeam Hot Springs	YOU	IBL	SPRG	114.746	44.272	1951	-149	-19.8	78	9 79
1202	10N 4E 33CBD1s	YOU	IBL	SPRG	115.997	44.158	1097	-136	-18.2	75	11 78
1203	10N 10E 31BCC1s	YOU	IBL	SPRG	115.650	44.160	1448	-140	-18.1	84	3 79
1204	9N 3E 25BAC1s	YOU	IBL	SPRG	116.061	44.090	975	-136	-17.2	80	11 78
1205	5N 7E 24BDD1s	YOU	IBL	SPRG	115.544	43.762		-138	-18.0	76	8 81
1206	3N 14E 28CAD1s	YOU	IBL	SPRG	114.863	43.562		-146	-19.5	87	7 81
1207	Old Boundary Spring	JNT	LAS	SPRG	120.51	40.50		-102	-14.0	-1	79
1208	Old Boundary Spring	JNT	LAS	SPRG	120.51	40.50		-101	-13.6	-1	75
1209	Cascade Springs	JNT	LAS	SPRG	120.49	40.48		-98	-13.8	-1	76
1210	Domingo Spring	JNT	LAS	SPRG	120.45	40.41		-96	-13.4	-1	79
1211	White Sulphur Spring	JNT	LAS	SPRG	120.55	40.40		-93	-13.0	-1	77

Under TEMP Column

-1 = No temperature reported, thought to be <20°C

999 = No temperature reported, known to be >100°C

APPENDIX B, continued

REF Symbol Key

Key to references for this and other appendices, refer to reference section for complete citation.

REF	FIRST AUTHOR	REF	FIRST AUTHOR	REF	FIRST AUTHOR
BEN	BENSON, 1987	FRN	FOURNIER, 1977	NAT	NATHENSON, 1982
BER	BERGER, 1987	GFG	CURRENT STUDY	NEH	NEHRING, 1980
BLK	BLACKETT, 1989	GLA	GLANCY, 1986	ROH	ROHRS, 1980
BNT	BENOIT, 1982	HIG	HIGGINS, 1983	RTH	ROTH, 1988
BNS	BENSON, 1983	IGR	INGRAHAM, 1986	SZE	SZECSODY, 1982
BOU	BOUGHTON, 1986	ING	INGRAHAM, 1982	TRX	TREXLER, 1980
BOW	BOWMAN, 1982	JNK	JANIK, 1983	TXL	TREXLER, 1980
BSN	BENSON, 1983	KRK	KIRK, 1987	VTZ	VUATAZ, 1987
CGT	CALIF. GEOTHERM	LLS	LYLES, 1985	WCH	WELCH, 1985
CLA	CLASSEN, 1985	LYL	LYLES, 1988	WEL	WELCH, 1981
COL	COLE, 1983	MAR	MARINER, 1976	WHT	WHITE, 1987
DAY	DAY, 1987	MCK	MACKAY, 1983	WLC	WELCH, 1986
DEN	TREXLER, 1982	MJR	REED, 1975	WNF	WINOGRAD, 1972
DTT	TREXLER, 1981	MNR	MARINER, 1975	WNP	WINOGRAD, 1976
FLN	FLYNN, 1984	MPE	MARINER, 1983	YNG	YOUNG, 1982
FOU	FOURNIER, 1979	MYP	MARINER, 1989	YOU	YOUNG, 1985

APPENDIX C

CARBON AGE DATES

Carbon age dates from this study and the literature search. A partial reference is listed before each group of data, complete reference is available in the references section. Ages are corrected based on either the permil PDB $\delta^{13}\text{C}$ or the Log Ionic Activity Product (IAP) of calcium carbonate (CaCO_3) in the soil, as determined from field measurements. The method applied is indicated for each data group, along with the approximate correction factor (see Section 3.4, correction of carbon age dates). Where no other name is provided, sample names are taken from the Township and Range designation for sample. LOC is location of sample, see Appendix A for key to location codes.

Sample Name	Sample Date	Temp LOC	$\delta^{14}\text{C}$ ‰	A dpm/g	A pmc	$\delta^{13}\text{C}$ PDB	Log		max? C1 Age	min? C2 Age	Correc	
							IAP CaCO_3	Apparent Age			Factor C1	Factor C2
CURRENT STUDY									$\delta^{13}\text{C}$	$\delta^{13}\text{C}$		
DESERT PK SCALE	03 88	DPK	160		0.5	-2.9		-43801	-32060	-25993	-12	-25
WARM SPRINGS	02 89	HCV	65		0.6	-0.6		-42294	-17528	-11460	-12	-25
ELKO JR HIGH	02 89	ELK	80		1.6	-0.8		-34185	-11798	-5730	-12	-25
OXBOW 45 SCALE		DXV	350		2.1	-5.1		-31937	-24864	-18796	-12	-25
OXBOW 74 SCALE		DXV	350		2.4	-5.8		-30833	-24823	-18755	-12	-25
OXBOW 76 SCALE		DXV	350		3.7	-6.2		-27255	-21796	-15728	-12	-25
BEOVAWE SCALE	03 88	BEO	160		8.4	-4.0		-20477	-11395	-5327	-12	-25
BEOVAWE INJECT	04 88	BEO	160		6.1	-0.7		-23122	370	6437	-12	-25
BEOVAWE 2-13	10 89	BEO	160		8.7	-4.4		-20187	-11892	-5825	-12	-25
SZECSDY, 1982, Carson City Nevada									$\delta^{13}\text{C}$	$\delta^{13}\text{C}$		
CARSON HOT SP		CEV	50		2.16	15.9	-14.7	-15202	-13952	-10812	-17	-25
CEV 48	04 81	CEV	15		9.07	66.9	-15.7	-3323	-2617	523	-17	-25
PRISON HOT SP	10 81	CEV	35		11.76	86.7	-12.6	-1180	1345	4485	-17	-25
CEV 52	04 81	CEV	15		12.37	91.2	-16.0	-762	-212	2928	-17	-25
CEV 10	01 81	CEV	12		12.41	91.5	-15.6	-734	25	3164	-17	-25
CEV 177	10 81	CEV	14		14.63	107.9	-17.3	629	532	3672	-17	-25
NEHRING, 1980, Reno Nevada												
STEAMBOAT #26	06 77	SMA	90			0.46		-44491				
STEAMBOAT #8	06 77	SMA	90			0.97		-38323				
STEAMBOAT #5	06 77	SMA	90			1.21		-36495				
STEAMBOAT NR#27	06 77	SMA	85			1.64		-33981				
MARINER, 1989, Boise Idaho									$\delta^{13}\text{C}$	$\delta^{13}\text{C}$		
4N2E 28CBBB1	01 88	BOI	43		9.1	-9.9		-19815	-15297	-12157	-17	-25
3N2E 2CDD1	01 88	BOI	72		5.4	-10.5		-24129	-20098	-16958	-17	-25
3N2E 10AABB1	01 88	BOI	68		6.2	-10.4		-22987	-18876	-15737	-17	-25
3N2E 12CDD1	01 88	BOI	78		3.2	-10.7		-28455	-24579	-21440	-17	-25

Appendix C, continued

Carbon Age Dates

Sample Name	Sample Date	Temp °C	$\delta^{14}\text{C}$ ‰	A dpm/g	A pmc	$\delta^{13}\text{C}$ ‰	Log	max? C1 Age	min? C2 Age	Correc Factor		
							IAP CaCO ₃			Apparent Age	C1	C2
YOUNG, 1985, Idaho Batholith								$\delta^{13}\text{C}$	$\delta^{13}\text{C}$			
BIG CREEK HS	08 80	IDA	94		0.7	-5.5	-41020	-31642	-28502	-17	-25	
19N 2E HOT SP	06 80	IDA	43		12.3	-10.65	-17324	-13410	-10270	-17	-25	
18N 6E HOT SP	06 80	IDA	62		12.6	-11.55	-17125	-13881	-10741	-17	-25	
16N 4E HOT SP	06 79	IDA	50		10.0	-8.60	-19035	-13353	-10214	-17	-25	
SUNBEAM HOT SP	09 79	IDA	78		7.1	-7.50	-21867	-15053	-11914	-17	-25	
SLATE CREEK HS	09 79	IDA	50		27.3	-8.95	-10733	-5381	-2241	-17	-25	
9N 3E HOT SP	11 78	IDA	80		<0.7	-8.35	>-41020	-35094	-31954	-17	-25	
8N 5E HOT SP	02 79	IDA	51		16.1	-10.65	-15098	-11184	-8044	-17	-25	
JACOBSON, 1983, Dixie Valley Nevada								$\delta^{13}\text{C}$	$\delta^{13}\text{C}$			
HYDER HOT SP	07 79	DXV	80	993	0.7	-1.7	-41020	-24864	-18796	-12	-25	
SOU HOT SPRINGS	07 79	DXV	85	993	0.7	-2.2	-41020	-26995	-20927	-12	-25	
MCCOY HOT SP	03 79	DXV	49	958	4.2	-4.0	-26207	-17125	-11057	-12	-25	
ART WELL #1	03 79	DXV	19	945	5.5	-9.1	-23978	-21691	-15623	-12	-25	
DIXIE HOT SP	03 79	DXV	70	892	10.8	-2.2	-18399	-4375	1693	-12	-25	
KYLE HOT SP		DXV	77	833	16.7	-8.6	-14796	-12042	-5974	-12	-25	
MIDDLEGATE SP		DXV	1	557	44.3	-10.1	-6731	-5306	762	-12	-25	
WHITE ROCK CAN		DXV	1	114	88.6	-11.2	-1001	-430	5637	-12	-25	
PARK CANYON SP		DXV	1	0	100.0	-11.8	0	139	6207	-12	-25	
GLANCY, 1986, Fallon Nevada								$\delta^{13}\text{C}$				
HOWARD WOLF		FAL	30		2.50	18.4	-7.98	-14000	-8775		-15	
RONALD ALBAUGH		FAL	30		4.10	30.2	-6.89	-9900	-3463		-15	
KENNAMETAL INC		FAL	30		4.62	34.1	-8.72	-8900	-4411		-15	
FALLON-MORI		FAL	30		5.41	39.9	-9.96	-7600	-4211		-15	
US NAVY #3		FAL	30		6.97	51.4	-8.85	-5500	-1135		-15	
FALLON #3		FAL	30		6.97	51.4	-9.23	-5500	-1483		-15	
FALLON #1		FAL	30		7.14	52.7	-9.41	-5300	-1443		-15	
PONTE SUBDIV		FAL	30		8.36	61.7	-10.98	-4000	-1419		-15	
BEN PECK		FAL	30		11.73	86.5	-10.68	-1200	1609		-15	
COUNTRY CLUB ES		FAL	30		11.87	87.5	-12.68	-1100	290		-15	
FLYNN, 1983, Reno Nevada								$\delta^{13}\text{C}$	$\delta^{13}\text{C}$			
STEAMBOAT SP	07 82	SMA	96	-998	0.03	0.2	-6.2	-51376	-42989	-39849	-17	-25
NEWBURG WELL	07 82	SMA	90	-987	0.18	1.3	-6.6	-35902	-28032	-24892	-17	-25
WARREN EST WELL	07 82	SMA	90	-885	1.56	11.5	-10.3	-17880	-13689	-10549	-17	-25
GADDA WELL	07 82	SMA	90	-782	2.96	21.8	-11.8	-12593	-9526	-6386	-17	-25
MILES WELL	07 82	SMA	89	-776	3.04	22.4	-10.1	-12368	-8015	-4876	-17	-25
DESJARDIN WELL	07 82	SMA	77	-552	6.07	44.8	-11.2	-6638	-3140	0	-17	-25
MCKAY WELL	07 82	SMA	54	-337	8.99	66.3	-13.9	-3398	-1685	1455	-17	-25
MOANA LANE WELL	07 82	SMA	40	-188	11.01	81.2	-15.5	-1722	-910	2230	-17	-25

Appendix C, continued

Carbon Age Dates

Sample Name	Sample		Temp °C	$\delta^{14}\text{C}$ ‰	A dpm/g	A pmc	$\delta^{13}\text{C}$ ‰	Log		max? C1 Age	min? C2 Age	Correc Factor	
	Date	LOC						IAP CaCO ₃	Apparent Age			C1 Age	C2 Age
WHITE, 1987, Beatty Nevada										CaCO ₃	$\delta^{13}\text{C}$		
W1		OAV	30	-931	0.94	6.9	-2.5	-8.7	-22103	-18123	-12366	-4	-11
W13		OAV	30	-658	4.64	34.2	-6.3	-8.4	-8870	-4061	-4692	-11	-11
W6		OAV	30	-650	4.75	35.0	-5.6	-8.5	-8679	-4003	-3735	-12	-11
W2		OAV	30	-611	5.27	38.9	-5.3	-8.5	-7806	-3181	-2524	-9	-11
W15		OAV	30	-353	8.77	64.7	-7.0	-8.3	-3600	1626	-97	-13	-11
W17		OAV	30	-71	12.59	92.8	-8.0	-8.2	-614	4930	1912	-16	-11
W3		OAV	30	-2.2	13.53	99.8	-5.3		-18		5284		-11
W5		OAV	30	0.01	13.56	100.0	-4.9	-8.4	0	4926	5823	-9	-11
LYLES, 1988, Las Vegas Valley Nevada											$\delta^{13}\text{C}$		
MARTIN WELL	06 85	LVS	22			1.9	-6.7		-32765	-27947			-12
IND SP PRISON	06 85	LVS	23			4.9	-6.6		-24933	-19990			-12
POINT B WELL	06 86	LVS	25			6.1	-7.1		-23122	-18783			-12
CORN CREEK WELL	12 86	LVS	19			7.0	-7.7		-21984	-18316			-12
IND SP AFB WELL	09 85	LVS	24			7.3	-6.9		-21637	-17062			-12
INDIAN SPRINGS	06 86	LVS	25			7.7	-7.8		-21196	-17635			-12
HOLLAND WELL	08 82	LVS	26			11.3	-6.2		-18025	-12566			-12
TULE SPRING	06 85	LVS	21			13.9	-7.0		-16313	-11857			-12
CORN CREEK SP	06 85	LVS	21			13.9	-8.3		-16313	-13265			-12
MIFFLIN WELL	08 82	LVS	18			16.4	-7.7		-14946	-11278			-12
STEWART WELL	06 86	SPM	10			31.6	-8.0		-9524	-6172			-12
GRAPEVINE SP	06 85	SPM	27			46.0	-9.1		-6420	-4133			-12
CORTNEY WELL	08 82	LVS	23			48.4	-7.9		-5999	-2543			-12
SANDSTONE SP	06 85	SPM	17			49.6	-10.4		-5797	-4614			-12
ADAMS WELL	08 82	LVS	21			50.1	-8.2		-5714	-2566			-12
PAHUTE IND RES	07 85	LVS	19			57.0	-8.7		-4647	-1989			-12
GILBERT WELL	08 82	SPM	16			61.4	-8.8		-4032	-1468			-12
RED SPRING	06 85	SPM	19			62.0	-10.6		-3952	-2926			-12
WILLOW SPRING	06 85	LVS	10			79.2	-9.6		-1928	-83			-12
BIG TIMBER SP	06 85	AMG	11			87.3	-8.8		-1123	1441			-12
WIREGRASS SP	10 86	SHM	10			96.8	-10.2		-269	1075			-12
HWY MAINT WELL	09 82	SPM	11			100.0	-10.1		0	1425			-12
DEER CREEK SP#2	06 85	SPM	8			100.0	-9.6		0	1845			-12
MT CHARLS LODGE	08 82	SPM	10			100.0	-9.8		0	1674			-12

Appendix C, continued

Carbon Age Dates

Sample Name	Sample Date	LOC	Temp °C	$\delta^{14}\text{C}$ ‰	A dpm/g	A pmc	$\delta^{13}\text{C}$ ‰	Log	Apparent Age	max?	min?	Correc	
								IAP CaCO_3		C1 Age	C2 Age	Factor C1	C2
GROVE, 1969, Nevada Test Site										$\delta^{13}\text{C}$	$\delta^{13}\text{C}$		
NTS WELL C1		YCF	35	-970	0.41	3.0	-13.8		-28989	-30168	-24100	-12	-25
NTS WELL 1		LVS	33	-935	0.88	6.5	-12.0		-22597	-22590	-16522	-12	-25
FAIRBANKS SP		AMG	28	-931	0.94	6.9	-7.2		-22103	-17869	-11801	-12	-25
POINT OF ROCKS		AMG	32	-900	1.36	10.0	-7.9		-19035	-15611	-9543	-12	-25
INDIAN SPRINGS		LVS	25	-890	1.49	11.0	-11.0		-18248	-17498	-11430	-12	-25
NTS WELL 2		YCF		-850	2.03	15.0	-14.5		-15683	-17259	-11192	-12	-25
NTS WELL U20a2		PHM		-847	2.07	15.3	-13.4		-15520	-16475	-10407	-12	-25
NTS WELL 5B		YCF	24	-840	2.17	16.0	-20.8		-15150	-19733	-13665	-12	-25
NTS WELL 8		PHM	27	-718	3.82	28.2	-5.8		-10465	-4397	1671	-12	-25
CORN CREEK SP		LVS	11	-164	11.34	83.6	-20.1		-1481	-5762	306	-12	-25
CLAASSEN, 1985, Amargosa Desert Nevada										$\delta^{13}\text{C}$	CaCO_3		
FAIRBANK SPRING		AMG	30			1.9	-5		-32765	-27092		-11	
C27	04 71	AMG	31			7.0	-3.6	-8.4	-21992	-14267	-17034	-11	-8
C16	03 74	AMG	30			10.0		-8.5	-19042		-14377		
C30	06 79	AMG	30			10.3	-4.4	-8.2	-18798	-12297	-13359	-11	-10
NTS WELL VH1	02 81	CRF	36			12.0	-8.5		-17535	-15454		-11	
ASH TREE SPRING	03 74	AMG	20			13.8		-8.8	-16379		-12489		
C25	03 71	AMG	25			15.6	-5.6	-8.6	-15365	-10416	-10955	-11	-11
C3	11 72	AMG	30			15.6		-8.6	-15359		-11025		
C23	03 71	AMG	26			17.1	-7.1	-8.8	-14606	-11261	-10642	-11	-12
C15	03 74	AMG	30			18.4		-8.3	-14000		-8840		
C17	03 74	AMG	30			18.9		-8.2	-13778		-8276		
C4	03 74	AMG	30	-807	2.62	19.3	-7.1	-8.0	-13605	-10260	-7592	-11	-16
C13	03 74	AMG	27			19.3		-8.8	-13605		-9736		
NTS WELL H1	10 80	FMC	33			19.8	-11		-13393	-13171		-11	
C11	03 74	AMG	26			20.8		-8.3	-12986		-7881		
C5	11 72	AMG	23	-786	2.90	21.4	-6.8	-8.9	-12751	-9107	-9210	-11	-11
C8	03 74	AMG	23	-781	2.97	21.9	-7.3	-8.4	-12560	-9406	-7754	-11	-14
C10	06 79	AMG	30			24.8	-5.2	-8.6	-11531	-6092	-7117	-11	-10
NTS WELL 8	03 71	PHM	27			25.4	-12.1		-11333	-11812		-11	
C21	06 79	AMG	30			27.4	-8.4	-8.5	-10707	-8535	-6215	-11	-15
C18	03 74	AMG	24			27.8		-8.3	-10587		-5424		
C9	03 74	AMG	30			28.4		-8.4	-10410		-5656		
NTS WELL UE25b1	09 81	FMC	36			28.8	-10.4		-10294	-9659		-11	
NTS WELL J13	03 71	FMC	31	-707	3.97	29.2	-7.3	-9.5	-10177	-7020	-7889	-11	-10
C47	03 71	AMG	24			31.4	-6.2	-8.4	-9580	-5305	-4771	-11	-12
NTS WELL J12	03 71	FMC	27	-690	4.20	32.2	-7.9	-9.6	-9368	-7163	-7158	-11	-11

Appendix C, continued

Carbon Age Dates

Sample Name	Sample Date	LOC	Temp °C	$\delta^{14}\text{C}$ ‰	A dpm/g	A pmc	$\delta^{13}\text{C}$ pdb	Log IAP CaCO ₃	Apparent Age	max? C1 Age	min? C2 Age	Correc Factor C1 C2
BOUGHTON, 1986, Nevada Test Site										$\delta^{13}\text{C}$		
NTS WELL C1	09 83	CRF	37	992	0.11	0.8	-3.8		-39916	-30409		-12
NTS WELL A	06 82	CRF	27	944	0.76	5.6	-8.9		-23829	-21358		-12
NTS WELL Ue15d	09 83	CRF	30	936	0.87	6.4	-4.1		-22725	-13847		-12
NTS WELL Ue16d	06 82	CRF	25	932	0.92	6.8	-8.7		-22224	-19565		-12
NTS WELL U19c	06 82	PHM	39	928	0.98	7.2	-11.6		-21751	-21471		-12
NTS WELL 2	06 82	CRF	35	900	1.36	10.0	-11.2		-19035	-18465		-12
NTS WELL 4	09 83	CRF	28	802	2.69	19.8	-10.9		-13388	-12593		-12
NTS WELL 8	06 82	PHM	27	748	3.42	25.2	-11.3		-11395	-10898		-12
NTS WELL J13	06 82	FMC	31	707	3.97	29.3	-7.8		-10148	-6587		-12
BENSON, 1983, Yucca Mountain Nevada										$\delta^{13}\text{C}$		
NTS WELL USWH6	06 84	YCM	42			10.0	-7.3		-19035	-15646		-11
NTS WELL USWH3	03 84	YCM	27			10.5	-4.9		-18632	-11947		-11
NTS WELL USWH4	05 82	YCM	35			11.8	-7.4		-17667	-14390		-11
NTS WELL USWVH1	02 81	CRF	36			12.2	-8.5		-17392	-15260		-11
NTS WELL USWH6	07 84	YCM	37			12.4	-7.1		-17257	-13638		-11
NTS WELL Ue25c1	09 83	YCM	42			15.0	-7.1		-15683	-12064		-11
NTS WELL Ue25c3	05 84	YCM	41			15.7	-7.5		-15306	-12140		-11
NTS WELL USWH6	10 82	YCM	38			16.3	-7.5		-14996	-11830		-11
NTS WELL Ue25c2	03 84	YCM	41			16.6	-7.0		-14846	-11109		-11
NTS WELL Ue25b1	09 81	YCM	36			16.7	-10.4		-14796	-14332		-11
NTS WELL USWH5	07 82	YCM	37			18.2	-10.3		-14085	-13541		-11
NTS WELL UE25b1	07 82	YCM	37			18.9	-8.6		-13773	-11738		-11
NTS WELL USWH5	07 82	YCM	36			21.4	-10.3		-12746	-12202		-11
NTS WELL USWG4	12 82	YCM	36			22.0	-9.1		-12517	-10950		-11
NTS WELL USWH1	12 80	YCM	35			23.9	-11.4		-11832	-12128		-11
NTS WELL J13	03 71	FMC	31			29.2	-7.3		-10177	-6787		-11
NTS WELL J12	03 71	FMC	27			32.2	-7.9		-9368	-6632		-11
NTS WELL UE29a2	01 82	FMC	23			60.0	-13.1		-4223	-5667		-11
NTS WELL UE29a2	01 82	FMC	25			62.3	-12.6		-3912	-5035		-11

APPENDIX D

PALEOCLIMATE DATA

Deuterium analyses of Great Basin packrat middens from two sources, the current study and one previous study. Oxygen-18 analyses from three sources, ice cores from the Greenland Ice Sheet, plankton obtained from sub-polar Indian Ocean deep sea cores, and layered calcite continuously deposited in Devil's Hole, Nevada. A partial reference is provided before each group of data, complete references are available in the reference section. Packrat midden age dates and macrofossils for isotope analysis for the current study provided courtesy of Dr. Peter Wigand, Desert Research Institute, Reno, Nevada.

CURRENT STUDY, Great Basin Packrat Middens

SAMPLE	LOC	LONG	LAT	DEUT ‰	ISO MAT	CARB AGE	+/-	DATE MAT
SC110388PEW1	SCY	119.64	39.26	-60	J	5650	150	N
SC111389MJ1	SCY	119.64	39.26	-55	J	MJ		
HV200589PEW1	HVY	119.68	39.49	-57	J	9800	340	N
HV111289MJ1	HVY	119.68	39.49	-48	J	MJ		
SM110389CLN2(1)	SMD	119.82	40.32	-64	J	11790	130	N
SM110389CLN3(1)	SMD	119.83	40.35	-73	J	10810	150	N
PH180589PEW2(1)	PHS	119.66	39.88	-64	J	21460	420	N
PH140889PEW2(1,5)	PHS	119.64	39.88	-71	J	24580	470	N
PH180589PEW3(2,1)	PHS	119.64	39.88	-71	J	16280	160	N
PH140889PEW2(1,3)	PHS	119.64	39.88	-79	J	11910	110	N
PH140889PEW2(1,4)	PHS	119.64	39.88	-49	J	11530	160	N
PH140889PEW2(1,2)	PHS	119.64	39.88	-59	J	8560	120	N
PH211089PEW1(1,2)	PHS	119.64	39.88	-65	J	29630	590	J
PH211089PEW1(1,3)	PHS	119.64	39.88	-55	J	28560	390	J
PH211089PEW1(1,4)	PHS	119.64	39.88	-53	J	11730	100	J
PH211089PEW1(1,5)	PHS	119.64	39.88	-77	J	23110	410	J
PH211089PEW1(1,6)	PHS	119.64	39.88	-40	J	29410	770	J
PH211089PEW1(1,7) ^t	PHS	119.64	39.88	-89	J	12440	130	J
PH211089PEW1(1,7) ^m	PHS	119.64	39.88	-77	J	12340	190	J
PH211089-MJ	PHS	119.64	39.88	-71	J	MJ		
PR100588PEW1(4,1)	PRG	115.40	37.41	-38	J	9540	120	
PR100588PEW1(4,2)	PRG	115.40	37.41	-34	J	5820	90	
PR100588PEW1(5,1)	PRG	115.40	37.41	-52	J	11710	150	
PR100588PEW1(5,3)	PRG	115.40	37.41	-61	J	22730	1080	
PR101189MJ1	PRG			X	J	MJ		

See next page for letter key

APPENDIX D, continued

Paleoclimate Data

SIEGEL, 1983, Snake Range Packrat Middens

SAMPLE	LOC	LONG	LAT	DEUT ‰	ISO MAT	CARB AGE	+/-	DATE MAT
AC-2A	SNR	114.2	39.0	-104	S	34040	4300	N
AC-6	SNR			-114	J	29920	2000	N
LC-2A	SNR			-110	J	27280	970	S
LC-2B	SNR			-117	P	17960	1100	P
SV-2	SNR			-119	P	17350	435	P
SC-5	SNR			-86	P	13340	430	P
LC-2C	SNR			-88	P	13100	210	P
SC-4	SNR			-96	P	12235	150	P
LC-4	SNR			-96	P	12100	150	P
LC-6	SNR			-92	S	11080	115	P
SC-2	SNR			-96	S	10450	290	J
BA-1	SNR			-98	S	9680	700	P
SV-3	SNR			-76	J	6490	190	J
CH-1A	SNR			-76	J	6120	80	J
CH-1B	SNR			-85	J	4220	60	J
LC-J2	SNR			-96	J	0		J
LC-J1	SNR			-96	J	0		J
LC-S	SNR			-104	S	0		S
SC-P	SNR			-88	PM	0		P

LEGEND

SNR - Snake Range, Nevada - Utah Border	HVA - Hidden Valley, Sparks, Nevada
SMD - Smoke Creek Desert, Northwest Nevada	PHS - Painted Hills, North of Reno
SCY - Silver City, Southeast of Reno	PRG - Paharanagat Range, Southern Nevada
ISO - Material Analyzed for isotope content	DATE - Material analyzed for carbon age
MAT	MAT
MJ - Modern Juniper	S - Symphoricarpos
J - Juniperus	P - Pinus longaeva
N - Neotoma fecal pellets	PM - Pinus Monophylla

APPENDIX D, continued

Paleoclimate Data

DANSGAARD, 1969, Greenland Ice Core

Oxygen-18 data reported normalized from 0 to 1 and permil

AGE (years)	^{18}O (norm)	^{18}O ‰	AGE (years)	^{18}O (norm)	^{18}O ‰	AGE (years)	^{18}O (norm)	^{18}O ‰
1655	0.94	-28.86	9043	0.87	-29.93	12595	0.24	-39.90
1720	0.91	-29.34	9268	0.87	-29.92	12690	0.21	-40.28
1767	0.93	-29.07	9383	0.84	-30.49	12828	0.26	-39.64
1840	0.97	-28.42	9500	0.83	-30.58	12892	0.17	-41.02
2038	0.97	-28.43	9607	0.86	-30.10	13002	0.18	-40.89
2253	0.98	-28.30	9694	0.88	-29.83	13072	0.18	-40.77
2325	0.90	-29.45	9917	0.82	-30.77	13234	0.30	-38.87
2444	0.90	-29.46	10160	0.83	-30.63	13267	0.09	-42.21
2802	0.93	-28.97	10209	0.76	-31.63	13421	0.17	-41.02
3194	0.95	-28.69	10275	0.76	-31.64	13511	0.16	-41.11
3594	0.99	-28.14	10284	0.75	-31.77	13621	0.09	-42.30
3692	0.91	-29.28	10350	0.75	-31.79	13771	0.12	-41.73
4086	0.93	-28.95	10361	0.75	-31.87	13926	0.23	-40.08
4609	0.95	-28.69	10414	0.75	-31.86	14012	0.24	-39.83
4672	1.00	-27.92	10476	0.71	-32.45	14166	0.37	-37.77
4748	0.97	-28.46	10538	0.70	-32.58	14256	0.08	-42.32
4875	0.98	-28.19	10572	0.66	-33.20	14393	0.04	-43.04
4987	0.97	-28.43	10644	0.65	-33.47	14520	0.00	-43.65
5119	0.94	-28.89	10699	0.62	-33.82	14641	0.20	-40.46
5247	0.96	-28.59	10784	0.61	-34.09	14827	0.20	-40.46
5367	0.96	-28.56	10853	0.53	-35.31	14932	0.31	-38.71
5495	0.95	-28.72	10937	0.54	-35.17	14941	0.16	-41.06
5706	0.95	-28.71	10965	0.40	-37.32	15404	0.22	-40.12
5784	0.95	-28.77	11018	0.26	-39.57	16162	0.15	-41.25
5974	0.96	-28.62	11111	0.23	-39.98	17147	0.44	-36.80
6155	0.98	-28.31	11216	0.35	-38.22	18276	0.30	-38.95
6366	0.92	-29.22	11287	0.35	-38.08	20190	0.42	-37.11
6505	0.93	-29.00	11391	0.46	-36.36	21182	0.11	-41.90
6569	0.96	-28.61	11441	0.46	-36.47	21587	0.14	-41.50
6603	1.00	-27.92	11570	0.45	-36.57	22782	0.20	-40.56
6754	0.98	-28.17	11636	0.56	-34.81	23847	0.20	-40.44
6911	0.98	-28.24	11733	0.57	-34.64	25496	0.26	-39.50
7141	0.96	-28.52	11794	0.36	-37.93	27684	0.36	-37.94
7324	0.93	-29.02	11850	0.37	-37.82	28205	0.36	-37.93
7618	0.94	-28.93	11907	0.18	-40.80	28836	0.40	-37.36
7846	0.94	-28.83	11984	0.15	-41.33	29312	0.40	-37.36
8104	0.87	-29.91	12144	0.21	-40.39	30703	0.53	-35.38
8310	0.92	-29.21	12216	0.28	-39.30	32813	0.52	-35.42
8424	0.88	-29.84	12281	0.33	-38.44	33974	0.49	-35.91
8566	0.87	-29.96	12343	0.32	-38.60	34723	0.49	-35.96
8692	0.88	-29.73	12402	0.33	-38.39	35494	0.32	-38.63
8773	0.92	-29.21	12481	0.33	-38.39	39488	0.32	-38.67
8986	0.92	-29.18	12484	0.28	-39.18			

APPENDIX D, continued

Paleoclimate Data

MARTINSON, 1987, Sub-polar Indian Ocean Deep Sea Cores
Oxygen-18 data reported normalized from 0 to 1

AGE (years)	^{18}O (norm)	AGE (years)	^{18}O (norm)	AGE (years)	^{18}O (norm)	AGE (years)	^{18}O (norm)	AGE (years)	^{18}O (norm)
210	1.00	37370	0.27	79250	0.60	139980	0.07	210800	0.72
2310	0.97	39690	0.24	79660	0.60	141330	0.25	215540	0.89
2480	0.97	41000	0.31	81790	0.52	142280	0.20	220140	0.68
4200	0.97	42930	0.31	84130	0.53	142810	0.17	222520	0.45
6270	0.92	43880	0.29	86310	0.49	145240	0.13	224890	0.25
7810	0.94	43940	0.29	90100	0.41	147110	0.12	225160	0.23
9140	0.78	44820	0.27	90950	0.42	149340	0.04	227360	0.30
10310	0.66	45570	0.27	92230	0.43	152140	0.07	229790	0.37
11440	0.48	47300	0.33	94060	0.49	152580	0.07	231850	0.45
12050	0.45	48900	0.36	96210	0.58	155090	0.08	233200	0.53
12580	0.41	50210	0.38	96380	0.59	157100	0.04	237030	0.75
13700	0.24	50390	0.39	99380	0.56	159890	0.19	240190	0.78
14990	0.13	51570	0.28	99960	0.55	161340	0.19	241190	0.79
16160	0.05	52670	0.32	103290	0.60	161830	0.19	244180	0.42
17310	0.00	53690	0.32	103800	0.60	162790	0.24	247600	0.24
17850	0.01	54840	0.39	105080	0.54	164110	0.18	250370	0.41
18310	0.01	55450	0.38	106050	0.50	165350	0.18	253430	0.15
19130	0.05	56050	0.38	107550	0.47	165990	0.19	254620	0.24
19220	0.05	57600	0.37	110790	0.47	167770	0.26	257180	0.24
19690	0.05	58930	0.30	112280	0.47	168890	0.19	259820	0.22
20330	0.05	58960	0.30	115910	0.62	171370	0.31	260680	0.18
20860	0.03	60440	0.25	118690	0.80	173670	0.31	263900	0.27
21400	0.08	62970	0.26	122190	0.91	175050	0.28	265670	0.23
21940	0.03	64090	0.24	122560	0.90	176900	0.24	266700	0.21
22380	0.08	65220	0.21	123790	0.87	179730	0.21	267480	0.12
22850	0.11	66970	0.23	123820	0.87	180910	0.21	269820	0.17
23170	0.11	68250	0.26	125000	0.89	181700	0.23	027168	0.46
23360	0.11	68830	0.28	125190	0.85	182640	0.25	273420	0.19
23930	0.14	69190	0.29	126580	0.63	183300	0.21	275840	0.20
24110	0.14	70240	0.27	128310	0.46	183370	0.20	277360	0.27
24460	0.15	70820	0.25	129700	0.34	184170	0.23	278370	0.21
24860	0.20	71120	0.24	129840	0.32	185190	0.22	280160	0.38
25350	0.24	72230	0.34	131090	0.16	188290	0.40	282330	0.37
25420	0.24	73250	0.34	132810	0.27	189610	0.47	283330	0.53
26500	0.24	73910	0.38	134230	0.08	191080	0.55	285340	0.60
27950	0.21	74340	0.40	135100	0.03	193070	0.69	288170	0.64
29730	0.24	75320	0.48	135340	0.01	193180	0.70	288540	0.63
31450	0.23	76370	0.50	136590	0.08	196070	0.64	291460	0.56
33210	0.27	77310	0.54	137970	0.09	200570	0.55		
35560	0.23	78300	0.60	139020	0.04	205530	0.70		

APPENDIX D, continued

Paleoclimate Data

WINOGRAD, 1988, Great Basin Calcite Deposition, Devils Hole
Oxygen-18 data reported normalized from 0 to 1

AGE (years)	^{18}O (norm)	AGE (years)	^{18}O (norm)	AGE (years)	^{18}O (norm)
53200	0.69	140000	0.00	227000	0.56
56000	0.71	142200	0.03	229500	0.55
58600	0.77	144900	0.09	231500	0.51
61000	0.84	146600	0.40	233900	0.48
62500	0.84	148000	0.56	236100	0.48
64700	0.89	151300	0.71	239000	0.48
68000	0.80	154000	0.78	240800	0.50
70000	0.71	156000	0.80	242900	0.62
72400	0.71	158600	0.80	245000	0.70
74500	0.63	160800	0.71	247000	0.79
77100	0.63	162900	0.80	249500	0.62
79000	0.63	165600	0.70	252000	0.50
81700	0.63	168000	0.68	254000	0.47
84100	0.56	170200	0.70	256400	0.43
86500	0.56	173000	0.71	258600	0.36
89200	0.56	175000	0.62	262000	0.30
91000	0.62	178600	0.70	264000	0.36
93800	0.62	179600	0.74	266500	0.40
96500	0.62	182100	0.80	269000	0.48
98500	0.55	184800	0.80	271200	0.44
101000	0.55	187200	0.80	273000	0.80
103500	0.50	188600	0.70	275500	0.80
105700	0.49	190800	0.78	277600	0.83
107500	0.44	193000	0.70	279700	0.89
110500	0.48	195800	0.62	282500	0.90
112600	0.40	198900	0.62	285000	0.69
115400	0.49	201000	0.62	287000	0.70
117300	0.54	203100	0.62	289000	0.80
119800	0.54	205500	0.62	291000	0.77
121500	0.49	207000	0.53	294000	0.66
123300	0.49	211000	0.50	296000	0.59
126000	0.40	212600	0.53	299200	0.80
128400	0.29	215800	0.49	301000	0.95
130600	0.16	218100	0.50	303500	0.99
132900	0.11	219800	0.55	306000	1.00
135000	0.09	222200	0.69	309000	0.83
137100	0.04	224600	0.62		